Characterization of the PASTA kinases as antibiotic targets in *S. aureus* and *L. monocytogenes*

By

Adam J. Schaenzer

A dissertation submitted in partial fulfillment of

the requirements for the degree of:

Doctor of Philosophy

(Molecular and Cellular Pharmacology)

UNIVERSITY OF WISCONSIN-MADISON

2018

Date of final oral examination: 9/4/2018

The dissertation is approved by the following members of the Final Oral Committee:

Dr. John-Demian Sauer, Assistant Professor, Medical Microbiology and Immunology
Dr. Rob Striker, Associate Professor, Medicine
Dr. Warren Rose, Associate Professor, Pharmacy Practice
Dr. Mark Burkard, Associate Professor, Medicine
Dr. Joseph Dillard, Professor, Medical Microbiology and Immunology

Characterization of the PASTA kinases as antibiotic targets in *S. aureus* and *L. monocytogenes*

By

Adam J. Schaenzer

Under the supervision of Dr. John-Demian Sauer

at the University of Wisconsin-Madison

DISSERTATION ABSTRACT

In order to combat the rise of antibiotic-resistant infections, it is imperative that novel antibiotic strategies are developed and implemented. Signal transduction systems including those governed by protein kinases are gaining increased attention as potential targets for antibiotics or antibiotic adjuvants due to the past clinical successes in targeting eukaryotic kinases. A subset of eukaryotic-like serine/threonine kinases known as the Penicillin-binding protein And Ser/Thr kinase-associated (PASTA) kinases are of particular interest as potential targets for antibiotic adjuvants due to their roles in maintaining β-lactam resistance. Here, we utilize a three-step microbiologic-biochemical-*in silico* approach to discover and characterize novel inhibitors of the PASTA kinases Stk1 and PrkA from the human pathogens *Staphylococcus aureus* and *Listeria monocytogenes*, respectively. We identify the imidazopyridine aminofurazans and pyrazolopyridazines as respective inhibitors of PrkA and Stk1 that can sensitize their respective organisms to β-lactams. We further perform *in silico* modeling, medicinal chemistry, and protein mutagenesis to probe the structure-activity relationships of these compounds with their kinase targets. Finally, we present our initial findings in identifying downstream substrates of *S. aureus* Stk1 which are important in the maintenance of β-lactam resistance. Understanding both the pharmacology of PASTA kinase inhibition and PASTA kinase signaling circuits will aid in the further development of these molecules as potential β-lactam adjuvants.

DEDICATION

I dedicate this dissertation to Mrs. Fran Grant and Dr. Shannon Colton. It's because of both of you and the SMART team program that I wound up down the path of molecular biology. This is all your fault (but in a good way).

I also dedicate this dissertation to all of those who have died to an antibiotic-resistant infection. Your passing has not gone unnoticed, and we will continue to fight the pathogens that have cut short your lives.

ACKNOWLEDGEMENTS

Science is rarely performed in a vacuum (unless, of course, you're a physicist and study these sorts of things). It takes a support network of friends, family members, and colleagues to be successful. Below is just a fraction of those who have helped me on this 5 year journey.

Most graduate students go through their training with a single primary advisor; I was blessed with three co-advisors over the course of my graduate school career. Drs. John-Demian Sauer, Warren Rose, and Rob Striker have given me three unique perspectives in mentoring and scientific outlook. They have successfully taught me both simple and hard lessons about the intricacies of science and life in general. I will always be grateful for them sticking with me through this time of growth.

I'd also like to thank the members of the Sauer lab both past and present for being the perfect blend of scientific hooligans to call a lab family. Dan Pensinger has the patience of a saint, and without him the lab would have certainly burned to the ground a long time ago. I thank Courtney "McDoogs" Mcdougal and Hans Smith for more than occasionally feeding into my shenanigans. CY Kao has become my partner-in-crime in the staphylococcal camp of the lab, and I hope that I have not corrupted his mind too much in the process. Will Vincent was my emotional rock, and I can only hope that I have helped him nearly as much as he has helped me these past years. I'd like to thank Erin Theisen for humoring my hypochondriasis on countless occasions and for her infamous eye-roll when I say something that's too out there. Grischa Chen always had insightful scientific input to all of our experiments. I'd also like to give a shout-out to all of the undergrads that have shared "The Kids' Room" office with me; it's a shame we never got that band "Adam and the Undergrads" up and running (I blame our manager). In particular, I'd like to say thank you to Drew Rust for working with me as I learned how to be a mentor. Finally, I'd like to thank our adoptive Sauer lab members Laurie Ristow and Tu Anh Huynh. You both have the Sauer lab spirit, and add to what makes the lab special. It has been a pleasure working alongside all of you.

There are also many colleagues outside of the Sauer lab that I'd wish to thank, too many to list here. We've all made wonderful memories together during my time in Madison, and I wouldn't change that for anything. In particular, I need to give a shout-out to Nate Wlodarchak and Akshat "Woodhouse" Sharma. Nate taught me practically everything I know about protein purification and designing enzymatic assays and is a riot to boot. Akshat has always been my fellow diva and the "Cersei" to my "Dany". It is probably for the best that the three of us never truly worked in the same workspace, as we would never have gotten anything done!

Finally, I'd like to thank my family for simply being there this whole time, not only for graduate school but also for all the times before and what is to come.

"TCGAAATAAGATAAAATAGTAGGATCG"

TABLE OF CONTENTS

LIST OF FIGURES

LIST OF TABLES AND SCHEMA

Chapter 1: PASTA kinases as potential antibiotic targets

Authors and their contributions

Adam J. Schaenzer: Planned, organized, and wrote the manuscript

John-Demian Sauer: Supervised writing and editing the manuscript

This chapter was published, in part, in Trends in Microbiology on January 2018:

> **Pensinger DA, Schaenzer AJ, Sauer JD.** 2018. Do shoot the messenger: PASTA kinases as virulence determinants and antibiotic targets. Trends Microbiol. PMID: 28734616.

Excerpts taken were directly written by Adam J. Schaenzer

INTRODUCTION: ANTIBIOTICS AND ANTIBIOTIC RESISTANCE

The rise and fall of the "Golden Age" of antibiotics

In 1928, Alexander Fleming accidentally discovered that secretions from the fungus *Penicillium rubens* possess antimicrobial properties[1,2]. The isolation and eventual widespread use of the active compound, known as penicillin, is considered one of the greatest medical advances of the 20th century; by the end of World War II in 1945, annual production of this life saving antibiotic in the United States had surpassed 6.8 trillion units[3]. Following in Fleming's footsteps, Selman Waksman and colleagues discovered the antibiotic streptomycin in 1944[4]. Waksman's successful platform of methodically screening soil bacteria for antibiotics became the backbone for natural product discovery and heralded the dawn of the "Golden Age" of antibiotics[4–6]. It was during this time (approximately the 1940s through the 1960s) when most of our clinically utilized antibiotic classes were discovered[4,6,7]. By the beginning of the 1970's, many believed that infectious diseases would soon be conquered.

During the "Golden Age", there was a steady discovery of novel antibiotic classes based on natural products. However, eventually antibiotic dereplication and diminishing returns led to the abandonment of the Waksman platform by most pharmaceutical companies by the 1980s[4,6,8–11]. Attempts to find new leads then shifted towards synthetic compound platforms using high-throughput screening of synthetic compounds against select targets predicted to be essential by genomics. This platform proved to be insufficient, however, with many compounds showing biochemical activity *in vitro* but failing to penetrate the cell wall or outer membrane to reach their targets[6,12,13]. Furthermore, it has been argued that synthetic libraries lack the chemical complexity required for effective antimicrobial properties, contributing to the dismal progress of this platform[13]. To date, only two classes of synthetic antibiotics have been successfully developed using this platform[6,14]: the oxazolidinones and the quinolones. This decline in lead compounds combined with a decreased return on investment and unclear FDA

approval requirements has led to the exodus of many pharmaceutical companies from the antibiotic market in the 1990s and early 2000s[8,15–17].

Since antibiotics put a selective pressure on the bacteria they target, the evolution of antibiotic resistance was inevitable. For a period of time, the discovery of novel antibiotics and derivatization of previously identified classes was able to keep pace with the rise of resistance. However, antibiotic development fell into a sharp decline with the death of the Waksman platform and the exodus of the pharmaceutical industry. When combined with misuse of antibiotics in both the medical and agricultural arenas[18], this allowed for the rise of widespread antibiotic resistance that some refer to as the "antibiotic resistance crisis"[18] or the "post-antibiotic era"[19]. Of particular concern are multidrug-resistant *Mycobacterium tuberculosis*, *Neisseria gonorrhoeae*, and the ESKAPE pathogens (*Enterococcus faecium*, *Staphylococcus aureus*, *Klebsiella pneumoniae*, *Acinetobacter baumannii*, *Pseudomonas aeruginosa*, and *Enterobacter* species) which have now become serious health threats across the globe[7,20,21]. If nothing is done to stem the rise of resistance, the global death toll due to antibiotic-resistant infections is predicted to escalate to 10 million deaths per year by 2050 and carry a 100 trillion dollar price tag in lost global GDP[7,20].

Mechanisms of antibiotic resistance

For millions of years microorganisms have coevolved in almost every conceivable ecological niche, struggling for survival in a constant state of biochemical warfare. They have been using their natural products to outcompete their neighbors long before we ever appropriated them for our medicines. As such, it should come as little surprise that resistance mechanisms for these natural product antibiotics were also already present in the environment before the modern antibiotic era[22,23]. Some of these genes have origins with the antibiotic-producer to prevent self-intoxication, while others may have evolved from "proto-resistance genes" which performed some basic physiologic function before adopting a resistance function

over generations of antibiotic selection[24]. Regardless of their origin, these resistance genes can then be mobilized at random through horizontal gene transfer into other bacterial species, including human pathogens[25,26].

Bacteria have evolved a wide variety of mechanisms to avoid killing by antibiotics (**Table 1.1**) including antibiotic destruction/modification, target modification, increased efflux, decreased permeability, and target bypass[27]. Of these, destruction or modification is the most direct method of resistance and possibly the most diverse with at least seven established types of inactivating modifications (**Table 1.1**)[24]. For example, the aminoglycosides can be chemically modified with 3 different moieties by aminoglycoside-modifying enzymes: acetylation, phosphorylation, and nucleotidylation[24,28]. Other antibiotics such as the macrolides, tetracyclines, and rifampin can be glycosylated[29], monooxygenated[30], and ADP-ribosylated[31], respectively. These modifications tend to block antibiotic activity through steric inhibition[27]. On the other hand, some antibiotics can be enzymatically broken down rather than simply adorned with chemical moieties. Examples of this antibiotic degradation include hydrolysis of β-lactams by β-lactamases[32,33] and linearization of streptogramin B by the C-O lyase virginiamycin B lyase[34].

In opposition to modifying the antibiotic itself, an alternative approach is modification of the antibiotic target which can yield the same net effect of diminished antibiotic affinity. These modifications can occur either through mutation of the target's inherent amino acid sequence or through enzymatic modifications. Resistance via target mutation is well documented for antibiotics such as the rifamycins[35], fluoroquinolones[36], and oxazolidinones[37]. Resistance to rifampin can be achieved through various one-step mutations which alter the amino acid sequence of the β-subunit of the RNA polymerase, thereby decreasing rifampin's affinity but leaving the polymerase's enzymatic activities intact[35]. In the case of the fluoroquinolones, accumulation of mutations in both DNA gyrase and topoisomerase IV are needed for drastic

resistance to these drugs[36]. In the final example, linezolid's affinity for the ribosome can be abolished by mutation of ribosomal proteins L3, L4, or domain V of the 23S ribosomal RNA[37].

Besides direct mutations to the genome, enzymatic modification of antibiotic targets also inhibits antibiotic activity; examples of this mechanism are particularly prevalent against ribosome-targeting antibiotics, the most infamous of which is the methylation of A2058 on domain V of the 23rRNA[38,39]. Catalyzed by the erythromycin ribosomal methylation (erm) proteins, methylation of this single adenine base is capable of granting resistance to the macrolides, lincosamides, and streptogramin B[39]. However, because this modification also decreases ribosome efficiency, the erm proteins are translationally regulated so that protein is only synthesized in the presence of the antibiotic[40]. On the other hand, formation of 8-methyladenosine on A2503 of the 23S rRNA by the methyltransferase Cfr increases resistance to linezolid (though intriguingly not the more recently approved tedizolid[41]), the phenicols, lincosamides, and streptrogramin A[42,43]. Indeed, the ability of two accessory methylation sites to cripple 5 classes of antibiotics demonstrates the effectiveness of this resistance strategy.

The ability to bypass the antibiotic target altogether is another successful antibiotic resistance strategy. The most infamous example of this strategy is the utilization of the β-lactam-resistant penicillin-binding protein (PBP) PBP2A in methicillin-resistant *S. aureus* (MRSA). The transpeptidase domain of PBP2A is resistant to the vast majority of β-lactams which, when coupled with the transglycosylase domain of other PBPs, allows for continued cell wall synthesis even while the transpeptidase domains of all other PBPs are inactivated[44–46]. Another example of target bypass is vancomycin resistance in the enterococci. Acquisition of any 1 of 9 gene clusters known as the *van* clusters allows for the modification of the terminal D-Ala-D-Ala peptide on the pentapeptide stem of cell wall precursors, modifying them to either D-Ala-D-Lac or D-Ala-D-Ser[47,48]. Both modifications decrease the affinity for vancomycin, though the removal of a single hydrogen bond by D-Ala-D-Lac is much more pronounced, leading to a 1,000-fold decrease in affinity for the antibiotic[48].

Finally, both the decreased permeability and increased efflux resistance mechanisms are complementary defenses which lower internal concentrations of the target antibiotics. Increased efflux is achieved using efflux pumps driven by the proton motive force (with the exception of the ABC transporters which are driven by ATP hydrolysis)[49]. A classic example of efflux resistance is the resistance of many *Enterobacteriaceae* to the tetracyclines, with some pumps such as Tet(A) and Tet(A)-1 of *Klebsiella pneumoniae* allowing for high-level tetracycline resistance[50,51]. The macrolides are another example of an antibiotic class susceptible to efflux; this is particularly important in the streptococci where the majority of macrolide resistance in *S. pneumoniae* is achieved via the proton-driven pump MefA[40]. On the other hand, efflux-driven macrolide resistance in *S. aureus* is relatively uncommon, though overexpression of the ABC transporter MsrA can grant this bacteria high-level resistance to 14- and 15-membered macrolides[40].

Unlike efflux, the decreased permeability strategy decreases the ability of antibiotics to even access the cytosolic compartment in the first place. This is a particularly useful strategy for gram-negative bacteria whose outer membrane provides a daunting barrier for many antibiotics. Hydrophilic antibiotics such as the β-lactams must pass through hydrated channels known as porins in order to enter the periplasm[52,53]. Access for these antibiotics can be restricted either by decreased expression of the relevant porin[53,54] or by voltage-dependent porin inactivation[53,55,56]. For hydrophobic antibiotics such as the aminoglycosides and macrolides which could naturally diffuse through the lipid bilayers, lipopolysaccharide (LPS) can act as a barrier to passage through the outer membrane with intact LPS possessing more protective properties than truncated forms[57,58]. Unlike their gram-negative counterparts, gram-positive bacteria do not possess an outer membrane or LPS to protect against antibiotic insult. Instead, they utilize mechanisms such as capsular polysaccharides[59] or modified teichoic acids to mask the intrinsic negative charge of the bacterial surface and repel antimicrobial peptides[60,61], daptomycin[62,63], and vancomycin[60].

The resistance mechanisms described above collectively grant resistance to every antibiotic class in use in the clinic today. In order to combat the “Antibiotic Resistance Crisis”, either novel antibiotic classes or methods to salvage established antibiotics must be implemented.

Resistance spotlight: the β-lactams

Among antibiotic classes, the β-lactams are one of the oldest and arguably the most successful, comprising ~65% of the world market for antibiotics[64]. The β-lactam antibiotics include the penams (i.e. penicillins), cephems (i.e. cephalosporins and cephamycins), carbapenems, and the monobactams, all of which possess a highly reactive β-lactam ring at their cores (**Figure 1.1**). These antibiotics mimic the D-Ala-D-Ala moiety of peptidoglycan and irreversibly inhibit the transpeptidase domain of penicillin-binding proteins (PBPs), leading to a defective cell wall[65]. While it was originally thought that β-lactam-mediated killing was simply lysis as the result of an imbalance of cell wall synthases and hydrolases, there is also evidence that instead the β-lactams induce a futile cycle of cell wall metabolism which leads to death independent of lysis[66]. In any case, they inhibit a highly conserved bacterial enzyme which has no homolog in humans and are relatively cheap to synthesize[64], making them ideal antibiotics.

Like with all antibiotics, resistance to the β-lactams poses a significant threat to modern medicine. The two predominant β-lactam resistance mechanisms are the production of β-lactamases which degrade the antibiotic and the use of PBPs with low affinity for the β-lactams[67]. The β-lactamases are the resistance mechanism of choice for the gram-negative bacteria and are a particularly diverse class of enzyme with over 890 unique protein sequences[33]. Modification of the target PBPs is the favored mechanism of gram-positive bacteria[68], the most infamous of which is PBP2A from methicillin-resistant *S. aureus* which is resistant to almost all β-lactams[44,45]. These widespread resistance mechanisms have seriously compromised the utility of β-lactams in the clinic.

Because of their previous success and prominent place in global healthcare, there have been considerable efforts to salvage the efficacy of the β-lactams. The development of β-lactam/β-lactamase inhibitor combination therapies have certainly aided in the extension of β-lactam utility. The early β-lactamase inhibitors clavulanic acid, sulbactam, and tazobactam are β-lactam derivatives that are collectively able to inhibit the class A narrow-spectrum and class A extended-spectrum β-lactamases[69]. As these early inhibitors were thwarted by the rise of the class C cephalosporinases and class A and D carbapenemases[70], the newer inhibitors avibactam, vaborbactam, and relebactam were developed as necessary coverage[69,71,72]. Unfortunately, complete coverage of such a vast class of enzymes remains challenging. This is made painfully evident by the rise of the class B metallo-β-lactamases such as VIM-I, IMP-I, and NDM-I[73]. Unlike the other classes of β-lactamases, which utilize an active site serine and a covalent intermediate to hydrolyze their targets, the metallo-β-lactamases utilize metal ions (usually zinc) and a non-covalent mechanism of action[74]. This fundamental difference renders them immune to all currently-implemented β-lactamase inhibitors. While there are some promising leads for metallo-β-lactamase inhibitors[75], there are currently none in clinical trials, and so it will be some time before such compounds are implemented.

For bacteria which wield modified PBPs rather than β-lactamases as their resistance mechanism, direct modification of the β-lactams themselves is needed. This is exemplified in the fifth-generation cephalosporins ceftaroline and ceftobiprole. Both of these β-lactams bind with high affinity to PBP2A of MRSA and PBP2x from penicillin-resistant *S. pneumoniae*[76–79]. This makes ceftaroline and ceftobiprole the only β-lactams with appreciable activity against MRSA. However, resistance to even these antibiotics eventually appeared (resistance mutants are discussed in more detail in **Chapter 3**)[80–84]. To date, notable resistance to ceftaroline or ceftobiprole has not been seen *S. pneumoniae*.

COMBATTING ANTIBIOTIC RESISTANCE

Revival of the Waksman platform

In order to combat antibiotic resistance and preserve antibiotics for future generations, a combination of robust antibiotic stewardship programs and continued antibiotic discovery and development are needed. For the sake of brevity, this section will focus on antibiotic discovery and development, and the cultural and economic implications of antibiotic stewardship will not be discussed here.

Historically, antibiotic platforms have focused on the development of small-molecule compounds with direct antimicrobial properties, including both the discovery of novel natural products and the derivatization of these compounds[6]. Derivatization of established antibiotics is a faster and financially easier method for antibiotic development and is useful for optimizing potency, efficacy, and desirable pharmacologic properties of a compound. However, these derivatives must fight against already established antibiotic resistance mechanisms. Furthermore, some antibiotic classes such as the glycopeptides and lipopeptides are not as amenable to chemical modification as other classes such as the β-lactams and the quinolones[85], resulting in limited feasibility of this approach for those antibiotic classes. Overall, derivatization alone is not a viable option for combatting resistance.

The Waksman platform and the boom in natural product discovery were crucial in fueling the past “Golden Age” of antibiotics[4], and it is predicted that nature’s reservoir of antimicrobial products is far from exhausted[10]. However, in order to revitalize this once successful antibiotic platform, the issues of sampling limitations and dereplication must be addressed. In other words, current efforts to discover natural products are hampered by the fact that only a fraction of the vast microbial biodiversity is cultivable under laboratory conditions[86], and continued screening of those specimens that are cultivable only yields previously-established antibiotics[4,6,8]. To overcome the latter, a method to rapidly remove known antibiotics from the

pipeline and/or a method to enrich a sample for producers of novel compounds is needed. In 2013, Cox *et al.* developed a platform known as the antibiotic resistance platform (ARP) consisting of an extensive array of known antibiotic resistance genes within the same genetic background under various gene expression and cell permeability conditions[11]. Compounds with known resistance mechanisms can then be swiftly identified in screened extracts and then excluded from further development. Alternatively, an approach developed by Thaker *et al.* enriches for antibiotic producers by wielding the concept that antibiotic producers must also have an established resistance to protect themselves from their own products[87]. The platform initially screens samples for organisms with resistance to a particular antibiotic class (glycopeptides, for example), followed by a secondary genomic screen for genetic fingerprints of that antibiotic's synthetic gene clusters. The data from the secondary screen can then be analyzed genetic variations that may produce novel compounds within that antibiotic class. This approach allowed Thaker *et al.* to discover an unusual glycopeptide, pekiskomycin[87]. Both of these screening platforms may prove effective for more rapid dereplication.

A significant proportion of natural product biodiversity is almost certainly locked away in microorganisms that are not cultivable in the laboratory. The inability to grow under laboratory conditions could stem from any number of reasons: perhaps a lack or an excess of specific nutrients, a lack of interspecies signaling from a symbiotic partner, or that they are simply outcompeted by other less-fastidious organisms under traditional culture conditions. Whatever the case, finding specific culture conditions for these organisms has proven to be an arduous task[86]. As such, efforts have shifted in the past two decades towards culturing loosely segregated microbial communities in a more natural environment with the goal of growth in natural levels of nutrients and allowance for free diffusion of metabolites among species. For example, Kaeberlein *et al.* designed agar-based diffusion chambers which, when incubated on the floor of a marine aquarium, allowed for the isolation of microcolonies of previously unidentified marine bacterial species[88]. A separate effort by Zengler *et al.* encapsulated

individual bacteria from marine and soil samples in gel microdroplets and incubated these segregated communities in growth columns with a continuous flow of low organic medium (or seawater for marine habitats)[89]. Once microcolonies were formed, the microdroplets were sorted by flow cytometry and grown in enriched media to identify novel isolated species. Continued efforts to increase access to these traditionally uncultivable species are an important step towards increasing the rates of natural product discovery.

An additional challenge beyond cultivating new microbial species is coaxing these organisms to relinquish their secondary metabolite repertoire. Genomic studies have uncovered copious “cryptic” or “silent” biosynthetic gene clusters which are predicted to produce novel secondary metabolites but are inactive under standard laboratory conditions[90]. In some cases, nutritional modifications to the growth medium are enough to activate certain clusters[91]. In other cases, genetic manipulations are necessary such as exogenous expression of the gene cluster in a suitable surrogate host and manipulation of gene promoters[92,93] and regulatory genes[91,94]. Intriguingly, a subset of mutations in the *rpoB* gene associated with rifampin resistance have been found to globally awaken silent biosynthetic gene clusters in various actinomycetes[95]. When genetic approaches are taken, however, it is important to consider that successful production of secondary metabolites from these gene clusters may be more complex than simply overexpressing the genes in the cluster. Excessive production of the metabolite may prove to be toxic to the host without simultaneous overexpression of protective resistance factors, or metabolite production may be limited by the availability of required metabolic precursor molecules. Even shuttling such large genetic clusters among hosts is challenging in and of itself[90]. Nevertheless, exploration of these cryptic gene clusters will almost certainly yield novel lead compounds for further antibiotic development.

Alternative antibiotic strategies

Whether an antibiotic is a derivative or is in a novel class of its own, the eventual development of resistance against it is inevitable. That being said, strategies designed to slow the development of resistance and prolong the use of established antibiotics are worthy of consideration. Some potential strategies such as antibiotic adjuvants need not have direct antibiotic effects of their own, while other strategies such as living antibiotics and polypharmacy provide complex antimicrobial effects which may prove difficult for a bacterium to completely circumvent. In either case, resistance to the antibiotic effects may be slowed.

Polypharmacy is potentially the simplest of these strategies to implement, as the main components are antibiotics which have already been established. The concept of polypharmacy is that when a group of antibiotics (preferably from different classes) are formulated together, the ability of the bacteria to evolve resistance against all components of the therapy simultaneously is limited, decreasing the probability of survivors with developed resistance. This strategy has already proven effective for antiviral therapies against viruses such as HIV[96]. The greatest drawback to this strategy is the risk of emergent drug-drug interactions among the antibiotics within the therapy (e.g., antagonistic interactions between bacteriostatic and bactericidal antibiotics[97]) as well as interactions between the antibiotics and other pharmaceuticals the patient may be taking. The latter case is particularly relevant for elderly patients who may already be taking cocktails of other pharmaceuticals for a variety of other ailments[98]. The presence of hypersensitivity in the patient to any of the antibiotics used in the therapy must also be considered[99].

A particularly intriguing antibiotic strategy is the concept of “living antibiotics”, i.e., the utilization of microorganisms to kill pathogenic bacteria. The greatest example of this strategy is phage therapy. Experimentation with using bacteriophage to treat human infections has been around in the United States and Europe since the 1930s, but has only recently regained interest due to the increasing predicament of widespread resistance to small molecule antibiotics[100]. As

such, there has been a considerable accumulation of knowledge on the subject, including research into delivery mechanisms, safety experiments, and combination therapy with traditional antibiotics (reviewed in [101,102]). Of particular interest are the recently documented "compassionate use" cases; one case involved treatment of diabetic toe ulcers caused by a recalcitrant *S. aureus* infection[103], while another particularly striking case involved the successful treatment of a systemic multidrug-resistant *Acinetobacter baumannii* infection[104]. Beyond these anecdotal successes, there was also a promising controlled clinical trial in 2009 for phage therapy to treat chronic otitis caused by antibiotic resistant *Pseudomonas aeruginosa*[105]. As with any antibiotic strategy, there still remains the risk of the evolution of resistance against phage[106]; however, formulations with complementary phage that target different surface receptors may reduce the risk to manageable levels[107].

Another example of a potential living antibiotic is the use of predatory bacteria such as *Bdellovibrio bacteriovorus*. *B. bacteriovorus* is a predator of gram-negative bacterium whose life cycle alternates between an extracellular predatory stage and a lethal growth stage within the prey cell's periplasm[108]. In 2016, a proof of concept demonstrated that injections of *B. bacteriovorus* into zebrafish larvae synergized with the host's immune system to increase survival against a lethal dose of *Shigella*[109]*.* The *Bdellovibrio* persisted in the host for over 24 hours without any pathogenic effect, eventually being cleared by host neutrophils and macrophages. Because they are living organisms, there are some unique considerations that must be taken into account. For example, as an obligate aerobe, there may be certain niches in the body where *Bdellovibrio* will not survive. In addition, efficacy of this treatment is limited to gram-negative infections. Nonetheless, many of the antibiotic resistant species of concern are gram-negative bacteria[7], so this caveat may be of relatively minor concern. There are also other epidemiologic considerations as well such as effects on the host microbiome[110] and the potential of the living antibiotic to spread between hosts. Overall, a considerable amount of research is still needed before the implementation of a living antibiotic.

Unlike the strategies described above, antibiotic adjuvants enhance the activity of antibiotics without any antibiotic effects of their own[111]. β-lactamase inhibitors are the greatest example of successful implementation of an antibiotic adjuvant. These compounds irreversibly bind and inhibit β-lactamases, sparing their partner β-lactam from hydrolytic inactivation by the enzyme. The discovery of clavulanic acid in the 1970's[112] gave rise to a relatively successful clinical campaign of combining various β-lactams with β-lactamase inhibitors (reviewed in [113] and as discussed above). This success has encouraged the exploration of using antibiotic adjuvants with other antibiotic classes. For example, interest in targeting aminoglycoside kinases led to the discovery of a pyrazolopyrimidine scaffold which inhibits the dominant gram-negative aminoglycoside kinase APH(3')-I[114,115]. Besides targeting active antibiotic resistance mechanisms, potential antibiotic adjuvants can also act in a passive manner such as in the case of the opioid receptor agonist loperamide's effects on tetracycline antibiotic uptake. Loperamide decreases the electrical component of the proton motive force, leading to an increase in the pH gradient across the inner membrane which enhances tetracycline antibiotic uptake[116]. Finally, antibiotic adjuvants don't even have to act on the bacteria *per se*, but could instead modulate the host's immune response for increased bacterial clearance. A screen for macrophage enhancers identified streptazolin as a macrophage stimulant which upregulates the NF-κB signaling pathway, allowing for the increased killing of *Streptococcus mutans*[117]. It is worth noting that a compound which stimulates the immune system rather than targeting the bacteria may be less susceptible to the evolution of bacterial resistance.

Each of the strategies discussed above comes with its own advantages and disadvantages. It will likely take a combination of most of them in order to appreciably slow the rise of antibiotic resistance. Indeed, continued efforts in antibiotic development, antibiotic stewardship, and better understanding the evolution and dissemination of resistance mechanisms will be needed to prevent complete regression into a post-antibiotic era.

A case for eukaryotic-like ser/thr protein kinases as antibiotic targets

All known organisms require signaling systems to maintain dynamic order among the complex biochemical processes required for life. One prevalent mode for rapid signal transduction is through reversible protein phosphorylation by kinases[118–121]. Protein kinases utilize the γ-phosphate of ATP as a substrate to phosphorylate their target proteins[122]. Eukaryotic protein kinases share a conserved bi-lobed structure known as the Hanks-type kinase domain[123] which possesses the following conserved motifs (**Figure 1.2)**: the P-loop and AxK motif which coordinate the substrate phosphates, the HRD motif and the activation loop which are important for regulation of kinase activation[124], and the catalytic DFG triad. The orientation of these various motifs are controlled by a pair of hydrophobic amino acid sets known as the catalytic C-spine and the regulatory R-spine; when ATP enters the active site, the adenine rings complete and stabilize the C-spine, and the phosphates lock into place along the R-spine and prime the kinase for catalysis[125]. The kinases activate by autophosphorylation on serines, threonines, or tyrosines in their activation loop which dramatically increases their catalytic activity. The prevailing model was that the unphosphorylated activation loop denies the protein substrate access to the active site as an autoinhibitory mechanism and that phosphorylation of the loop relieves this autoinhibiton. However, while this appears to be the case for some kinases, it is not necessarily true for all kinases[126]. The activation loop of Src kinase, for example, performs an allosteric regulatory function on the dynamics of the kinase's C-lobe[127]. In either case, the kinase is activated upon phosphorylation of the activation loop, allowing the enzyme to phosphorylate its targets on serine, threonine, and tyrosine residues.

Bacterial protein phosphorylation was traditionally thought to be distinct from eukaryotic protein phosphorylation. Rather than phosphorylation on serines, threonines, and tyrosines, phosphorylation occurs on histidine and aspartate residues in a mechanism catalyzed by two-component systems[128]. Two-component systems consist of a transmembrane sensor histidine kinase and its cognate response regulator. When the extracellular sensor detects a stimulus,

the signal is transduced across the cell membrane to the intracellular histidine kinase which consists of an ATP-binding domain and a phosphotransfer domain[129]. The activated kinase binds ATP through the ATP-binding domain and autophosphorylates the phosphotransfer domain on a conserved histidine residue[129]. The phosphoryl group on this histidine is then shuttled onto a conserved aspartate residue in the response regulator, leading to conformational changes in the response regulator which modulates its ability to bind to its target DNA sequences[129]. This modification in DNA binding ultimately leads to changes in gene transcription as an output in response to the external stimulus. Unlike the ser/thr/tyr kinases, histidine kinases are fairly monogamous with their cognate response regulator, usually acting on only one or two with relatively little cross-talk (**Figure 1.3**)[130,131]. For a time, these two-component systems were thought to be the sole source of protein phosphorylation in bacteria. However, in 1991, a ser/thr protein kinase was discovered in the gram-negative bacterium *Myxococcus xanthus*[132]. The kinase, called Pkn1, was able to specifically phosphorylate protein substrates on serine and threonine but not tyrosine residues. This discovery led to the further identification of at least 26 of these ser/thr kinases in *M. xanthus*, most displaying the highly conserved sequence motifs of eukaryotic kinases[133]. It is now apparent that these eukaryotic-like Ser/Thr kinases (eSTKs) are prevalent throughout bacteria and play important roles in bacterial physiology[120,134–138], with some bacteria such as *M. tuberculosis* possessing as many as 11 eSTKs[139]. Unlike their two-component system counterparts which shift a phosphoryl group from their own histidine to the target and thus must “reload” with a new phospohistidine, the eSTKs directly phosphorylate their targets without dephosphorylating themselves (**Figure 1.3**) which allows for exponential amplification of the signal.

Given their important roles in bacterial physiology, bacterial protein kinases have gained considerable interest as potential antibiotic targets. Initial efforts focused on developing inhibitors for the histidine kinases of two-component systems (reviewed in [140]) as they have no known homologs in eukaryotes. Furthermore, some two-component systems are essential (such

as WalRK[141]) while others are important for maintaining antibiotic resistance (such as VraRS in *S. aureus*[142] and VanRS in the enterococci[143]), making them appealing targets. As early as 1993, candidate molecules were identified as inhibitors of systems such as KinA/Spo0F in *E. coli* and *Bacillus subtilis*[144,145], Algr1/Algr2 in *P. aeruginosa*[146], VanRS in *E. faecium*[147], and WalRK in *S. aureus*[148]. Unfortunately, many of the lead chemical scaffolds which demonstrated antibacterial activity either act independently of histidine kinase inhibition (likely through membrane disruption)[149] or possess other pharmacologic liabilities such as poor bioavailability and high protein binding[150]. As such, there has yet to be any histidine kinase inhibitors put forth for clinical trials.

At first glance, inhibition of bacterial eSTKs may seem counterintuitive as the high structural homology between eSTK kinase domains and eukaryotic kinases would imply complications of poor selectivity and off-target effects. However, decades of eukaryotic protein kinase research have revealed mechanisms to achieve relative kinase inhibitor selectivity even in the context of the highly conserved active site[151–158]. For example, certain kinases such as p38 and Abelson tyrosine kinase (Abl) possess the capability of shuffling their catalytic DFG motif ~180° around the axis of its Cα backbone, flipping their sidechains out of the active site ("DFG-out") and back ("DFG-in")[159,160]. This flexibility allows for shifts between DFG-in/kinase active, DFG-in/kinase inactive, and DFG-out/kinase inactive conformations. When in the DFG-out position, a hydrophobic allosteric pocket is exposed where the DFG phenylalanine would rest when in the DFG-in conformation[161]. Type-II kinase inhibitors such as imatinib and sorafenib exploit this pocket, locking the kinase into the DFG-out inactive conformation (**Figure 1.4**)[162,163]. Hari *et al.* determined that the identities of the gatekeeper residue (discussed in more detail below) and the xDFG residue dictate the ability of a kinase to adopt the DFG-out conformation and thus the relative susceptibility to type-II inhibitors[164]. The selectivity of the type-II inhibitors for kinases which can more readily adopt the DFG-out conformation was further established by profiling the selectivity of kinase inhibitors hybridized among type-II inhibitors[165].

On the opposite side of the active site from the DFG motif lays another deep pocket which sits behind the binding site of ATP's adenine rings. The entrance to this pocket (which will be called the "back pocket" here and in **Chapter 2**) is guarded by a residue on the roof of the active site known as the gatekeeper residue (**Figure 1.2**)[166,167]. The identity of the gatekeeper residue dictates access to the back pocket, with larger residues such as methionine and isoleucine blocking entry[167]. This concept is exemplified by the inhibitor lapatinib's ability to inhibit epidermal growth factor receptor kinase (EGFR) which sports a small threonine gatekeeper (**Figure 1.5**)[168]. Therefore, the gatekeeper residue can be used as a guide to design inhibitors which are selective for kinases with small gatekeepers.

Additional selectivity can be gained by exploiting allosteric regions outside of the active site, as these are less conserved among kinases. For example, a pyrazolobenzothiazine compound inhibits focal adhesion kinase 3 (FAK3) by burrowing into an allosteric pocket beneath the αC helix within the kinase's C-lobe [169], and a compound known as PD318088 inhibits MAP kinase kinase 1 (MEK1) and MEK2 by binding to an allosteric pocket formed by the αC helix and β-sheets of the kinase's N-lobe[170]. Even interfering with accessory domains outside of the kinase domain such as pleckstrin homology domains[171] can indirectly inhibit kinase activity while remaining selective for kinases which possess such domains. Taken together, these distinguishing features demonstrate that relative selectivity can be achieved among eukaryotic kinases; therefore, it should also be possible to target bacterial eSTKs with inhibitors that can distinguish between eSTKs and eukaryotic kinases.

The appeal for targeting bacterial eSTKs as an antibiotic strategy stems from the clinical successes of eukaryotic kinase inhibitors[172,173]. As of 2015, there are 27 FDA-approved protein kinase inhibitors in clinical use as anticancer therapies and immunomodulatory drugs[173,174]. It has taken the accumulation of an enormous wealth of knowledge and resources to develop and implement so many successful drugs. There are a wide variety of kinase inhibitor libraries available for screening campaigns from both commercial vendors and through collaborations

with pharmaceutical companies such as GlaxoSmithKline[175] and Pfizer[176]. Furthermore, there is no lack of tools available for probing kinase/inhibitor binding[177], kinase profiling[178], basic kinase biology[179], and computational techniques[180]. Overall, these resources and knowledge bases can be repurposed with relative ease to create a robust platform to study bacterial eSTK inhibitors for antibiotic development.

With regards to potential targets, a subfamily of eSTK known as the Penicillin-binding protein and Ser/Thr kinase-associated (PASTA) kinases has received particular attention due to their roles in maintaining β-lactam resistance. The focus of this dissertation is on the investigation of the PASTA kinases as pharmacologic targets.

PASTA KINASES AS TARGETS FOR β-LACTAM ADJUVANTS

PASTA kinase structure and function

The PASTA kinases are a subfamily of eSTK found in the phyla *Firmicutes* and *Actinobacteria*[181] and are generally found in single copy (though with some exceptions such as *Corynebacterium glutamicum*[182]). They have been found to be essential in the mycobacteria[183,184] but are dispensable in the other phyla tested to date. The PASTA kinases consist of an intracellular N-terminal Hanks-type Ser/Thr kinase domain connected by a single transmembrane helix to a set of 1-5 C-terminal tandem PASTA repeats with some species possessing an additional C-terminal Ig-like domain (**Figure 1.6**)[185,186]. While the intracellular kinase domain shows relatively high sequence identity among species[181], the extracellular PASTA domains suffer low sequence conservation both among species and among PASTA domains within the same protein[181,185]. Nevertheless, the kinase domain possesses the requisite motifs and fold of a Hanks-type kinase, and the PASTA domains all share a highly-conserved fold regardless of their low sequence conservation.

The PASTA domains of the PASTA kinases share the same fold as those on high-molecular-weight PBPs such as PBP2x of *S. pneumoniae*[187–189]. However, while the PASTA pair on PBP2x lays in a compact sandwich[187], those of the PASTA kinases remain in an extended conformation[188–190]. This linearization is likely the result of an extra pair of short beta strands on the N-terminus of each of the kinases' individual PASTA domains which act as bracers and prevent the extracellular structure from folding over on itself[188,190]. This arrangement of the extracellular domain led to the proposal that the PASTA kinases may behave like eukaryotic receptor tyrosine kinases[191], the extracellular domain dimerizing on a bound ligand and sending a signal across the membrane to allow for dimerization and activation of the kinase domains[190].

Since PASTA domains can be found on both the PASTA kinases and on PBPs, the ligand was proposed to be muropeptides or polymerized peptidoglycan. This proved to be the case for the *B. subtilis* PASTA kinase PrkC when it was discovered that PrkC-dependent awakening of dormant spores required the presence of muropeptides, minimally the disaccharide-tripeptide[192]. Furthermore, the identity of the third peptide in the ligand proved to be important for recognition by the PrkC PASTA domains[192,193]; the presence of a meso-DAP at position 3 of the muropeptide was recognized by Arg500 on PASTA domain 3 (as numbered in **Figure 1.6**) while the presence of L-lysine at this position prevented recognition. Strikingly, when the native PrkC was replaced with the PASTA kinase Stk1 from *S. aureus* (a bacteria which uses L-lysine over meso-DAP), spores were able to respond to both L-lysine and meso-DAP muropeptides[194], suggesting that this discrimination mechanism is not reciprocated. In *M. tuberculosis*, the PASTA kinase PknB recognizes the minimum unit of MurNAc-tetrapeptide with meso-DAP in position 3 and amidated D-isoglutamate in position 2[195]. Intriguingly, the extracellular domain of *S. aureus* Stk1 was demonstrated to recognize lipid II rather than free muropeptides, leading to stimulation of kinase activity[196]. Finally, *S. pneumoniae* StkP was found to recognize β-lactams as well as synthetic peptidoglycan[197]. In an overwhelming majority of cases, cell wall muropeptides appear to be the natural ligand of the PASTA domains.

Once a signal is detected, a signal needs to be transduced across the membrane in order for the kinase domain to respond. Dimerization experiments performed with a λ phage cI fusion protein system[198] revealed that both the extracellular domain and transmembrane helix of the *B. subtilis* PASTA kinase PrkC are capable of dimerization in the absence of a ligand[199]. This has also been found to be the case for the PASTA kinase StkP from *S. pneumoniae*[200]. However, *S. aureus* Stk1 is an example where PASTA dimerization has failed to be seen, even in the presence of excess muropeptides[189] implying that not all PASTA kinases function through an extracellular dimerization mechanism. Another argument against an extracellular activation mechanism was put forth by Mir *et al.* in that the highly flexible juxtamembrane linker which connects the intracellular kinase domain to the transmembrane helix is too flexible to allow for a signal to be transduced from the dimerized PASTA domains outside the cell to the intracellular kinase domain[195]. They propose that the PASTA domains act like a tether to guide localization instead of as a signal transduction mechanism. Indeed, the intact PASTA domains are required for localization of *M. tuberculosis* PknB[195], *S. aureus* Stk1[196], and *S. pneumoniae* StkP[201,202] to the cell poles and septa. In the case of *S. pneumoniae*, StkP's PASTA domains are also important for the localization of PBP2x to the septa[203], and PASTA domain 4 specifically recruits the non-autolytic peptidoglycan hydrolase LytB[202]. Intriguingly, PASTA domains 1-3 were found to be interchangeable and act like a molecular tape measure to regulate the thickness of septal peptidoglycan[202]. In the end, it appears that the PASTA kinases in general sense muropeptides and peptidoglycan through their PASTA domains, though the functions of the PASTA domains may diverge among species.

Much of what is known about the mechanics of the PASTA kinases' intracellular domains stems from structural studies of *M. tuberculosis* PknB. As with their eukaryotic counterparts, the kinase domains are activated by phosphorylation of serines and threonines in the activation loop[204–208]. This means that two kinase domains need to arrange in a fashion where the activation loops are inserted into the active sites for productive phosphorylation.

Various crystal structures of the PknB kinase domain reveal that the molecules can dimerize in a “back-to-back” conformation with their N-lobes[206,209,210] or in an asymmetric “front-to-front” conformation via interdigitation of the αG helices in their C-lobes[204] (**Figure 1.7**). It is interesting to note that in the front-to-front model, the asymmetric orientation of the monomers positions the activation loop of one monomer in the active site of the other monomer[204]. Lombana *et al.* demonstrate that the back-to-back conformation is important for kinase activity both *in vitro* and in the bacteria by mutating the N-lobe dimer interface[211]; on the other hand, Meiczkowski *et al.* demonstrate that the front-to-front conformation is also important for activation by disrupting the complementary hydrophobic amino acids on the αG helix[204]. These data support an elegant model of activation where an initial pair of inactive kinases are brought together (either by dimerization of the extracellular domains or by simple localization and proximity) and dimerize back-to-back through their N-lobes, stabilizing an allosteric active conformation regardless of phosphorylation status[211,212]. The activated back-to-back dimer can then activate neighboring kinase domains by trans-phosphorylation of their activation loops in the front-to-front orientation. This mechanism ultimately leads to an amplified response of activated kinase domains and the rapid phosphorylation of kinase substrates.

Over the years, the PASTA kinases have been found to play important roles in various bacterial physiologic processes, including cell wall homeostasis[213–217], germination[192,218], metabolism[219,220], biofilm formation[221], and virulence[184,222–230]. While there is some overlap of the roles PASTA kinases play in various species, there has most likely been some evolutionary rewiring of PASTA kinase signaling circuitry to better suit each species’ particular needs. For example, *B. subtilis* utilizes PrkC to regulate sporulation[192], a physiologic process which is unused by other organisms such as *S. aureus* and *L. monocytogenes*. The PASTA kinase PrkA is crucial for the intracellular survival of *L. monocytogenes*, as demonstrated by an exquisite decrease in bacterial burden of the Δ*prkA* mutant *in vivo*[222]. *Staphylococcus epidermidis*, a pathogen well-renowned for the formation of biofilms, uses its PASTA kinase Stk1 to regulate

biofilm formation[221] as do *B. subtilis*[199] and *B. anthracis*[231]. Finally, StkP appears to play a much more prominent role in regulating cell division of *S. pneumoniae* than do the PASTA kinases from other bacteria[201,202,215], perhaps necessitated to maintain the complex ovococcoid shape.

Interestingly, many pathogenic bacteria utilize their respective PASTA kinases in the regulation of virulence. *L. monocytogenes*[222], *E. faecalis*[224], *S. epidermidis*[221], and *S. pyogenes*[232] all require their respective PASTA kinases for optimal virulence, though the kinase substrates which mediate this response have yet to be determined. The *S. aureus* PASTA kinase Stk1 is one of the most well-studied kinases with respect to its role in virulence and its direct impact on expression of validated virulence factors. Despite this, strain differences as well as multiple infection models have led to conflicting data such that the role of Stk1 in *S. aureus* virulence is unclear. Deletion of *stk1* in the SH1000 strain led to significant attenuation in a murine model of pyelonephritis, with the Δ*stk1* mutant demonstrating ~100-fold lower bacterial burdens in the kidney[226]. In contrast, deletion of *stk1* in the methicillin-resistant *S. aureus* (MRSA) USA300 or methicillin-sensitive (MSSA) Newman strains resulted in no loss of virulence in skin and soft tissue infection (SSTI) and bacteremia models respectively and, in fact, may have resulted in increased virulence in the SSTI model[223,229]. Expression of virulence factors in *S. aureus* is controlled through activity of the accessory gene regulator (*agr*) system[233,234]. The Δ*stk1* mutant in the USA300 MRSA strain demonstrated enhanced *agr* activity, evident by elevated levels of several downstream virulence determinants including the virulence transcriptional regulator SarA[223]. Additionally, Stk1 was found to positively regulate activity of the alternate sigma factor SigB[223] which itself is inversely correlated with levels of SarA[235]. SarA itself may be further regulated directly by Stk1 *via* phosphorylation on threonine[227] and/or cysteine[228] residues. Threonine phosphorylation results in a reduced affinity of phosphorylated SarA for various gene promoters[227]. Failure to phosphorylate the conserved redox-sensing cysteine residues was found to increase α-hemolysin expression and ultimately virulence in the MSSA strain Newman[228]. Taken together, these studies highlight a role for Stk1

in negatively regulating virulence factor expression in multiple strains of *S. aureus*. It remains to be determined if the contradictory virulence phenotypes of Δ*stk1* mutants in different studies is due to genuine differences in Stk1 function in different strains, or instead is due to differences in the infection model used in each study.

Importantly, genetic deletion of homologs in the *Firmicutes* has been linked to increased susceptibility to β-lactam antibiotics in every genus tested to date. The PASTA kinases have been shown to be important for β-lactam resistance in *S. aureus*[213,223,236], *L. monocytogenes*[222,237], the streptococci[232,238], and the enterococci[224,239–241] with variations in the resistance profiles between species and strains. For example, the PASTA kinase phenotype in the staphylococci is more pronounced against the penicillinase-stable penams[223] while *L. monocytogenes* and the enterococci are sensitized 10- to 100-fold to the cephalosporins[222,224,237]. In the latter case, the bias towards the cephalosporins might be due to the intrinsic resistance of the enterococci and *L. monocytogenes* towards this subclass[242–244]. The mechanics behind these variations among species have yet to be determined. Regardless, the essentiality of the PASTA kinases in the mycobacteria and their ability to modulate β-lactam resistance in the *Firmicutes* has led to interest in the PASTA kinases as potential direct antibiotic targets in the mycobacteria and β-lactam adjuvants in the *Firmicutes*.

Targeting the PASTA kinases: a brief history

Initial efforts to pharmacologically target the PASTA kinases were focused on targeting PknB in *M. tuberculosis* due to its essentiality. The indolocarbazoles staurosporine, K252a, and K252b were identified in a small 18-compound screen against purified PknB kinase domain *in vitro* as compounds which inhibited autophosphorylation and phosphorylation of the PknB substrate GarA (**Figure 1.8**)[183]. Additionally, an *in silico* screen for compounds which docked into the PknB active site identified the type II topoisomerase inhibitor mitoxantrone which was then further validated as a PknB inhibitor *in vitro* (**Figure 1.8**)[210]. Although these early hits had

biochemical activity against PknB and revealed valuable insights into PASTA kinase biochemistry, they had little activity against *M. tuberculosis* with the most promising MIC being 20 µM. Later efforts incorporated comprehensive medicinal chemistry campaigns to identify effective PknB inhibitors with improved microbiologic activity [245,246]. After screening ~54,000 compounds, Lougheed *et al.* identified 12 lead compounds with incremental increases in antibacterial activity with the lowest MICs being 16 µM and 5 µM in broth and an *ex vivo* macrophage model of infection, respectively [245]. Chapman *et al.* pushed these limits even further with the identification of an aminopyrimidine pharmacophore, yielding a compound with a biochemical IC_{50} of 0.176 µM and an MIC of 8 µM (**Figure 1.8**)[246].

Despite their lack of essentiality, the critical role of the non-essential PASTA kinases in β-lactam resistance and virulence has led to interest in identification of PASTA kinase inhibitors as either combination therapies to augment β-lactam activity or as antivirulence therapies. The highly non-selective indolocarbazole staurosporine inhibits PASTA kinases from *L. monocytogenes, B. subtilis, S. epidermidis* and *E. faecalis* [192,221,237,239] while activity against *S. aureus* Stk1 is controversial [237,247]. In all cases, staurosporine was identified as a singled out compound rather than being identified in a broad inhibitor library screen. In some of these cases staurosporine has been demonstrated to potentiate β-lactam activity as has been observed with PASTA kinase mutant bacteria. Based on these preliminary studies, combination activity with other structurally distinct scaffolds has been achieved in various MRSA strains and in *L. monocytogenes* **(Figure 1.8)** [237,247,248]. Both the sulfonamide and triarylimidazole scaffolds were identified as Stk1 inhibitors by initial screens against live MRSA in the presence of a β-lactam antibiotic followed by validation of Stk1 in an *in vitro* phosphorylation assay[247,248]. The strategy of screening against live bacteria is reminiscent of the old Waksman platform and faces head-on the challenge of finding scaffolds that can access the bacterial cytosol. In contrast, the initial approaches to identify PknB inhibitors focused on *in silico* or biochemical approaches[183,210].

While these strategies would undoubtedly reveal more inhibitor scaffolds than a microbiological assay on a larger scale, they are plagued with dead-end hits that fail to access their target.

In this doctoral dissertation, we utilize a microbiologic-biochemical-*in silico* approach to identify and characterize inhibitors of the PASTA kinases Stk1 and PrkA from *S. aureus* and *L. monocytogenes*, respectively. We screen kinase inhibitor libraries against live bacteria to identify lead compounds which potentiate β-lactam activity followed by target validation using both genetic and biochemical means. In the final stages, we utilize *in silico* modeling to characterize structure-activity relationships (SAR) and to guide modifications to our lead scaffolds which influence their biochemical and microbiologic activities. This workflow utilizes the strengths of each approach while attempting to minimize false leads for future pharmacologic development.

Chapter 2 details the discovery of the imidazopyridine aminofurazan scaffold as an inhibitor of *L. monocytogenes* PrkA. We explore the ability of this scaffold to sensitize the bacteria to β-lactam antibiotics and identify key structural features on the scaffold that modulate activity both biochemical and microbiologic activity. Importantly, we present data which support the hypothesis that the imidazopyridine aminofurazan scaffold exploits the back pocket of the active site, one of the distinct features that can dictate inhibitor selectivity.

In Chapter 3, we identify the pyrazolopyridazine scaffold as an *S. aureus* Stk1 inhibitor. We demonstrate that this scaffold is effective against a variety of *S. aureus* lineages and can exquisitely sensitize a ceftaroline-resistant isolate to ceftaroline. Finally, we discover that a positively-charged piperazine side chain is critical for both biochemical and microbiologic activity.

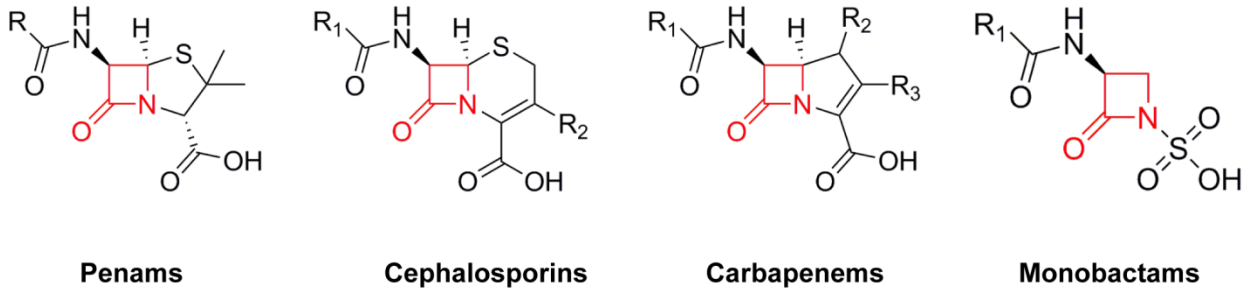

Figure 1.1: β-lactam antibiotic structures

The β-lactam antibiotics can be broken down into 4 subfamilies. The namesake β-lactam ring is displayed in red.

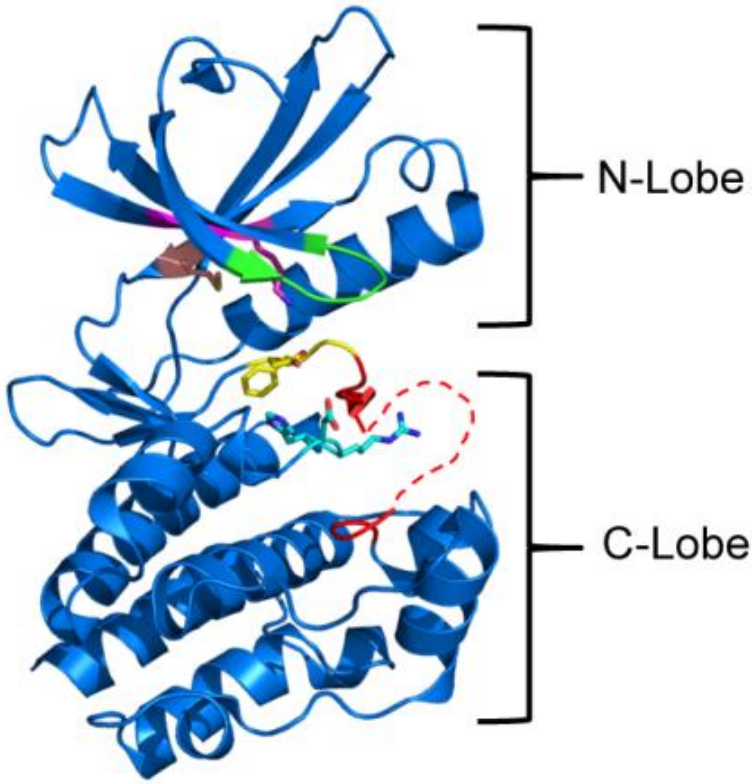

Figure 1.2: Anatomy of a Hanks-type ser/thr kinase

The Hanks-type ser/thr kinases share a characteristic bi-lobed structure with an N-lobe comprised predominantly of β-sheets and a C-lobe comprised of α-helices. Features of the active site include the P-loop (green), AxK motif (magenta sticks), catalytic DFG triad (yellow sticks), activation loop (red dashed line), HRD motif (cyan sticks), and gatekeeper residue (peach sticks). PDB ID: 1O6Y.

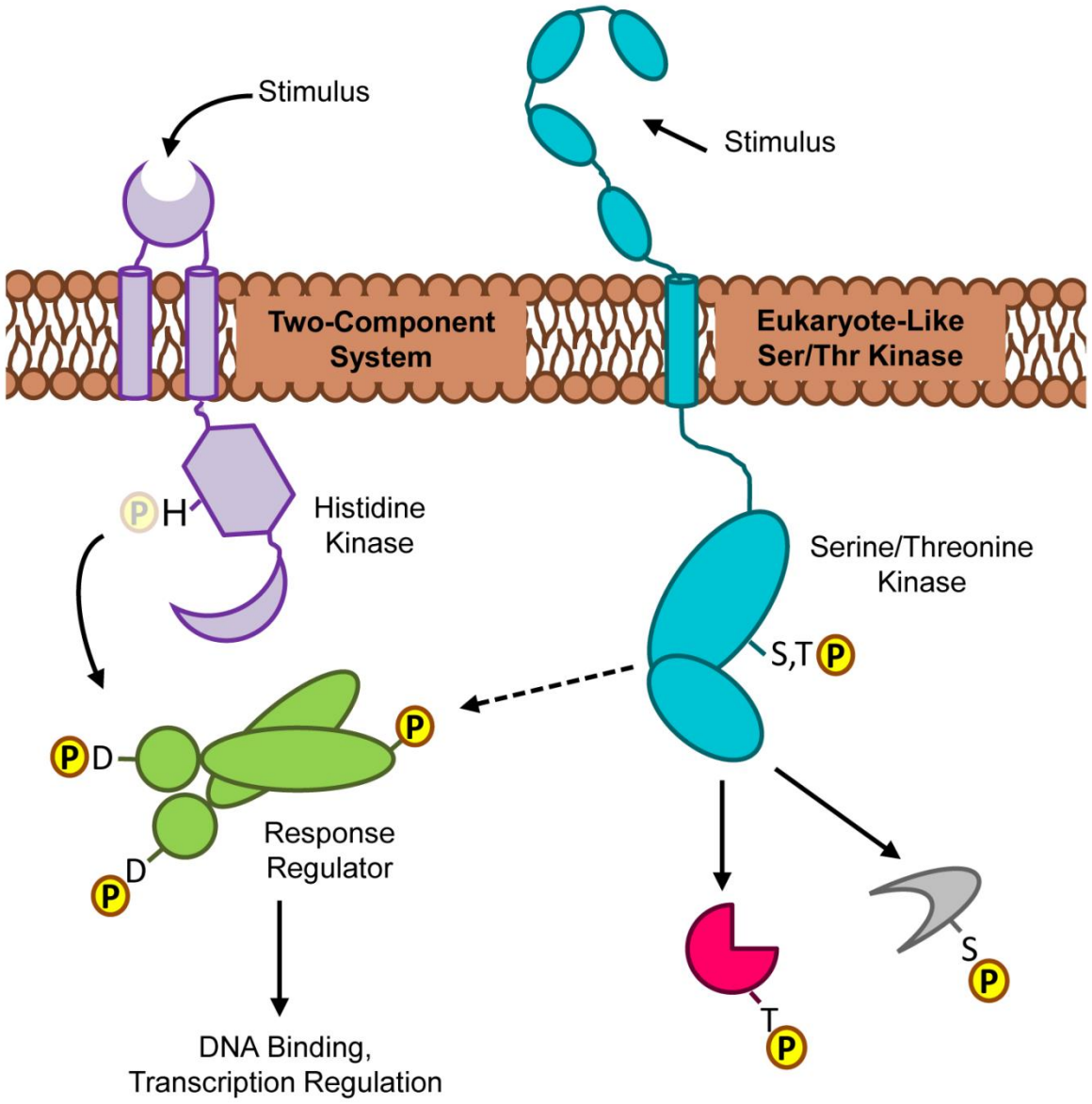

Fibure 1.3: Prokaryotic protein phosphorylation in signal transduction

Bacteria utilize both two-component systems (TCS, *Left)* and eukaryotic-like ser/thr kinases (eSTKs, *Right*) in signal transduction. TCSs autophosphorylate on histidine residues upon stimulation, then transfer the phosphoryl group from the histidine to aspartate residues in the cognate response regulator. eSTKs autophosphorylate on serine and threonine residues, then phosphorylate their substrates on serines and threonines as well. eSTKs are also able to cross-talk with certain response regulators. Note that not all eSTKs are membrane-associated.

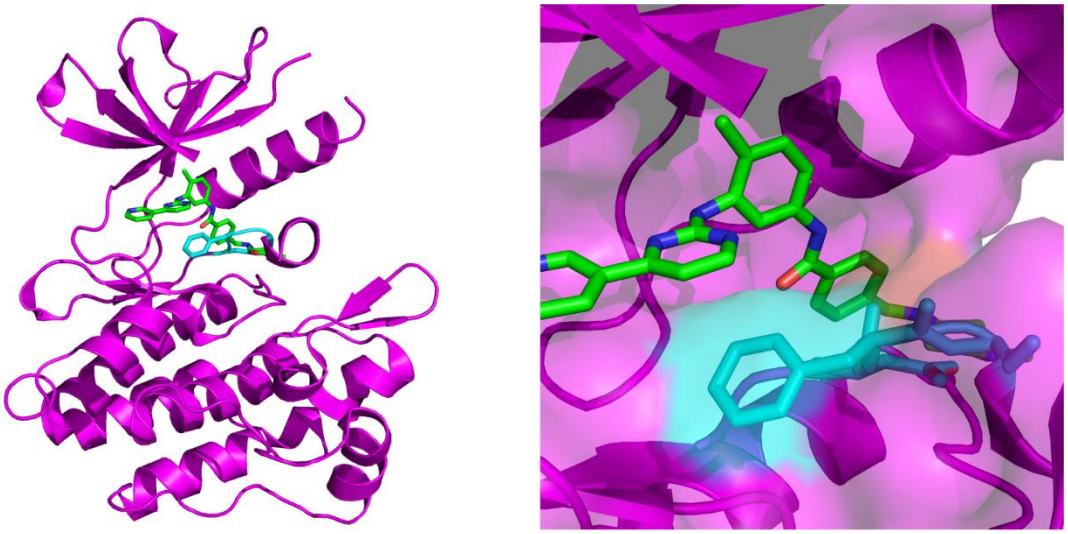

Figure 1.4: Imatinib stabilizes the DFG-out conformation of Abl kinase

Imatinib (green sticks) exploits an allosteric pocket behind the catalytic DFG triad (cyan sticks) which is accessible only when the triad is rolled forward into the “DFG-out” conformation. This locks Abl kinase (magenta cartoon) into an inactive conformation. PDB ID: 2HYY

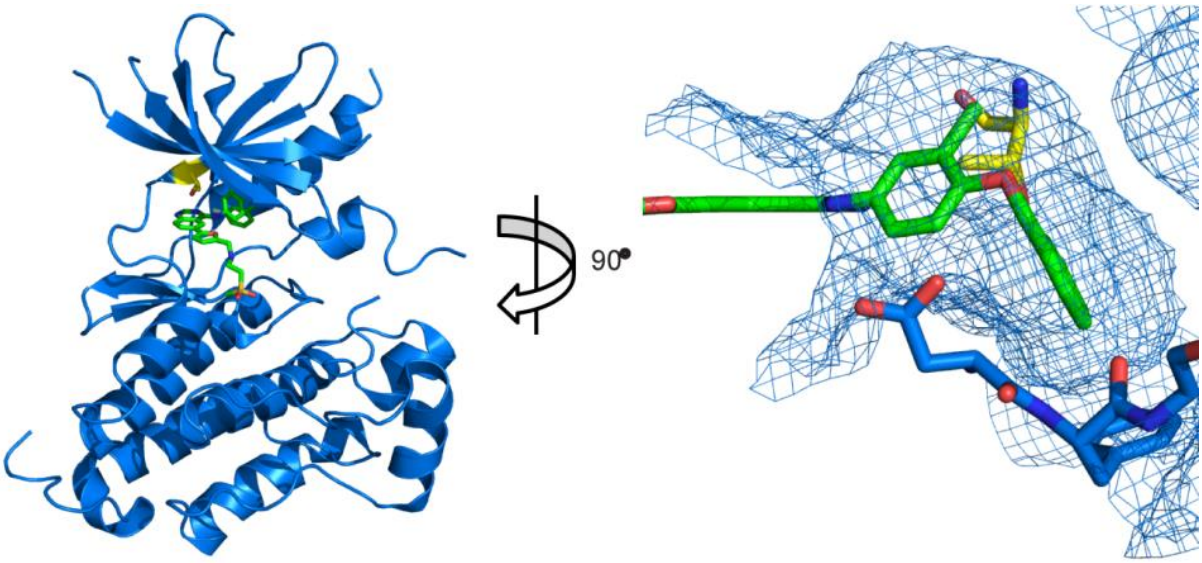

Figure 1.5: Lapatinib accesses the back pocket of EGFR kinase

The relatively small gatekeeper residue of EFGR kinase (yellow sticks) allows entrance of lapatinib (green sticks) into the back pocket behind the nucleotide binding cleft. EFGR's catalytic DFG triad is displayed in marine sticks, and the depth of the back pocket is displayed in marine mesh. PDB ID: 1XKK

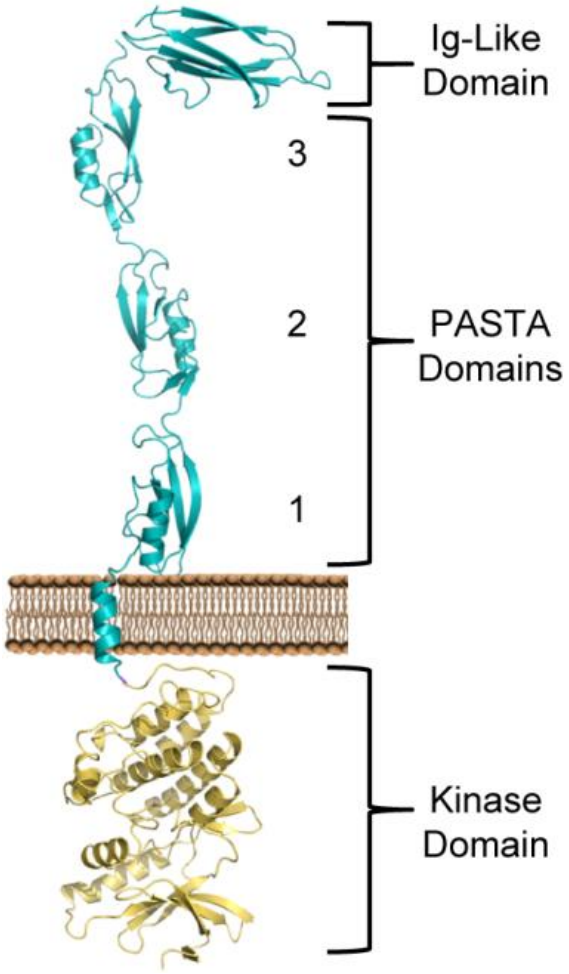

Figure 1.6: Structural features of the PASTA kinases

The PASTA kinases consist of an intracellular Hanks-type ser/thr kinase domain (shown in gold) attached by a single transmembrane helix to a set of 1-5 extracellular PASTA domains (teal). Some PASTA kinases also possess an extra C-terminal Ig-like domain. Note the PASTA domain numbering scheme which is used throughout this dissertation. Model is a combination of the following PDB IDs: 4EQM, 3PY9

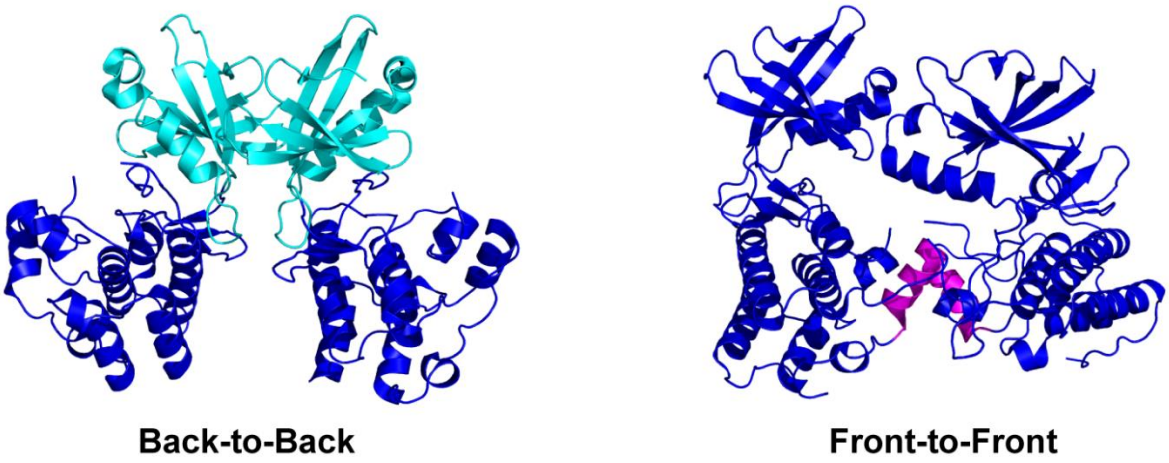

Figure 1.7: PknB kinase domain forms two distinct dimers

The PknB kinase domain is capable of forming both a symmetric back-to-back dimer (*Left*, PDB ID: 2FUM) and an asymmetric front-to-front dimer (*Right*, PDB ID: 3F69). The back-to-back dimer is stabilized through interactions in the N-lobe (cyan), while the front-to-front dimer is stabilized by interdigitation of the αG helix (magenta).

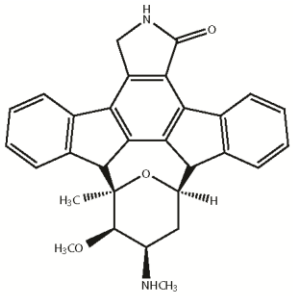

Staurosporine
Targets: PknB, PrkA, IreK, Stk1(?)
IC_{50}: 0.6 µM
MIC: 25 µM < MIC < 50 µM
Family: Indolocarbazole

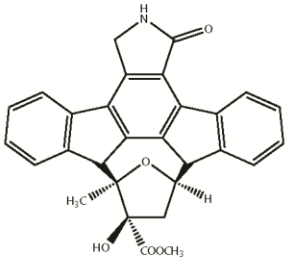

K252a
Targets: PknB
IC_{50}: 0.096 µM
MIC: 20 µM
Family: Indolocarbazole

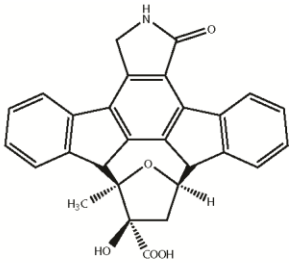

K252b
Targets: PknB
IC_{50}: 0.106 µM
MIC: > 40 µM
Family: Indolocarbazole

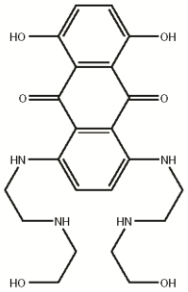

Mitoxantrone
Targets: PknB
IC_{50}: 0.8 µM
MIC: 400 µM
Family: anthracenedione

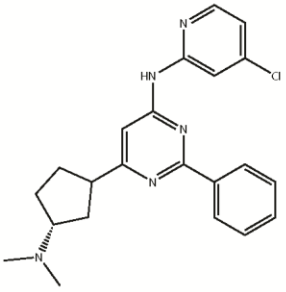

Aminopyrimidine 16c
Targets: PknB
IC_{50}: 0.176 µM
MIC: 8 µM
Family: Aminopyrimidine

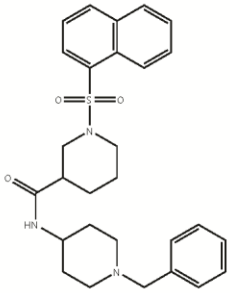

ST085384
Targets: Stk1
Family: Sulfonamide

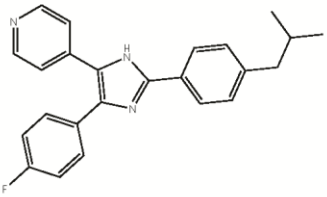

Triarylimidazole 12
Targets: Stk1
Family: Triarylimidazole

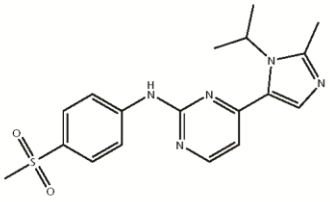

AZD5438
Targets: PrkA
Family: Imidazole sulfone

Figure 1.8: Previously-established PASTA kinase inhibitors

Targets include *M. tuberculosis* PknB, *E. faecalis* IreK, *L. monocytogenes* PrkA, and *S. aureus* Stk1. For antitubercular compounds, MICs and IC_{50}s are displayed where available.

Table 1.1: Antibiotic resistance mechanisms (adapted from Morar *et al*[24])

Antibiotic Class	Mechanism of Action	Resistance Mechanisms
β-lactams	Cell wall inhibition	Hydrolysis Efflux Altered target
Glycopeptides	Cell wall inhibition	Altered target
Lipopeptides	Membrane disruption	Altered target
Cationic peptides	Membrane disruption	Altered target Efflux
Aminoglycosides	Protein translation inhibition	Phosphorylation Acetylation Nucleotidylation Efflux Altered target
Macrolides	Protein translation inhibition	Hydrolysis Glycosylation Phosphorylation Efflux Altered target
Tetracyclines	Protein translation inhibition	Monooxygenation Efflux Altered target
Lincosamides	Protein translation inhibition	Nucleotidylation Efflux Altered target
Streptogramins	Protein translation inhibition	C-O lyase Acetylation Efflux Altered target
Oxazolidinones	Protein translation inhibition	Efflux Altered target
Phenicols	Protein translation inhibition	acetylation Efflux Altered target
Quinolones	DNA replication inhibition	acetylation Efflux Altered target
Sulfonamides	C1 metabolism disruption	Efflux Altered target
Rifamycins	Transcription inhibition	ADP-ribosylation Efflux Altered target

Chapter 2: A screen for kinase inhibitors identifies antimicrobial imidazopyridine aminofurazans as specific inhibitors of the *Listeria monocytogenes* PASTA kinase PrkA

Authors and their contributions

Adam J. Schaenzer: Planned, designed, and conducted all experiments unless otherwise noted. Organized data and wrote this manuscript.

Nathan Wlodarchak: Planned, designed, and conducted IC_{50} experiments.

David H. Drewry: Aided in the selection and acquisition of aminofurazan derivatives.

William J. Zuercher: Aided in the selection and acquisition of aminofurazan derivatives.

Warren E. Rose: Contributed intellectually to the design of the experiments.

Rob Striker: Supervised all research and contributed intellectually to the design of experiments.

John-Demian Sauer: Supervised all research and contributed intellectually to the design of experiments.

This chapter was published in the Journal of Biological Chemistry on October 2017:

Schaenzer AJ, Wlodarchak N, Drewry DH, Zuercher WJ, Rose WE, Striker R, Sauer JD. 2017. A screen for kinase inhibitors identifies antimicrobial imidazopyridine aminofurazans as specific inhibitors of the *Listeria monocytogenes* PASTA kinase PrkA. J Biol Chem. PMID: 28821610.

ABSTRACT

Bacterial signaling systems such as protein kinases and quorum sensing have become increasingly attractive targets for the development of novel antimicrobial agents in a time of rising antibiotic resistance. The family of bacterial Penicillin-binding-protein And Serine/Threonine kinase-Associated (PASTA) kinases is of particular interest due to the role of these kinases in regulating resistance to β-lactam antibiotics. As such, small-molecule kinase inhibitors that target PASTA kinases may prove beneficial as treatments adjunctive to β-lactam therapy. Despite this interest, only limited progress has been made in identifying functional inhibitors of the PASTA kinases that have both activity against the intact microbe and high kinase specificity. Here, we report the results of a small-molecule screen that identified GSK690693, an imidazopyridine aminofurazan-type kinase inhibitor that increases the sensitivity of the intracellular pathogen *Listeria monocytogenes* to various β-lactams by inhibiting the PASTA kinase PrkA. GSK690693 potently inhibited PrkA kinase activity biochemically and exhibited significant selectivity for PrkA relative to the *Staphylococcus aureus* PASTA kinase Stk1. Furthermore, other imidazopyridine aminofurazans could effectively inhibit PrkA and potentiate β-lactam antibiotic activity to varying degrees. The presence of the 2-methyl-3-butyn-2-ol (alkynol) moiety was important for both biochemical and antimicrobial activity. Finally, mutagenesis studies demonstrated residues in the back pocket of the active site are important for GSK690693 selectivity. These data suggest that targeted screens can successfully identify PASTA kinase inhibitors with both biochemical and antimicrobial specificity. Moreover, the imidazopyridine aminofurazans represent a family of PASTA kinase inhibitors that have the potential to be optimized for selective PASTA kinase inhibition.

INTRODUCTION

Antibiotics, in particular the β-lactams, are considered one of the greatest medical advances of the 20th century since their discovery and widespread use in the 1940's[6]. However, due to the misuse of these life-saving drugs, antibiotic-resistant strains of bacteria such as carbapenem-resistant Enterobacteriaceae (CRE), vancomycin-resistant *Enterococcus* (VRE), and methicillin-resistant *Staphylococcus aureus* (MRSA) are emerging at an alarming rate[7,20]. The rapid evolution of resistance to available antibiotics currently outpaces the rate of development of new, effective treatments and highlights the need for the development of truly novel antimicrobial strategies[8,15]. One new strategy is the pursuit of novel compounds that target microbial signaling cascades which are relatively overlooked by traditional methods of antibiotic development. Reversible protein phosphorylation by bacterial kinases is one such process that has been garnering attention within the past decade as a potential target for truly novel antibiotics[249,250].

Prokaryotic protein phosphorylation was originally thought to occur predominantly on histidine and aspartate residues phosphorylated by two-component systems (TCS) in a fashion distinct from eukaryotic kinases[128,129]. However, since the discovery of *pkn1*, a bacterial serine/threonine kinase with high structural homology to eukaryotic protein kinases[132], genomic studies have shown eukaryotic-like serine/threonine kinases (eSTKs) to be near ubiquitous in bacteria[135]. Specifically, many important Gram-positive pathogens have transmembrane eSTKs known as Penicillin-binding-protein And Ser/Thr kinase-Associated (PASTA) kinases[185]. In a variety of different pathogens, PASTA kinases have been found to regulate cell wall homeostasis[213–217], germination[192,218], metabolism[219,220], biofilm formation[221], and virulence[184,222–230]. The PASTA kinase PknB is essential in *Mycobacterium tuberculosis*[183,184], while genetic deletion of homologs in other species has been linked to increased susceptibility to β-lactam antibiotics[213,223,224,237]. These phenotypes have led to interest in PASTA kinases as potential antibiotic targets in pathogens ranging from *M. tuberculosis* and *S. aureus* to *Listeria*

monocytogenes. As a proof of principle, we previously demonstrated that pharmacologic inhibition of the PASTA kinase PrkA by the nonspecific kinase inhibitor staurosporine increases the susceptibility of the intracellular pathogen *L. monocytogenes* to β-lactams in broth culture[237]; however, staurosporine's high promiscuity amongst eukaryotic kinases makes it remarkably toxic and undermines its usefulness as a candidate for therapeutic development[251]. Staurosporine's hallmark toxicity highlights the necessity for kinase inhibitors that are selective for a limited number of targets.

Extensive efforts have been put forth to probe the biochemistry of eukaryotic kinases and identify structural features that can be exploited by selective kinase inhibitors for the treatment of a variety of human diseases, most notably cancer[157]. Such a wealth of established knowledge can be harnessed to probe bacterial kinase biochemistry and engineer inhibitors that act as selective antibiotics. Furthermore, the abundance of available small molecule kinase inhibitor libraries can be mined for bacterial kinase-selective scaffolds. Here, we report that GSK690693, an imidazopyridine aminofurazan (IPA) identified in a small molecule kinase inhibitor library, sensitizes *L. monocytogenes* to various β-lactams. We show that other members of the IPA family inhibit PrkA biochemically and sensitize *L. monocytogenes* to β-lactams to varying degrees. Finally, we demonstrate selectivity for the *L. monocytogenes* PASTA kinase both at the biochemical and microbiological level as compared to the *S. aureus* PASTA kinase Stk1 on an amino acid level. Taken together, our data validate the potential to exploit PASTA kinases as druggable targets and establish GSK690693 and other IPAs as both lead compounds and valuable tools to investigate PASTA kinase biology.

RESULTS

GSK690693 sensitizes *Listeria* to β-lactam antibiotics

In a wide variety of important gram-positive pathogens, PASTA kinases are essential for resistance to β-lactam antibiotics[213,224,237]. We have previously demonstrated that either genetic

deletion or pharmacologic inhibition of the PASTA kinase PrkA with staurosporine sensitizes *L. monocytogenes* to β-lactams[237]. To identify specific (and therefore potentially less toxic) inhibitors of PrkA, we screened 625 small molecule kinase inhibitors from the GlaxoSmithKline Published Kinase Inhibitor Set (PKIS)[175,252] and Selleck kinase inhibitor libraries against wild-type *L. monocytogenes* strain 10403s in the presence of a sublethal dose of the β-lactam ceftriaxone (**Figure 2.1A**). Sixteen compounds potentiated inhibition of *L. monocytogenes* growth by ceftriaxone at three standard deviations or more above the mean including the positive control staurosporine (**Figure 2.1A, blue dot**). Of these, nine compounds failed to show a dose-response, and an additional three showed β-lactam independence in secondary screens. The four remaining validated compounds were LY2228820, GSK690693, and our previously-published compounds staurosporine and AZD5438 (**Supplemental Figure S2.1**).We selected GSK690693 (**Figure 2.1A, green dot; Figure 2.1B**) for further analysis due to the presence of structural congeners in the screen (**Figure 2.1A, red dots**).

Based on our previous investigation of staurosporine, we hypothesized that GSK690693 would also sensitize *L. monocytogenes* to other β-lactam antibiotics. To test this hypothesis, we determined the MIC values of various antibiotics against wild-type *L. monocytogenes* in the presence and absence of 20 μM GSK690693 (**Table 2.1**). Importantly, GSK690693 sensitized *L. monocytogenes* to other β-lactams as well, including ceftriaxone, ampicillin, and meropenem, but had no β-lactam-independent effects up to 20 μM (**Supplemental Figure S2.2**), consistent with the lack of β-lactam-independent growth defects in Δ*prkA* mutants [237]. While GSK690693 had no effect on the MIC values of the non-β-lactams vancomycin or kanamycin, it did sensitize *L. monocytogenes* to the TarO inhibitor tunicamycin, consistent with the role of PASTA kinases in resistance to tunicamycin[222,236]. To confirm that GSK690693 potentiation of β-lactam and tunicamycin sensitivity was through PASTA kinase inhibition, we tested the sensitivity of the Δ*prkA* mutant to the same antibiotics in the presence and absence of 20 μM GSK690693. GSK690693 afforded the Δ*prkA* strain no additional sensitization to any antibiotic tested,

suggesting that the activity of GSK690693 is PrkA kinase-dependent (**Table 2.1)**. Finally, GSK690693 sensitized wild-type *L. monocytogenes* in a concentration-dependent manner to a fixed sub-inhibitory concentration of ceftriaxone, demonstrating the reciprocal dose dependency of the kinase inhibitor-β-lactam potentiation (**Figure 2.2**). Taken together, our data demonstrates that GSK690693 sensitizes *L. monocytogenes* to β-lactam antibiotics through PrkA inhibition.

GSK690693 inhibits PrkA *in vitro*

To assess the basis of kinase inhibitor/β-lactam potentiation at the biochemical level and to begin to understand biochemical determinants of activity, we assessed the kinase activity of the purified kinase domain of PrkA in the presence of increasing concentrations of GSK690693. Analysis by autoradiography revealed that GSK690693 robustly inhibited both PrkA autophosphorylation and phosphorylation of the nonspecific phosphoacceptor myelin basic protein (MBP) at concentrations as low as 2 μM (**Figure 2.3A**). Consistent with this finding, analysis of kinase inhibition in the Kinase-Glo® assay (Promega) resulted in a calculated IC_{50} value of 0.84 μM (**Table 2.2**). Finally, *in silico* docking of GSK690693 in the kinase domain of PrkA predicted the 2-methyl-3-butyn-2-ol (alkynol) moiety penetrating into the gatekeeper-guarded back pocket of the kinase active site, similar to the orientation and mechanism of inhibition previously reported for GSK690693 bound to the eukaryotic kinase AKT (**Figure 2.3B**)[253]. Taken together, our data demonstrate that GSK690693 can directly inhibit PrkA activity *in vitro*.

Various IPAs Display Biochemical and Microbiologic Activity

There were seven other members of the IPA family in our library screen (**Figure 2.1 – Red Dots**), three of which demonstrated potentiation with ceftriaxone at >2SD above the mean of the screen and whose structures are shown in **Table 2.3**. To determine if the IPAs represent

a broadly applicable scaffold for PASTA kinase inhibitors we tested 3 additional compounds for biochemical activity and ceftriaxone potentiation: GSK554170A, GSK614526A, and GSK902056A (**Figure 2.4A, Table 2.2**). All three compounds showed statistically similar biochemical activity to GSK690693; however, GSK554170A was 2-fold less potent than GSK690693 microbiologically, while GSK614526A was 4-fold more potent than GSK690693. Taken together, our data suggest that these variations in the R2 and R3 positions of the PIA scaffold may play a role in target accessibility and/or stability in the bacterial cytosol. In contrast, SB-747651A, an IPA which lacks the alkynol moiety, neither potentiated β-lactam sensitivity (**Figure 2.4A**) nor inhibited biochemical activity (**Figure 2.4B**). This is consistent with molecular modeling that implicates the alkynol moiety in stabilization of binding and kinase inhibition (**Figure 2.3B**). Taken together, our findings demonstrate that multiple compounds of the IPA family are capable of augmenting ceftriaxone activity to varying degrees and further suggest that the IPA pharmacophore can be further optimized for β-lactam sensitization.

GSK690693 displays selectivity for PrkA over Stk1

As PASTA kinases are highly conserved in a variety of important human pathogens, we hypothesized that GSK690693 may act on other PASTA kinases as well. Surprisingly, we observed that GSK690693 was significantly less potent against the purified kinase domain of Stk1, the PASTA kinase homolog from *Staphylococcus aureus* (**Figure 2.5A**), with a predicted IC_{50} greater than 40 µM by Kinase-Glo® assay (**Supplemental Figure S2.3A**). Consistent with this finding, neither the ceftriaxone nor oxacillin MIC for the MRSA strain LAC was altered in the presence of GSK690693, although there was a reproducibly minor slowdown in growth in the presence of GSK690693 relative to antibiotics alone (**Supplemental Figure S2.3D-E**) consistent with low level inhibition of Stk1 observed biochemically. In contrast, Δ*stk1* mutants are potently sensitized to both β-lactam antibiotics (**Supplemental Figure S2.3B-C)** as previously described[223]**.** Importantly, Stk1 can be biochemically inhibited by the kinase inhibitor

indirubin-3'-monoxime, which shows relative selectivity for Stk1 over PrkA (**Supplemental Figure S2.4**). Consistent with this, three recent papers have identified small molecule inhibitors of Stk1 that are structurally distinct from the IPAs we identified as PrkA inhibitors[247,248,254]. These data suggest that GSK690693 selectively inhibits the kinase activity of PrkA relative to Stk1 and highlight the possibility of designing non-broad spectrum, pathogen-specific inhibitors.

Intrigued by the divergent activity against the two kinase domains, we utilized *in silico* modeling to identify potential structural deviations that might explain the selectivity. Examination of the back pockets of the Stk1 and PrkA kinase domains revealed high sequence conservation with only four divergent residues: S62 (Stk1)/A63(PrkA), M73/V74, L85/I86, and F150/T151 (**Figure 2.5B**). As F150 and T151 sit at the entrances of their respective kinase's back pocket just upstream of the catalytic DFG motif, we hypothesized that a bulky "xDFG" residue at this position (such as Stk1's F150) may deny GSK690693's alkynol group access to the pocket while a smaller residue (such as PrkA's T151) may be permissible. However, when these residues are swapped between kinases, we found that PrkA T151F has greatly reduced intrinsic kinase activity (**Supplemental Figure S2.5**), whereas Stk1 F150T sensitivity to GSK690693 is unaffected (**Figure 2.5C**). Alternatively, the three other divergent residues (M73/V74, L85/I86, and S62/A63) might alter the size and polarity of the pocket in a way that generates selectivity. Strikingly, an Stk1 S62A/M73V/L85I triple mutant is more sensitive to GSK690693 relative to the wild-type kinase domain (**Figure 2.5C**), although there is also a minor decrease in intrinsic kinase activity. Overall, our data suggests that, at least in part, selectivity of GSK690693 for PrkA over Stk1 is not due to the xDFG residue but rather is mediated by the size and charge of the back pocket that stabilizes the alkynol moiety facilitating inhibition. Additional point mutants altering the character of the back pocket in addition to synthesizing alkynol modifications will help to establish a formal SAR and may instruct the rational design of species specific kinase inhibitors in the future.

DISCUSSION

Eukaryotic kinases have been a target of the pharmaceutical industry for decades owing to their central role in a variety of cancers and other diseases[255,256]. As of 2015, 27 protein kinase inhibitors are FDA-approved for use in the clinic[174]. In light of this relative success in eukaryotes, prokaryotic protein kinases have begun to be investigated as potentially novel antibiotic targets. A highly conserved family of bacterial kinases, the PASTA kinases, have high levels of conservation with eukaryotic kinases and play central roles in processes ranging from metabolism and basic bacterial physiology to regulation of virulence and β-lactam antibiotic susceptibility. As such, efforts are being put forth to identify small molecule inhibitors of the PASTA kinases [237,246,247,257]. As these efforts progress, it will be important to consider the need for a better understanding of the biochemistry of PASTA kinase inhibition to aid in the development of selective kinase inhibitors. Here, we present GSK690693 and other IPAs as novel inhibitors of the *L. monocytogenes* PASTA kinase PrkA and as a tool to better understand PASTA kinase biochemistry.

We identified 16 compounds, including GSK690693, that inhibited growth of *L. monocytogenes* in the presence of a sublethal dose of a β-lactam by performing a small (625 compound) primary screen of compounds known to possess a pharmacophore with kinase-inhibiting attributes. We chose GSK690693 above others due to its dependence on PrkA, its dependence on the presence of a β-lactam, and its dose dependence. Although several inhibitors with PrkA-specific activity may have been missed in our screen, the utilization of a microbiological screen rather than a biochemical screen immediately overcame a significant barrier that has been encountered in screens to identify *M. tuberculosis* PknB inhibitors, namely identification of compounds capable of entering into the bacterium[245].

Seven congeners of GSK690693 were also present in our screen, each possessing the characteristic alkynol moiety and IPA scaffold but varying in the position and molecular structures of their respective side chains. Those that we further characterized all had statistically

similar IC_{50}s though their microbiologic activity varied. This suggests a varying ability of these compounds to access their target in the bacterial cytosol or a difference in stability once in the cytosol, further exemplifying the need to modify "Lipinski's rule of 5" to account for the bacterial cell wall when performing antibiotic development. Our data indicate that modifications to the R2 or R3 position may be more important in dictating target accessibility rather than biochemical activity.

GSK690693's eukaryotic SAR has established that the alkynol moiety penetrates into AKT's gatekeeper-guarded back pocket to stabilize binding[253]. Interestingly, SB-747651A is completely unable to inhibit PrkA activity and sensitize *L. monocytogenes* to a β-lactam, likely due to the lack of the alkynol moiety on the IPA scaffold. Although effects of SB-747651A's R2 sidechain cannot be ruled out, it is worth noting that all other tested IPAs that possess the alkynol moiety have some efficacy against *L. monocytogenes* PrkA, regardless of the sidechain structure at R1 or R2.

Due to an expansion in our knowledge of the effects current antibiotics have on the human microbiome[258,259], one of the challenges of antimicrobial development has become finding antimicrobial compounds that are selective for the pathogen of interest without disruption of normal microbiota or collateral resistance effects. Therefore, we were intrigued to find that GSK690693 showed selectivity for the PrkA kinase domain over Stk1, the PASTA kinase from *S. aureus* that shows 49% identity with PrkA across its kinase domain (**Figure 3A; Figure 5A**). PASTA kinase inhibitors with varying degrees of biochemical activity have been identified for *M. tuberculosis* PknB[183,209,218,245,246,260], *E. faecalis* IreK[239], *B. subtilis* PrkC[192], *L. monocytogenes* PrkA [237], and staphylococcal Stk1 [221,247,248,254]; however, this work is the first to investigate the selectivity of an inhibitor between two PASTA kinases. Given the importance of the gatekeeper-guarded back pocket in the eukaryotic SAR of GSK690693, we investigated differences in the back pockets of PrkA and Stk1. Mutation of the most obvious amino acid residue (Stk1 F150T) at the entrance to the pocket did not alter selectivity; however, mutation of the three divergent

residues that contribute to the shape and depth of the back pocket profoundly affected the sensitivity of Stk1 to GSK690693 (**Figure 5C**). To our knowledge, investigations in human kinases have not implicated these internal residues as contributing to selectivity[151,261]. GSK690693 has been well established as relatively selective among eukaryotic kinases for isoforms of AKT [154,252,253], though this is the first time activity against specific bacterial kinases has been shown. Overall, GSK690693's selectivity between two highly similar kinases found in *L. monocytogenes* and *S. aureus* extends the concept that pathogen-specific inhibitors could be identified and developed [237].

The mechanism by which PrkA mediates tunicamycin resistance remains unknown. At low (non-lethal) concentrations, tunicamycin inhibits the activity of TarO, the enzyme required for the transfer of GlcNAc-1-phosphate from UDP-GlcNAc to undecaprenyl phosphate during wall teichoic acid (WTA) synthesis[262]. However, at higher (lethal) concentrations, tunicamycin also blocks the activity of MraY, the essential enzyme required for the transfer of phospho-MurNAc-pentapeptide to undecaprenyl phosphate during peptidoglycan synthesis[263]. Sensitization to tunicamycin through PrkA inhibition may be due to PrkA-mediated regulation of one or both of these proteins directly as substrates. Alternatively, PrkA may act on the pathways further upstream or downstream of these proteins. Additionally, it is unknown why treatment with GSK690693 can achieve the maximum-expected sensitivity to tunicamycin (i.e. match the phenotype of a Δ*prkA* mutant) but cannot do the same for the β-lactams. It is possible that the tunicamycin phenotype is dependent solely on kinase activity, while the β-lactam phenotype might be dependent on both kinase activity and other non-enzymatic roles of PrkA. If true, then inhibition of kinase activity by GSK690693 would only be able to achieve a fraction of the phenotype of the genetic deletion. Determining if there are kinase activity-independent functions of PrkA is an active area of investigation

As with tunicamycin, the exact mechanism by which PrkA mediates β-lactam resistance is not well understood. A considerable number of enzymes and proteins involved in cell wall

metabolism are directly phosphorylated by eSTKs in a variety of species, with examples including MurC[264], PBPa[265], DivIVA/Wag31[266], GpsB[214], and VraR[225]. Such a span of substrates leads to the conclusion that PrkA (and the PASTA kinases in general) may play a role in many aspects of cell wall metabolism such as muropeptide synthesis, PBP function and localization, and the orchestration of cell elongation and septation. These possibilities are still under investigation.

In conclusion, we have identified GSK690693 and other IPAs as novel inhibitors of the PASTA kinase PrkA with the potential for increased selectivity amongst PASTA kinases. We have shown that GSK690693 potentiates β-lactam activity against *Listeria* in both broth and macrophage models. Furthermore, we have begun to establish an SAR by demonstrating that the alkynol group and nature of the back pocket in which it is predicted to be bound is potentially important for PASTA kinase inhibition by IPAs. These studies represent a stepping stone in the development of new and selective antibiotic therapies that could breathe new life into an exhausted antibiotic class.

MATERIALS AND METHODS

Bacterial strains and growth conditions

All bacterial strains used in this study are listed in **Supplementary Table S2.1**. Conditional deletion of *prkA* (Δ*prkA*) was achieved as previously described[237]. All *L. monocytogenes* strains were grown in brain-heart infusion (BHI) medium at 30°C stationary overnight until stationary phase. Cultures were then back-diluted 1:50 for *in vitro* growth experiments. All *S. aureus* strains were grown in tryptic soy broth (TSB) medium at 37°C shaking overnight until stationary phase. Cultures were then back-diluted to an OD_{600} of 0.06 for *in vitro* growth experiments. *Escherichia coli* strains XL-1Blue and Rosetta BL21 were used for subcloning and protein expression, respectively. When needed, chloramphenicol (Sigma-Aldrich) was used at 10 μg/mL and carbenicillin (Sigma-Aldrich) was used at 100 μg/mL. For all

broth growth assays, GSK690693 (Selleck Chemicals, Houston, TX) was used at a final concentration of 20 μM (2% DMSO) unless otherwise specified in the figure legends.

Library screen

The PKIS1 and Selleck libraries were obtained via the University of Wisconsin Carbone Cancer Center's Small Molecule Screening Facility. Overnight cultures were back-diluted 1:50 into fresh BHI medium containing 1 μg/mL ceftriaxone and either library compounds (final concentration: 10 μM in 2% DMSO) or DMSO (final concentration: 2%). Growth was measured as an optical density at 600 nm (OD_{600}) on 15 minute intervals for 12 hours in a 96-well format using an Eon microplate spectrophotometer or Synergy HT microplate spectrophotometer (BioTek Instruments, Inc, Winooski, VT) (growth conditions: 37°C, linear shaking). Each compound was screened twice. Percent inhibition was calculated as $(1 – (OD_X / OD_{CRO})) * 100$, where OD_X is the endpoint OD_{600} for a culture treated with both ceftriaxone and compound X, and OD_{CRO} is the endpoint OD_{600} for a culture treated with ceftriaxone alone. Compounds that inhibited growth three standard deviations greater than the library mean were further verified for dose responsiveness and β-lactam dependence.

Minimal Inhibitory Concentration (MIC) determination

L. monocytogenes overnight cultures were back-diluted 1:50 into fresh BHI medium containing 2-fold dilutions of the antibiotics ampicillin, ceftriaxone, meropenem, tunicamycin, kanamycin, or vancomycin in the presence or absence of GSK690693. OD_{600} was measured to monitor growth of the microdilutions as described above. *S. aureus* overnight cultures were back-diluted to an OD_{600} of 0.06 into cation-adjusted Mueller-Hinton medium containing 2-fold dilutions of the antibiotic ceftriaxone in the presence or absence of GSK690693. OD_{600} was measured to monitor growth of the microdilutions for 16 hours. MICs were defined as the lowest

concentration of antibiotic required to prevent turbidity in broth visible by eye. Each MIC experiment was performed at least three times.

Kinase domain protein expression and purification

The *prkA* and *stk1* kinase domains (1-338 and 1-348, respectively) were subcloned into the expression vector pGEX-2T as previously described[237]. The plasmids were transformed into *E. coli* Rosetta BL21 cells, and protein expression was verified by SDS-PAGE. The bacteria were pelleted by centrifugation and resuspended in lysis buffer (25 mM Tris pH 8.0, 150 mM NaCl, 1 mM dithiothreitol [DTT], 10 mM $MgCl_2$) containing 2 µg/mL DNAse, 2 µg/mL aprotinin, 1 µg/mL leupeptin, and 25 µg/mL phenylmethylsulfonyl fluoride (PMSF). Cells were lysed by sonication, and cell debris was pelleted by centrifugation for 20 minutes. Supernatant was passed through GS4FF affinity resin columns at 4°C; columns were then rinsed with lysis buffer, and the protein eluted with elution buffer (50 mM Tris pH 8.0, 5 mM NaCl, 3 mM DTT, 20 mM reduced glutathione, 1 mM $MgCl_2$). Eluted protein was then digested overnight at 4°C with 1/20 w/w thrombin. Digested protein was passed through a HiPrep Q16 10FF anionic exchange column (Buffer A: 20 mM Tris pH 8.0, 1 mM DTT) via an ÄKTApurifier (GE Healthcare Life Sciences, Pittsburgh, PA); protein was eluted off the column with a 0-50% gradient of Buffer B (20 mM Tris pH 8.0, 1 mM DTT, 1 M NaCl). Target fractions were then combined and passed through GS4FF affinity columns as described above. The flowthrough was concentrated via spin columns and passed through a Sephadex75 size exclusion column on the ÄKTApurifier (Running Buffer: 10 mM Tris pH 8.0, 150 mM NaCl, 1 mM DTT, 10 mM $MgCl_2$). Fractions were tested for purity by SDS-PAGE and combined. For Stk1 purification, $MgCl_2$ was replaced with $MnCl_2$ throughout.

Generation of kinase mutants

All plasmids generated in this study are listed in **Supplementary Table S2.2**. To generate the Stk1-F150T mutant, plasmid pGEX-2T-Stk1 was digested with BamHI and KpnI (New England Biolabs) to remove the wild-type N-terminal Stk1 sequence. A gBlock gene fragment (Integrated DNA Technologies) consisting of the excised N-terminal sequence with a F150T (*T1404A, T1405C*) mutation was ligated into the digested plasmid to yield pGEX-2T-Stk1 F150T. To generate the PrkA T151F mutant, a similar process was performed on the pGEX-2T-PrkA plasmid, utilizing BamHI and EcoRI restriction sites and a gBlock gene fragment with a T151F (*A451T, C452T, A453T*) mutation to yield pGEX-2T-PrkA T151F. Finally, to generate the Stk1 S62A/M73V/L85I triple mutant, a similar process was performed on the pGEX-2T-Stk1 plasmid, utilizing BamHI and KpnI restriction sites and a gBlock gene fragment with a S62A (*T187A*), M73V (*A217G, G219T*), and L85I (*T253A, A255T*) mutations to yield pGEX-2T-Stk1 S62A/M73V/L85I. All mutant constructs were validated by sequencing. Mutant constructs were transformed into *E. coli* Rosetta BL21 cells and protein expression and purification were performed in the same fashion as the wild type constructs.

Generation of Δ*stk1* mutant

Regions 1000 bp in size directly upstream and downstream were amplified with primer pairs JDS88/BK34 and BK35/JDS89, respectively (**Supplemental Table S2.3**). These regions were fused by “splice by overlap” PCR and ligated into the plasmid pJB38 utilizing the SacI and XmaI restriction sites to yield pJB38-Δstk1. The construct was electroporated into the *S. aureus* strain RN4220 then transduced into LAC by phage transduction. Deletion of the *stk1* gene was then performed by pJB38-mediated allelic exchange as described by Bose *et al*[267]. Successful deletion of *stk1* was validated by PCR.

Kinase-Glo® assay

The kinase assays were performed using the KinaseGlo® reagent from Promega. All reactions were done in 50µL volume. The buffer used for all kinase assays was 10mM Tris-HCl pH 7.4, 150mM NaCl, 1mM DTT, and 1mM $MgCl_2$. Drugs in 5mM DMSO were diluted in kinase buffer to 1/2 the final concentration using a serial dilution from 20 to 0µM. The final DMSO concentration in the reactions was no more than 0.4%. PrkA 1-338 was added to the drugs to a final concentration of 2.0µM and allowed to incubate for 10min at 37C. ATP and MBP (Novatein Biosciences, Woburn, MA) were added for a final concentration of 100µM and 40µM respectively, initializing the reaction. After a half hour incubation, the reaction was stopped by the addition of 50µL of KinaseGlo® reagent, and the signal was allowed to stabilize for 10min at room temperature per the product manual. The plate was read using luminescence detection on a Synergy HT detector (BioTek) and the data were collected using the Gen5 2.0 software (BioTek). The data were transformed to log scale and non-linear regression was performed in PRISM using the variable slope 4-parameter model for enzyme inhibition to determine IC_{50}.

In vitro protein phosphorylation

2 µM kinase domain, 10 µM MBP (Novatein Biosciences, Woburn, MA), and various concentrations of kinase inhibitors were incubated on ice for 10 minutes, then added to a mixture of 10 mM Tris pH 7.4, 150 mM NaCl, 1 mM $MgCl_2$ (50 µM $MnCl_2$ for Stk1 and its mutants), 50 µM ATP, and 1 µCi of [γ-^{32}P] ATP. Reactions were incubated at 37°C for 1 hour and terminated by the addition of 6X SDS loading buffer. Samples were run on an SDS-PAGE gel then fixed for 2 hours in fixation solution (40% methanol, 5% glycerol, 10% glacial acetic acid). Fixed gels were dried for 1 hour and blots visualized by autoradiography.

In silico Modeling

The primary sequences of the PrkA and Stk1 kinase domains (residues 1-270) were threaded onto the crystal structure of the kinase domain of PknB from *Mycobacterium*

tuberculosis (PDB ID 1O6Y) using the Phyre2 server's one-to-one threading[268]. Hydrogen atoms and Gasteiger-Huckel charges were added, and energy minimization was performed using SYBYL-X1.2[269]. The structure of GSK690693 was downloaded as a MOL2 file from the ZINC database[270]. Hydrogen atoms and Gasteiger-Huckel charges were added, and energy minimization was performed using SYBYL-X1.2. GSK690693 was docked into a 66x66x66 unit grid encompassing the kinases' active site clefts using the docking program Autodock's Lamarckian genetic algorithm[271]. Models were visualized using PyMOL[272]. The reference crystal structure of GSK690693 bound to human AKT (PDB ID 3d0e) was directly downloaded from the PDB and visualized in PyMOL without modifications.

ACKNOWLEDGEMENTS AND FUNDING INFORMATION

The PKIS was supplied by GlaxoSmithKline, LLC and the Structural Genomics Consortium under an open access Material Transfer and Trust Agreement: http://www.sgc-unc.org".
The SGC is a registered charity (number 1097737) that receives funds from AbbVie, Bayer Pharma AG, Boehringer Ingelheim, Canada Foundation for Innovation, Eshelman Institute for Innovation, Genome Canada, Innovative Medicines Initiative (EU/EFPIA) [ULTRA-DD grant no. 115766], Janssen, Merck & Co., Novartis Pharma AG, Ontario Ministry of Economic Development and Innovation, Pfizer, São Paulo Research Foundation-FAPESP, Takeda, and Wellcome Trust [106169/ZZ14/Z]

Supported by grant UL1TR000427 from the Clinical and Translational Science Award (CTSA) program of the National Center for Advancing Translational Sciences, NIH.

Supported by grant AI121704 from the National Institute of Allergy and Infectious Diseases, NIH.

RT and NW supported by the Hartwell Foundation.

JDS supported by The Wisconsin Partnership Program

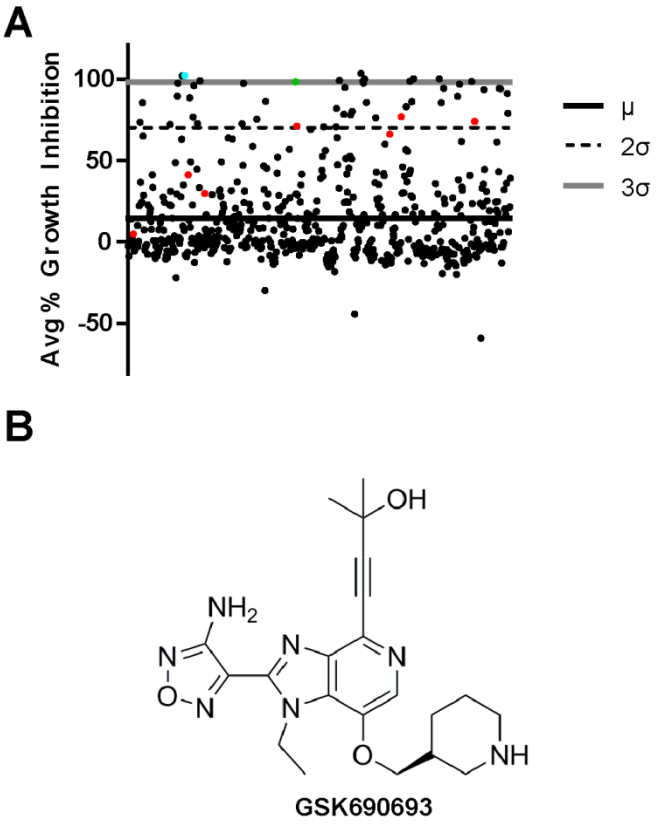

Figure 2.1: Library screen identifies GSK690693 as a compound that sensitizes *L. monocytogenes* to ceftriaxone. A) Scatter plot representing percent growth inhibition of WT *L. monocytogenes* in the presence of a combination of a sublethal dose (1 μg/mL) of the β-lactam ceftriaxone and each compound in the screen. The solid black line represents the library mean (μ), and the dashed black line and gray line represent two (2σ) and three (3σ) standard deviations above the library mean, respectively. The cyan, green, and red data points represent staurosporine, GSK690693, and other compounds from the IPA family, respectively. **B)** Skeletal structure of GSK690693.

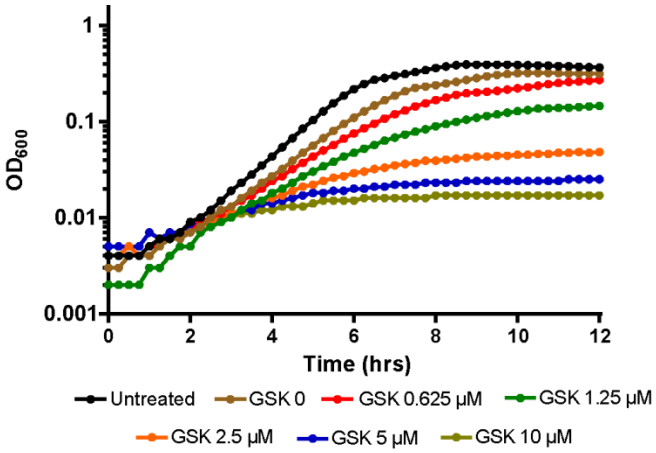

Figure 2.2: GSK690693 potentiates the inhibitory action of ceftriaxone in a dose-dependent manner. Growth curves of WT *L. monocytogenes* grown in the presence of 2.5 µg/mL ceftriaxone and increasing concentrations (µM) of GSK690693. Curves are representative of 3 independent trials.

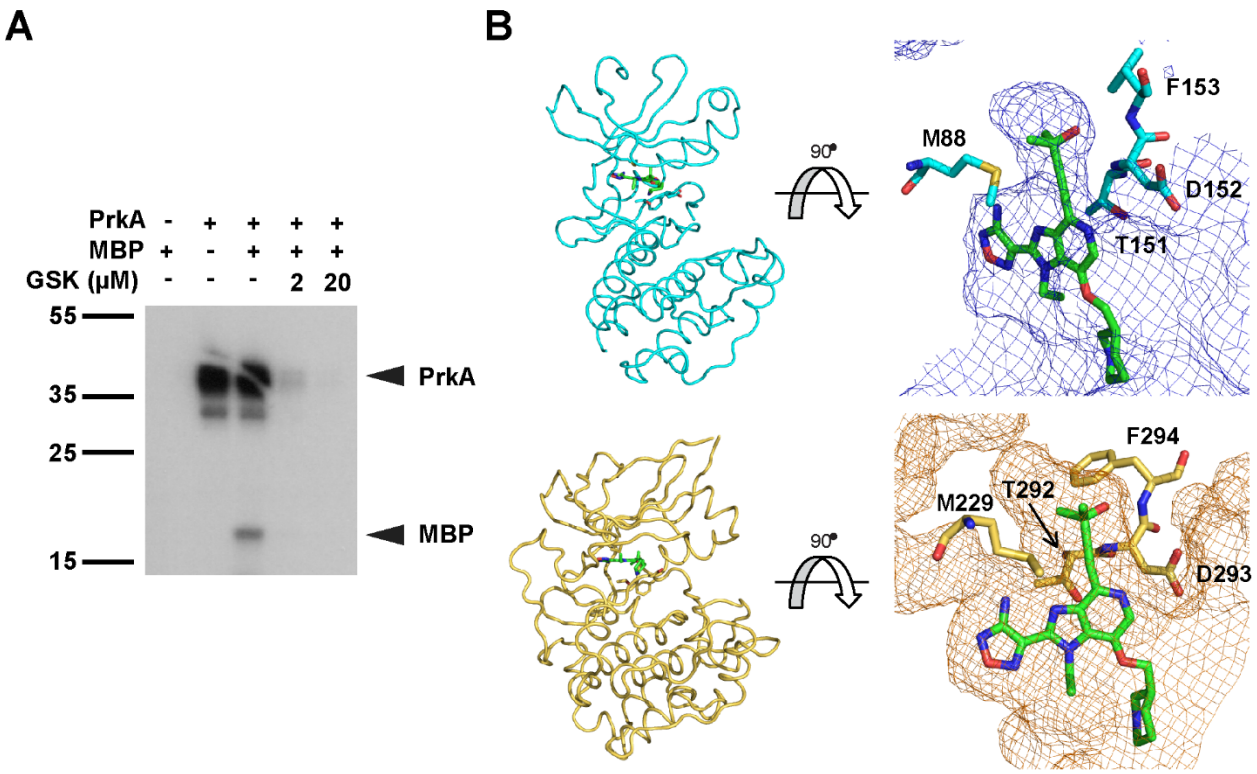

Figure 2.3: GSK690693 inhibits the PrkA kinase domain *in vitro*. A) Autoradiography blot of purified PrkA kinase domain from *L. monocytogenes* and the non-specific phosphoacceptor substrate myelin basic protein (MBP) in the presence or absence of GSK690693. Blot is representative of 3 independent trials. **B)** (top) GSK690693 docked *in silico* into the threaded model of the kinase domain of PrkA (bottom) crystal structure of GSK690693 bound to human AKT (PDB ID 3d0e). Gatekeeper methionine and xDF residues are represented as sticks.

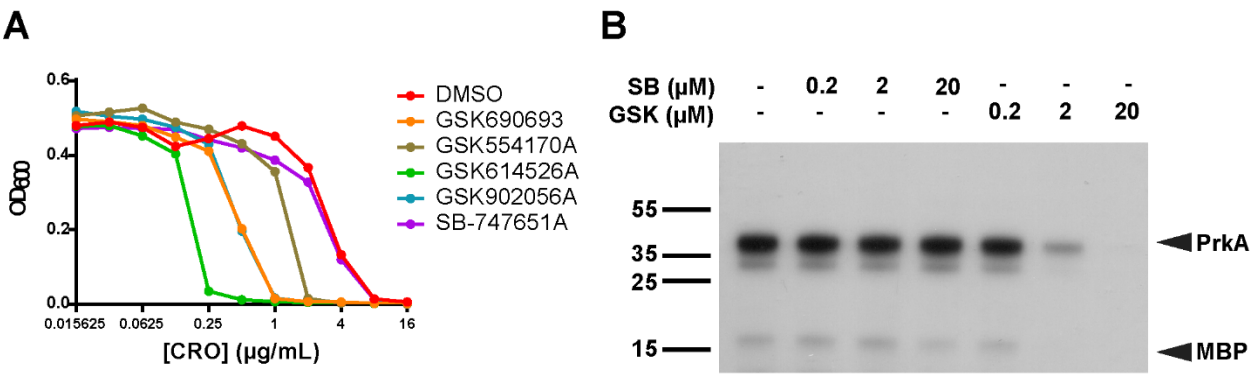

Figure 2.4: IPAs potentiate ceftriaxone activity to varying degrees. A) Dose-response curves of *L. monocytogenes* growth vs. ceftriaxone in the presence and absence of 10 µM IPAs. Curves are representative of 3 independent trials. **B)** Autoradiography blot of purified PrkA kinase domain and MBP in the presence or absence of GSK690693 or SB-747651A. Blot is representative of 3 independent trials.

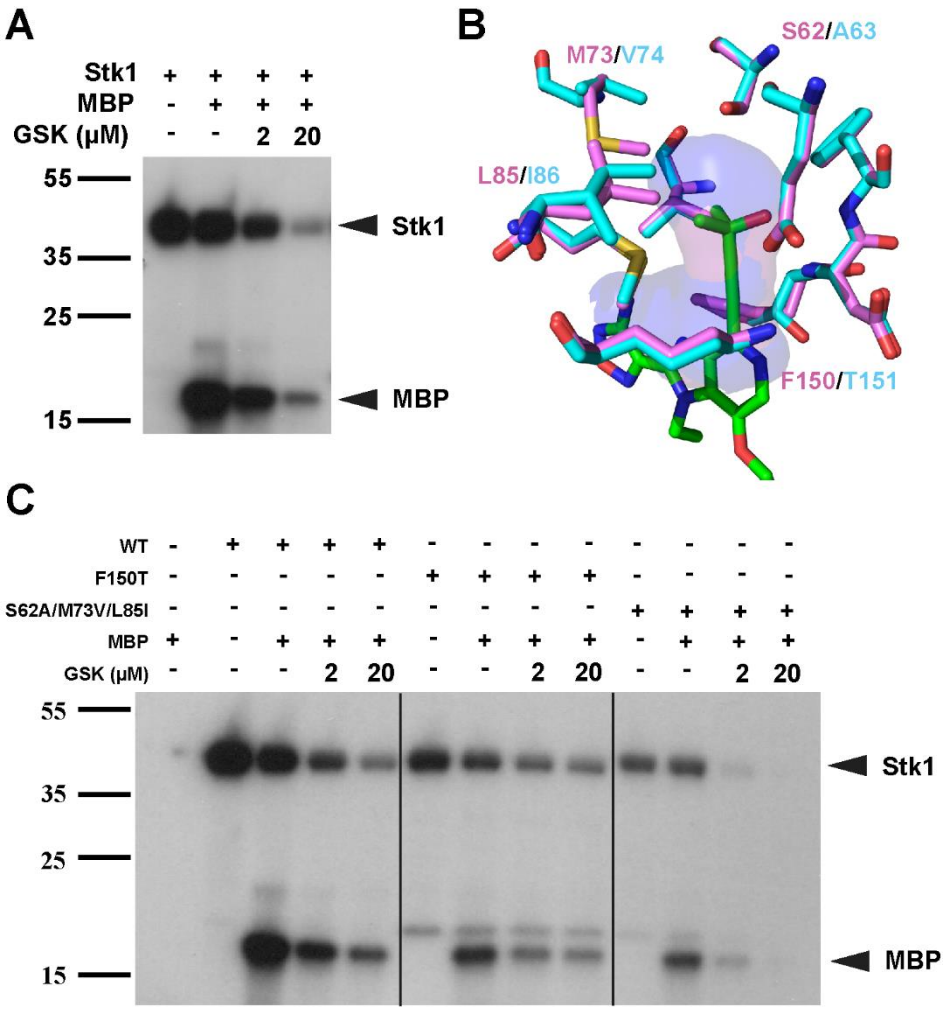

Figure 2.5: Residues of the back pocket play a role in GSK690693 selectivity A) Autoradiography blot of purified Stk1 kinase domain from *S. aureus* and MBP in the presence or absence of GSK690693. **B)** Stick figure representation of the amino acids that constitute the back pocket of the PrkA (cyan) and Stk1 (violet) kinase domains. GSK690693 (green sticks) is docked into the back pocket, which is represented by the translucent cavity surface. **C)** Autoradiography blot of purified WT Stk1, F150T mutant, S62A/M73V/L85I triple mutant, and MBP in the presence or absence of GSK690693. Blots are representative of 3 independent trials.

	MIC (µg/mL)			
	10403s		Δ*prkA*	
GSK690693	**-**	**+**	**-**	**+**
Ceftriaxone	8 [4, 8]	1 [0.5, 1]	0.0625 [0.03125, 0.25]	0.0625 [0.03125, 0.25]
Ampicillin	0.25 [0.25, 0.25]	0.0625 [0.0625, 0.125]	0.03125 [0.03125, 0.03125]	0.03125 [0.03125, 0.03125]
Meropenem	0.25 [0.25, 0.25]	0.125 [0.125, 0.25]	0.03125 [0.03125, 0.0625]	0.0625 [0.0625, 0.0625]
Tunicamycin	32 [32, 32]	0.5 [0.5, 1]	0.5 [0.5, 1]	0.5 [0.5, 1]
Vancomycin	2 [2, 4]	2 [2, 4]	1 [1, 1]	1 [1, 1]
Kanamycin	8 [8, 8]	8 [8, 8]	8 [8, 8]	8 [8, 8]

Table 2.1: Minimum Inhibitory Concentrations (MIC) of various antibiotics against WT and Δ*prkA* strains +/- 20µM GSK690693. Data presented as median of at least three biological replicates with the range in brackets.

Compound	Relative IC_{50} [95% CI] (μM)	Ceftriaxone MIC (μg/mL)
DMSO	*N/A*	8
GSK690693	0.84 [0.34, 2.00]	1
GSK554170A	0.45 [0.080, 2.49]	2
GSK614526A	0.42 [0.010, 17.17]	0.25
GSK902056A	0.41 [0.10, 1.63]	1
SB-747651A	*N/A*	8

Table 2.2: Summary of biochemical and microbiology data for various IPAs against *L. monocytogenes*. N/A: Not applicable.

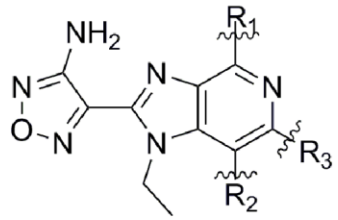

Compound	R1	R2	R3
GSK690693	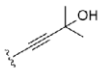	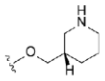	H
GSK554170A	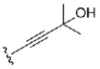	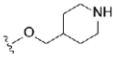	H
GSK614526A	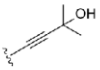	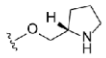	H
GSK902056A		H	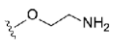
SB-747651A	H	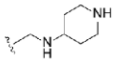	H

Table 2.3: Structures of various IPA family compounds

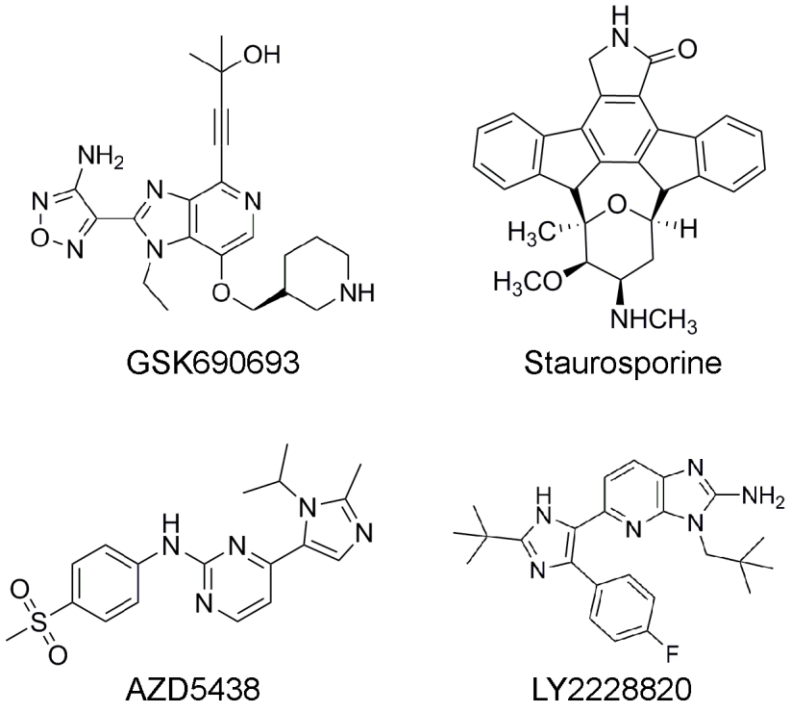

Figure S2.1: Validated hits from the kinase inhibitor library screen. Compounds displayed were identified as compounds that passed the primary screen (sensitize *L. monocytogenes* to a β-lactam) then passed secondary screens for dose dependence, β-lactam dependence, and PrkA dependence.

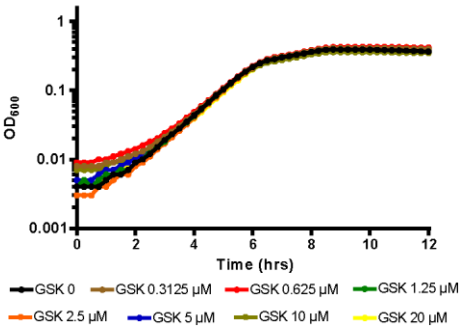

Figure S2.2: GSK690693 is nontoxic to *L. monocytogenes.* WT *L. monocytogenes* was grown for 12 hours in the presence of varying concentrations of GSK690693. Curves are representative of 3 independent trials.

A

Compound	IC_{50} (μM)	Ceftriaxone MIC (μg/mL)	Oxacillin MIC (μg/mL)
DMSO	*N/A*	32	16
GSK690693	> 40	32	16

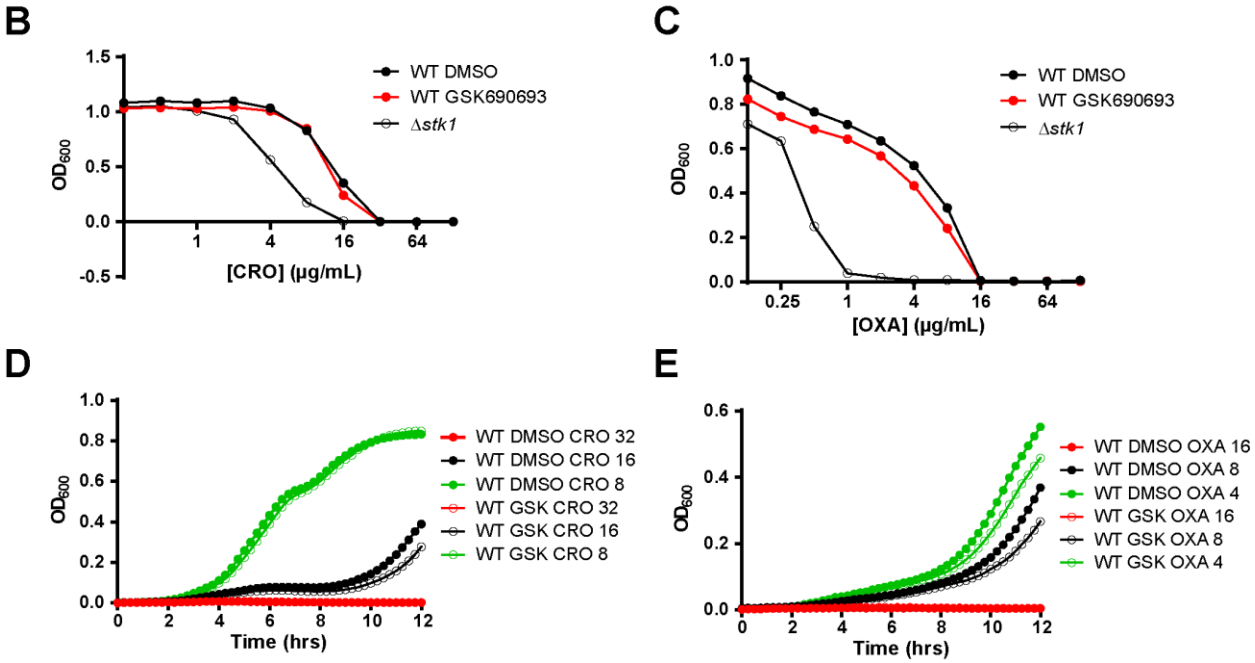

Figure S2.3: GSK690693 is unable to potentiate β-lactam activity against *S. aureus*. A) Summary of biochemical and microbiology data for GSK690693 against *S. aureus* Stk1. IC_{50} values were determined by Kinase-Glo® assay. N/A: Not applicable. **B-C)** Dose-response curves of WT *S. aureus* LAC and Δ*stk1* growth vs **B)** ceftriaxone and **C)** oxacillin in the presence and absence of 20 μM GSK690693. Curves are representative of 3 independent trials. **D-E)** Growth curves for data presented in **B)** and **C)**, respectively.

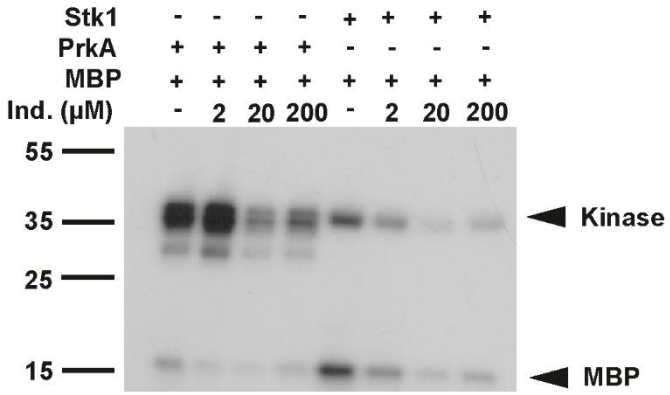

Figure S2.4: Indirubin-3'-monoxime shows selectivity for Stk1 over PrkA. Autoradiography blots of purified PrkA kinase domain from *L. monocytogenes* or purified Stk1 kinase domain from *S. aureus* and the non-specific phosphoacceptor substrate myelin basic protein (MBP) in the presence or absence of indirubin-3'-monoxime.

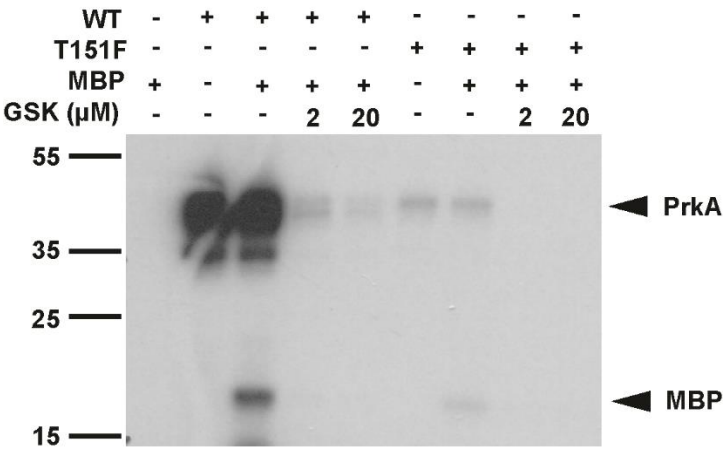

Figure S2.5: PrkA T151F mutant has reduced activity. Autoradiography blot of purified WT PrkA kinase domain (WT), T151F mutant (T151F), and MBP in the presence or absence of GSK690693. Blot is representative of two independent trials.

Strain	Description	Reference
E. coli		
XL1-Blue	Competent strain of *E. coli* for routine sub-cloning	Agilent Genomics
Rosetta™ (DE3)	BL21 derivative for enhanced expression of proteins with codons rarely found in *E. coli*; Cam^R	EMD Millipore
JDS1509	Rosetta™ (DE3) carrying pGEX-2T-PrkA; Cam^R, Amp^R	237
JDS299	Rosetta™ (DE3) carrying pGEX-2T-Stk1; Cam^R, Amp^R	237
JDS951	XL1-Blue carrying pGEX-2T-Stk1 F150T; Amp^R	this work
JDS999	Rosetta™ (DE3) carrying pGEX-2T-Stk1 F150T; Cam^R, Amp^R	this work
JDS937	XL1-Blue carrying pGEX-2T-PrkA T151F; Amp^R	this work
JDS385	Rosetta™ (DE3) carrying pGEX-2T-PrkA T151F; Cam^R, Amp^R	this work
JDS1350	XL1-Blue carrying pGEX-2T-Stk1 S62A/M73V/L85I; Amp^R	this work
JDS1362	Rosetta™ (DE3) carrying pGEX-2T-Stk1 S62A/M73V/L85I; Cam^R, Amp^R	this work
L. monocytogenes		
10430s	Streptomycin-resistant derivative of strain 10403	273
S. aureus		
RN4220	Heavily mutagenized shuttle strain that accepts foreign DNA	274
LAC	Community-acquired USA300 MRSA strain isolated from LA County	275
JDS827	LAC Δ*stk1*	this work

Supplemental Table S2.1: Strains used in this study.

Plasmid	Description	Reference
pGEX-2T	Commercial plasmid for expressing fusion proteins with thrombin-cleavable N-terminal GST tags; Amp^R	GE Healthcare Life Sciences
pJB38	Allelic-exchange plasmid for *S. aureus*; Amp^R (*E. coli*), Cam^R (*S. aureus*)	267
pGEX-2T-Stk1	pGEX-2T plasmid for expression of the Stk1 kinase domain (residues 1-348) from *S. aureus*; Amp^R	237
pGEX-2T-PrkA	pGEX-2T plasmid for expression of the PrkA kinase domain (1-338) from *L. monocytogenes*; Amp^R	237
pGEX-2T-Stk1 F150T	pGEX-2T plasmid for expression of the Stk1 kinase domain with F150T mutation; Amp^R	this work
pGEX-2T-PrkA T151F	pGEX-2T plasmid for expression of the PrkA kinase domain with T151F mutation; Amp^R	this work
pGEX-2T-Stk1 S62A/M73V/L85I	pGEX-2T plasmid for expression of the Stk1 kinase domain with S62A/M73V/L85I triple mutation; Amp^R	this work
pJB38-Δ*stk1*	pJB38 containing fusion of 1 kb upstream and downstream of the *stk1* gene for allelic exchange; Amp^R (*E. coli*), Cam^R (*S. aureus*)	this work

Supplemental Table S2.2: Plasmids used in this study.

Primer	Sequence (5' → 3') (Restriction Sites Lower Case)	Reference
JDS88 (Stk1 KO A)	TATTATgagctcGGTCTGTTTGGTGGTGTGAATGAC	this work
BK34 (Stk1 KO B)	ATACATCATCATAGCTGACTTCTTTTTCAGCTTACCTATCATACTTTATCACCTTCAATAGC	this work
BK35 (Stk1 KO C)	GCTATTGAAGGTGATAAAGTATGATAGGTAAGCTGAAAAAGAAGTCAGCTATGATGATGTAT	this work
JDS89 (Stk1 KO D)	ATTATAcccgggCAATTCCTAAACTTACATGTTTCACCATATCG	this work

Supplementary Table S2.3: Primers used in this study.

Supplementary Table S2.4: Tabulated *L. monocytogenes* library screen data

Compound	Trial 1 % Inhib.	Trial 2 % Inhib.	AVG % Inhib.	Std Dev
3-Methyladenine	8.266	0.795	4.530	5.283
A66	20.949	27.571	24.260	4.683
A-674563	65.920	87.779	76.850	15.457
A-769662	30.083	51.416	40.750	15.084
AEE788 (NVP-AEE788)	19.145	25.027	22.086	4.159
Afatinib (BIBW2992)	45.728	45.103	45.415	0.442
AG-1024	107.775	99.148	103.461	6.100
AG-1478 (Tyrphostin AG-1478)	23.759	39.195	31.477	10.915
AG-490	10.927	46.392	28.659	25.077
AMG 900	39.921	88.077	63.999	34.052
AMG-208	20.700	2.449	11.575	12.905
AMG458	19.895	38.003	28.949	12.805
Amuvatinib (MP-470)	26.919	-3.514	11.702	21.520
Apatinib (YN968D1)	8.300	17.139	12.719	6.250
ARQ 197 (Tivantinib)	36.759	89.866	63.312	37.552
ARRY334543	67.325	74.367	70.846	4.979
Arry-380	13.922	30.849	22.386	11.970
AS-252424	63.812	77.645	70.729	9.782
AS-604850	36.056	46.349	41.202	7.278
AS-605240	20.700	6.283	13.491	10.194
AS703026 (Pimasertib)	10.204	-7.348	1.428	12.411
AST-1306	17.590	17.359	17.474	0.163
AT7519	17.590	9.265	13.428	5.886
AT7867	101.166	99.148	100.157	1.427
AT9283	37.856	73.454	55.655	25.171
Aurora A Inhibitor I	16.035	-1.810	7.112	12.619
Axitinib	-1.916	-21.649	-11.783	13.954
AZ 960	96.838	97.019	96.929	0.128
AZ628	39.570	55.291	47.430	11.116
AZD0855	45.967	71.459	58.713	18.026
AZD2014	1.386	1.643	1.514	0.182
AZD4547	23.172	53.365	38.269	21.349
AZD5438	95.784	99.106	97.445	2.349
AZD6244 (Selumetinib)	16.313	-14.948	0.682	22.105
AZD7762	25.364	7.987	16.676	12.288
AZD8330	17.201	9.265	13.233	5.612
AZD8931	1.652	-0.958	0.347	1.846
Barasertib (AZD1152-HQPA)	4.713	37.371	21.042	23.093
Baricitinib (LY3009104, inc b28050)	20.879	19.873	20.376	0.712
BEZ235 (NVP-BEZ235)	-0.259	-0.515	-0.387	0.181

Compound	Trial 1 % Inhib.	Trial 2 % Inhib.	AVG % Inhib.	Std Dev
BGJ398 (NVP-BGJ398)	16.035	8.413	12.224	5.389
BI 2536	10.098	73.454	41.776	44.799
BI6727 (Volasertib)	45.894	67.809	56.851	15.497
BIBF1120 (Vargatef)	11.756	31.443	21.599	13.921
BIRB 796 (Doramapimod)	20.700	0.319	10.510	14.411
BIX02188	10.982	6.283	8.632	3.322
BIX02189	25.364	27.583	26.473	1.568
BKM120 (NVP-BKM120)	22.003	71.982	46.992	35.341
BMS 777607	40.914	6.283	23.598	24.487
BMS-265246	-0.680	-12.886	-6.783	8.631
BMS-599626 (AC480)	29.984	58.247	44.116	19.985
BMS794833	26.219	-23.994	1.112	35.506
Bosutinib (SKI-606)	71.414	72.938	72.176	1.078
Brivanib (BMS-540215)	-0.673	31.701	15.514	22.892
Brivanib Alaninate (BMS-582664)	100.829	99.485	100.157	0.950
BS-181 HCl	106.220	97.870	102.045	5.904
BX-795	-4.568	-34.185	-19.376	20.943
BX-912	18.367	0.319	9.343	12.762
BYL719	39.608	10.122	24.865	20.850
CAL-101 (GS-1101)	5.490	38.003	21.746	22.990
CAY10505	11.814	51.714	31.764	28.214
CCT128930	20.597	49.329	34.963	20.317
CCT129202	14.869	15.655	15.262	0.556
CCT137690	11.814	69.001	40.408	40.438
Cediranib (AZD2171)	40.756	51.289	46.022	7.448
CEP33779	49.928	88.129	69.029	27.012
CH5424802	3.679	-9.380	-2.851	9.234
CHIR-124	93.676	98.510	96.093	3.418
CHIR-98014	20.949	35.320	28.135	10.162
CI-1033 (Canertinib)	17.141	25.773	21.457	6.104
CI-1040 (PD184352)	-8.959	26.031	8.536	24.742
CP 673451	16.812	-2.662	7.075	13.771
CP-724714	-21.283	10.969	-5.157	22.806
Crenolanib (CP-868596)	22.354	41.580	31.967	13.595
Crizotinib (PF-02341066)	91.300	98.454	94.877	5.058
CX-4945 (Silmitasertib)	69.433	83.010	76.222	9.600
CYC116	-10.398	-0.106	-5.252	7.278
Cyt387	23.759	42.176	32.968	13.022
Dabrafenib (GSK2118436)	74.773	37.679	56.226	26.230
Dacomitinib (PF299804, PF-00299804)	20.949	99.106	60.027	55.265
Danusertib (PHA-739358)	34.127	56.186	45.156	15.597
Dasatinib (BMS-354825)	17.556	46.392	31.974	20.390

Compound	Trial 1 % Inhib.	Trial 2 % Inhib.	AVG % Inhib.	Std Dev
DCC-2036 (Rebastinib)	20.597	21.311	20.954	0.505
Deforolimus (Ridaforolimus)	29.156	49.227	39.191	14.192
Desmethyl Erlotinib (CP-473420)	7.119	4.610	5.865	1.774
Dinaciclib (SCH727965)	4.826	-9.380	-2.277	10.045
Dovitinib (TKI-258)	1.398	1.546	1.472	0.105
Dovitinib Dilactic Acid (TKI258 Dilactic Acid)	19.350	47.430	33.390	19.855
E7080 (Lenvatinib)	16.035	-4.366	5.834	14.426
ENMD-2076	73.178	98.296	85.737	17.761
Enzastaurin (LY317615)	28.327	52.835	40.581	17.330
Erlotinib HCl	5.955	31.186	18.571	17.840
Everolimus (RAD001)	13.827	41.237	27.532	19.382
Flavopiridol HCl	5.490	15.052	10.271	6.762
Foretinib (GSK1363089, XL880)	77.214	83.247	80.231	4.266
GDC-0068	17.439	29.624	23.531	8.616
GDC-0879	76.800	89.175	82.987	8.751
GDC-0941	10.098	40.206	25.152	21.289
GDC-0980 (RG7422)	17.084	28.465	22.774	8.048
Gefitinib (Iressa)	16.313	45.619	30.966	20.722
GI261520A	10.890	-6.919	1.986	12.593
Golvatinib (E7050)	22.790	74.563	48.677	36.609
GR105659X	5.317	9.816	7.566	3.182
GR269666A	-1.039	-28.036	-14.537	19.089
GSK1000163A	0.899	9.002	4.951	5.730
GSK1023156A	-4.854	-3.941	-4.398	0.646
GSK1030058A	1.086	0.112	0.599	0.689
GSK1030059A	10.072	12.352	11.212	1.612
GSK1030061A	1.672	-23.590	-10.959	17.863
GSK1030062A	-2.527	-8.298	-5.412	4.081
GSK1059615	21.866	16.933	19.399	3.488
GSK1070916	13.922	39.493	26.708	18.082
GSK1120212 (Trametinib)	23.057	39.493	31.275	11.622
GSK1173862A	5.829	-2.917	1.456	6.185
GSK1220512A	-6.897	-16.809	-11.853	7.008
GSK1326255A	-5.036	-11.375	-8.205	4.482
GSK1392956A	4.969	5.212	5.090	0.172
GSK1511931A	-0.540	-3.838	-2.189	2.332
GSK1713088A	1.310	-27.591	-13.140	20.436
GSK1751853A	-0.136	-15.810	-7.973	11.083
GSK180736A	1.063	3.511	2.287	1.731
GSK1819799A	-1.317	0.412	-0.452	1.223
GSK182497A	-0.578	-15.186	-7.882	10.329
GSK1838705A	10.408	77.645	44.027	47.544

Compound	Trial 1 % Inhib.	Trial 2 % Inhib.	AVG % Inhib.	Std Dev
GSK1904529A	18.799	30.155	24.477	8.030
GSK192082A	3.841	50.431	27.136	32.944
GSK200398A	5.468	-16.032	-5.282	15.203
GSK204925A	-5.779	-3.750	-4.764	1.435
GSK2110236A	-2.635	1.791	-0.422	3.130
GSK2126458	7.246	18.331	12.789	7.838
GSK2163632A	-5.385	-4.387	-4.886	0.706
GSK2186269A	7.557	7.012	7.284	0.386
GSK2213727A	0.045	-12.031	-5.993	8.539
GSK2219385A	-1.156	0.263	-0.447	1.003
GSK2220400A	-2.981	-1.087	-2.034	1.339
GSK237700A	-15.639	-8.936	-12.287	4.739
GSK237701A	0.180	-7.746	-3.783	5.604
GSK238063A	0.162	-11.286	-5.562	8.095
GSK238583A	0.949	-13.809	-6.430	10.436
GSK248233A	-4.854	-6.998	-5.926	1.516
GSK269962B	-1.132	1.312	0.090	1.729
GSK270822A	9.892	13.189	11.541	2.331
GSK299115A	-5.987	-20.000	-12.993	9.909
GSK300014A	-1.401	-20.256	-10.828	13.332
GSK312948A	0.587	-21.367	-10.390	15.524
GSK317314A	1.619	2.024	1.821	0.286
GSK317315A	8.540	-6.919	0.811	10.931
GSK317354A	9.221	-1.087	4.067	7.289
GSK319347A	10.515	14.811	12.663	3.037
GSK461364	82.507	94.462	88.485	8.453
GSK466314A	7.275	-10.697	-1.711	12.709
GSK466317A	-0.763	-8.586	-4.675	5.532
GSK554170A	23.022	36.636	29.829	9.627
GSK561866B	-0.601	-1.457	-1.029	0.605
GSK571989A	-0.231	-4.514	-2.373	3.028
GSK579289A	-1.156	2.364	0.604	2.489
GSK586581A	15.138	43.007	29.072	19.707
GSK605714A	0.532	-9.486	-4.477	7.084
GSK614526A	78.777	69.295	74.036	6.705
GSK619487A	77.948	75.993	76.971	1.383
GSK620503A	-0.540	-2.163	-1.351	1.148
GSK625137A	-3.597	7.886	2.144	8.119
GSK635416A	5.468	-15.365	-4.949	14.731
GSK690693	98.343	98.454	98.398	0.078
GSK711701A	0.532	2.212	1.372	1.188
GSK718429A	-2.450	0.836	-0.807	2.324

Compound	Trial 1 % Inhib.	Trial 2 % Inhib.	AVG % Inhib.	Std Dev
GSK938890A	73.430	69.103	71.266	3.060
GSK943949A	64.307	68.085	66.196	2.672
GSK949675A	28.249	54.255	41.252	18.389
GSK953913A	0.901	-8.886	-3.993	6.921
GSK969786A	9.532	4.257	6.895	3.730
GSK978744A	-2.635	-4.705	-3.670	1.464
GSK980961A	11.255	5.812	8.533	3.849
GSK994854A	-8.923	-6.234	-7.578	1.902
GW275616X	-6.889	-5.469	-6.179	1.004
GW275944X	0.139	4.657	2.398	3.195
GW276655X	-0.393	0.412	0.010	0.569
GW278681X	-1.220	-28.036	-14.628	18.961
GW279320X	-4.137	-14.445	-9.291	7.289
GW280670X	-4.496	-20.586	-12.541	11.377
GW282449A	0.949	-25.146	-12.098	18.452
GW282536X	-4.830	-15.486	-10.158	7.535
GW282974X	-7.813	-7.953	-7.883	0.099
GW284372X	-1.401	-18.477	-9.939	12.075
GW284408X	6.796	8.288	7.542	1.055
GW290597X	-5.594	-0.884	-3.239	3.331
GW296115X	-12.067	-5.660	-8.863	4.530
GW297361X	0.347	-5.587	-2.620	4.196
GW300653X	-0.899	0.349	-0.275	0.883
GW300657X	3.118	-22.034	-9.458	17.785
GW300660X	11.151	17.097	14.124	4.204
GW301784X	-2.124	-24.701	-13.413	15.965
GW301789X	2.572	-2.340	0.116	3.474
GW301888X	-8.354	-19.787	-14.071	8.084
GW305074X	32.686	41.151	36.919	5.986
GW305178X	-3.802	-9.149	-6.475	3.781
GW335962X	-4.115	-2.985	-3.550	0.798
GW352430A	1.271	-10.386	-4.558	8.243
GW396574X	-2.450	-2.985	-2.718	0.378
GW405841X	11.331	13.468	12.400	1.511
GW406108X	10.791	17.097	13.944	4.459
GW406731X	-7.628	-5.278	-6.453	1.662
GW407323A	1.803	5.804	3.803	2.829
GW410563A	-6.281	-19.589	-12.935	9.410
GW416469X	11.794	-7.808	1.993	13.860
GW416981X	3.660	-16.477	-6.408	14.239
GW427984X	-1.439	-6.071	-3.755	3.276
GW429374A	20.111	24.146	22.129	2.853

Compound	Trial 1 % Inhib.	Trial 2 % Inhib.	AVG % Inhib.	Std Dev
GW432441X	8.036	-1.915	3.060	7.036
GW434756X	26.768	14.593	20.681	8.609
GW435821X	1.439	-1.884	-0.223	2.350
GW439255X	-0.360	-0.209	-0.285	0.106
GW441756X	0.226	-26.257	-13.016	18.726
GW441806A	-2.450	-2.221	-2.336	0.162
GW442130X	-2.796	-14.286	-8.541	8.124
GW445012X	1.439	-3.838	-1.200	3.731
GW445014X	-1.619	-8.025	-4.822	4.530
GW445015X	35.291	15.310	25.301	14.129
GW445017X	-2.518	-3.559	-3.038	0.736
GW450241X	12.714	16.503	14.609	2.680
GW458344X	-2.709	-9.362	-6.035	4.704
GW458787A	0.901	-4.987	-2.043	4.164
GW459057A	-0.678	-14.254	-7.466	9.600
GW461104A	-2.878	6.211	1.667	6.427
GW513184X	7.721	0.072	3.896	5.409
GW549034X	-4.530	-13.830	-9.180	6.576
GW549390X	2.728	2.173	2.451	0.392
GW559768X	-2.485	-20.256	-11.370	12.566
GW561436X	8.633	5.373	7.003	2.305
GW566221B	8.036	1.915	4.975	4.328
GW567808A	1.672	-21.367	-9.848	16.291
GW568326X	5.648	-21.589	-7.970	19.260
GW568377B	10.700	4.912	7.806	4.093
GW569293E	20.666	10.580	15.623	7.131
GW569530A	2.033	-18.477	-8.222	14.503
GW572399X	11.794	1.973	6.883	6.945
GW572401X	-7.998	-3.941	-5.969	2.869
GW572738X	-1.439	-4.676	-3.057	2.289
GW574782A	-5.409	-4.896	-5.153	0.363
GW574783B	-1.582	-18.033	-9.807	11.633
GW575533A	8.276	13.064	10.670	3.386
GW575808A	-7.074	-2.603	-4.838	3.161
GW576484X	-7.194	-16.957	-12.076	6.904
GW576609A	-3.375	-6.043	-4.709	1.886
GW576924A	7.817	-3.362	2.228	7.905
GW577921A	-1.259	3.699	1.220	3.506
GW578748X	13.963	-0.917	6.523	10.522
GW580496A	-0.023	-4.687	-2.355	3.298
GW580509X	2.756	-21.145	-9.194	16.901
GW581744X	4.383	-18.922	-7.269	16.479

Compound	Trial 1 % Inhib.	Trial 2 % Inhib.	AVG % Inhib.	Std Dev
GW583373A	-2.338	6.769	2.215	6.440
GW589933X	-11.882	-5.278	-8.580	4.669
GW589961A	-0.899	-7.467	-4.183	4.644
GW607049C	-3.389	-22.034	-12.711	13.184
GW607117X	15.228	-2.028	6.600	12.202
GW612286X	2.395	-17.811	-7.708	14.287
GW615311X	-3.751	-19.366	-11.559	11.042
GW616030X	4.599	-2.587	1.006	5.081
GW618013X	9.221	7.612	8.416	1.138
GW620972X	-7.194	-5.513	-6.354	1.189
GW621431X	6.214	9.362	7.788	2.225
GW621823A	-4.091	-10.086	-7.088	4.240
GW621970X	0.540	4.536	2.538	2.826
GW622055X	7.998	-13.143	-2.572	14.949
GW627512B	1.063	1.218	1.141	0.109
GW627834A	-5.224	-2.794	-4.009	1.718
GW631581B	14.193	19.752	16.972	3.930
GW632046X	-0.046	-0.693	-0.369	0.457
GW632580X	70.683	57.013	63.848	9.666
GW633459A	9.083	-9.364	-0.141	13.044
GW641155A	-1.687	0.712	-0.487	1.697
GW642125X	-0.524	16.809	8.142	12.256
GW642138X	-2.242	-4.987	-3.614	1.941
GW643971X	-8.172	-13.404	-10.788	3.700
GW644007X	0.360	-2.722	-1.181	2.179
GW654652C	2.750	-0.787	0.981	2.501
GW659386A	-3.777	-6.350	-5.064	1.820
GW659893X	-4.460	-7.987	-6.223	2.493
GW673715X	11.974	7.523	9.749	3.147
GW678313X	0.360	3.699	2.029	2.361
GW679410X	-0.208	6.412	3.102	4.681
GW680191X	-7.990	-15.957	-11.974	5.634
GW680908A	-19.094	-7.571	-13.332	8.148
GW680975X	2.214	-15.810	-6.798	12.745
GW682841X	-8.923	-4.705	-6.814	2.982
GW683109X	-3.351	-2.587	-2.969	0.540
GW683134A	4.856	13.189	9.023	5.892
GW683768X	-7.074	-2.794	-4.934	3.026
GW684626B	-1.259	-7.467	-4.363	4.390
GW693481X	2.196	-1.987	0.104	2.958
GW693881A	10.330	4.612	7.471	4.044
GW693917X	0.540	-4.676	-2.068	3.688

Compound	Trial 1 % Inhib.	Trial 2 % Inhib.	AVG % Inhib.	Std Dev
GW694234A	13.963	-14.032	-0.034	19.795
GW694590A	7.536	10.007	8.771	1.747
GW695874X	4.925	-8.475	-1.775	9.475
GW701032X	11.625	6.412	9.018	3.686
GW701427A	12.336	2.195	7.266	7.171
GW703087X	-13.271	-16.809	-15.040	2.501
GW708336X	-2.518	-1.326	-1.922	0.843
GW708893X	-7.074	-2.412	-4.743	3.296
GW711782X	2.380	-8.886	-3.253	7.967
GW734508X	-3.957	10.956	3.500	10.545
GW743024X	14.583	19.010	16.796	3.131
GW759710A	3.660	-12.698	-4.519	11.567
GW768505A	-8.898	1.912	-3.493	7.644
GW769076X	-0.046	-1.839	-0.943	1.268
GW770220A	10.971	9.281	10.126	1.195
GW770249A	-1.317	-0.487	-0.902	0.587
GW771127A	5.523	-0.487	2.518	4.250
GW772405X	-3.166	2.812	-0.177	4.227
GW775608X	-0.180	2.861	1.341	2.150
GW778894X	-0.948	-0.187	-0.568	0.537
GW779439X	-1.317	2.512	0.597	2.708
GW780056X	-1.401	-21.589	-11.495	14.275
GW780159X	-1.872	-12.186	-7.029	7.293
GW781673X	-2.820	-0.502	-1.661	1.640
GW782612X	1.641	-0.187	0.727	1.293
GW782907X	2.518	-6.071	-1.777	6.073
GW782912X	-0.540	-2.442	-1.491	1.346
GW784307A	-1.711	2.173	0.231	2.746
GW784684X	1.086	4.912	2.999	2.705
GW784752X	-2.338	-8.863	-5.600	4.613
GW785404X	-2.635	1.027	-0.804	2.590
GW785804X	0.347	-3.487	-1.570	2.711
GW785974X	-1.079	-1.326	-1.203	0.174
GW786460X	-3.984	-14.255	-9.119	7.263
GW794607X	3.841	-16.477	-6.318	14.367
GW794726X	-3.957	2.024	-0.967	4.229
GW795493X	-10.402	-15.405	-12.904	3.537
GW796920X	-0.231	-0.693	-0.462	0.326
GW796921X	-1.132	-3.787	-2.460	1.877
GW799251X	8.993	9.002	8.997	0.007
GW801372X	-2.666	-24.924	-13.795	15.738
GW805758X	-1.079	-0.768	-0.923	0.220

Compound	Trial 1 % Inhib.	Trial 2 % Inhib.	AVG % Inhib.	Std Dev
GW806742X	-1.872	-4.687	-3.279	1.990
GW806776X	0.716	-0.787	-0.035	1.063
GW807930X	-2.878	0.349	-1.264	2.282
GW809885X	1.310	-26.257	-12.473	19.493
GW809897X	-3.536	-2.287	-2.912	0.883
GW810372X	4.745	-19.811	-7.533	17.364
GW810576X	-1.619	-3.559	-2.589	1.372
GW811168X	3.841	-9.364	-2.761	9.337
GW811761X	-3.237	-13.050	-8.143	6.938
GW813360X	0.226	-21.367	-10.571	15.269
GW814408X	-0.578	-20.585	-10.581	14.147
GW817394X	1.480	11.064	6.272	6.777
GW817396X	-2.698	-4.117	-3.408	1.004
GW819077X	-9.663	-6.043	-7.853	2.560
GW819230X	0.360	-7.188	-3.414	5.337
GW820759X	7.927	8.811	8.369	0.625
GW824645A	2.214	-12.476	-5.131	10.387
GW827099X	-4.317	-11.654	-7.985	5.188
GW827102X	-7.074	-4.514	-5.794	1.810
GW827105X	6.448	-0.487	2.980	4.904
GW827106X	-5.076	-10.851	-7.964	4.083
GW827396X	-1.132	1.012	-0.060	1.517
GW828525X	-4.712	-9.362	-7.037	3.288
GW828529X	-0.208	-6.487	-3.347	4.440
GW829055X	-4.460	-9.786	-7.123	3.766
GW829115X	-9.353	-8.025	-8.689	0.939
GW829874X	4.564	-11.142	-3.289	11.106
GW829877X	-9.663	-8.717	-9.190	0.668
GW829906X	-6.864	-0.187	-3.526	4.721
GW830263A	-8.183	-3.559	-5.871	3.270
GW830365A	-7.443	-3.176	-5.310	3.017
GW830900A	-1.259	-4.117	-2.688	2.021
GW831090X	8.091	13.637	10.864	3.922
GW831091X	6.818	13.311	10.064	4.591
GW832467X	-1.259	-2.442	-1.851	0.837
GW833373X	-7.258	-5.278	-6.268	1.400
GW837331X	3.957	-8.025	-2.034	8.473
GW843682X	-2.635	-1.839	-2.237	0.563
GW846105X	21.223	12.352	16.787	6.273
GW852849X	-6.889	-6.234	-6.561	0.463
GW853606X	-4.115	-1.457	-2.786	1.879
GW853609X	-9.083	-6.596	-7.839	1.758

Compound	Trial 1 % Inhib.	Trial 2 % Inhib.	AVG % Inhib.	Std Dev
GW856804X	1.310	-15.588	-7.139	11.949
GW861893X	-6.281	-30.258	-18.270	16.955
GW869810X	6.835	21.842	14.338	10.612
GW874091X	-0.786	0.836	0.025	1.147
GW876790X	-6.715	-6.170	-6.443	0.385
Hesperadin	11.370	27.157	19.263	11.163
HMN-214	19.534	7.135	13.334	8.767
IC-87114	-4.956	-10.756	-7.856	4.101
Imatinib (Gleevec)	19.543	12.966	16.254	4.651
Imatinib Mesylate	17.970	41.753	29.861	16.817
IMD 0354	97.324	97.880	97.602	0.393
INCB28060	23.172	10.546	16.859	8.928
Indirubin	-19.455	-3.428	-11.442	11.333
INK 128 (MLN0128)	0.621	-1.325	-0.352	1.376
JNJ-38877605	-6.059	40.206	17.074	32.714
JNJ-7706621	23.032	32.268	27.650	6.531
Ki8751	5.539	27.157	16.348	15.286
KRN 633	14.091	11.395	12.743	1.907
Ku-0063794	-2.624	-6.070	-4.347	2.437
KU-55933	87.157	85.309	86.233	1.306
KU-60019	30.418	24.601	27.509	4.113
KW2449	6.317	7.987	7.152	1.181
KX2-391	39.570	27.571	33.570	8.484
Lapatinib Ditosylate (Tykerb)	30.399	53.608	42.004	16.412
LDN193189	16.030	33.234	24.632	12.165
Linifanib (ABT-869)	16.313	43.557	29.935	19.264
Linsitinib (OSI-906)	74.728	38.918	56.823	25.322
LY2228820	98.445	96.592	97.519	1.310
LY2603618 (IC-83)	26.570	97.019	61.795	49.815
LY2784544	16.812	7.135	11.974	6.843
LY294002	6.784	47.938	27.361	29.100
Masitinib (AB1010)	17.970	55.412	36.691	26.476
MGCD-265	5.151	-13.312	-4.081	13.055
Milciclib (PHA-848125)	14.625	26.677	20.651	8.522
MK-2206 2HCl	86.743	86.082	86.413	0.467
MK-2461	-21.930	-22.099	-22.014	0.119
MK-5108 (VX-689)	91.591	87.281	89.436	3.047
MLN8054	88.814	93.814	91.314	3.536
MLN8237	16.727	69.330	43.028	37.196
Motesanib Diphosphate (AMG-706)	6.784	37.629	22.206	21.811
Mubritinib (TAK 165)	11.814	20.417	16.116	6.084
Neratinib (HKI-272)	19.145	5.431	12.288	9.697

Compound	Trial 1 % Inhib.	Trial 2 % Inhib.	AVG % Inhib.	Std Dev
Nilotinib (AMN-107)	44.070	49.485	46.777	3.828
NU7441 (KU-57788)	21.300	31.148	26.224	6.963
NVP-ADW742	24.599	98.196	61.397	52.041
NVP-BGT226	21.651	35.320	28.486	9.666
NVP-BHG712	-13.483	9.687	-1.898	16.383
NVP-BSK805	66.271	97.914	82.092	22.374
NVP-BVU972	1.003	-3.445	-1.221	3.145
NVP-TAE226	5.972	-12.772	-3.400	13.254
ON-01910	4.373	5.005	4.689	0.447
OSI-027	7.246	26.379	16.812	13.528
OSI-420	7.598	30.849	19.224	16.441
OSI-930	38.581	33.120	35.851	3.861
OSU-03012	85.085	85.825	85.455	0.523
Palomid 529	10.760	25.186	17.973	10.201
Pazopanib HCl	10.927	29.897	20.412	13.414
PCl-32765 (Ibrutinib)	24.813	59.463	42.138	24.501
PD 0332991 (Palbociclib) HCl	56.499	73.711	65.105	12.171
PD0325901	73.485	83.247	78.366	6.903
PD153035 HCl	24.599	47.680	36.140	16.321
PD173074	18.367	28.009	23.188	6.817
PD318088	103.887	96.592	100.240	5.158
PD98059	6.706	6.709	6.707	0.003
Pelitinib (EKB-569)	22.255	7.561	14.908	10.390
PF-00562271	22.003	61.550	41.776	27.964
PF-03814735	19.192	84.799	51.995	46.391
PF-04217903	5.541	40.206	22.874	24.512
PF-04691502	5.490	18.927	12.208	9.502
PF-05212384 (PKI-587)	17.435	27.869	22.652	7.378
PH-797804	27.273	43.070	35.171	11.170
PHA-665752	74.314	81.701	78.007	5.224
PHA-680632	29.640	36.528	33.084	4.870
PHA-767491	12.868	32.638	22.753	13.980
PHA-793887	8.649	-97.231	-44.291	74.869
Phenformin HCl	16.381	38.003	27.192	15.289
PHT-427	101.555	85.517	93.536	11.341
PI-103	5.127	39.691	22.409	24.440
Piceatannol	17.821	41.070	29.446	16.440
PIK-293	6.544	24.292	15.418	12.550
PIK-294	9.354	26.677	18.016	12.249
PIK-75	5.539	-0.532	2.503	4.293
PIK-90	2.430	-4.366	-0.968	4.805
PIK-93	28.086	30.990	29.538	2.054

Compound	Trial 1 % Inhib.	Trial 2 % Inhib.	AVG % Inhib.	Std Dev
PKI-402	6.544	33.830	20.187	19.294
PLX-4720	8.441	39.948	24.195	22.279
Ponatinib (AP24534)	96.890	91.906	94.398	3.524
PP-121	26.570	59.165	42.868	23.048
PP242	9.003	23.398	16.200	10.179
Quercetin (Sophoretin)	11.462	29.359	20.411	12.655
Quizartinib (AC220)	28.086	42.918	35.502	10.488
R406	5.490	12.668	9.079	5.076
R406 (Free Base)	11.370	-10.330	0.520	15.345
R788 (Fostamatinib)	5.490	19.523	12.506	9.923
R935788 (Fostamatinib Disodium, R788)	1.625	18.629	10.127	12.024
Raf265 Derivative	64.163	34.426	49.295	21.027
Rapamycin (Sirolimus)	11.756	48.711	30.233	26.132
Regorafenib (BAY 73-4506)	82.896	88.072	85.484	3.660
Roscovitine (Seliciclib, CYC202)	7.613	38.144	22.878	21.589
Ruxolitinib (INCB018424)	9.815	11.395	10.605	1.117
SAR131675	6.737	-2.597	2.070	6.600
Saracatinib (AZD0530)	11.341	-16.237	-2.448	19.501
SB 202190	0.984	46.392	23.688	32.108
SB 203580	10.098	46.649	28.374	25.846
SB 415286	18.138	86.885	52.512	48.612
SB 431542	-4.816	37.629	16.406	30.013
SB 525334	19.145	0.319	9.732	13.312
SB-210313	-1.132	3.412	1.140	3.213
SB-216385	-0.971	-1.075	-1.023	0.073
SB216763	-3.573	42.526	19.476	32.597
SB-220025-A	-2.338	7.327	2.495	6.834
SB-220455	-2.057	0.712	-0.672	1.958
SB-221466	-5.076	-17.660	-11.368	8.898
SB-223133	-0.948	-3.187	-2.067	1.584
SB-226879	-1.079	-4.676	-2.877	2.543
SB-236687	-6.351	-11.489	-8.920	3.633
SB-239272	-0.208	-7.987	-4.097	5.500
SB-242717	-4.115	-2.221	-3.168	1.339
SB-242718	-2.427	-2.887	-2.657	0.326
SB-242719	17.759	-14.254	1.752	22.636
SB-242721	-2.124	-28.258	-15.191	18.480
SB-245392	-4.460	28.909	12.224	23.596
SB-250715	-2.820	-4.896	-3.858	1.468
SB-251505	-4.317	-1.326	-2.821	2.115
SB-251527	-2.878	-8.025	-5.451	3.640
SB-253226	-12.436	-7.189	-9.813	3.711

Compound	Trial 1 % Inhib.	Trial 2 % Inhib.	AVG % Inhib.	Std Dev
SB-253228	-0.524	21.915	10.696	15.866
SB-254169	27.158	-6.919	10.120	24.096
SB-264865	-3.351	-2.287	-2.819	0.752
SB-264866	0.407	-22.256	-10.925	16.025
SB-278538	2.033	-12.920	-5.443	10.574
SB-278539	-0.719	-7.467	-4.093	4.771
SB-284847-BT	-0.136	-21.589	-10.862	15.170
SB-285234-W	2.395	-14.032	-5.818	11.615
SB-333612	10.252	18.772	14.512	6.025
SB-347804	-2.698	5.094	1.198	5.510
SB-358518	46.001	52.424	49.213	4.542
SB-360741	2.380	10.011	6.196	5.396
SB-361058	-2.265	-2.794	-2.530	0.374
SB-376719	-1.341	-1.839	-1.590	0.352
SB-390523	-1.070	-19.362	-10.216	12.934
SB-390527	-1.259	-6.350	-3.805	3.600
SB-400868-A	1.672	-22.256	-10.292	16.920
SB-409513	9.532	10.119	9.826	0.415
SB-409514	2.937	-18.033	-7.548	14.828
SB-431533	9.712	5.652	7.682	2.871
SB-431542-A	-1.341	0.454	-0.443	1.269
SB-437013	12.529	11.536	12.032	0.702
SB-476429-A	0.949	-20.700	-9.876	15.308
SB590885	67.325	78.241	72.783	7.719
SB-590885-AAD	11.255	16.910	14.083	3.999
SB-610251-B	-2.265	-3.750	-3.008	1.050
SB-614067-R	4.022	10.771	7.397	4.772
SB-630812	23.921	11.235	17.578	8.970
SB-633825	1.079	-3.280	-1.100	3.082
SB-657836-AAA	1.844	18.085	9.964	11.484
SB-675259-M	0.540	-1.326	-0.393	1.319
SB-678557-A	9.776	25.309	17.543	10.984
SB-682330-A	63.850	9.086	36.468	38.724
SB-686709-A	-2.450	3.129	0.339	3.945
SB-698596-AC	2.196	11.811	7.003	6.799
SB-711237	-1.401	-13.143	-7.272	8.303
SB-725317	-6.169	-12.128	-9.148	4.213
SB-732881-H	4.925	-12.476	-3.775	12.304
SB-732941	3.859	4.312	4.086	0.320
SB-734117	9.591	15.111	12.351	3.903
SB-735465	8.902	-9.808	-0.453	13.230
SB-735467	1.491	-20.700	-9.605	15.692

Compound	Trial 1 % Inhib.	Trial 2 % Inhib.	AVG % Inhib.	Std Dev
SB-736290	-8.923	-2.603	-5.763	4.469
SB-736302	-6.715	-12.553	-9.634	4.128
SB-737198	13.269	14.020	13.644	0.531
SB-738482	0.587	-22.256	-10.834	16.153
SB-738561	-0.899	0.628	-0.136	1.080
SB-739245-AC	9.200	6.759	7.980	1.726
SB-739452	-1.132	-5.587	-3.360	3.150
SB-741905	-1.799	3.419	0.810	3.690
SB-742864	3.841	-17.811	-6.985	15.310
SB-742865	-1.502	5.212	1.855	4.748
SB-742865	81.327	69.404	75.365	8.431
SB-743899	0.000	0.907	0.454	0.641
SB-744941	45.956	-8.475	18.741	38.488
SB-750140	-1.980	-7.021	-4.501	3.564
SB-751148	-11.882	-5.087	-8.484	4.804
SB-751399	-3.536	-7.087	-5.311	2.511
SB-772077-B	9.036	6.112	7.574	2.068
SB-814597	-0.540	-4.955	-2.747	3.122
Semaxanib (SU5416)	4.443	-13.196	-4.376	12.473
SGX-523	3.470	32.474	17.972	20.509
SKF-62604	-0.763	7.012	3.124	5.497
SKF-86002-A2	1.672	-19.366	-8.847	14.876
SKF-86055	1.853	-15.143	-6.645	12.018
SNS-032 (BMS-387032)	12.584	46.392	29.488	23.906
SNS-314	95.857	93.041	94.449	1.991
Sorafenib (Nexavar)	100.000	97.423	98.711	1.822
Sotrastaurin (AEB071)	24.701	64.812	44.757	28.362
SP600125	17.590	3.301	10.446	10.104
Staurosporine	105.831	98.722	102.276	5.027
SU11274	43.242	59.278	51.260	11.340
Sunitinib Malate (Sutent)	64.785	82.474	73.630	12.508
TAE684 (NVP-TAE684)	62.299	95.876	79.088	23.742
TAK-285	98.089	99.152	98.620	0.752
TAK-733	13.922	32.042	22.982	12.813
TAK-901	26.219	35.917	31.068	6.857
Tandutinib (MLN518)	19.213	45.361	32.287	18.489
Telatinib (BAY 57-9352)	-0.132	45.753	22.810	32.445
Temsirolimus (Torisel)	-21.802	61.340	19.769	58.791
TG 100713	12.088	5.882	8.985	4.388
TG100-115	49.466	76.571	63.018	19.166
TG101209	25.165	59.463	42.314	24.253
TG101348 (SAR302503)	28.327	49.627	38.977	15.062

Compound	Trial 1 % Inhib.	Trial 2 % Inhib.	AVG % Inhib.	Std Dev
TGX-221	17.590	30.990	24.290	9.476
Thiazovivin	13.703	-1.810	5.946	10.969
Tideglusib	97.707	81.346	89.526	11.569
Tie2 Kinase Inhibitor	51.798	37.380	44.589	10.195
Tivozanib (AV-951)	24.587	22.897	23.742	1.195
Tofacitinib (CP-690550)	13.617	9.274	11.445	3.071
Tofacitinib Citrate (CP-690550 Citrate)	18.968	12.242	15.605	4.756
Torin 1	3.297	-11.500	-4.102	10.463
Torin 2	-11.610	-28.458	-20.034	11.913
TPCA-1	30.053	51.669	40.861	15.285
Triciribine (Triciribine Posphate)	2.641	40.979	21.810	27.109
TSU-68 (SU6668)	100.389	97.018	98.703	2.383
TWS119	2.041	-9.478	-3.719	8.145
Tyrphostin AG 879 (AG 879)	51.457	94.065	72.761	30.128
U0126-EtOH	21.699	80.412	51.055	41.517
Vandetanib (Zactima)	3.884	44.588	24.236	28.782
Vatalinib 2HCl (PTK787)	10.513	39.175	24.844	20.267
Vemurafenib (PLX4032)	-11.565	-47.817	-29.691	25.634
VX-680 (MK-0457, Tozasertib)	40.756	64.691	52.723	16.924
VX-702	12.088	-4.716	3.686	11.883
WAY-600	24.813	49.329	37.071	17.335
WHI-P154	17.057	9.698	13.377	5.204
Wortmannin	3.297	1.219	2.258	1.469
WP1066	98.853	99.152	99.003	0.211
WP1130	98.946	99.702	99.324	0.535
WYE-125132	3.030	12.370	7.700	6.604
WYE-354	-51.992	-66.134	-59.063	10.000
WYE-687	13.570	54.098	33.834	28.658
WZ3146	10.982	15.655	13.318	3.305
WZ4002	5.151	-8.626	-1.738	9.742
WZ8040	93.392	94.888	94.140	1.058
XL147	-5.230	17.784	6.277	16.273
XL-184 (Cabozantinib)	26.670	34.278	30.474	5.380
XL765	26.919	43.344	35.132	11.614
Y-27632 2HCl	12.584	36.598	24.591	16.980
YM201636	30.029	32.268	31.149	1.583
ZM 336372	21.300	37.705	29.502	11.600
ZM-447439	10.927	38.918	24.922	19.792
ZSTK474	9.270	29.897	19.583	14.586

Chapter 3: GW779439X and its pyrazolopyridazine derivatives inhibit the serine/threonine kinase Stk1 and act as antibiotic adjuvants against β-lactam-resistant *Staphylococcus aureus*

Authors and their contributions

Adam J. Schaenzer: Planned, designed, and conducted all experiments unless otherwise noted. Organized data and wrote this manuscript.

Nathan Wlodarchak: Contributed intellectually to the design of the experiments.

David H. Drewry: Performed the chemical synthesis of pyrazolopyridazine derivatives.

William J. Zuercher: Contributed intellectually to the design of the experiments.

Warren E. Rose: Contributed to the selection of *S. aureus* strains and selection of antibiotics for MIC analysis and interpretation of MIC results.

Carla A Ferrer: Performed the chemical synthesis of pyrazolopyridazine derivatives.

John-Demian Sauer: Supervised all research and contributed intellectually to the design of experiments.

Rob Striker: Supervised all research and contributed intellectually to the design of experiments.

This chapter was accepted for publication in ACS Infectious Diseases on July 2018:

> **Schaenzer AJ, Wlodarchak N, Drewry DH, Zuercher WJ, Rose WE, Ferrer CA, Sauer JD, Striker R**. 2018. GW779439X and its pyrazolopyridazine derivatives inhibit the serine/threonine kinase Stk1 and act as antibiotic adjuvants against β-lactam-resistant *Staphylococcus aureus*. ACS Infect Dis. doi: 10.1021/acsinfecdis.8b00136. [Epub ahead of print]. PMID:30059625.

ABSTRACT AND TOC ART

As antibiotic resistance rises, there is a need for strategies such as antibiotic adjuvants to conserve already-established antibiotics. A family of bacterial kinases known as the Penicillin-binding-protein And Serine/Threonine kinase-Associated (PASTA) kinases has attracted attention as targets for antibiotic adjuvants for β-lactams. Here, we report that the pyrazolopyridazine GW779439X sensitizes methicillin-resistant *Staphylococcus aureus* (MRSA) to various β-lactams through inhibition of the PASTA kinase Stk1. GW779439X potentiates β-lactam activity against multiple MRSA and MSSA isolates, including the sensitization of a ceftaroline-resistant isolate to ceftaroline. *In silico* modeling was used to guide the synthesis of GW779439X derivatives. The presence and orientation of GW779439X's methylpiperazine moiety was crucial for robust biochemical and microbiologic activity. Taken together, our data provide a proof of concept for developing the pyrazolopyridazines as selective Stk1 inhibitors which act across *S. aureus* isolates.

For Table of Contents Use Only

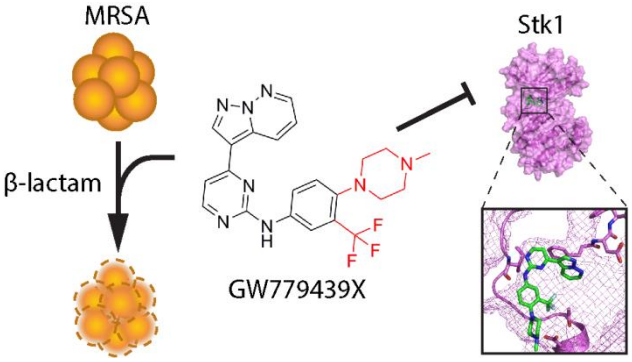

INTRODUCTION

The β-lactams are one of the oldest and most successful classes of antibiotics; however, they are also arguably the most affected by antibiotic resistance. Methicillin-resistant *Staphylococcus aureus* (MRSA) quickly evolved as a form of β-lactam resistance, and it continues to be a relevant threat in the clinic and the community.[7] Unfortunately, resistance to front-line MRSA treatments such as vancomycin, daptomycin, ceftaroline, and linezolid has begun to appear in the clinic,[80,276–278] highlighting the need for novel antibiotic strategies. One such strategy is the utilization of antibiotic adjuvants to preserve the efficacy of current antibiotics.[111] This strategy has already proven successful in the case of β-lactam/β-lactamase inhibitor combination therapy to treat various β-lactamase-expressing gram-negative infections and penicillin-resistant *S. aureus.*[279] However, because MRSA strains utilize the intrinsically β-lactam resistant penicillin-binding protein PBP2A as their primary resistance mechanism, alternative adjuvants are needed to augment β-lactams in these strains.

Over the past decade, there has been an increased interest in exploring bacterial signal transduction mechanisms, in particular those regulated by protein kinases, as potential antibiotic and antivirulence targets.[249,250] While prokaryotic protein kinases were originally thought to only phosphorylate proteins on histidine and aspartate residues,[128,129] it is now well-established that eukaryotic-like serine/threonine protein kinases (eSTKs) are near ubiquitous in bacteria.[135] Of note, a subset of eSTK known as the Penicillin-binding protein And Ser/Thr kinase-Associated (PASTA) kinases has been demonstrated to be crucial for cell wall homeostasis,[213–217,222–224,237,239,280] virulence,[223,229,250] biofilm formation,[221] germination,[192,218] and metabolism[219,220] in a variety of *Firmicutes* and *Actinobacteria*. Intriguingly, while the PASTA kinase PknB is essential for the viability of *Mycobacterium tuberculosis,*[183,184] deletion of PknB homologs in the *Firmicutes* decreases resistance to the β-lactam antibiotics (reviewed in [9]). This characteristic makes the PASTA kinases attractive targets for potential β-lactam adjuvants.

Eukaryotic protein kinases have been extensively studied and successfully exploited in the clinic as therapeutic targets for anti-cancer treatments.[157] As such, there is established knowledge and resources such as small-molecule protein kinase inhibitor libraries that can be repurposed for the identification of eSTK-targeting scaffolds. We and others have published multiple PASTA kinase inhibitors.[237,245–248,254,280] Here, we report that GW779439X, a pyrazolopyridazine identified in a small-molecule kinase inhibitor library screen, increases the sensitivity of the MRSA strain LAC to β-lactam antibiotics via inhibition of the PASTA kinase Stk1. In addition, GW779439X also sensitizes a variety of other MRSA and further enhances β-lactam activity against methicillin-sensitive *S. aureus* (MSSA) isolates in a similar fashion. Finally, using a series of GW779439X congeners we propose a preliminary structure-activity relationship (SAR) for the pyrazolopyridazine pharmacophore's activity against the Stk1 kinase domain. Taken together, our data demonstrate that GW779439X and the pyrazolopyridazines are promising lead compounds for further optimization as Stk1 inhibitors as adjuvants to β-lactams for certain MRSA strains.

RESULTS

GW779439X sensitizes MRSA to β-lactams

In a variety of gram-positive pathogens, including *S. aureus*, genetic deletion of the PASTA kinases results in increased sensitivity to β-lactam antibiotics.[213,223,224,237] Through a kinase inhibitor library screen, we have previously identified the compound GSK690693 as a potent inhibitor of the *Listeria monocytogenes* PASTA kinase PrkA which sensitizes the organism to β-lactams.[280] However, GSK690693 showed only minor biochemical activity against the *S. aureus* PASTA kinase Stk1 and no appreciable activity microbiologically as a β-lactam adjuvant against *S. aureus*. Therefore, to identify inhibitors of Stk1 that could function as β-lactam adjuvants, we screened 1,147 small molecule kinase inhibitors from the GlaxoSmithKline Published Kinase Inhibitor Sets 1 and 2 (PKIS1 and PKIS2)[175,252]and Selleck kinase inhibitor

libraries against the wild-type MRSA strain LAC in the presence of a sublethal dose of ceftriaxone. Thirty-one compounds potentiated ceftriaxone activity three standard deviations or greater than the library average (**Figure 3.1A**). Of these, twenty-five compounds failed to show a dose response in secondary screens, and an additional three demonstrated β-lactam independence. The three remaining compounds were NVP-ADW742, BI-2536, and GW779439X (**Supplemental Figure S3.1**). Of these, we selected GW779439X (**Figure 3.1A**, cyan dot, and **3.1B**) for further analysis both because it was the most potent compound in our secondary screens and due to the availability of molecular derivatives (**Figure 3.1A**, red dots).

Genetic deletion of *pknB* (which expresses Stk1 and will be referred to as *stk1* throughout this manuscript) has been shown to decrease resistance of MRSA to a variety of β-lactams.[213,223,247] We therefore hypothesized that if GW779439X acts through an Stk1-dependent mechanism, it should be able to potentiate other β-lactams beyond ceftriaxone. To test this hypothesis, we determined the minimum inhibitory concentration (MIC) values of a variety of antibiotics against LAC in the presence and absence of 5 μM GW779439X. Importantly, GW779439X has no intrinsic effects on bacterial growth below 20 μM (**Supplemental Figure S3.2**). As can be seen in **Table 3.1**, GW779439X was able to potentiate the activity of all β-lactams tested, particularly the penicillinase-resistant penicillins oxacillin and nafcillin to an MIC considered susceptible to these agents. Intriguingly, GW779439X also increased sensitivity 2-fold to ceftaroline, one of the few clinically-available β-lactams with anti-MRSA activity. Importantly, GW779439X was unable to further sensitize a Δ*stk1* mutant to any of the β-lactams tested. Consistent with the PASTA kinase literature, the MICs of non-β-lactams such as vancomycin or chloramphenicol remained unaffected in any condition tested. Taken together, these data support the hypothesis that GW779439X potentiates a variety of β-lactam antibiotics in an Stk1-dependent manner, and shifts the β-lactam class collectively towards sensitivity.

GW779439X biochemically inhibits Stk1 *in vitro*

Since GW779439X was originally designed to be a eukaryotic kinase inhibitor[281] and its effects on β-lactam MICs are Stk1-dependent, we hypothesized that GW779439X acts through direct inhibition of the Stk1 kinase domain. Using autoradiography, we monitored the *in vitro* kinase activity of the purified Stk1 kinase domain in the presence of increasing concentrations of GW779439X. Strikingly, we observed a robust inhibition of Stk1 autophosphorylation and phosphorylation of the nonspecific phosphosubstrate myelin basic protein (MBP) at concentrations of GW779439X as low as 2 μM (**Figure 3.2**). This is in contrast to the compound SB-747651A, a compound which failed to sensitize LAC to ceftriaxone in our library screen and which we've previously demonstrated has no intrinsic activity against the *L. monocytogenes* PASTA kinase PrkA (**Figure 3.2**).[280] When taken with our broth culture experiments, these data support the hypothesis that GW779439X potentiates β-lactam activity via direct inhibition of Stk1.

GW779439X potentiates oxacillin activity against various *S. aureus* strains

LAC was chosen as the MRSA strain for our primary screen for multiple reasons. It is a representative of the USA300 clonal lineage, and it is a particularly virulent and prevalent pulsed-field gel electrophoresis (PFGE) type among community-acquired MRSA infections in the United States.[282] To determine if GW779439X would be effective against additional clonal lineages, we determined the MIC of oxacillin against a variety of MRSA and MSSA isolates in the presence and absence of GW779439X (**Table 3.2**). At 5 μM GW779439X, we observed potentiation of oxacillin against representatives of PFGE types USA400, USA600, and USA800 as well as the hospital-acquired MRSA strain COL. Strikingly, GW779439X lowered the MIC at least 512-fold against ATCC BAA-2686, a MRSA isolate isolated from the blood of a patient with cystic fibrosis which evolved high-level resistance to ceftaroline; this phenotype was also observed when tested with ceftaroline (**Figure 3.3A**) in a ceftaroline-dependent manner (**Figure**

3.3B). Finally, GW779493X was also able to modestly potentiate oxacillin activity against the MSSA isolates Newman and NCTC8325 (**Table 3.2**). These data demonstrate that a broad range of *S. aureus* isolates are susceptible to β-lactam potentiation by GW779439X, and combination therapy with kinase inhibitors may represent a particularly powerful therapeutic option in the context of ceftaroline-resistant *S. aureus*.

A subset of pyrazolopyridazines retain biochemical and microbiologic activity

Since GW779439X was originally designed to target human CDK4, its direct utility as an antibiotic adjuvant is limited. In order to rationally design modifications which would minimize off-target effects, a better understanding of the GW779439X-Stk1 SAR is needed. To focus our efforts, we utilized the program Autodock4.2 to dock GW779439X into the active site of the Stk1 kinase domain (**Figure 3.4A**). GW779439X's core scaffold consistently docks into the Stk1 active site in a fashion similar to that of other pyrazolopyridazines in CDK2[281] with the aminopyrimidine moiety participating in a hydrogen bonding pattern with the backbone atoms of Ile90. The pyrazolopyridazine head pivots almost perpendicular to the active site floor, allowing for a potential parallel-displaced pi-stacking interaction with Phe150. The *p*-*N*-methyl piperazine tail reaches out of the active site and appears to anchor to Glu97 via salt bridge. Finally, the *m*-trifluoromethyl group comes to rest against Thr94. This model gave us an initial reference for selecting chemical modifications of GW779439X.

In our primary kinase inhibitor library screen (**Figure 3.1**), the pyrazolopyridazine family members as a group possessed modifications at four locations (**Figure 3.4B**). Based on our *in silico* model, we speculated that addition of sidechains at positions R2 and R4 would not be tolerated, so we chose to leave these positions unmodified. We retained the pyridazine nitrogen at the R3 position in order to remain consistent with GW779439X. Since we hypothesized the *p*-*N*-methyl piperazine is important for a stabilizing salt bridge with Glu97, we restricted the R1 position to the original aniline and allowed for modifications on this moiety at an R5 and R6

position which would come within proximity of Glu97 (**Figure 3.4C**). Utilizing **Scheme 3.1**, we ultimately synthesized seven compounds with R5 and R6 modifications to test both biochemically and microbiologically (**Table 3.3**).

Using autoradiography, we first tested the ability of our compound series to inhibit Stk1 activity *in vitro*. At an inhibitor concentration of 2 μM, the compounds CAF052 and CAF078 robustly inhibited Stk1 kinase activity like the GW779439X control (**Figure 3.5A**). In contrast, CAF070, CAF075, and CAF089 possessed very little activity at this concentration. The final two compounds, CAF045 and CAF077, displayed an intermediate phenotype with partial Stk1 inhibition. From these data, we hypothesized that the inhibition profile of our compound series would directly translate to the potentiation of oxacillin in broth culture. When tested against LAC with a sublethal concentration of oxacillin and an inhibitor concentration of 20 μM, the compounds CAF045, CAF052, CAF077, and CAF078 mimicked the GW779439X control with a near 100% inhibition of growth relative to bacteria treated with oxacillin alone (**Figure 3.5B**). In agreement with our autoradiography data, the compounds CAF070, CAF075, and CAF089 were significantly less effective at potentiating oxacillin in broth culture. To determine the potencies of the four most-efficacious compounds relative to GW779439X, we treated LAC with a sublethal dose of oxacillin and decreasing concentrations of the kinase inhibitors. We discovered that CAF078 had a potency similar to GW779439X, achieving complete inhibition of bacterial growth at submicromolar concentrations (**Figure 3.5C**). On the other hand, CAF052 was 4-fold less potent than GW779439X in broth culture. CAF045 and CAF077 were both 32-fold less potent than GW779439X with near-complete inhibition of growth occurring only as low as 10 μM. Taken together, our data demonstrate that multiple family members of the pyrazolopyridazine class of compounds retain both biochemical and microbiologic activity, though with a wide variation in potency. Importantly, our data suggest that the presence of the positive charge on the *p*-*N*-methyl piperazine tail is important for biochemical activity.

DISCUSSION

With the current rise of antibiotic resistance, it has become imperative that novel antibiotic strategies are developed for use in the clinic. The concept of antibiotic adjuvants (*i.e.* compounds which enhance the activity of established antibiotics) has gained considerable attention within the past decades,[111] particularly after the introduction and clinical success of the β-lactamase inhibitors. Due to their roles in virulence and β-lactam resistance, a highly conserved family of bacterial kinases known as the PASTA kinases are attractive targets for the development of β-lactam adjuvants.[250] Here, we present our findings on GW779439X, a pyrazolopyridazine protein kinase inhibitor which potentiates β-lactam activity against MRSA via inhibition of the PASTA kinase Stk1.

The intracellular kinase domain of the PASTA kinases has high structural homology to eukaryotic protein kinases, allowing for the knowledge and resources used in the eukaryotic kinase field to be easily repurposed for identification and development of bacterial PASTA kinase inhibitors. However, this also means that extra care must be taken to avoid nonspecific activity against eukaryotic kinases. Nonetheless, it is feasible to generate kinase inhibitors with relative selectivity amongst eukaryotic kinase targets,[154,155] and we have previously identified an inhibitor that can discriminate between *S. aureus* Stk1 and *L. monocytogenes* PrkA, two PASTA kinases with greater similarity than that between eukaryotic kinases and PASTA kinases.[280] This strongly suggests that PASTA kinase inhibitors with minimized off-target effects can be generated. Furthermore, by coadministrating a relatively selective antibiotic adjuvant, there is at least the theoretical potential of focusing the β-lactam activity against the target pathogenic species and blunting the effect of the β-lactam on microbiota that do not have a PASTA kinase whose catalytic active site is highly similar to the target PASTA kinase.

To identify inhibitors of Stk1, we screened three small-molecule ATP-competitive kinase inhibitor libraries (1,147 compounds total) against wild-type LAC in the presence of sublethal ceftriaxone. We chose a microbiologic approach rather than a biochemical approach as our

primary screen in order to focus our efforts on lead compounds which could access the bacterial cytosol, a hurdle that has proven challenging in biochemical screens for inhibitors of the *M. tuberculosis* PASTA kinase PknB.[245] Of the 31 hits in our primary screen, we selected GW779439X as our lead compound due to its dependence on the presence of a β-lactam and Stk1, its dose responsiveness, and the accessibility of synthesized derivatives. GW779439X possesses a pyrazolopyridazine scaffold that is structurally unique compared to other previously identified Stk1 inhibitors.[247,248,254] The sulfonamide and quinazoline scaffolds identified by Vornhagen *et al.* and Kant *et al.*, respectively, were absent from the inhibitor libraries we screened. On the other hand, SB-202190, an inhibitor identified by Boudreau *et al.*, was present in the Selleck library but failed to potentiate ceftriaxone activity against LAC, potentially due to differences in screening conditions (ceftriaxone in tryptic soy broth [TSB] reported here and oxacillin in cation-adjusted Mueller-Hinton media reported in Boudreau *et al*). We validated this hypothesis by testing the compound in both conditions and found that these conditions were indeed the cause of the discrepancy (**Supplemental Figure S3.3**). This data suggests that more potential Stk1 inhibitors could be identified by screening small molecule libraries under various growth conditions.

GW779439X potentiates the activity of a variety of β-lactam antibiotics in an Stk1-dependent manner. Interestingly, GW779439X can sensitize LAC to β-lactams to the same extent as a Δ*stk1* mutant. This is in contrast to our previous findings with the compound GSK690693 against *L. monocytogenes* which could not reach the same levels of sensitivity as a Δ*prkA* mutant.[280] This suggests that either GW779439X has a greater efficacy against Stk1 than GSK690693 against PrkA, or that the β-lactam phenotypes of Stk1 are solely dependent on its kinase activity while PrkA regulates additional effects which are independent of its enzymatic activity. The latter case would suggest that the functions of the Stk1 and PrkA signaling circuits do not completely overlap. Introduction of kinase-dead complements into their respective kinase mutants would shed light on this hypothesis.

It is intriguing that pharmacologic inhibition or genetic deletion of Stk1 potentiates different β-lactams to varying degrees. Ceftriaxone is only augmented 2-fold, while nafcillin and oxacillin (the mainstay therapies for MSSA infections) are more strikingly potentiated to below their respective clinical break points. These data suggest that while Stk1 inhibition may not be able to clinically sensitize MRSA to all β-lactams, it could allow for treatment of MRSA with a traditional MSSA therapy.

GW779439X is able to potentiate the activity of oxacillin against various *S. aureus* isolates, including both MRSA and MSSA isolates, but the potentiation is clearly strongest in PBP2A-containing strains. With the exception of USA800, the hospital-acquired MRSA isolates (COL, USA600) appear relatively recalcitrant towards GW779439X treatment while the community-acquired MRSA isolates (USA300, USA400) are sensitized by GW779439X to below the oxacillin clinical breakpoint. USA800 is also sensitized to oxacillin though it is a hospital-acquired MRSA isolate. Further investigation is needed to elucidate the mechanism responsible for the variations in β-lactam sensitization among MRSA isolates.

GW779439X's ability to sensitize the ceftaroline-resistant MRSA strain BAA-2686 to both oxacillin and ceftaroline is quite striking and brings their MICs well below the clinical susceptibility breakpoints of ≤ 2 μg/mL and ≤ 1 μg/mL, respectively. Ceftaroline's unique mechanism of action involves binding of a ceftaroline molecule into an allosteric binding site on PBP2A, leading to a conformational change which exposes the transpeptidase active site to acylation by a second ceftaroline molecule.[283] Low-level resistance to ceftaroline (MIC >1 – 8 μg/mL) can be achieved by select mutations in the allosteric binding site.[81,83] High-level resistance (MIC > 32 μg/mL) can be achieved directly by mutations in the PBP2A active site,[80] or indirectly by PBP2A-independent mechanisms such as mutations in PBP2, PBP4, LytD, and GdpP.[82,84] Although the exact resistance mechanism is unknown in BAA-2686, the exquisite augmentation of ceftaroline by GW779439X might hint at underlying players in the Stk1 signaling cascade.

In order to begin developing a GW779439X-Stk1 SAR, we synthesized seven pyrazolopyridazine derivatives with a focus on modifications to the *p*-*N*-methyl piperazine tail and *m*-trifluoromethyl sidechain. In general, we discovered that modifications to the *p*-*N*-methyl piperazine were detrimental to biochemical activity as demonstrated by the greatly reduced activity of CAF070 and CAF075 in both our *in vitro* and microbiology assays. This could be due to the loss of a stabilizing salt bridge with Glu^{97} by swapping the positively-charged piperazine for an electronegative sidechain (CAF070) and/or by the inability of a sidechain that can reach Glu97 (CAF075) (**Supplemental Figure S3.4**). This could be further validated by reversing or removing the charge at position 97. CAF077 is unique in the fact that it simply shifts the positive charge into the *meta*- position on the aniline moiety rather than completely eliminate it. While this is ultimately a detriment to biochemical activity, some intermediate inhibition is salvaged possibly by the formation of a hydrogen bond with Thr94 (**Supplemental Figure S3.4**). However, this moderate decrease in biochemical activity is enough to potently decrease the compound's microbiologic potency. These findings with CAF077 support the hypothesis that it is not only the presence of a positive charge, but also its optimal positioning on the sidechain that is important to stabilize the compound in the active site. On the other hand, modifications to the *m*-trifluoromethyl sidechain appear to be generally more forgiving; replacement with other electronegative sidechains such as fluorine (CAF052) or nitrile (CAF078) retain both biochemical and microbiologic activity on par with GW779439X. Interestingly, replacement with a nonpolar methyl sidechain (CAF089) greatly diminishes biochemical activity and abolishes microbiologic activity, while a complete lack of a sidechain (CAF045) creates an intermediate phenotype. We speculate that an electronegative sidechain at this position might add an additional stabilizing hydrogen bond with Thr94 (**Supplemental Figure S3.4**). A mutation of Thr94 to a nonpolar residue such as alanine might shed light on this hypothesis. Future work will be needed to elucidate the effects of modifications to the pyrazolopyridazine head.

Besides β-lactam sensitivity, Stk1 also regulates virulence in *S. aureus* (reviewed in [250]). Overall, there is conflicting evidence on the effects of Stk1 interference, with certain strains and infection models showing Stk1 as a positive regulator of virulence while others reveal Stk1 to be a negative regulator of virulence. While an increase in virulence due to Stk1 inhibition may be problematic, the tradeoff with increased sensitivity to antibiotics still needs to be considered. In any case, there is yet to be conclusive evidence about the effects of dysregulation of Stk1 on β-lactam therapy in an animal model of infection, a crucial experiment needed for further development of PASTA kinase inhibitors as β-lactam adjuvants.

Although it is well established that interference with PASTA kinase signaling augments β-lactam activity, our understanding of the exact signaling circuits required to maintain β-lactam resistance remains incomplete. Bacterial eSTKs have been found to phosphorylate a wide variety of candidate proteins across species such as DivIVA/Wag31,[266] Yvck/CuvA,[284,285] MurC,[264] VraR,[225] IreB,[239] and GpsB.[214] Of note, Stk1 has been found to play a role in regulating the activity of the class-A β-lactamase BlaZ in select *S. aureus* strains.[248] However, bacteria which lack a β-lactamase (such as *L. monocytogenes* and the *S. aureus* strains COL and Newman) are still sensitized to β-lactams when PASTA kinase signaling is disrupted,[223,237] notably against β-lactams that are resistant to hydrolysis by BlaZ like oxacillin and nafcillin. Overall, the current literature suggests that Stk1 and other PASTA kinases most likely act as master regulators of various components of the cell wall synthesis and division machinery, further emphasizing their attractiveness as antibiotic adjuvant targets.

In summary, we have identified the compound GW779439X as a novel inhibitor of the *S. aureus* PASTA kinase Stk1. We have demonstrated that GW779439X potentiates the activity of β-lactam antibiotics against various MRSA and MSSA isolates, some even crossing the breakpoint from resistant to sensitive. Finally, we have determined the importance of the *p*-*N*-methyl piperazine sidechain for biochemical and microbiologic activity. Future work with the pyrazolopyridazine scaffold may lead to the design of compounds with better selectivity for

staphylococcal PASTA kinases as antibiotic adjuvants to restore β-lactam activity and prolong the clinical utility of newer agents such as ceftaroline.

MATERIALS AND METHODS

Bacterial strains and growth conditions

All bacterial strains used in this study are listed in **Table S3.1**. Generation of the Δ*stk1* mutant strain was achieved as previously described.[280] All *S. aureus* strains were grown in tryptic soy broth (TSB) medium at 37°C shaking overnight until stationary phase. Cultures were then back-diluted to an OD_{600} of 0.06 for broth growth experiments. *Escherichia coli* strains XL-1Blue and Rosetta BL21 were used for subcloning and protein expression, respectively. When needed, chloramphenicol (Sigma-Aldrich) was used at 10 μg/mL and carbenicillin (Sigma-Aldrich) was used at 100 μg/mL.

Library screen

The PKIS1, PKIS2, and Selleck libraries were obtained via the University of Wisconsin Carbone Cancer Center's Small Molecule Screening Facility. Overnight cultures were back-diluted 1:100 into fresh TSB medium containing 10 μg/mL ceftriaxone and either library compounds (final concentration: 20 μM in 2% DMSO) or DMSO (final concentration: 2%). Growth was measured as an optical density at 600 nm (OD_{600}) on 15 minute intervals for 12 hours in a 96-well format using an Eon microplate spectrophotometer or Synergy HT microplate spectrophotometer (BioTek Instruments, Inc, Winooski, VT) (growth conditions: 37°C, linear shaking). Each compound was screened twice. Percent inhibition was calculated as $(1 - (OD_X / OD_{CRO})) * 100$, where OD_X is the endpoint OD_{600} for a culture treated with both ceftriaxone and compound X, and OD_{CRO} is the endpoint OD_{600} for a culture treated with ceftriaxone alone. Compounds that inhibited growth three standard deviations greater than the library mean were further verified for dose responsiveness and β-lactam dependence.

Minimum Inhibitory Concentration (MIC) determination

S. aureus overnight cultures were back-diluted to an OD_{600} of 0.06 into cation-adjusted Mueller-Hinton (CA-MH) medium containing 2-fold dilutions of the tested antibiotics in the presence or absence of 5 µM GW779439X. The CA-MH was supplemented with 2% NaCl when determining the MICs of nafcillin, oxacillin, or ceftaroline as per recommendation by the Clinical and Laboratory Standards Institute.[286] OD_{600} was measured to monitor growth of the microdilutions for 12 hours (with the exception of the *S. aureus* strain BAA-2686, which was grown for 24 hours due to its relatively long lag phase). MICs were defined as the lowest concentration of antibiotic required to prevent turbidity in broth visible by eye. Each MIC experiment was performed at least three times.

Kinase domain protein expression and purification

The *stk1* kinase domain (residues 1-348) was subcloned into the expression vector pGEX-2T as previously described.[237] Expression and purification of the GST-tagged Stk1 kinase domain was performed as previously described.[280] Briefly, protein expression was induced by addition of 1 mM Isopropyl β-D-1-thiogalactopyranoside (IPTG) overnight at 23°C. Cells were lysed by sonication, and the lysates were processed through GS4FF affinity resin columns. The GST tag was then cleaved by thrombin digestion, and liberated Stk1 kinase domain was further processed through a HiPrep Q16 10FF anionic exchange column and a Sephadex75 size-exclusion column to purity.

***In vitro* protein phosphorylation**

2 µM kinase domain, 10 µM MBP (Novatein Biosciences, Woburn, MA), and various concentrations of kinase inhibitors were incubated at 37°C for 10 minutes, then added to a mixture of 10 mM Tris pH 7.4, 150 mM NaCl, 50 µM $MnCl_2$, 50 µM ATP, and 1 µCi of [γ-^{32}P]

ATP. Reactions were incubated at 37°C for 30 minutes and terminated by the addition of 6X SDS loading buffer. Samples were run on an SDS-PAGE gel then fixed for 2 hours in fixation solution (40% methanol, 5% glycerol, 10% glacial acetic acid). Fixed gels were dried for 1 hour and blots visualized by autoradiography.

In Silico Modeling – In silico modeling was performed as previously described.[280] Briefly, the primary sequence of the Stk1 kinase domain (residues 1-270) was threaded onto the crystal structure of the kinase domain of PknB from *M. tuberculosis* (PDB ID 1O6Y) using the Phyre2 server's one-to-one threading.[268] Gatsieger-Huckel charges were added to Stk1 and compounds using SYBYL-X1.2.[269] Compounds were docked into a 66x66x66 unit grid encompassing the kinase's active site cleft using the docking program Autodock's Lamarckian genetic algorithm.[271] Models were visualized using PyMOL.[272]

Compound synthesis

Synthesis of 2-Chloro-4-((trimethylsilyl)ethynyl)pyrimidine (Compound **2**) - To a solution of $Pd(dppf)_2Cl_2$ (200 mg, 0.3 mmol), PPh_3 (200 mg, 0.7 mmol) and 2,4-dichloropyrimidine (1.0 g, 7.0 mmol) (Compound **1**) in anhydrous THF (25 mL) was added Et_3N (33 mL) under a N_2 atmosphere. Nitrogen was bubbled into the solution for 20 min before the addition of (trimethylsilyl)acetylene (1.0 mL, 7.0 mmol) followed by CuI (100 mg, 0.7 mmol). The mixture was then heated at 70 °C for 10 min. Upon completion, the mixture was cooled to room temperature, filtered and the solvent was removed under rotary evaporation. Purification by silica gel flash column chromatography (hexane:EtOAc 8:2) afforded 2-Chloro-4-((trimethylsilyl)ethynyl)pyrimidine (Compound **2**) (920 mg, 4.4 mmol, 68%) as a brown solid.

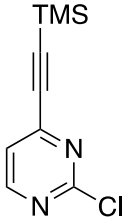

m.p. 49–50 °C; ^{1}H NMR (400 MHz, $CDCl_3$) δ 8.58 (d, *J* = 5.0 Hz, 1H), 7.31 (d, *J* = 5.0 Hz, 1H), 0.28 (s, 9H); ^{13}C NMR (100 MHz, $CDCl_3$) δ 161.6, 159.6, 152.8, 122.0, 103.7, 100.2, 0.5; LRMS *m/z* 211 $[M+H]^+$.

***Synthesis of* 3-(2-Chloropyrimidin-4-yl)pyrazolo[1,5-*b*]pyridazine** (Compound **4**)

Hydroxylamine-O-sulfonic acid (1.2 g, 10.7 mmol) was dissolved in H_2O (3 mL) and the pH was adjusted to 5-6 by the addition of a 2.5 M solution of $NaHCO_3$. Pyridazine (Compound **3**) (514 μL, 7.1 mmol) was added dropwise, and the solution was stirred at 70 °C for 2 hours. After cooling at room temperature, the solution was neutralized to pH 8-9 by the addition of a 2.5 M solution of $NaHCO_3$. Then, a solution of 2-chloro-4-[2-(trimethylsilyl)ethynyl]pyrimidine (Compound **2**) (0.5 g, 2.4 mmol) in CH_2Cl_2 (4 mL) was added, followed by a solution of KOH (0.8 g, 14.2 mmol) in H_2O (7 mL). The resulting solution turned dark/red and the stirring was continued for 18 h at room temperature. Upon completion, the mixture was diluted with CH_2Cl_2 (15 mL) and layers were separated. The organics were further extracted from the aqueous with CH_2Cl_2 (3 x 20 mL) and the combined organics were washed with brine (50 mL), dried over Na_2SO_4, filtered and the solvent was removed by rotary evaporation. Purification by silica gel flash column chromatography (hexane:EtOAc 7:3) afforded 3-(2-Chloropyrimidin-4-yl)pyrazolo[1,5-*b*]pyridazine (Compound **4**) (0.3 g, 1.4 mmol, 58%) as a brown solid.

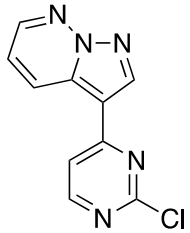

m.p. >250 °C; ^{1}H NMR (400 MHz, DMSO-d_6) δ 9.03 (s, 1H), 8.90 (dd, *J* = 9.0, 1.9 Hz, 1H), 8.73 (d, *J* = 5.3 Hz, 1H), 8.69 (dd, *J* = 4.5, 1.9 Hz, 1H), 8.06 (d, *J* = 5.4 Hz, 1H), 7.58 (dd, *J* = 9.1, 4.5 Hz, 1H); ^{13}C NMR (100 MHz, DMSO-d_6) δ 161.8, 160.3, 160.1, 144.6, 140.7, 132.9, 128.9, 120.2, 115.4, 108.3; LRMS *m/z* 232.0 $[M+H]^+$.

General Procedure 1 - To a solution of 3-(2-chloropyrimidin-4-yl)pyrazolo[1,5-*b*]pyridazine (Compound **4**) (1.0 mmol) in *sec*-BuOH (0.05 M) was added the aniline of interest (1.3 mmol) followed by TFA (3.7 M). The resulting mixture was stirred at 100 °C for 18 hours. Upon completion, the mixture was diluted with EtOAc and a saturated solution of $NaHCO_3$ was added. The layers were separated and the organics were further extracted from the aqueous with EtOAc (× 2). The combined organics were washed with brine, dried over Na_2SO_4, filtered and the solvent was removed by rotary evaporation. Purification by silica gel flash column chromatography (hexane:EtOAc or CH_2Cl_2:MeOH mixtures) afforded the desired Compound **5**.

N-(4-(4-Methylpiperazin-1-yl)phenyl)-4-(pyrazolo[1,5-b]pyridazin-3-yl)pyrimidin-2-amine (***CAF045***)

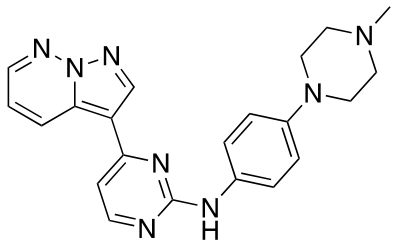

Reaction of 3-(2-chloropyrimidin-4-yl)pyrazolo[1,5-*b*]pyridazine (Compound **4**) (50 mg, 0.22 mmol), 4-(4-methylpiperazin-1-yl)aniline (45 mg, 0.24 mmol) and TFA (58 μL) in *sec*-BuOH (4 mL) according to General Procedure **1** afforded the title compound after purification by silica gel flash column chromatography (CH_2Cl_2:MeOH 9:1) (48 mg, 0.12 mmol, 70%) as a yellow solid. m.p. 150 °C decomp; ^{1}H NMR (400 MHz, Methanol-d_4) δ 9.03 (dd, *J* = 9.1, 1.9 Hz, 1H), 8.67 (s, 1H), 8.50 (dd, *J* = 4.5, 2.0 Hz, 1H), 8.36 (d, *J* = 5.4 Hz, 1H), 7.56–7.54 (m, 2H), 7.30 (dd, *J* = 9.1, 4.5 Hz, 1H), 7.20 (d, *J* = 5.3 Hz, 1H), 7.09–7.06 (m, 2H), 3.29–3.26 (m, 4H), 2.77–2.74 (m, 4H), 2.46 (s, 3H); ^{13}C NMR (100 MHz, $CDCl_3$) δ 161.0, 159.9, 158.4, 148.1, 143.1, 139.4, 133.2, 131.9, 130.1, 123.2, 117.8, 116.9, 111.0, 107.4, 55.3, 49.9, 46.3; LRMS *m/z* 387 $[M+H]^+$; HRMS (ESI) calculated for $[M+H]^+$: 387.1967, found 387.20447

*N-(3-Fluoro-4-(4-methylpiperazin-1-yl)phenyl)-4-(pyrazolo[1,5-b]pyridazin-3-yl)pyrimidin-2-amine (**CAF052**)*

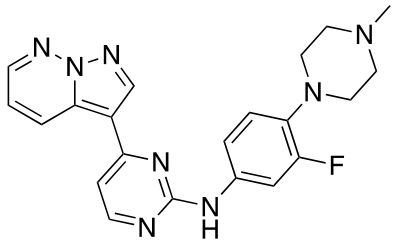

Reaction of 3-(2-chloropyrimidin-4-yl)pyrazolo[1,5-*b*]pyridazine (Compound **4**) (35 mg, 0.15 mmol), 3-fluoro-4-(4-methylpiperazin-1-yl)aniline (35 mg, 0.17 mmol) and TFA (41 μL) in *sec*-BuOH (3 mL) according to General Procedure **1** afforded the title compound after purification by silica gel flash column chromatography (CH_2Cl_2:MeOH 9:1) (30 mg, 0.15 mmol, 49%) as a brown solid.

m.p. 170 °C decomp; ^{1}H NMR (400 MHz, Methanol-d_4) δ 9.15 (dd, *J* = 9.2, 1.9 Hz, 1H), 8.70 (s, 1H), 8.53 (dd, *J* = 4.4, 2.0 Hz, 1H), 8.43 (d, *J* = 5.3 Hz, 1H), 7.85 (bs, 1H), 7.68 (dd, *J* = 14.8, 2.5 Hz, 1H), 7.38–7.32 (m, 2H), 7.26 (d, *J* = 5.6 Hz, 1H), 7.08 (d, *J* = 9.2 Hz, 1H), 3.18 (bs, 4H), 2.74 (bs, 4H), 2.44 (s, 3H); ^{13}C NMR (100 MHz, $CDCl_3$) δ 160.3, 160.0, 158.3, 155.8 (d, *J* = 245.2 Hz), 143.2, 139.5, 135.8 (d, *J* = 9.2 Hz), 134.7 (d, *J* = 10.7 Hz), 133.1, 129.7, 119.2 (d, *J* = 4.8 Hz), 118.1, 116.4 (d, *J* = 3.1 Hz), 110.8, 109.6 (d, *J* = 25.3 Hz), 108.1, 55.4, 51.0 (d, *J* = 2.8 Hz), 46.3; LRMS *m/z* 405 $[M+H]^+$; HRMS (ESI) calculated for $[M+H]^+$: 405.1873, found 405.19572.

*4-((4-(Pyrazolo[1,5-b]pyridazin-3-yl)pyrimidin-2-yl)amino)-2-(trifluoromethyl)benzonitrile (**CAF070**)*

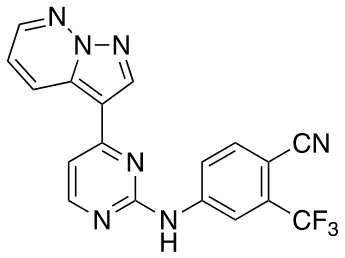

Reaction of 3-(2-chloropyrimidin-4-yl)pyrazolo[1,5-*b*]pyridazine (Compound **4**) (36 mg, 0.16 mmol), 4-amino-2-(trifluoromethyl)benzonitrile (32 mg, 0.17 mmol) and TFA (42 μL) in *sec*-BuOH (3 mL) according to General Procedure **1** afforded the title compound after purification by silica gel flash column chromatography (hexane:EtOAc 3:7) (15 mg, 0.16 mmol, 25%) as a yellow solid.

m.p. > 250 °C; ^{1}H NMR (400 MHz, DMSO-d_6) δ 10.49 (s, 1H), 9.13 (dd, *J* = 9.1, 2.0 Hz, 1H), 8.95 (s, 1H), 8.65 (dd, *J* = 4.5, 2.0 Hz, 1H), 8.63 (d, *J* = 5.3 Hz, 1H), 8.49 (d, *J* = 2.1 Hz, 1H), 8.23 (dd, *J* = 8.7, 2.2 Hz, 1H), 8.08 (d, *J* = 8.6 Hz, 1H), 7.59 (d, *J* = 5.4 Hz, 1H), 7.51 (dd, *J* = 9.1, 4.5 Hz, 1H); ^{13}C NMR (100 MHz, DMSO-d_6) δ 159.7, 159.0, 158.2, 145.3, 144.2, 140.1, 136.3, 132.6, 132.0 (d, *J* = 3.1 Hz), 131.5 (d, *J* = 9.8 Hz), 129.3, 128.7 (d, *J* = 11.7 Hz), 122.7 (d, *J* = 273.6 Hz), 120.8, 119.2, 116.3, 115.5 (q, *J* = 5.1 Hz), 109.7 (d, *J* = 30.7 Hz); LRMS *m/z* 382 $[M+H]^+$; HRMS (ESI) calculated for $[M+H]^+$: 382.0950, found 382.10433.

*N-(4-Methoxy-3-(trifluoromethyl)phenyl)-4-(pyrazolo[1,5-b]pyridazin-3-yl)pyrimidin-2-amine (**CAF075**)*

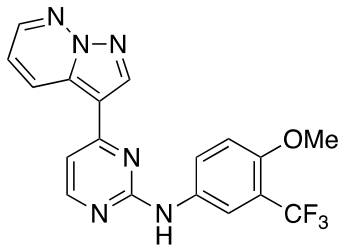

Reaction of 3-(2-chloropyrimidin-4-yl)pyrazolo[1,5-*b*]pyridazine (Compound **4**) (45 mg, 0.19 mmol), 4-methoxy-3-(trifluoromethyl)aniline (41 mg, 0.21 mmol) and TFA (53 μL) in *sec*-BuOH

(4 mL) according to General Procedure **1** afforded the *title* compound after purification by silica gel flash column chromatography (hexane:EtOAc 3:7) (32 mg, 0.08 mmol, 43%) as a yellow solid.

m.p. 220 °C decomp; ^{1}H NMR (400 MHz, DMSO-d_6) δ 9.65 (s, 1H), 9.06 (bd, *J* = 8.8 Hz, 1H), 8.90 (s, 1H), 8.62 (dd, *J* = 4.5, 1.9 Hz, 1H), 8.48 (d, *J* = 5.3Hz, 1H), 8.09 (d, *J* = 2.7 Hz, 1H), 7.90 (dd, *J* = 9.2, 2.6 Hz, 1H), 7.42 (dd, *J* = 9.1, 4.5 Hz, 1H), 7.38 (d, *J* = 5.3 Hz, 1H), 7.28 (d, *J* = 9.0 Hz, 1H), 3.88 (s, 3H); ^{13}C NMR (100 MHz, Methanol-d_4) δ 160.9, 160.1, 157.1, 154.0, 143.8, 139.8, 133.6, 132.2, 130.0, 126.8, 123.9 (d, *J* = 272.5 Hz), 121.4 (q, *J* = 5.7 Hz), 119.0, 113.1, 110.9, 107.9, 56.5; LRMS *m/z* 387 $[M+H]^+$; HRMS (ESI) calculated for $[M+H]^+$: 387.1103, found 387.11939.

N-(3-(4-Methylpiperazin-1-yl)phenyl)-4-(pyrazolo[1,5-b]pyridazin-3-yl)pyrimidin-2-amine (***CAF077***)

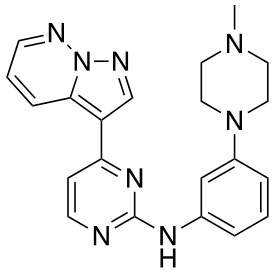

Reaction of 3-(2-chloropyrimidin-4-yl)pyrazolo[1,5-*b*]pyridazine (Compound **4**) (40 mg, 0.17 mmol), 3-(4-methylpiperazin-1-yl)aniline (36 mg, 0.19 mmol) and TFA (47 μL) in *sec*-BuOH (3 mL) according to General Procedure **1** afforded the *title* compound after purification by silica gel flash column chromatography (CH_2Cl_2:MeOH 9:1) (31 mg, 0.08 mmol, 46%) as a yellow solid.

m.p. 139–140 °C; ^{1}H NMR (400 MHz, $CDCl_3$) δ 8.90 (dd, *J* = 9.0, 2.0 Hz, 1H), 8.49 (s, 1H), 8.40 (d, *J* = 5.3 Hz, 1H), 8.37 (dd, *J* = 4.4, 2.0 Hz, 1H), 7.33 (bs, 1H), 7.27–7.23 (m, 2H), 7.11 (dd, *J* = 9.1, 4.4 Hz, 1H), 7.07 (dd, *J* = 7.6, 1.5 Hz, 1H), 7.03 (d, *J* = 5.2 Hz, 1H), 6.69 (ddd, *J* = 8.2, 2.5, 0.9 Hz, 1H), 3.24–3.22 (m, 4H), 2.57–2.54 (m, 4H), 2.34 (s, 3H); ^{13}C NMR (100

MHz, $CDCl_3$) δ 160.6, 159.9, 158.4, 152.0, 143.2, 140.4, 139.5, 133.2, 130.0, 129.6, 118.0, 112.4, 111.0, 110.9, 108.5, 108.0, 55.2, 48.9, 46.1; LRMS *m/z* 387 $[M+H]^+$; HRMS (ESI) calculated for $[M+H]^+$: 387.1967, found 387.20611.

*2-(4-Methylpiperazin-1-yl)-5-((4-(pyrazolo[1,5-b]pyridazin-3-yl)pyrimidin-2-yl)amino)benzonitrile (**CAF078**)*

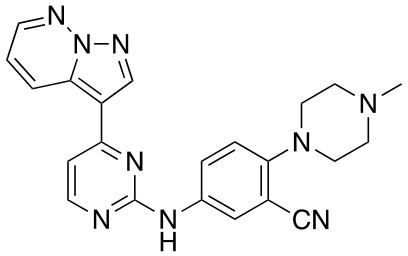

Reaction of 3-(2-chloropyrimidin-4-yl)pyrazolo[1,5-*b*]pyridazine (Compound **4**) (35 mg, 0.15 mmol), 5-amino-2-(4-methylpiperazin-1-yl)benzonitrile (36 mg, 0.17 mmol) and TFA (41 μL) in *sec*-BuOH (3 mL) according to General Procedure **1** afforded the *title* compound after purification by silica gel flash column chromatography (CH_2Cl_2:MeOH 9:1) (38 mg, 0.09 mmol, 61%) as a yellow solid.

m.p. 231-232 °C, ^{1}H NMR (400 MHz, $CDCl_3$) δ 8.88 (dd, *J* = 9.1, 2.0 Hz, 1H), 8.49 (s, 1H), 8.40–8.38 (m, 2H), 8.17 (d, *J* = 2.6 Hz, 1H), 7.50 (dd, *J* = 8.8, 2.7 Hz, 1H), 7.42 (bs, 1H), 7.24 (dd, *J* = 9.1, 4.4 Hz, 1H), 7.1 (d, *J* = 5.3 Hz, 1H), 7.04 (d, *J* = 8.8 Hz, 1H), 3.23–3.20 (m, 4H), 2.67–2.65 (m, 4H), 2.38 (s, 3H); ^{13}C NMR (100 MHz, $CDCl_3$) δ 160.2, 160.1, 158.3, 151.3, 143.3, 139.7, 134.2, 133.1, 129.4, 126.0, 125.7, 119.7, 118.5, 118.3, 110.6, 108.7, 106.8, 55.2, 51.9, 46.1; LRMS *m/z* 412 $[M+H]^+$; HRMS (ESI) calculated for $[M+H]^+$: 412.1920, found 412.20171.

*N-(3-Methyl-4-(4-methylpiperazin-1-yl)phenyl)-4-(pyrazolo[1,5-b]pyridazin-3-yl)pyrimidin-2-amine (**CAF089**)*

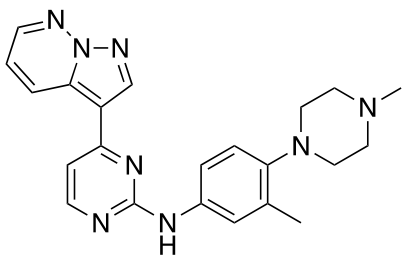

Reaction of 3-(2-chloropyrimidin-4-yl)pyrazolo[1,5-*b*]pyridazine (Compound **4**) (33 mg, 0.14 mmol), 3-methyl-4-(4-methylpiperazin-1-yl)aniline (38 mg, 0.16 mmol) and TFA (39 μL) in *sec*-BuOH (3 mL) according to General Procedure **1** afforded the *title* compound after purification by silica gel flash column chromatography (CH_2Cl_2:MeOH 9:1) (27 mg, 0.14 mmol, 47%) as a brown solid.

m.p > 250 °C; ^{1}H NMR (400 MHz, $CDCl_3$) δ 8.90 (dd, *J* = 9.1, 2.0 Hz, 1H), 8.49 (s, 1H), 8.39–8.37 (m, 2H), 7.45 (d, *J* = 2.6 Hz, 1H), 7.35 (dd, *J* = 8.5, 2.7 Hz, 1H), 7.10–7.06 (m, 3H), 7.02 (d, *J* = 5.3 Hz, 1H), 3.00–2.97 (m, 4H), 2.66 (bs, 4H), 2.42 (s, 3H), 2.34 (s, 3H); ^{13}C NMR (100 MHz, $CDCl_3$) δ 160.7, 159.9, 158.4, 143.1, 139.5, 135.1, 133.6, 133.2, 129.9, 123.9, 119.9, 119.6, 117.9, 111.0, 107.8, 55.6, 51.5, 45.8, 18.0; LRMS *m/z* 401 $[M+H]^+$; HRMS (ESI) calculated for $[M+H]^+$: 401.2124, found 401.22196.

ACKNOWLEDGEMENTS AND FUNDING

The PKIS was supplied by GlaxoSmithKline, LLC and the Structural Genomics Consortium under an open access Material Transfer and Trust Agreement: http://www.sgc-unc.org".
The SGC is a registered charity (number 1097737) that receives funds from AbbVie, Bayer Pharma AG, Boehringer Ingelheim, Canada Foundation for Innovation, Eshelman Institute for Innovation, Genome Canada, Innovative Medicines Initiative (EU/EFPIA) [ULTRA-DD grant no. 115766], Janssen, Merck & Co., Novartis Pharma AG, Ontario Ministry of Economic Development and Innovation, Pfizer, São Paulo Research Foundation-FAPESP, Takeda, and Wellcome Trust [106169/ZZ14/Z]

Supported by grant UL1TR000427 from the Clinical and Translational Science Award (CTSA) program of the National Center for Advancing Translational Sciences, NIH.

Supported by grant AI121704 from the National Institute of Allergy and Infectious Diseases, NIH.

RS and NW supported by the Hartwell Foundation and a Veteran's Affairs Merit Award.

AS supported by the PhRMA Foundation.

JDS supported by The Wisconsin Partnership Program

The SGC is a registered charity (number 1097737) that receives funds from AbbVie, Bayer Pharma AG, Boehringer Ingelheim, Canada Foundation for Innovation, Eshelman Institute for Innovation, Genome Canada, Innovative Medicines Initiative (EU/EFPIA) [ULTRA-DD grant no. 115766], Janssen, Merck & Co., Novartis Pharma AG, Ontario Ministry of Economic Development and Innovation, Pfizer, São Paulo Research Foundation-FAPESP, Takeda, and Wellcome Trust [106169/ZZ14/Z]

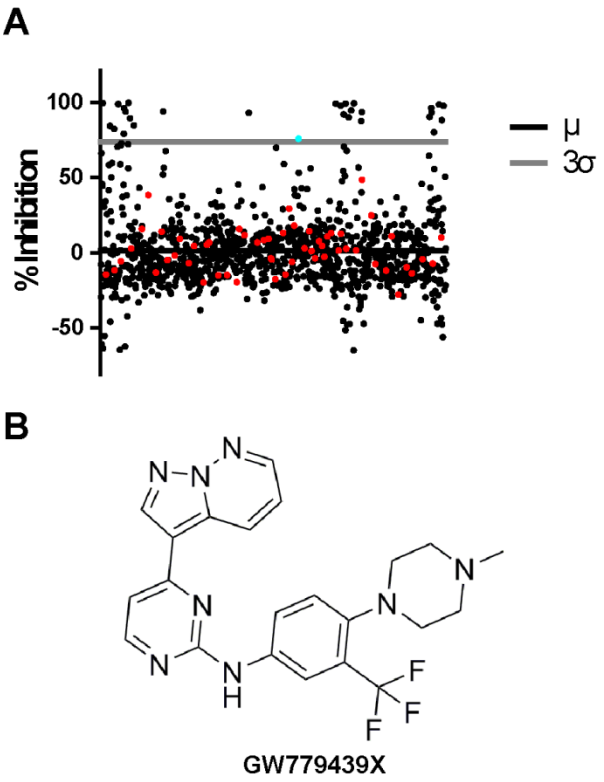

Figure 3.1: Library screen identifies GW779439X as a compound that potentiates ceftriaxone activity against MRSA. A) Scatter plot representing percent growth inhibition of WT LAC in the presence of a combination of a sublethal concentration (10 μg/mL) of ceftriaxone and compounds in the screen. The solid black line represents the library average (μ), and the grey line represents the three standard deviations (3σ) above the library average. The cyan and red dots represent GW779439X and other compounds from the pyrazolopyridazine family, respectively. **B)** Skeletal structure of GW779439X.

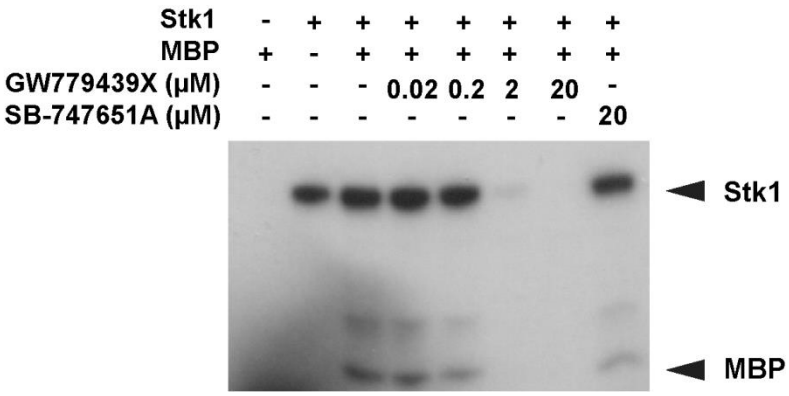

Figure 3.2: GW779439X directly inhibits Stk1 kinase activity *in vitro*. Autoradiography blot of purified Stk1 kinase domain and the nonspecific phosphosubstrate myelin basic protein (MBP) untreated or in increasing concentrations of GW779439X. SB-747651A is an imidazopyridine aminofurazan kinase inhibitor present in the initial library screen which shows no Stk1 activity. Blot is representative of 3 independent trials.

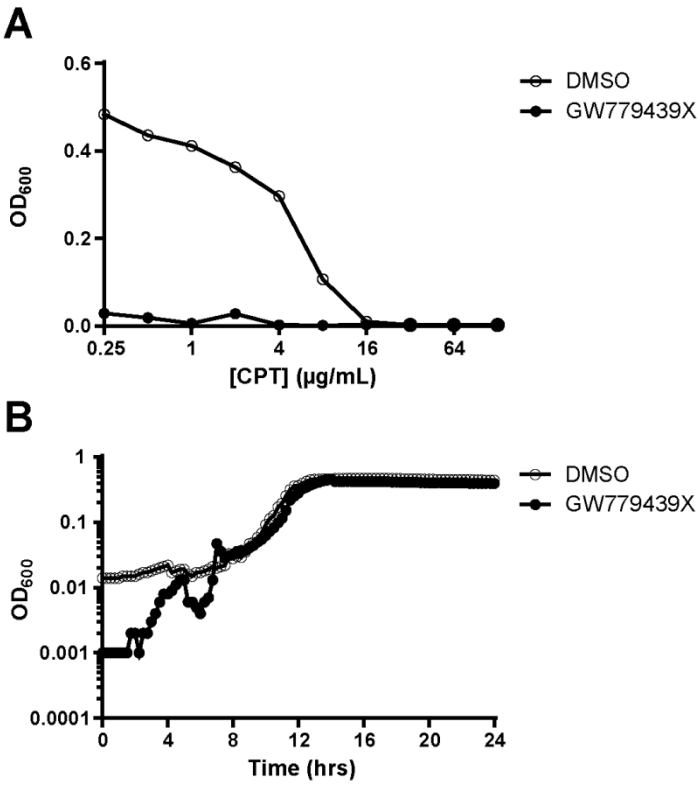

Figure 3.3: GW779439X potentiates ceftaroline activity against a ceftaroline-resistant MRSA strain. MRSA strain BAA-2686 was back-diluted into increasing concentrations of ceftaroline in the presence or absence of 5 µM GW779439X. **B)** BAA-2686 was back-diluted into 5 µM GW779439X and growth was monitored for 24 hours. Dose-response curves and growth curves are representative of 3 independent trials.

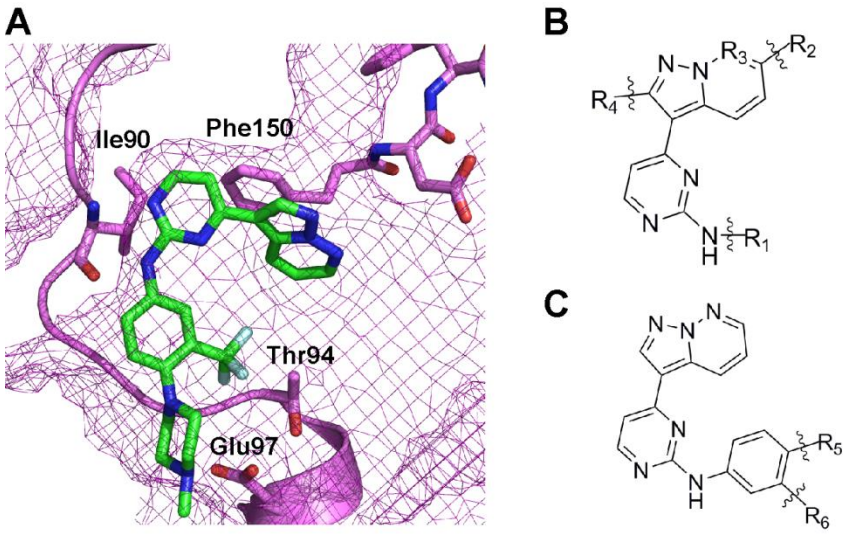

Figure 3.4: The pyrazolopyridazine scaffold docks in the Stk1 active site. A) GW779439X docked *in silico* into the Stk1 active site. GW779439X is displayed as green sticks, Stk1 residues of note are displayed as violet sticks. Stk1 backbone is displayed as violet cartoon, and Stk1 Van der Waals radii are displayed as violet mesh. **B)** Skeletal structure of the pyrazolopyridazine scaffold that was present in the kinase inhibitor library screen. **C)** Skeletal structure of our restricted pyrazolopyridazine scaffold used for medicinal chemistry.

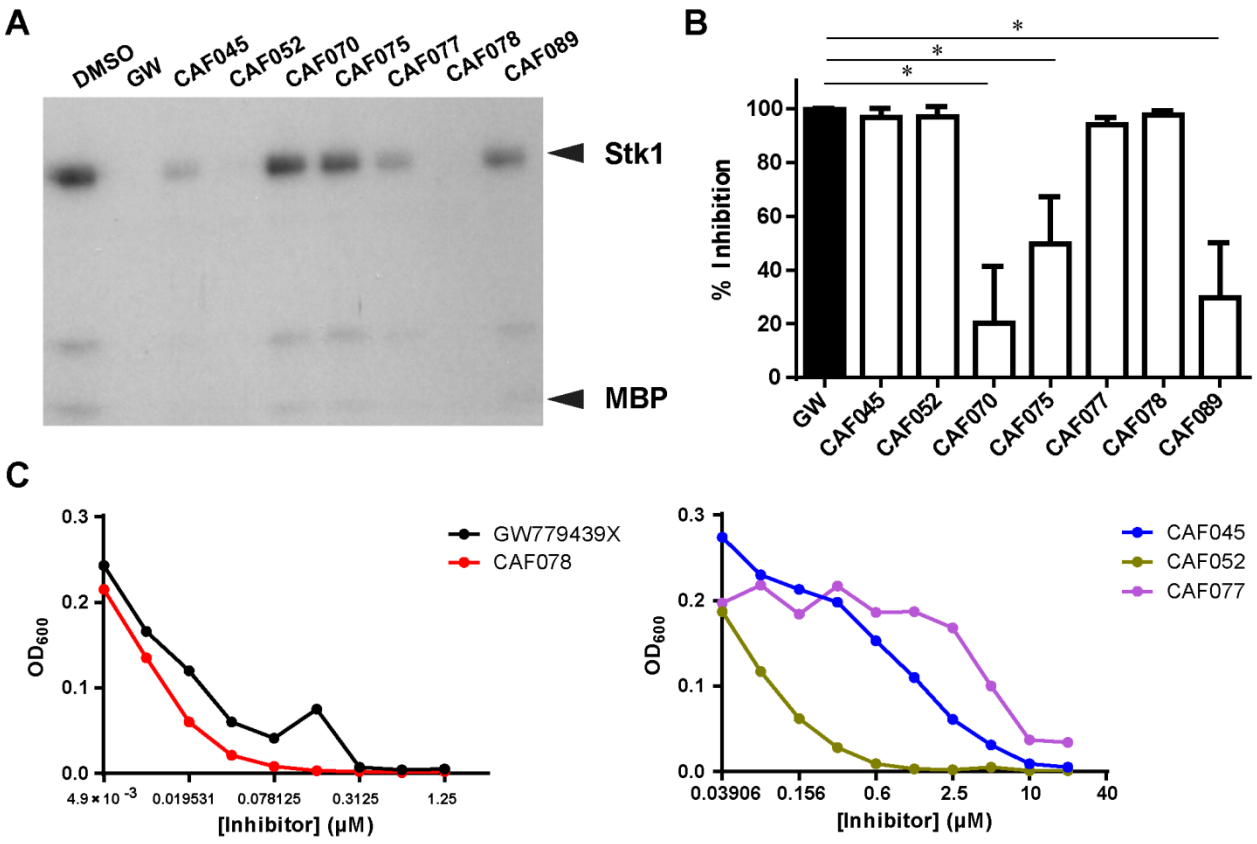

Figure 3.5: GW779439X's *p-N*-methyl piperazine sidechain is important for biochemical and microbiologic activity. A) Autoradiography blot of Stk1 kinase domain and MBP untreated or in the presence of 2 μM GW779439X (GW) or other kinase inhibitors. Blot is representative of 3 independent trials. **B)** WT LAC was back-diluted into cation-adjusted Mueller Hinton media with a sublethal concentration (8 μg/mL) of oxacillin in the presence of 20 μM GW or other kinase inhibitors. Percent inhibition for each compound was calculated relative to bacteria grown in oxacillin and DMSO. Error bars represent the standard deviation of 3 independent trials. * = statistically significant by student's T-test. **C)** WT LAC was back-diluted into a sublethal concentration (8 μg/mL) of oxacillin in increasing concentrations of **Left)** GW779439X or CAF078 or **Right)** CAF045, CAF052, or CAF077. Dose-response curves are representative of 3 independent trials.

Scheme 3.1: Synthesis of pyrazolopyridazine analogs

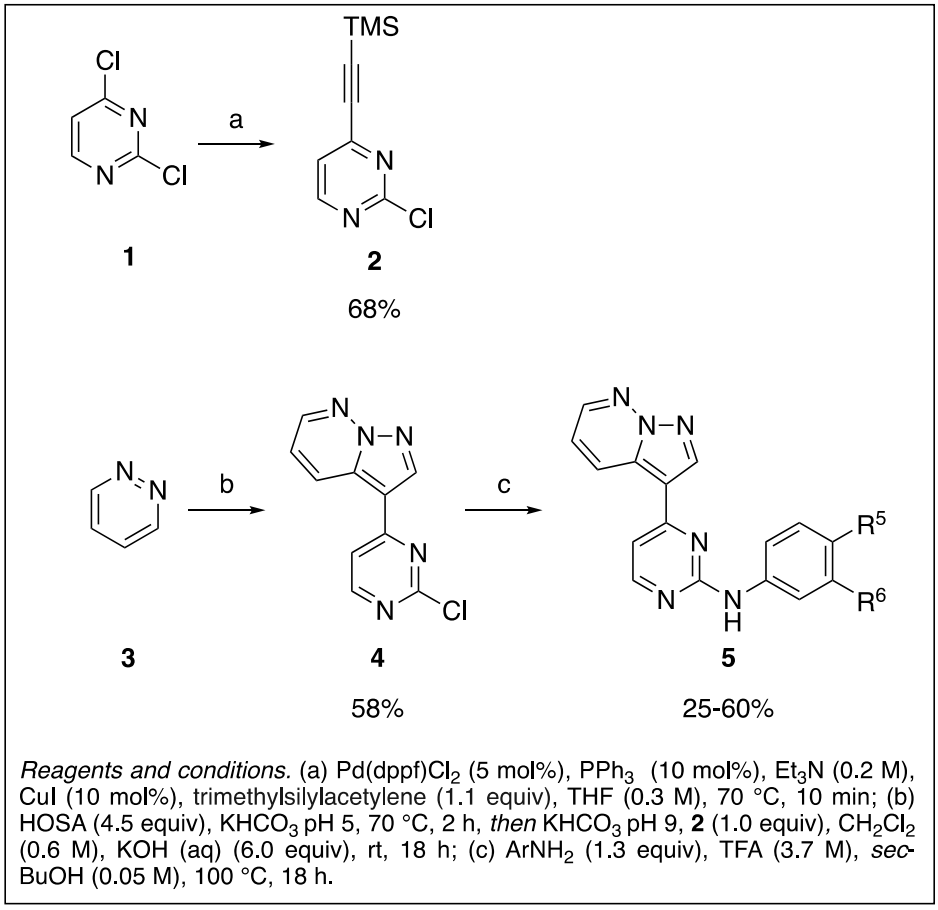

Reagents and conditions. (a) $Pd(dppf)Cl_2$ (5 mol%), PPh_3 (10 mol%), Et_3N (0.2 M), CuI (10 mol%), trimethylsilylacetylene (1.1 equiv), THF (0.3 M), 70 °C, 10 min; (b) HOSA (4.5 equiv), $KHCO_3$ pH 5, 70 °C, 2 h, *then* $KHCO_3$ pH 9, **2** (1.0 equiv), CH_2Cl_2 (0.6 M), KOH (aq) (6.0 equiv), rt, 18 h; (c) $ArNH_2$ (1.3 equiv), TFA (3.7 M), *sec*-BuOH (0.05 M), 100 °C, 18 h.

Table 3.1: Minimum Inhibitory Concentration (MIC) of various antibiotics against WT LAC and Δ*stk1* strains +/- 5 µM GW779439X. Data represented as median of at least 3 independent trials with the range in brackets.

	MIC (µg/mL)							
	LAC (WT)				Δ*stk1*			
GW779439X	**-**		**+**		**-**		**+**	
Ceftriaxone	**32**	[32, 32]	**16**	[16, 16]	**16**	[16, 16]	**16**	[16, 32]
Oxacillin	**16**	[16, 32]	**1**	[1, 4]	**1**	[1, 4]	**1**	[1, 4]
Nafcillin	**16**	[16, 16]	**2**	[1, 2]	**2**	[1, 2]	**2**	[1, 2]
Meropenem	**0.25**	[0.25, 0.5]	**0.125**	[0.125, 0.125]	**0.125**	[0.0625, 0.125]	**0.125**	[0.0625, 0.125]
Ceftaroline	**1**	[0.5, 1]	**0.5**	[0.5, 0.5]	**0.5**	[0.5, 0.5]	**0.5**	[0.5, 0.5]
Vancomycin	**1**	[1, 2]	**1**	[1, 2]	**1**	[1, 2]	**1**	[1, 2]
Chloramphenicol	**4**	[8, 4]	**4**	[8, 4]	**4**	[8, 4]	**4**	[8, 4]

Table 3.2: MIC of oxacillin for various *S. aureus* isolates +/- 5 µM GW779439X. Data represented as median of at least 3 independent trials with the range in brackets.

	Oxacillin MIC (µg/mL)	
GW779439X	**-**	**+**
USA400 (MW2)	**16** [16, 32]	**2** [1, 4]
USA600	**16** [16, 16]	**8** [8, 8]
USA800	**4** [4, 8]	**1** [0.5, 2]
COL	**256** [256, 256]	**64** [64, 64]
ATCC BAA-2686	**128** [64,128]	**0.25** [0.25, 0.5]
Newman	**0.25** [0.125, 0.5]	**0.125** [0.0625, 0.125]
NCTC8325	**0.125** [0.125, 0.25]	**0.0625** [0.0625, 0.125]

Table 3.3: Structures of various pyrazolopyridazine compounds

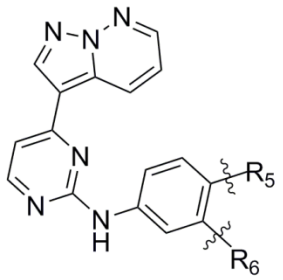

Compound	R5	R6
GW779439X	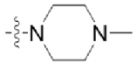	
CAF045	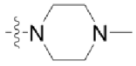	
CAF052	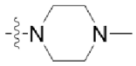	
CAF070		
CAF075		
CAF077		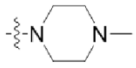
CAF078	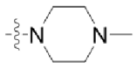	
CAF089	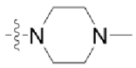	

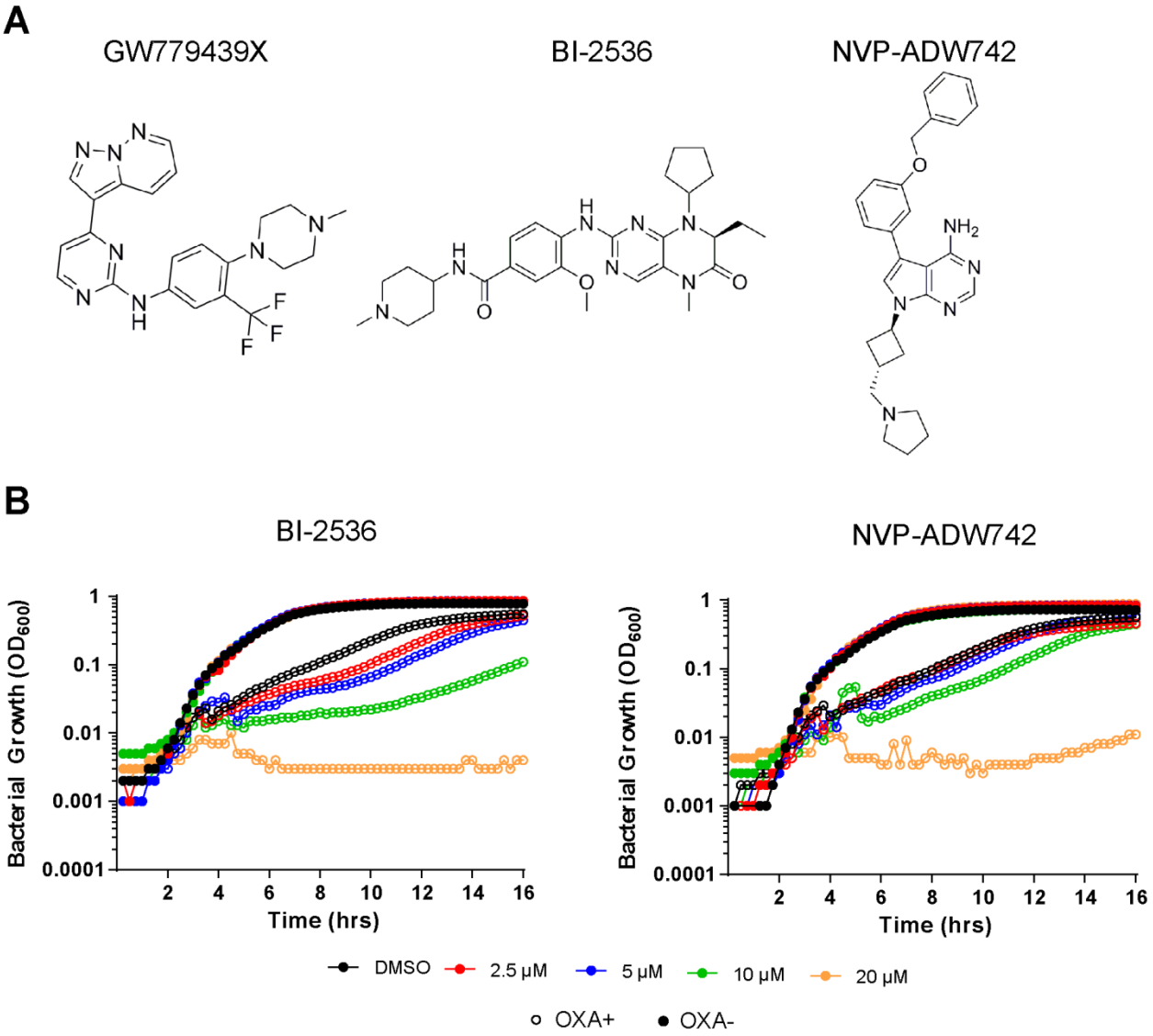

Figure S3.1: A) Three compounds (GW779439X, BI-2536, and NVP-ADW742) were identified in the kinase inhibitor library screen and were found to be β-lactam-dependent. **B)** WT *S. aureus* was grown in increasing concentrations of BI-2536 (*left*) or NVP-ADW742 (*right*) in the presence (open circles) or absence (filled circles) of 8 µg/mL oxacillin. Growth curves are representative of 2 independent trials.

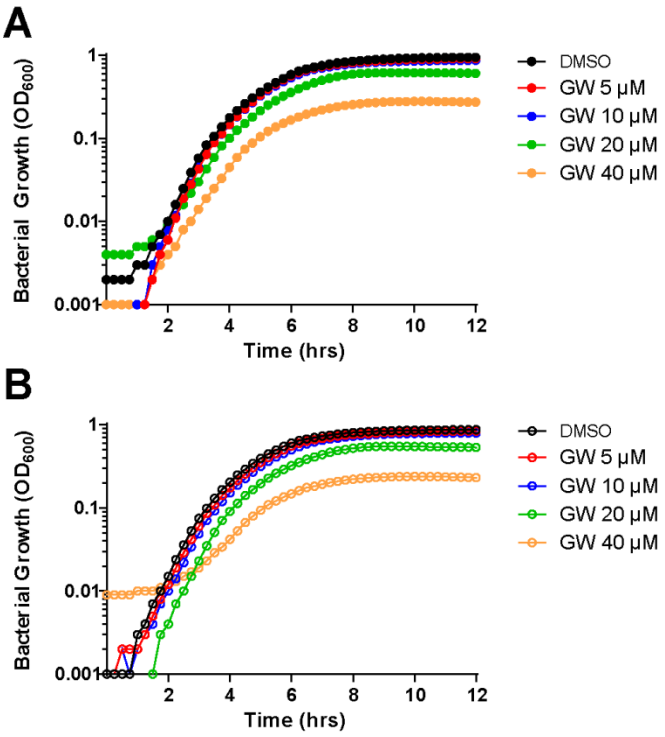

Figure S3.2: Cultures of **A)** WT LAC or **B)** Δ*stk1* were back-diluted into cation-adjusted Mueller-Hinton media with increasing concentrations of GW779439X, and the OD_{600} was monitored for 12 hours. Growth curves are representative of 3 independent trials.

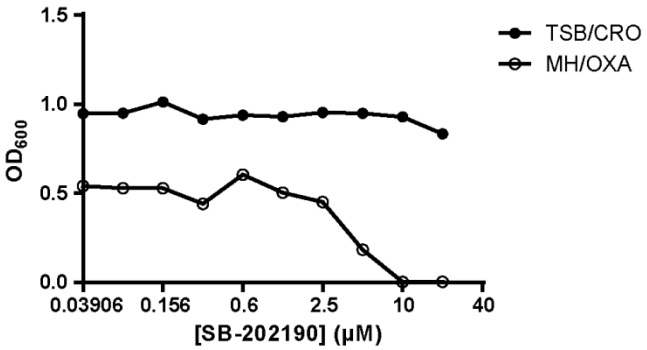

Figure S3.3: Cultures of *S. aureus* LAC were back-diluted into increasing concentrations of SB-202190 in growth conditions similar to the initial kinase inhibitor library screen (TSB + 10 µg/mL ceftriaxone [CRO]) or conditions described by Boudreau *et al* (cation-adjusted Mueller-Hinton media + 2% NaCl + 8 µg/mL oxacillin [OXA]). Curves are representative of 3 independent trials.

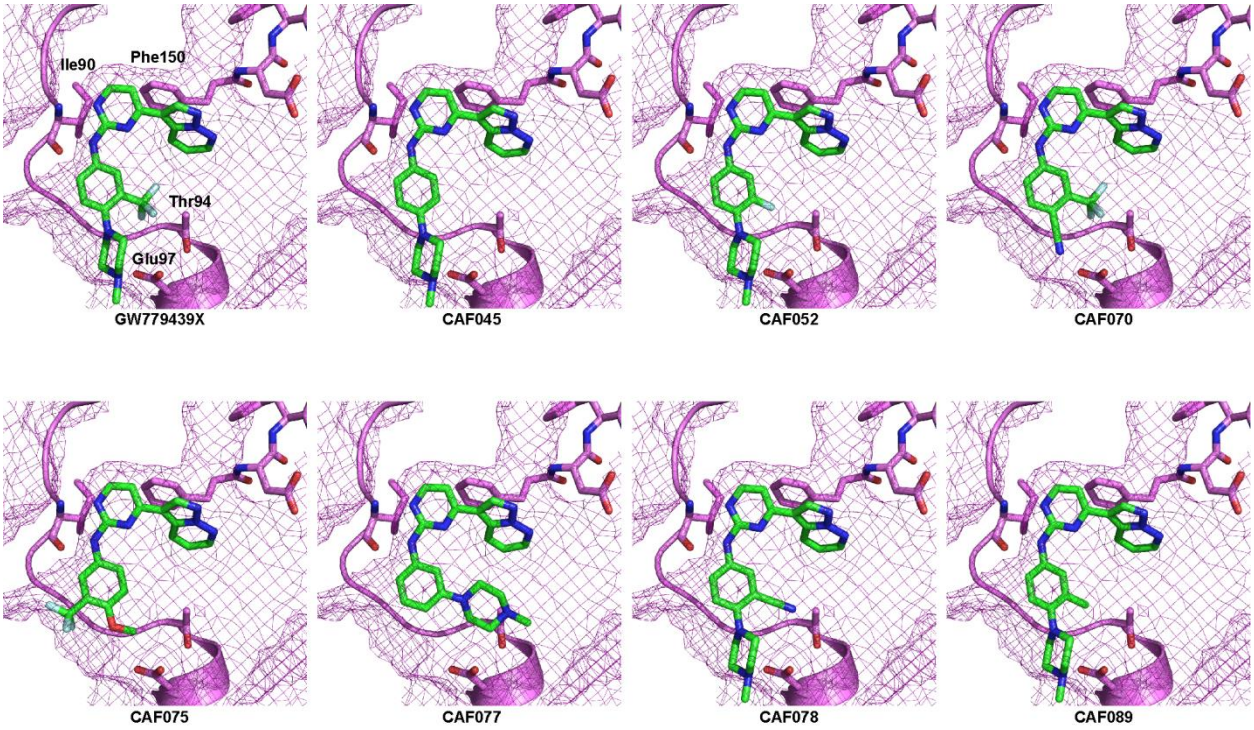

Figure S3.4: *In silico* modeling of GW779439X and its derivatives in the active site of the Stk1 kinase domain. Inhibitors are depicted as green sticks, and the Stk1 kinase domain depicted in violet cartoon, sticks, and mesh.

Table S3.1: Strains used in this study

Strain	Description	Reference
E. coli		
JDS299	Rosetta™ (DE3) carrying pGEX-2T-Stk1; Cam^R, Amp^R	237
S. aureus		
LAC	Community-acquired USA300 MRSA strain isolated from LA County	275
JDS827	LAC Δ*stk1*	280
MW2	Community-acquired USA400 MRSA strain isolated from ND, USA	287
COL	Hospital-acquired MRSA strain isolated from Colindale, England	288
USA600	Hospital-acquired MRSA strain NRS-22	289
USA800	Hospital-acquired MRSA strain NRS387	289
ATCC BAA-2686	Ceftaroline-resistant MRSA strain isolated from the blood of a cystic fibrosis patient	ATCC®
Newman	MSSA strain Newman	290
RN6390B NCTC8325	*rsbU* $^-$ MSSA strain NCTC8325	291

Supplemental Table S3.2: Tabulated *S. aureus* library screen data

Compound	Trial 1 % Inhib.	Trial 2 % Inhib.	AGV % Inhib.	Std. Dev
3-Methyladenine	-62.839	4.092	-29.373	33.466
A66	-21.812	6.208	-7.802	14.010
A-674563	78.537	53.908	66.222	12.314
A-769662	-123.833	2.367	-60.733	63.100
AEE788 (NVP-AEE788)	-5.197	96.681	45.742	50.939
Afatinib (BIBW2992)	14.745	74.427	44.586	29.841
AG-1024	100.501	98.673	99.587	0.914
AG-1478 (Tyrphostin AG-1478)	-137.770	10.674	-63.548	74.222
AG-490	-40.349	-3.836	-22.092	18.256
AH20685XX	-3.105	-4.110	-3.607	0.502
AH2635	-1.499	-3.271	-2.385	0.886
AH5015X	-2.419	-4.163	-3.291	0.872
AMG 900	-111.289	0.938	-55.176	56.114
AMG-208	4.571	-0.442	2.064	2.507
AMG458	-44.390	10.138	-17.126	27.264
Amuvatinib (MP-470)	78.585	-9.956	34.315	44.270
Apatinib (YN968D1)	-41.045	5.226	-17.910	23.135
ARQ 197 (Tivantinib)	-63.345	60.965	-1.190	62.155
ARRY334543	-72.822	30.058	-21.382	51.440
Arry-380	-44.948	21.215	-11.866	33.081
AS-252424	-4.808	56.409	25.800	30.609
AS-604850	-76.725	37.919	-19.403	57.322
AS-605240	3.444	21.571	12.507	9.063
AS703026 (Pimasertib)	-23.231	5.973	-8.629	14.602
AST-1306	-16.218	1.991	-7.113	9.105
AT7519	-26.487	2.212	-12.137	14.350
AT7867	-15.091	98.341	41.625	56.716
AT9283	99.062	17.684	58.373	40.689
Aurora A Inhibitor I	-27.865	-0.996	-14.430	13.435
Axitinib	-31.501	-3.353	-17.427	14.074
AZ 960	80.209	88.745	84.477	4.268
AZ628	-97.073	5.672	-45.700	51.373
AZD0855	16.468	38.827	27.648	11.180
AZD2014	-0.009	-0.337	-0.173	0.164
AZD4547	63.974	36.062	50.018	13.956
AZD5438	11.916	29.790	20.853	8.937
AZD6244 (Selumetinib)	-37.936	-5.090	-21.513	16.423
AZD7762	100.000	19.469	59.735	40.265
AZD8330	-40.513	-18.695	-29.604	10.909
AZD8931	-35.003	-23.562	-29.283	5.721
Barasertib (AZD1152-HQPA)	-28.686	26.659	-1.014	27.672
Baricitinib (LY3009104, inc b28050)	2.585	6.403	4.494	1.909
BEZ235 (NVP-BEZ235)	-32.038	11.701	-10.168	21.869
BGJ398 (NVP-BGJ398)	-28.240	-8.628	-18.434	9.806
BI 2536	69.035	95.754	82.394	13.360
BI6727 (Volasertib)	16.934	24.252	20.593	3.659
BIBF1120 (Vargatef)	-28.418	1.954	-13.232	15.186

Compound	Trial 1 % Inhib.	Trial 2 % Inhib.	AGV % Inhib.	Std. Dev
BIRB 796 (Doramapimod)	-39.011	-15.155	-27.083	11.928
BIX02188	-34.502	-10.841	-22.671	11.831
BIX02189	-32.498	-7.633	-20.066	12.433
BKM120 (NVP-BKM120)	-63.624	5.047	-29.288	34.335
BMS 777607	-37.383	-22.124	-29.753	7.629
BMS-265246	-30.495	-2.655	-16.575	13.920
BMS-599626 (AC480)	-40.751	14.306	-13.222	27.529
BMS794833	11.638	-11.300	0.169	11.469
Bosutinib (SKI-606)	58.579	82.437	70.508	11.929
Brivanib (BMS-540215)	-37.265	1.761	-17.752	19.513
Brivanib Alaninate (BMS-582664)	99.196	98.649	98.922	0.273
BS-181 HCl	98.497	99.226	98.861	0.364
BX-795	-24.358	-5.199	-14.779	9.580
BX-912	41.515	-19.912	10.802	30.713
BYL719	-28.830	5.248	-11.791	17.039
CAL-101 (GS-1101)	-33.798	8.799	-12.500	21.298
CAY10505	-135.819	7.012	-64.403	71.415
CCT128930	78.537	39.348	58.942	19.594
CCT129202	-22.229	25.664	1.717	23.946
CCT137690	11.080	18.446	14.763	3.683
Cediranib (AZD2171)	69.839	73.172	71.506	1.667
CEP33779	51.292	94.319	72.806	21.513
CH5424802	-68.027	5.344	-31.341	36.686
CHIR-124	14.704	45.511	30.108	15.404
CHIR-98014	-27.666	11.746	-7.960	19.706
CI-1033 (Canertinib)	26.542	47.986	37.264	10.722
CI-1040 (PD184352)	-12.064	28.782	8.359	20.423
CP 673451	4.947	45.796	25.372	20.425
CP-724714	99.875	-9.292	45.291	54.583
Crenolanib (CP-868596)	82.718	75.703	79.211	3.507
Crizotinib (PF-02341066)	92.359	100.000	96.180	3.820
CX-4945 (Silmitasertib)	-19.861	42.117	11.128	30.989
CYC116	-4.070	-13.717	-8.893	4.823
Cyt387	-109.059	-15.319	-62.189	46.870
Dabrafenib (GSK2118436)	-66.010	47.906	-9.052	56.958
Dacomitinib (PF299804, PF-00299804)	90.801	96.874	93.837	3.036
Danusertib (PHA-739358)	-36.193	2.051	-17.071	19.122
Dasatinib (BMS-354825)	-45.442	6.200	-19.621	25.821
DCC-2036 (Rebastinib)	-29.617	13.533	-8.042	21.575
Deforolimus (Ridaforolimus)	4.155	72.400	38.278	34.122
Desmethyl Erlotinib (CP-473420)	-53.905	-5.633	-29.769	24.136
Dinaciclib (SCH727965)	-83.014	-1.396	-42.205	40.809
Dovitinib (TKI-258)	-27.212	10.543	-8.334	18.877
Dovitinib Dilactic Acid (TKI258 Dilactic Acid)	45.240	99.422	72.331	27.091
E7080 (Lenvatinib)	98.497	14.159	56.328	42.169
ENMD-2076	100.125	99.336	99.731	0.394
Enzastaurin (LY317615)	-17.962	15.464	-1.249	16.713
Erlotinib HCl	-26.944	6.007	-10.468	16.475
Everolimus (RAD001)	6.166	29.747	17.956	11.790

Compound	Trial 1 % Inhib.	Trial 2 % Inhib.	AGV % Inhib.	Std. Dev
Flavopiridol HCl	-46.063	4.690	-20.687	25.376
Foretinib (GSK1363089, XL880)	84.450	94.306	89.378	4.928
GDC-0068	-23.354	4.478	-9.438	13.916
GDC-0879	-4.558	25.887	10.664	15.222
GDC-0941	-18.767	18.938	0.086	18.853
GDC-0980 (RG7422)	-50.523	3.082	-23.720	26.802
Gefitinib (Iressa)	-36.193	2.533	-16.830	19.363
GI230329A	-22.217	0.363	-10.927	11.290
GI261520A	5.719	26.078	15.899	10.179
GI261590A	19.025	-11.429	3.798	15.227
GI261656A	-2.693	6.545	1.926	4.619
GI262866A	8.351	16.141	12.246	3.895
GI98581X	-1.499	-7.549	-4.524	3.025
Golvatinib (E7050)	76.078	93.452	84.765	8.687
GR105659X	3.295	0.124	1.710	1.585
GR269666A	7.650	7.795	7.723	0.072
GSK1000163A	-13.944	7.865	-3.039	10.904
GSK1007102B	12.949	27.731	20.340	7.391
GSK1014915A	-3.014	-3.477	-3.246	0.232
GSK1023156A	3.122	20.418	11.770	8.648
GSK1024304A	-8.285	1.651	-3.317	4.968
GSK1024306A	-13.467	-2.561	-8.014	5.453
GSK1030058A	7.912	15.315	11.613	3.701
GSK1030059A	-10.206	9.625	-0.291	9.915
GSK1030061A	5.971	8.684	7.328	1.357
GSK1030062A	3.840	6.286	5.063	1.223
GSK1033723A	-9.785	3.244	-3.271	6.515
GSK1034945A	-14.730	-3.295	-9.012	5.718
GSK1059615	10.081	13.496	11.788	1.707
GSK1070916	-69.199	3.439	-32.880	36.319
GSK1120212 (Trametinib)	-48.014	14.426	-16.794	31.220
GSK1122999D	3.854	7.588	5.721	1.867
GSK1173862A	32.753	53.749	43.251	10.498
GSK1220512A	7.669	14.544	11.107	3.438
GSK1229496A	-5.032	0.391	-2.320	2.712
GSK1229782A	5.581	-1.396	2.093	3.489
GSK1229959A	-2.100	-0.316	-1.208	0.892
GSK1269851A	15.309	20.888	18.098	2.790
GSK1287544A	-9.785	22.937	6.576	16.361
GSK1292139B	-14.154	2.759	-5.698	8.457
GSK1307810A	-9.421	8.989	-0.216	9.205
GSK1321561A	98.500	7.456	52.978	45.522
GSK1321565A	-0.183	1.370	0.594	0.776
GSK1322949A	12.522	-0.585	5.969	6.553
GSK1323434A	-6.897	4.272	-1.312	5.585
GSK1325775A	-11.965	7.678	-2.144	9.822
GSK1326180A	10.693	-3.271	3.711	6.982
GSK1326255A	-1.770	14.993	6.612	8.381
GSK1379706A	-15.650	-3.699	-9.674	5.975

Compound	Trial 1 % Inhib.	Trial 2 % Inhib.	AGV % Inhib.	Std. Dev
GSK1379708A	-11.049	-8.643	-9.846	1.203
GSK1379710A	-5.675	-8.057	-6.866	1.191
GSK1379712A	-9.700	-5.611	-7.655	2.045
GSK1379713A	-25.331	-22.384	-23.858	1.474
GSK1379714A	-3.470	-7.271	-5.371	1.900
GSK1379715A	-3.319	-8.683	-6.001	2.682
GSK1379716A	15.890	-1.581	7.155	8.736
GSK1379717A	-13.693	12.218	-0.738	12.956
GSK1379720A	-6.959	-6.180	-6.570	0.390
GSK1379721A	6.852	-6.910	-0.029	6.881
GSK1379722A	-3.212	-10.769	-6.991	3.779
GSK1379723A	-7.012	6.669	-0.172	6.841
GSK1379724A	-14.548	-36.808	-25.678	11.130
GSK1379725A	-7.173	-5.450	-6.312	0.862
GSK1379727A	-4.039	-3.171	-3.605	0.434
GSK1379729A	-0.889	-10.832	-5.860	4.971
GSK1379730A	-0.091	-5.479	-2.785	2.694
GSK1379731A	-2.616	-0.982	-1.799	0.817
GSK1379732A	-12.073	-20.054	-16.063	3.991
GSK1379735A	-0.991	-7.151	-4.071	3.080
GSK1379737A	-1.829	-2.160	-1.994	0.166
GSK1379738A	23.562	11.697	17.629	5.933
GSK1379741A	-7.746	-1.883	-4.815	2.931
GSK1379742A	-7.388	-4.198	-5.793	1.595
GSK1379745A	-21.514	7.797	-6.858	14.656
GSK1379746A	-3.961	13.429	4.734	8.695
GSK1379748A	-18.493	-24.714	-21.603	3.110
GSK1379751A	5.032	2.164	3.598	1.434
GSK1379753A	5.198	20.795	12.996	7.798
GSK1379754A	-0.991	1.306	0.158	1.148
GSK1379757A	-3.854	1.956	-0.949	2.905
GSK1379760A	8.950	11.907	10.429	1.479
GSK1379761A	3.426	53.377	28.401	24.975
GSK1379762A	-11.235	-14.153	-12.694	1.459
GSK1379763A	-12.212	-16.793	-14.502	2.290
GSK1379765A	1.209	3.743	2.476	1.267
GSK1379766A	-15.377	21.799	3.211	18.588
GSK1379767A	9.116	6.510	7.813	1.303
GSK1379788A	4.818	5.293	5.056	0.238
GSK1379800A	-12.887	-15.151	-14.019	1.132
GSK1379812A	-8.351	-1.486	-4.919	3.432
GSK1379825A	-7.493	-3.271	-5.382	2.111
GSK1379859A	-2.192	-6.112	-4.152	1.960
GSK1379860A	-1.674	-1.495	-1.585	0.090
GSK1379874A	-20.171	-55.647	-37.909	17.738
GSK1379878A	-6.103	-7.536	-6.819	0.717
GSK1379879A	-13.348	-1.529	-7.438	5.909
GSK1379880A	-7.127	5.534	-0.797	6.331
GSK1379882A	-5.353	-5.346	-5.349	0.004

Compound	Trial 1 % Inhib.	Trial 2 % Inhib.	AGV % Inhib.	Std. Dev
GSK1379883A	4.186	1.371	2.779	1.407
GSK1379896A	-0.913	-10.537	-5.725	4.812
GSK1379899A	3.640	-0.443	1.598	2.042
GSK1379901A	-12.513	3.472	-4.520	7.992
GSK1379944A	-7.243	-2.664	-4.953	2.289
GSK1383280A	-6.321	-10.358	-8.339	2.018
GSK1383281A	-6.909	24.209	8.650	15.559
GSK1389063A	6.698	15.503	11.101	4.403
GSK1392956A	10.262	23.948	17.105	6.843
GSK1398460A	29.589	-17.703	5.943	23.646
GSK1398463A	-15.892	-16.141	-16.017	0.124
GSK1398467A	33.059	-9.800	11.630	21.430
GSK1398468A	80.728	35.332	58.030	22.698
GSK1398470A	97.460	90.150	93.805	3.655
GSK1398471A	23.961	-13.397	5.282	18.679
GSK1398472A	53.056	76.406	64.731	11.675
GSK1398473A	10.959	-5.690	2.634	8.325
GSK1398474A	46.788	17.914	32.351	14.437
GSK1398475A	21.627	-5.867	7.880	13.747
GSK1398477A	9.717	-13.489	-1.886	11.603
GSK1440913A	-13.693	1.750	-5.972	7.722
GSK1487252A	99.078	4.525	51.802	47.277
GSK1511931A	-12.982	2.497	-5.243	7.740
GSK1520489A	1.143	-10.832	-4.844	5.987
GSK1535721A	-9.315	-1.278	-5.296	4.019
GSK1558669A	-0.733	38.180	18.723	19.457
GSK1576028A	-10.258	0.136	-5.061	5.197
GSK1581427A	55.906	14.339	35.122	20.783
GSK1581428A	-9.892	-0.773	-5.332	4.560
GSK1627798A	-16.678	-35.896	-26.287	9.609
GSK1645872A	-4.156	-8.459	-6.308	2.151
GSK1645895A	-2.831	-8.641	-5.736	2.905
GSK1649598A	8.193	5.408	6.800	1.393
GSK1653537A	7.387	17.011	12.199	4.812
GSK1653539A	14.155	-8.746	2.705	11.451
GSK1660437A	8.558	7.795	8.177	0.382
GSK1660450B	42.865	-4.304	19.281	23.585
GSK1669917A	-18.786	5.635	-6.576	12.210
GSK1669921A	6.791	3.941	5.366	1.425
GSK1693850A	-17.013	-6.773	-11.893	5.120
GSK1713088A	8.322	25.485	16.903	8.581
GSK1723980B	10.185	25.183	17.684	7.499
GSK1751853A	20.579	21.038	20.808	0.229
GSK175726A	9.957	-4.720	2.619	7.338
GSK1804250A	21.785	-0.016	10.885	10.901
GSK180736A	3.554	10.868	7.211	3.657
GSK1819799A	4.554	14.539	9.546	4.992
GSK182497A	3.715	10.270	6.992	3.278
GSK1838705A	3.554	22.912	13.233	9.679

Compound	Trial 1 % Inhib.	Trial 2 % Inhib.	AGV % Inhib.	Std. Dev
GSK189015A	35.077	-2.972	16.053	19.025
GSK1904529A	-30.027	15.368	-7.329	22.697
GSK190937A	-2.141	-13.272	-7.707	5.566
GSK1917008A	-3.836	-12.434	-8.135	4.299
GSK192082A	6.139	10.760	8.449	2.310
GSK198271A	-16.748	-35.162	-25.955	9.207
GSK200398A	4.208	28.944	16.576	12.368
GSK2008607A	7.617	7.804	7.710	0.093
GSK204559A	-12.887	34.164	10.638	23.525
GSK204607A	-12.225	-33.882	-23.053	10.829
GSK204919A	6.745	-7.014	-0.135	6.880
GSK204925A	10.986	19.622	15.304	4.318
GSK205189A	5.297	-4.426	0.436	4.861
GSK2110236A	27.579	35.240	31.410	3.830
GSK2126458	30.314	0.938	15.626	14.688
GSK2137462A	-12.714	-21.262	-16.988	4.274
GSK2163632A	16.306	34.134	25.220	8.914
GSK2177277A	-3.902	9.191	2.645	6.547
GSK2181306A	-3.744	-0.843	-2.294	1.451
GSK2186269A	19.496	43.252	31.374	11.878
GSK2188764A	39.141	12.150	25.646	13.496
GSK2189892A	-10.698	4.272	-3.213	7.485
GSK2192730A	-6.648	6.318	-0.165	6.483
GSK2193613A	-5.359	-0.883	-3.121	2.238
GSK2197149A	-8.025	-16.016	-12.021	3.996
GSK2206003A	-0.365	0.105	-0.130	0.235
GSK2213727A	7.902	16.096	11.999	4.097
GSK2219329A	0.930	15.998	8.464	7.534
GSK2219385A	8.480	13.255	10.868	2.388
GSK2220400A	11.605	20.262	15.934	4.328
GSK2221681A	-11.736	-30.224	-20.980	9.244
GSK2224810A	-2.819	2.201	-0.309	2.510
GSK2225749A	0.229	-12.822	-6.297	6.525
GSK2227430A	-16.957	-19.123	-18.040	1.083
GSK2228768A	-13.233	9.065	-2.084	11.149
GSK223675A	-15.281	-37.174	-26.228	10.947
GSK223810A	-12.311	-20.322	-16.316	4.005
GSK2250882A	16.488	2.999	9.743	6.745
GSK2258759A	0.274	-9.168	-4.447	4.721
GSK2269905A	2.784	6.649	4.717	1.933
GSK2276055A	-10.024	3.064	-3.480	6.544
GSK2283293A	18.110	-0.286	8.912	9.198
GSK2286062A	-13.887	-14.308	-14.097	0.210
GSK2286096A	-16.331	7.001	-4.665	11.666
GSK2286295A	-3.535	2.557	-0.489	3.046
GSK2286775B	-3.744	-4.742	-4.243	0.499
GSK2288359A	-4.140	-8.444	-6.292	2.152
GSK2289044B	-6.091	2.128	-1.981	4.110
GSK2291363A	-8.887	1.017	-3.935	4.952

Compound	Trial 1 % Inhib.	Trial 2 % Inhib.	AGV % Inhib.	Std. Dev
GSK2296823A	-15.536	-3.421	-9.479	6.058
GSK2297099A	-5.571	-7.692	-6.632	1.061
GSK2297428A	-0.428	-0.443	-0.436	0.008
GSK2297430A	-4.242	-6.753	-5.497	1.256
GSK2297542A	-10.583	-2.664	-6.624	3.959
GSK2297543A	2.972	-7.549	-2.289	5.260
GSK2298859A	-8.740	1.245	-3.747	4.993
GSK2299009A	-13.195	10.757	-1.219	11.976
GSK2306394A	-2.819	-10.434	-6.627	3.807
GSK2328680A	-29.833	3.699	-13.067	16.766
GSK2333389A	35.378	13.227	24.303	11.075
GSK2334006A	-17.655	-28.286	-22.971	5.315
GSK2336394A	-1.702	-5.957	-3.829	2.128
GSK2342769A	-5.114	-6.849	-5.982	0.868
GSK2344444A	-17.237	-27.665	-22.451	5.214
GSK2347225A	4.497	15.411	9.954	5.457
GSK2358994A	-18.513	2.334	-8.090	10.423
GSK2363608B	9.674	-0.309	4.683	4.992
GSK2373690A	-15.562	-22.539	-19.051	3.489
GSK2373693A	-6.638	1.538	-2.550	4.088
GSK2373723A	-1.600	-8.942	-5.271	3.671
GSK2375584A	-13.117	3.390	-4.864	8.253
GSK2376236A	0.548	-12.223	-5.838	6.386
GSK237700A	10.802	2.018	6.410	4.392
GSK237701A	-12.555	5.049	-3.753	8.802
GSK238063A	2.707	15.412	9.059	6.352
GSK238583A	8.238	22.718	15.478	7.240
GSK248233A	17.468	31.957	24.713	7.245
GSK2576924A	0.558	2.557	1.558	0.999
GSK257997A	2.784	-1.278	0.753	2.031
GSK2587663A	-26.710	-35.835	-31.272	4.562
GSK2592465A	0.279	-0.408	-0.064	0.343
GSK2593067A	4.093	-0.506	1.793	2.300
GSK2593074A	-3.256	10.957	3.851	7.107
GSK260205A	-0.558	0.185	-0.186	0.372
GSK2603346A	-31.606	3.586	-14.010	17.596
GSK2603358A	1.581	2.162	1.872	0.290
GSK2606414A	-15.143	-14.463	-14.803	0.340
GSK2606590A	-30.440	-83.448	-56.944	26.504
GSK2608885A	-41.562	2.447	-19.557	22.004
GSK2608899A	4.186	4.534	4.360	0.174
GSK2634140A	5.581	5.917	5.749	0.168
GSK2634758A	0.465	-0.111	0.177	0.288
GSK2635225A	16.180	-16.105	0.037	16.142
GSK2645446A	17.399	-4.863	6.268	11.131
GSK269962B	10.178	21.717	15.948	5.769
GSK270822A	-18.749	7.865	-5.442	13.307
GSK292658A	1.820	-7.849	-3.014	4.834
GSK299115A	-3.122	-7.539	-5.330	2.208

Compound	Trial 1 % Inhib.	Trial 2 % Inhib.	AGV % Inhib.	Std. Dev
GSK299495A	5.023	-9.062	-2.020	7.043
GSK300014A	11.176	20.445	15.811	4.634
GSK301329A	6.317	3.729	5.023	1.294
GSK301362A	-6.724	1.235	-2.745	3.979
GSK306886A	13.607	-3.547	5.030	8.577
GSK312879A	-6.424	-4.407	-5.415	1.009
GSK312948A	8.238	21.532	14.885	6.647
GSK317314A	-25.050	4.433	-10.308	14.741
GSK317315A	5.551	8.487	7.019	1.468
GSK317354A	3.379	10.076	6.728	3.349
GSK319347A	5.058	17.837	11.447	6.390
GSK323521A	10.707	12.177	11.442	0.735
GSK323543A	-13.692	-20.530	-17.111	3.419
GSK326180A	-2.784	-10.456	-6.620	3.836
GSK327238A	5.488	9.771	7.630	2.142
GSK336313A	-8.510	-19.187	-13.848	5.338
GSK336735A	-8.164	-21.331	-14.747	6.583
GSK346294A	-30.106	-1.537	-15.821	14.284
GSK350559A	14.656	8.569	11.612	3.044
GSK357952A	-33.426	-32.634	-33.030	0.396
GSK361061A	-3.023	-8.842	-5.932	2.910
GSK361065A	9.488	1.767	5.627	3.861
GSK364507A	6.989	20.888	13.939	6.949
GSK398099A	-16.957	-19.433	-18.195	1.238
GSK429286A	1.735	-8.641	-3.453	5.188
GSK448459A	0.639	-5.269	-2.315	2.954
GSK461364	-12.461	77.212	32.376	44.837
GSK466314A	10.589	21.334	15.961	5.373
GSK466317A	2.959	7.457	5.208	2.249
GSK479719A	-0.091	-6.217	-3.154	3.063
GSK483724A	39.040	-3.072	17.984	21.056
GSK507274A	-13.693	-2.286	-7.990	5.704
GSK507358A	-1.057	13.034	5.988	7.045
GSK534911A	-10.643	-18.294	-14.468	3.826
GSK534913A	31.163	-2.977	14.093	17.070
GSK554170A	-9.565	4.785	-2.390	7.175
GSK561866B	23.604	24.596	24.100	0.496
GSK562689A	5.782	7.797	6.789	1.008
GSK571989A	31.554	35.240	33.397	1.843
GSK579289A	7.702	33.449	20.576	12.874
GSK580432A	0.432	-7.250	-3.409	3.841
GSK581271A	-13.447	-59.671	-36.559	23.112
GSK586581A	8.248	18.419	13.333	5.086
GSK605714A	4.302	10.658	7.480	3.178
GSK614526A	-17.254	1.617	-7.819	9.435
GSK619487A	7.231	54.342	30.786	23.556
GSK620503A	24.073	4.961	14.517	9.556
GSK625137A	-14.050	6.193	-3.929	10.122
GSK635416A	4.460	16.788	10.624	6.164

Compound	Trial 1 % Inhib.	Trial 2 % Inhib.	AGV % Inhib.	Std. Dev
GSK641502A	8.037	31.718	19.877	11.841
GSK683281A	1.209	1.767	1.488	0.279
GSK690693	64.075	18.359	41.217	22.858
GSK711701A	-3.841	2.025	-0.908	2.933
GSK718429A	6.233	24.098	15.166	8.933
GSK846226A	-10.007	-6.826	-8.417	1.590
GSK902056A	-12.958	-0.229	-6.594	6.365
GSK907232A	-8.030	-5.137	-6.583	1.447
GSK938890A	8.994	13.725	11.359	2.365
GSK943949A	7.147	8.328	7.737	0.590
GSK949675A	23.420	25.493	24.456	1.036
GSK953913A	5.813	14.539	10.176	4.363
GSK955403A	-11.285	5.635	-2.825	8.460
GSK969786A	-8.818	25.641	8.412	17.229
GSK977617A	-1.600	5.186	1.793	3.393
GSK977620A	-3.124	-6.554	-4.839	1.715
GSK978744A	3.813	12.460	8.136	4.323
GSK980961A	6.653	3.868	5.260	1.392
GSK986310C	-4.818	-0.026	-2.422	2.396
GSK993273A	21.361	-2.574	9.394	11.968
GSK994854A	8.826	30.664	19.745	10.919
GW271431X	-3.196	-4.742	-3.969	0.773
GW272142A	-10.122	1.245	-4.438	5.684
GW273749A	2.318	-10.484	-4.083	6.401
GW275568A	15.565	-11.367	2.099	13.466
GW275616X	-3.360	3.109	-0.125	3.234
GW275944X	2.258	-1.865	0.196	2.061
GW276655X	-1.154	5.129	1.987	3.142
GW278681X	-2.676	-0.111	-1.394	1.282
GW279320X	-15.332	3.729	-5.801	9.530
GW280670X	-15.225	5.753	-4.736	10.489
GW281179X	24.201	29.294	26.747	2.547
GW282449A	6.559	21.532	14.045	7.486
GW282450A	-6.317	-7.744	-7.031	0.714
GW282536X	4.974	11.822	8.398	3.424
GW282974X	2.776	22.109	12.443	9.666
GW284372X	5.551	3.447	4.499	1.052
GW284408X	5.887	0.124	3.006	2.882
GW284543A	1.711	-16.872	-7.580	9.292
GW290597X	13.233	26.983	20.108	6.875
GW296115X	10.122	15.344	12.733	2.611
GW297361X	5.645	7.360	6.503	0.857
GW300653X	-12.982	0.385	-6.299	6.684
GW300657X	9.665	17.282	13.474	3.809
GW300660X	-7.536	12.793	2.628	10.165
GW301784X	7.482	22.718	15.100	7.618
GW301789X	0.533	-3.178	-1.322	1.855
GW301888X	-0.511	2.018	0.753	1.265
GW305074X	22.221	9.873	16.047	6.174

Compound	Trial 1 % Inhib.	Trial 2 % Inhib.	AGV % Inhib.	Std. Dev
GW305178X	3.492	2.389	2.941	0.551
GW320571X	20.450	9.048	14.749	5.701
GW335962X	-1.199	2.213	0.507	1.706
GW345098X	4.000	6.905	5.453	1.453
GW352430A	5.310	15.606	10.458	5.148
GW396574X	4.245	10.570	7.407	3.162
GW405841X	-25.370	2.057	-11.656	13.713
GW406108X	-23.021	5.665	-8.678	14.343
GW406731X	7.529	-0.174	3.678	3.852
GW407034X	10.490	-3.271	3.610	6.880
GW407323A	-13.730	-12.708	-13.219	0.511
GW410563A	6.559	12.934	9.746	3.187
GW412617A	-0.686	-0.286	-0.486	0.200
GW416469X	-1.836	5.818	1.991	3.827
GW416981X	-6.118	-1.890	-4.004	2.114
GW424170A	-15.104	9.391	-2.856	12.247
GW427984X	-11.594	5.577	-3.009	8.586
GW429374A	33.542	57.225	45.383	11.841
GW432441X	7.756	3.410	5.583	2.173
GW434756X	0.961	-6.541	-2.790	3.751
GW435821X	-14.905	-0.671	-7.788	7.117
GW439255X	-14.691	5.313	-4.689	10.002
GW440132A	-4.955	32.751	13.898	18.853
GW440135A	1.209	2.755	1.982	0.773
GW440137A	3.070	26.473	14.771	11.702
GW440138A	5.116	9.771	7.444	2.328
GW440146A	-6.846	22.085	7.620	14.466
GW440148A	5.489	8.367	6.928	1.439
GW441756X	1.270	10.859	6.064	4.794
GW441806A	3.986	8.580	6.283	2.297
GW442130X	6.065	6.390	6.228	0.163
GW445012X	-12.235	1.353	-5.441	6.794
GW445014X	-14.691	3.113	-5.789	8.902
GW445015X	6.307	12.143	9.225	2.918
GW445017X	-16.827	-0.319	-8.573	8.254
GW450241X	15.221	12.857	14.039	1.182
GW457859A	29.734	0.110	14.922	14.812
GW458344X	-0.685	-5.683	-3.184	2.499
GW458787A	4.638	18.613	11.625	6.987
GW459057A	3.285	12.440	7.862	4.578
GW459135A	-16.195	2.903	-6.646	9.549
GW461104A	-7.429	4.345	-1.542	5.887
GW461484A	-17.482	-39.186	-28.334	10.852
GW461487A	2.034	-7.953	-2.959	4.994
GW466413A	-15.882	-9.475	-12.678	3.203
GW468513X	-6.484	-0.211	-3.347	3.137
GW475620X	-24.450	-60.219	-42.335	17.885
GW482059X	0.940	-1.281	-0.171	1.110
GW493036X	7.066	11.864	9.465	2.399

Compound	Trial 1 % Inhib.	Trial 2 % Inhib.	AGV % Inhib.	Std. Dev
GW494601A	-3.640	-2.321	-2.980	0.660
GW494610A	-14.166	-20.520	-17.343	3.177
GW494702A	1.116	-0.012	0.552	0.564
GW497681X	97.348	96.894	97.121	0.227
GW513184X	2.431	-5.745	-1.657	4.088
GW514784X	6.233	16.689	11.461	5.228
GW514786X	-13.050	-23.626	-18.338	5.288
GW515532X	-1.116	-1.396	-1.256	0.140
GW525701A	2.326	5.127	3.726	1.401
GW548057X	-2.009	-5.479	-3.744	1.735
GW549034X	1.577	6.843	4.210	2.633
GW549390X	-0.508	6.889	3.191	3.698
GW551191X	-1.860	-1.001	-1.431	0.430
GW552771X	0.651	-1.099	-0.224	0.875
GW554060X	-5.630	-7.962	-6.796	1.166
GW557777X	4.279	17.776	11.028	6.749
GW559768X	5.132	11.748	8.440	3.308
GW560106X	-11.933	-35.275	-23.604	11.671
GW560109X	26.854	-5.187	10.834	16.020
GW560116X	15.349	11.254	13.301	2.047
GW560459X	-2.831	-9.484	-6.157	3.326
GW561436X	-8.711	5.225	-1.743	6.968
GW566221B	9.061	8.699	8.880	0.181
GW567140X	2.318	-10.484	-4.083	6.401
GW567142A	11.608	5.783	8.695	2.912
GW567143X	9.169	14.339	11.754	2.585
GW567145X	-9.839	5.261	-2.289	7.550
GW567148X	1.956	5.285	3.621	1.665
GW567808A	2.193	6.708	4.451	2.257
GW568326X	6.391	17.183	11.787	5.396
GW568377B	5.142	18.516	11.829	6.687
GW569293E	7.270	6.690	6.980	0.290
GW569530A	3.453	7.103	5.278	1.825
GW569716A	-4.939	-7.331	-6.135	1.196
GW572399X	1.270	4.534	2.902	1.632
GW572401X	5.023	17.235	11.129	6.106
GW572738X	-18.749	5.401	-6.674	12.075
GW574782A	10.813	14.051	12.432	1.619
GW574783B	0.934	5.028	2.981	2.047
GW574783B	0.107	-3.051	-1.472	1.579
GW575533A	4.764	-1.965	1.400	3.364
GW575808A	3.813	22.308	13.061	9.247
GW576484X	-10.847	5.137	-2.855	7.992
GW576604X	11.811	-2.375	4.718	7.093
GW576609A	3.036	0.224	1.630	1.406
GW576924A	7.063	18.863	12.963	5.900
GW577382X	-3.288	-0.948	-2.118	1.170
GW577921A	-24.088	-3.575	-13.832	10.257
GW578342X	30.310	0.741	15.525	14.784

Compound	Trial 1 % Inhib.	Trial 2 % Inhib.	AGV % Inhib.	Std. Dev
GW578748X	9.497	8.289	8.893	0.604
GW579362A	-23.832	-1.878	-12.855	10.977
GW580496A	5.393	13.375	9.384	3.991
GW580509X	6.979	19.852	13.415	6.437
GW581744X	5.887	10.957	8.422	2.535
GW582764A	0.744	1.174	0.959	0.215
GW582868A	-35.424	2.220	-16.602	18.822
GW583340C	-7.588	86.253	39.332	46.920
GW583373A	-18.322	3.201	-7.560	10.761
GW589933X	6.233	7.983	7.108	0.875
GW589961A	-12.555	2.673	-4.941	7.614
GW591947A	-16.260	-21.452	-18.856	2.596
GW595885X	-3.023	-6.056	-4.540	1.517
GW599550X	-5.479	-8.430	-6.955	1.475
GW607049C	3.621	0.976	2.298	1.322
GW607117X	7.482	10.167	8.825	1.342
GW608005X	-4.478	-3.673	-4.076	0.402
GW612286X	13.695	17.381	15.538	1.843
GW615311X	5.551	13.132	9.342	3.790
GW616030X	3.882	6.972	5.427	1.545
GW618013X	6.065	12.890	9.477	3.412
GW620972X	-11.808	3.201	-4.303	7.504
GW621431X	8.974	14.544	11.759	2.785
GW621581X	-1.918	-0.527	-1.222	0.695
GW621823A	8.835	5.711	7.273	1.562
GW621970X	-8.711	4.521	-2.095	6.616
GW622055X	12.520	29.141	20.831	8.311
GW622475X	5.032	1.643	3.337	1.695
GW627512B	5.023	6.292	5.658	0.634
GW627834A	-0.594	4.103	1.755	2.349
GW630813X	11.563	7.588	9.576	1.988
GW630823A	-12.196	1.624	-5.286	6.910
GW631581B	10.554	13.952	12.253	1.699
GW632046X	7.962	13.056	10.509	2.547
GW632580X	-8.284	3.993	-2.145	6.138
GW633459A	7.147	9.376	8.261	1.115
GW635815X	-31.879	-4.496	-18.187	13.691
GW639905A	-14.306	-17.725	-16.015	1.710
GW641155A	3.463	13.181	8.322	4.859
GW642125X	7.669	10.833	9.251	1.582
GW642138X	3.127	10.270	6.699	3.572
GW643971X	-0.337	5.730	2.696	3.033
GW644007X	-11.274	1.089	-5.092	6.181
GW654607A	-8.137	-1.278	-4.707	3.430
GW654652C	3.127	13.278	8.202	5.075
GW659008A	88.311	22.234	55.272	33.038
GW659009A	-4.536	5.727	0.596	5.131
GW659386A	-14.798	3.553	-5.622	9.175
GW659386A	-6.047	-1.594	-3.820	2.226

Compound	Trial 1 % Inhib.	Trial 2 % Inhib.	AGV % Inhib.	Std. Dev
GW659893X	6.821	13.375	10.098	3.277
GW663929X	-3.301	24.280	10.490	13.790
GW664114X	-2.718	-9.638	-6.178	3.460
GW673715X	5.801	0.920	3.361	2.440
GW678313X	-23.875	0.649	-11.613	12.262
GW679395X	-1.209	-0.012	-0.611	0.598
GW679396X	-11.159	-2.286	-6.723	4.437
GW679410X	6.821	26.373	16.597	9.776
GW679662X	-1.713	-0.860	-1.287	0.426
GW680061X	-5.889	-1.069	-3.479	2.410
GW680191X	3.231	3.224	3.228	0.003
GW680338X	0.838	-3.569	-1.366	2.204
GW680903X	-9.422	-3.885	-6.654	2.768
GW680908A	1.566	6.988	4.277	2.711
GW680975X	7.315	12.637	9.976	2.661
GW681170A	-20.049	-41.930	-30.989	10.940
GW681251X	-16.259	-39.369	-27.814	11.555
GW682569X	-5.353	-2.738	-4.046	1.308
GW682841X	21.530	36.533	29.031	7.502
GW683109X	5.813	20.844	13.329	7.515
GW683134A	-10.420	2.937	-3.741	6.678
GW683134A	-7.588	-48.573	-28.081	20.493
GW683768X	7.616	14.648	11.132	3.516
GW684083X	-14.059	-33.150	-23.605	9.546
GW684088X	-14.425	-27.663	-21.044	6.619
GW684374X	-1.803	-6.653	-4.228	2.425
GW684626B	-14.584	2.145	-6.220	8.365
GW684941X	1.395	-0.309	0.543	0.852
GW689066X	-4.201	-8.114	-6.157	1.956
GW692089A	4.930	-0.506	2.212	2.718
GW693028X	-0.186	0.976	0.395	0.581
GW693481X	7.492	13.957	10.724	3.232
GW693542X	-1.488	-2.285	-1.887	0.398
GW693881A	7.744	16.091	11.917	4.173
GW693917X	-5.934	4.697	-0.619	5.316
GW694077X	-20.490	6.164	-7.163	13.327
GW694234A	7.986	17.678	12.832	4.846
GW694590A	14.184	19.224	16.704	2.520
GW695874X	6.139	8.586	7.362	1.223
GW696155X	13.674	32.304	22.989	9.315
GW697465A	-20.028	-33.722	-26.875	6.847
GW697999A	-3.014	-2.529	-2.771	0.242
GW701032X	6.317	13.957	10.137	3.820
GW701424A	-5.766	-8.046	-6.906	1.140
GW701427A	6.307	10.167	8.237	1.930
GW702865X	-9.560	-16.638	-13.099	3.539
GW703087X	11.672	16.400	14.036	2.364
GW707818B	98.227	10.871	54.549	43.678
GW708336X	-16.293	4.169	-6.062	10.231

Compound	Trial 1 % Inhib.	Trial 2 % Inhib.	AGV % Inhib.	Std. Dev
GW708893X	5.369	13.355	9.362	3.993
GW709199X	22.512	6.510	14.511	8.001
GW709213X	-4.390	-3.468	-3.929	0.461
GW711782X	5.393	11.822	8.608	3.214
GW734508X	-13.516	4.873	-4.322	9.195
GW743024X	12.109	21.523	16.816	4.707
GW759710A	-3.012	-3.669	-3.340	0.329
GW767488X	13.116	35.960	24.538	11.422
GW768504A	23.769	46.076	34.922	11.153
GW768505A	33.179	43.640	38.410	5.230
GW769076X	1.480	8.779	5.129	3.649
GW770220A	-11.915	9.097	-1.409	10.506
GW770249A	3.966	9.009	6.488	2.521
GW771127A	8.499	16.479	12.489	3.990
GW772405X	7.072	19.292	13.182	6.110
GW775604X	-2.648	-4.110	-3.379	0.731
GW775608X	-5.614	1.881	-1.867	3.748
GW775610X	-1.674	0.976	-0.349	1.325
GW776245A	0.093	15.306	7.699	7.606
GW777257X	2.998	-5.241	-1.122	4.120
GW778894X	20.923	11.046	15.985	4.938
GW779439X	76.915	74.876	75.895	1.020
GW780056X	13.695	11.649	12.672	1.023
GW780159X	2.204	6.099	4.151	1.948
GW781483X	8.930	11.155	10.043	1.112
GW781673X	3.813	14.847	9.330	5.517
GW782612X	11.522	19.777	15.649	4.128
GW782907X	0.580	16.313	8.446	7.867
GW782912X	-9.352	4.697	-2.327	7.024
GW784041A	43.628	-2.779	20.424	23.204
GW784307A	10.036	14.350	12.193	2.157
GW784684X	36.201	49.751	42.976	6.775
GW784752X	11.579	3.817	7.698	3.881
GW785404X	3.468	8.282	5.875	2.407
GW785804X	7.408	10.949	9.179	1.771
GW785974X	-15.118	5.929	-4.595	10.524
GW786460X	3.666	7.678	5.672	2.006
GW787226A	97.765	3.495	50.630	47.135
GW789449X	-3.023	-5.857	-4.440	1.417
GW792479X	1.302	3.150	2.226	0.924
GW794607X	7.482	13.329	10.406	2.923
GW794726X	-7.323	4.785	-1.269	6.054
GW795493X	8.739	6.292	7.516	1.224
GW796920X	7.011	12.360	9.686	2.675
GW796921X	6.065	17.255	11.660	5.595
GW799251X	-8.818	9.889	0.536	9.353
GW800172X	-12.592	14.952	1.180	13.772
GW801372X	4.880	1.371	3.126	1.754
GW805758X	26.957	4.961	15.959	10.998

Compound	Trial 1 % Inhib.	Trial 2 % Inhib.	AGV % Inhib.	Std. Dev
GW806290X	92.081	5.080	48.580	43.500
GW806742X	51.144	33.649	42.396	8.748
GW806776X	6.149	8.136	7.143	0.994
GW807930X	-9.672	5.313	-2.180	7.492
GW809885X	5.216	6.905	6.061	0.845
GW809893X	24.003	17.921	20.962	3.041
GW809897X	5.393	7.651	6.522	1.129
GW810083X	-5.246	1.851	-1.697	3.549
GW810372X	9.917	18.962	14.440	4.523
GW810437X	-15.701	-22.073	-18.887	3.186
GW810445X	-6.424	-2.112	-4.268	2.156
GW810576X	-12.982	4.433	-4.275	8.708
GW810578X	2.034	0.495	1.265	0.769
GW811168X	12.100	23.113	17.606	5.507
GW811603A	-4.283	-10.665	-7.474	3.191
GW811761X	-8.604	11.209	1.302	9.907
GW812171X	-7.740	19.180	5.720	13.460
GW813244A	-6.424	-4.407	-5.415	1.009
GW813349X	-2.515	-1.579	-2.047	0.468
GW813360X	12.268	16.393	14.330	2.063
GW814408X	8.416	13.763	11.089	2.674
GW817394X	4.797	9.905	7.351	2.554
GW817396X	-15.118	3.817	-5.651	9.468
GW818933X	1.395	-1.495	-0.050	1.445
GW818941X	-6.968	16.415	4.723	11.692
GW819077X	11.073	17.135	14.104	3.031
GW819230X	-12.769	9.889	-1.440	11.329
GW819776X	-6.091	5.408	-0.342	5.749
GW820759X	8.248	25.306	16.777	8.529
GW823670X	-23.098	-28.441	-25.770	2.671
GW824645A	5.635	11.946	8.791	3.155
GW824645A	-10.956	-22.695	-16.825	5.869
GW827099X	-6.362	14.465	4.052	10.413
GW827102X	4.764	17.135	10.950	6.186
GW827105X	6.065	14.442	10.253	4.188
GW827106X	15.066	12.317	13.692	1.374
GW827396X	2.707	2.704	2.706	0.002
GW827654A	-10.636	-22.725	-16.680	6.045
GW828205X	7.442	21.334	14.388	6.946
GW828206X	2.419	1.371	1.895	0.524
GW828525X	3.753	11.668	7.710	3.957
GW828529X	3.966	1.928	2.947	1.019
GW829055X	2.875	0.764	1.820	1.056
GW829058X	-14.422	8.708	-2.857	11.565
GW829115X	-14.905	-0.055	-7.480	7.425
GW829116X	-3.632	-8.444	-6.038	2.406
GW829350X	8.626	8.480	8.553	0.073
GW829351X	1.711	-20.896	-9.592	11.304
GW829874X	17.305	20.642	18.974	1.669

Compound	Trial 1 % Inhib.	Trial 2 % Inhib.	AGV % Inhib.	Std. Dev
GW829877X	4.332	14.449	9.390	5.059
GW829906X	2.371	6.972	4.672	2.300
GW830263A	7.011	8.580	7.795	0.785
GW830365A	2.517	14.947	8.732	6.215
GW830707A	-11.514	1.689	-4.913	6.602
GW830899A	-18.074	-13.376	-15.725	2.349
GW830900A	-14.905	1.705	-6.600	8.305
GW831090X	16.172	21.114	18.643	2.471
GW831091X	6.485	14.248	10.366	3.881
GW832467X	-14.798	9.625	-2.586	12.211
GW833373X	-0.853	4.004	1.575	2.429
GW835314X	-15.422	-25.801	-20.612	5.189
GW837331X	-16.186	-0.759	-8.473	7.714
GW839464X	-6.317	-3.781	-5.049	1.268
GW843682X	9.258	21.512	15.385	6.127
GW846105X	-12.128	5.401	-3.364	8.765
GW852849X	6.492	6.292	6.392	0.100
GW853606X	5.023	10.271	7.647	2.624
GW853609X	1.490	3.410	2.450	0.960
GW854278X	-1.499	-6.255	-3.877	2.378
GW855857X	-2.174	5.660	1.743	3.917
GW856795X	-9.839	-9.804	-9.822	0.018
GW856804X	0.010	-3.471	-1.730	1.741
GW856805X	-2.413	-4.564	-3.489	1.076
GW857175X	20.744	26.572	23.658	2.914
GW861893X	21.503	22.817	22.160	0.657
GW867253X	-5.285	10.074	2.395	7.679
GW867587X	7.950	-1.281	3.335	4.616
GW867588X	-8.285	14.969	3.342	11.627
GW868318X	-11.491	-16.324	-13.908	2.416
GW869516X	-30.924	-12.237	-21.580	9.344
GW869640X	-8.510	3.516	-2.497	6.013
GW869641X	-20.307	-19.123	-19.715	0.592
GW869810X	-6.789	28.897	11.054	17.843
GW869979X	-5.359	-0.783	-3.071	2.288
GW872411X	-4.497	-5.658	-5.078	0.581
GW873004X	4.902	-6.355	-0.726	5.629
GW874091X	9.517	23.999	16.758	7.241
GW876019X	-14.013	-4.041	-9.027	4.986
GW876731X	-5.012	17.928	6.458	11.470
GW876790X	0.446	2.482	1.464	1.018
Hesperadin	-30.495	13.385	-8.555	21.940
HMN-214	-18.973	-15.708	-17.341	1.633
IC-87114	-38.885	-19.027	-28.956	9.929
Imatinib (Gleevec)	-8.153	6.476	-0.839	7.315
Imatinib Mesylate	-5.898	24.536	9.319	15.217
IMD 0354	100.000	98.459	99.230	0.770
INCB28060	-47.852	1.300	-23.276	24.576
Indirubin	-48.571	8.084	-20.244	28.328

Compound	Trial 1 % Inhib.	Trial 2 % Inhib.	AGV % Inhib.	Std. Dev
INK 128 (MLN0128)	3.449	6.115	4.782	1.333
JNJ-38877605	-42.627	11.894	-15.367	27.261
JNJ-7706621	33.500	9.845	21.673	11.828
Ki8751	-28.491	20.354	-4.068	24.422
KRN 633	-22.354	3.319	-9.518	12.836
Ku-0063794	-18.096	3.208	-7.444	10.652
KU-55933	-46.917	12.666	-17.126	29.791
KU-60019	31.371	-27.655	1.858	29.513
KW2449	60.927	-2.655	29.136	31.791
KX2-391	-44.669	11.389	-16.640	28.029
Lapatinib Ditosylate (Tykerb)	-27.078	14.499	-6.289	20.789
LDN193189	16.934	24.877	20.905	3.972
Linifanib (ABT-869)	68.231	-2.774	32.728	35.502
Linsitinib (OSI-906)	-36.863	4.270	-16.297	20.567
LY2228820	97.996	97.788	97.892	0.104
LY2603618 (IC-83)	64.042	42.385	53.213	10.828
LY2784544	-31.872	-11.062	-21.467	10.405
LY294002	-47.453	-1.134	-24.293	23.160
Masitinib (AB1010)	-24.397	43.160	9.382	33.779
MGCD-265	61.302	34.071	47.687	13.616
Milciclib (PHA-848125)	-19.303	25.681	3.189	22.492
MK-2206 2HCl	-23.995	52.328	14.167	38.161
MK-2461	-84.455	-5.922	-45.189	39.267
MK-5108 (VX-689)	46.969	61.868	54.419	7.449
MLN8054	87.265	97.008	92.137	4.872
MLN8237	50.402	90.929	70.665	20.263
Motesanib Diphosphate (AMG-706)	-34.048	8.516	-12.766	21.282
Mubritinib (TAK 165)	-2.021	12.818	5.399	7.420
Neratinib (HKI-272)	99.249	2.765	51.007	48.242
Nilotinib (AMN-107)	-22.654	78.191	27.768	50.422
NU7441 (KU-57788)	-112.125	9.424	-51.351	60.775
NVP-ADW742	99.330	99.131	99.231	0.099
NVP-BGT226	33.937	22.376	28.157	5.781
NVP-BHG712	3.275	0.938	2.107	1.169
NVP-BSK805	36.167	99.732	67.950	31.782
NVP-BVU972	-94.254	-0.818	-47.536	46.718
NVP-TAE226	-68.604	-3.707	-36.155	32.448
ON-01910	-30.996	-12.279	-21.637	9.358
OSI-027	1.045	21.840	11.443	10.397
OSI-420	-10.941	2.188	-4.376	6.565
OSI-930	17.595	18.805	18.200	0.605
OSU-03012	89.812	90.253	90.033	0.220
Palomid 529	-24.321	10.674	-6.823	17.497
Pazopanib HCl	-30.027	21.737	-4.145	25.882
PCl-32765 (Ibrutinib)	-109.895	15.498	-47.199	62.697
PD 0332991 (Palbociclib) HCl	0.268	35.923	18.095	17.827
PD0325901	-31.635	8.130	-11.753	19.883
PD153035 HCl	-45.576	-2.388	-23.982	21.594
PD173074	-20.601	35.951	7.675	28.276

Compound	Trial 1 % Inhib.	Trial 2 % Inhib.	AGV % Inhib.	Std. Dev
PD318088	100.000	89.491	94.746	5.254
PD98059	-24.108	-5.752	-14.930	9.178
Pelitinib (EKB-569)	25.110	-4.757	10.176	14.933
PF-00562271	-58.328	3.082	-27.623	30.705
PF-03814735	-48.014	7.727	-20.144	27.870
PF-04217903	-31.233	6.876	-12.179	19.054
PF-04691502	-46.899	12.997	-16.951	29.948
PF-05212384 (PKI-587)	-16.794	7.816	-4.489	12.305
PH-797804	-126.341	-3.171	-64.756	61.585
PHA-665752	99.464	99.324	99.394	0.070
PHA-680632	-20.225	27.765	3.770	23.995
PHA-767491	-41.603	11.389	-15.107	26.496
PHA-793887	-31.747	-5.088	-18.418	13.329
Phenformin HCl	-30.453	6.744	-11.854	18.599
PHT-427	-22.354	90.265	33.956	56.310
PI-103	-36.059	12.376	-11.841	24.218
Piceatannol	10.655	15.648	13.151	2.497
PIK-293	-43.275	6.208	-18.534	24.742
PIK-294	9.408	12.461	10.934	1.527
PIK-75	4.571	-16.372	-5.900	10.471
PIK-90	53.538	-7.080	23.229	30.309
PIK-93	-36.506	-7.412	-21.959	14.547
PKI-402	-50.801	5.047	-22.877	27.924
PLX-4720	-44.102	1.375	-21.363	22.739
Ponatinib (AP24534)	63.932	49.558	56.745	7.187
PP-121	-75.889	17.731	-29.079	46.810
PP242	-10.105	-4.511	-7.308	2.797
Quercetin (Sophoretin)	-82.857	7.905	-37.476	45.381
Quizartinib (AC220)	-21.603	7.412	-7.096	14.507
R406	0.488	10.853	5.670	5.183
R406 (Free Base)	12.336	-4.535	3.900	8.436
R788 (Fostamatinib)	-67.526	2.724	-32.401	35.125
R935788 (Fostamatinib Disodium, R788)	-65.854	-4.243	-35.048	30.805
Raf265 Derivative	95.540	79.634	87.587	7.953
Rapamycin (Sirolimus)	28.954	51.556	40.255	11.301
Regorafenib (BAY 73-4506)	94.114	93.142	93.628	0.486
Roscovitine (Seliciclib, CYC202)	-43.834	-3.160	-23.497	20.337
Ruxolitinib (INCB018424)	-24.859	0.221	-12.319	12.540
SAR131675	-38.341	2.167	-18.087	20.254
Saracatinib (AZD0530)	-31.769	-1.520	-16.645	15.125
SB 202190	-27.480	32.352	2.436	29.916
SB 203580	-13.941	31.291	8.675	22.616
SB 415286	-93.449	-0.849	-47.149	46.300
SB 431542	-18.767	14.306	-2.230	16.537
SB 525334	-33.500	-25.332	-29.416	4.084
SB-202620	24.450	20.622	22.536	1.914
SB-210313	5.142	21.038	13.090	7.948
SB-210486	-13.692	-14.129	-13.910	0.219
SB-211742	1.488	-11.872	-5.192	6.680

Compound	Trial 1 % Inhib.	Trial 2 % Inhib.	AGV % Inhib.	Std. Dev
SB-211743	-7.188	-3.592	-5.390	1.798
SB-213663	2.326	0.086	1.206	1.120
SB-216385	8.653	16.140	12.397	3.744
SB216763	-25.201	12.666	-6.268	18.933
SB-217146-A	-5.246	-3.990	-4.618	0.628
SB-217360	-2.108	-8.643	-5.376	3.267
SB-217780	-12.772	1.372	-5.700	7.072
SB-219952	-3.648	2.675	-0.487	3.162
SB-219980	7.602	1.747	4.674	2.927
SB-220025-A	-10.526	2.673	-3.927	6.600
SB-220455	4.974	18.516	11.745	6.771
SB-221466	5.145	4.987	5.066	0.079
SB-222516	-3.327	-3.470	-3.399	0.071
SB-222517	-6.357	-2.789	-4.573	1.784
SB-222903	0.744	-0.506	0.119	0.625
SB-223132	25.011	14.236	19.623	5.387
SB-223133	6.233	13.763	9.998	3.765
SB-226605	-9.046	-0.412	-4.729	4.317
SB-226879	-12.449	2.937	-4.756	7.693
SB-229482	-0.365	-3.267	-1.816	1.451
SB-236560	28.582	-9.980	9.301	19.281
SB-236687	4.710	8.235	6.472	1.762
SB-238039-R	10.814	8.214	9.514	1.300
SB-239272	6.485	19.874	13.179	6.695
SB-242717	3.727	10.371	7.049	3.322
SB-242718	7.492	16.479	11.985	4.493
SB-242719	7.986	16.788	12.387	4.401
SB-242721	19.908	16.689	18.298	1.609
SB-245391	8.763	6.380	7.571	1.192
SB-245392	12.109	36.462	24.285	12.176
SB-249175	-2.100	-4.320	-3.210	1.110
SB-250715	10.986	12.161	11.574	0.587
SB-251505	-11.487	6.897	-2.295	9.192
SB-251527	-10.526	3.905	-3.311	7.216
SB-253226	6.752	23.203	14.977	8.226
SB-253228	7.060	8.977	8.018	0.959
SB-254169	9.497	15.899	12.698	3.201
SB-264865	6.149	20.941	13.545	7.396
SB-264866	7.398	17.579	12.489	5.090
SB-278538	11.596	27.363	19.479	7.883
SB-278539	-9.886	3.553	-3.166	6.719
SB-282852	-10.467	65.282	27.407	37.874
SB-282975-A	9.474	-1.082	4.196	5.278
SB-284847-BT	6.727	22.224	14.475	7.748
SB-284851-BT	-13.578	-0.268	-6.923	6.655
SB-284852-BT	2.605	5.917	4.261	1.656
SB-285234-W	12.352	20.346	16.349	3.997
SB-300079	-26.287	11.668	-7.310	18.977
SB-317651	-9.785	13.603	1.909	11.694

Compound	Trial 1 % Inhib.	Trial 2 % Inhib.	AGV % Inhib.	Std. Dev
SB-317658	-4.708	-4.304	-4.506	0.202
SB-317661	-8.712	-6.156	-7.434	1.278
SB-326892	-2.059	-8.088	-5.073	3.014
SB-331032	-6.601	-16.141	-11.371	4.770
SB-333612	-9.458	4.873	-2.293	7.166
SB-333613	-11.044	-6.826	-8.935	2.109
SB-334860	-16.504	-17.787	-17.145	0.642
SB-334865	-2.419	6.510	2.046	4.464
SB-340867	9.677	-4.465	2.606	7.071
SB-341528	15.814	7.103	11.459	4.355
SB-341556	-6.206	10.200	1.997	8.203
SB-342409	-5.889	2.790	-1.549	4.339
SB-342411	-10.353	0.110	-5.121	5.232
SB-347804	-10.206	2.937	-3.634	6.571
SB-358518	11.850	9.674	10.762	1.088
SB-360737	-1.209	1.964	0.377	1.587
SB-360741	19.664	31.806	25.735	6.071
SB-361058	1.912	3.606	2.759	0.847
SB-373598	1.860	-1.989	-0.064	1.925
SB-376715	1.116	1.174	1.145	0.029
SB-376719	12.888	16.041	14.464	1.577
SB-381891	-8.313	2.332	-2.990	5.322
SB-381904	-1.826	-5.058	-3.442	1.616
SB-386023-B	-15.037	-52.172	-33.604	18.568
SB-390523	3.318	2.760	3.039	0.279
SB-390526	-11.096	-12.134	-11.615	0.519
SB-390527	-11.487	5.577	-2.955	8.532
SB-390530	-1.279	-11.486	-6.382	5.104
SB-390532	-1.860	1.174	-0.343	1.517
SB-390534	-2.520	3.137	0.309	2.829
SB-390765	4.186	5.127	4.656	0.470
SB-390766	0.558	1.964	1.261	0.703
SB-390767	-12.772	0.363	-6.205	6.567
SB-390769	1.302	2.755	2.029	0.726
SB-390770	-12.376	12.351	-0.013	12.364
SB-390771	0.548	-1.791	-0.622	1.170
SB-400868-A	42.911	75.293	59.102	16.191
SB-404290	-16.195	0.968	-7.614	8.581
SB-404321	-20.782	-64.426	-42.604	21.822
SB-405367	-14.166	-19.899	-17.033	2.866
SB-408010	-2.210	-16.304	-9.257	7.047
SB-409513	-11.274	5.929	-2.672	8.601
SB-409514	-0.073	-0.210	-0.142	0.068
SB-428218-A	-2.413	-5.857	-4.135	1.722
SB-431533	-9.992	5.929	-2.032	7.961
SB-431542-A	13.320	24.397	18.858	5.539
SB-437013	10.641	8.083	9.362	1.279
SB-476429-A	6.139	11.353	8.746	2.607
SB-477794-AAA	-7.066	-5.346	-6.206	0.860

Compound	Trial 1 % Inhib.	Trial 2 % Inhib.	AGV % Inhib.	Std. Dev
SB-517081	-14.548	-29.675	-22.112	7.564
SB-517389	0.000	-14.542	-7.271	7.271
SB-548492	46.301	-6.428	19.937	26.365
SB-589132	1.581	11.254	6.418	4.836
SB590885	58.746	15.141	36.943	21.802
SB-590885-AAD	10.514	15.218	12.866	2.352
SB-601273	-5.652	-11.668	-8.660	3.008
SB-601436	32.029	2.002	17.016	15.014
SB-610250	8.186	7.993	8.089	0.097
SB-610251-B	4.591	4.700	4.646	0.055
SB-614067-R	14.097	15.046	14.572	0.474
SB-625086-M	0.737	-11.329	-5.296	6.033
SB-627772-A	-1.461	-3.793	-2.627	1.166
SB-630812	-11.487	29.425	8.969	20.456
SB-633825	-15.759	0.209	-7.775	7.984
SB-642057	50.468	-30.285	10.091	40.377
SB-642124-AAA	-13.608	-18.967	-16.288	2.680
SB-657836-AAA	8.191	11.482	9.837	1.646
SB-660566	-26.727	-32.013	-29.370	2.643
SB-675259-M	-3.265	0.825	-1.220	2.045
SB-678557-A	8.416	16.770	12.593	4.177
SB-682330-A	6.727	43.965	25.346	18.619
SB-684387-B	14.298	33.155	23.726	9.428
SB-686709-A	10.554	25.690	18.122	7.568
SB-693162	-0.744	-1.297	-1.021	0.276
SB-693578	5.105	-5.161	-0.028	5.133
SB-698596-AC	9.255	14.830	12.042	2.787
SB-707548-A	-38.172	-34.032	-36.102	2.070
SB-708998	-11.558	5.293	-3.133	8.426
SB-708999	-14.670	-24.737	-19.704	5.034
SB-710363	-13.329	-20.365	-16.847	3.518
SB-710397-B	-14.286	1.764	-6.261	8.025
SB-710903	-11.850	17.389	2.769	14.620
SB-711237	5.384	13.329	9.356	3.973
SB-711239	-5.460	-0.652	-3.056	2.404
SB-711805	-5.694	16.335	5.320	11.014
SB-711880	6.103	-3.572	1.265	4.838
SB-725317	0.272	5.358	2.815	2.543
SB-731254-M	-4.279	-3.175	-3.727	0.552
SB-731284	-7.188	-6.156	-6.672	0.516
SB-731579	-2.831	-2.213	-2.522	0.309
SB-732881-H	13.107	27.165	20.136	7.029
SB-732932	-9.046	-26.932	-17.989	8.943
SB-732941	6.485	16.867	11.676	5.191
SB-733371	-4.497	0.078	-2.209	2.288
SB-733416	-15.882	-3.799	-9.841	6.041
SB-733887	-17.495	0.867	-8.314	9.181
SB-733894	-8.672	-1.591	-5.131	3.541
SB-734117	5.813	20.262	13.038	7.224

Compound	Trial 1 % Inhib.	Trial 2 % Inhib.	AGV % Inhib.	Std. Dev
SB-734909	-13.348	1.372	-5.988	7.360
SB-735216	-11.159	-5.691	-8.425	2.734
SB-735297	-7.603	16.562	4.480	12.083
SB-735464	-5.782	-11.604	-8.693	2.911
SB-735465	11.932	23.410	17.671	5.739
SB-735467	6.223	14.416	10.320	4.097
SB-736290	3.381	13.852	8.617	5.236
SB-736302	1.925	5.822	3.874	1.948
SB-736398	-0.457	-5.269	-2.863	2.406
SB-736715	-10.238	-15.024	-12.631	2.393
SB-737198	5.801	1.219	3.510	2.291
SB-737447	-6.852	-2.321	-4.586	2.266
SB-737856	-6.745	2.686	-2.030	4.715
SB-738004	-7.696	-6.753	-7.225	0.472
SB-738481	-2.140	-0.704	-1.422	0.718
SB-738482	5.216	10.068	7.642	2.426
SB-738561	-13.730	0.649	-6.540	7.189
SB-739245-AC	10.295	9.475	9.885	0.410
SB-739452	5.226	7.263	6.244	1.019
SB-741905	-15.332	1.793	-6.769	8.562
SB-742034-AC	2.355	3.833	3.094	0.739
SB-742251	1.346	-2.375	-0.515	1.861
SB-742352-AC	1.674	6.905	4.290	2.616
SB-742609	-0.558	1.371	0.407	0.965
SB-742864	11.176	14.120	12.648	1.472
SB-742865	6.233	23.269	14.751	8.518
SB-743341	-18.582	-44.490	-31.536	12.954
SB-743899	-14.157	5.225	-4.466	9.691
SB-744941	-3.012	-2.384	-2.698	0.314
SB-747651-A	-12.714	6.356	-3.179	9.535
SB-750140	1.577	9.905	5.741	4.164
SB-750250-M	14.249	-0.485	6.882	7.367
SB-751148	0.961	-0.671	0.145	0.816
SB-751399	6.401	13.957	10.179	3.778
SB-772077-B	7.492	18.904	13.198	5.706
SB-814597	-14.905	3.201	-5.852	9.053
Semaxanib (SU5416)	-85.320	-4.189	-44.754	40.566
SGX-523	-36.595	5.911	-15.342	21.253
SKF-104365	19.126	34.138	26.632	7.506
SKF-104493-B2	-5.563	-2.176	-3.869	1.693
SKF-105561	-5.353	-7.223	-6.288	0.935
SKF-105942	-6.638	-11.604	-9.121	2.483
SKF-106164-A2	-6.769	-7.630	-7.199	0.430
SKF-12778	-9.512	2.334	-3.589	5.923
SKF-18267	-11.125	-10.288	-10.706	0.418
SKF-18355	3.277	0.211	1.744	1.533
SKF-31736	-11.858	-7.179	-9.518	2.340
SKF-62604	11.186	25.306	18.246	7.060
SKF-86002-A2	3.033	5.522	4.277	1.245

Compound	Trial 1 % Inhib.	Trial 2 % Inhib.	AGV % Inhib.	Std. Dev
SKF-86055	4.040	15.207	9.624	5.583
SKF-96418	2.140	4.138	3.139	0.999
SKF-97184	-14.831	0.398	-7.216	7.615
SKF-97236	-0.558	-2.285	-1.422	0.864
SKF-97255	2.977	0.778	1.878	1.099
SKF-97263	-12.772	-0.142	-6.457	6.315
SKF-97293	-3.937	-5.062	-4.499	0.562
SKF-97359	-4.497	43.990	19.746	24.243
SKF-97416	-1.644	-5.690	-3.667	2.023
SKF-97510	-14.960	26.722	5.881	20.841
SKF-97560	-14.615	-11.115	-12.865	1.750
SKF-97620	-1.302	-1.396	-1.349	0.047
SKF-97623	-1.194	-4.863	-3.028	1.834
SNS-032 (BMS-387032)	32.708	96.333	64.520	31.813
SNS-314	8.981	49.723	29.352	20.371
Sorafenib (Nexavar)	90.751	90.157	90.454	0.297
Sotrastaurin (AEB071)	34.288	7.174	20.731	13.557
SP600125	-20.100	-3.650	-11.875	8.225
Staurosporine	-9.080	96.018	43.469	52.549
SU11274	50.134	17.298	33.716	16.418
Sunitinib Malate (Sutent)	-9.115	48.565	19.725	28.840
TAE684 (NVP-TAE684)	93.298	99.324	96.311	3.013
TAK-285	87.030	99.904	93.467	6.437
TAK-733	-25.436	2.903	-11.266	14.169
TAK-901	-61.394	7.012	-27.191	34.203
Tandutinib (MLN518)	-20.777	24.825	2.024	22.801
Telatinib (BAY 57-9352)	-22.091	13.354	-4.368	17.722
Temsirolimus (Torisel)	-7.105	63.812	28.354	35.458
TG 100713	-59.381	-4.092	-31.737	27.644
TG100-115	-19.724	-14.712	-17.218	2.506
TG101209	73.798	86.780	80.289	6.491
TG101348 (SAR302503)	74.634	36.936	55.785	18.849
TGX-221	99.499	-28.540	35.480	64.019
Thiazovivin	-30.745	-4.757	-17.751	12.994
Tideglusib	-45.835	-4.959	-25.397	20.438
Tie2 Kinase Inhibitor	10.207	25.000	17.603	7.397
Tivozanib (AV-951)	10.207	33.407	21.807	11.600
Tofacitinib (CP-690550)	-34.883	-0.722	-17.803	17.080
Tofacitinib Citrate (CP-690550 Citrate)	-17.878	0.337	-8.771	9.108
Torin 1	-57.075	20.173	-18.451	38.624
Torin 2	-68.604	-3.418	-36.011	32.593
TPCA-1	-88.490	-5.826	-47.158	41.332
Triciribine (Triciribine Posphate)	-38.874	20.676	-9.099	29.775
TSU-68 (SU6668)	46.024	3.208	24.616	21.408
TWS119	-39.011	-17.146	-28.078	10.932
Tyrphostin AG 879 (AG 879)	20.454	52.431	36.443	15.989
U0126-EtOH	-36.461	91.894	27.716	64.177
Vandetanib (Zactima)	97.721	99.517	98.619	0.898
Vatalinib 2HCl (PTK787)	-29.759	7.937	-10.911	18.848

Compound	Trial 1 % Inhib.	Trial 2 % Inhib.	AGV % Inhib.	Std. Dev
Vemurafenib (PLX4032)	-37.383	-3.761	-20.572	16.811
VX-680 (MK-0457, Tozasertib)	-40.483	4.656	-17.913	22.569
VX-702	-21.913	-1.781	-11.847	10.066
WAY-600	-49.686	11.925	-18.881	30.806
WHI-P154	-78.403	-8.426	-43.414	34.989
Wortmannin	-30.560	-0.530	-15.545	15.015
WP1066	8.637	29.225	18.931	10.294
WP1130	88.014	88.388	88.201	0.187
WYE-125132	-101.812	6.655	-47.579	54.233
WYE-354	-22.730	51.881	14.575	37.305
WYE-687	-121.882	9.692	-56.095	65.787
WZ3146	43.770	15.376	29.573	14.197
WZ4002	-12.210	4.757	-3.727	8.484
WZ8040	99.123	96.239	97.681	1.442
XL147	-36.729	14.403	-11.163	25.566
XL-184 (Cabozantinib)	-21.716	11.508	-5.104	16.612
XL765	-28.616	-20.465	-24.540	4.076
Y-27632 2HCl	-26.542	14.596	-5.973	20.569
YM201636	33.250	67.810	50.530	17.280
ZM 336372	-51.359	8.263	-21.548	29.811
ZM-447439	-6.300	11.990	2.845	9.145
ZSTK474	-20.643	5.718	-7.463	13.181

Chapter 4: Summary, Conclusions, and Future Directions

Authors and their contributions

Adam J. Schaenzer: Planned, organized, and wrote the manuscript

John-Demian Sauer: Supervised writing and editing the manuscript

Ever since the widespread use of penicillin, humans have been in an antibiotic arms race with bacterial pathogens, oscillating between the rise of new antibiotics and the inevitable development of antibiotic resistance. As such, continued development of novel antibiotics and antibiotic strategies is imperative to slow the rise of resistance and prevent relapse into a "post antibiotic era"[19]. Dysregulation of bacterial signal transduction has become an increasingly attractive target for antibiotic development due to the clinical successes in targeting eukaryotic signaling molecules like protein kinases[172–174]. In the *Firmicutes* and *Actinobacteria*, a family of eSTKs known as the PASTA kinases have gained attention as potential targets for β-lactam adjuvants due to their established roles in maintaining β-lactam resistance (reviewed in [250]). Indeed, various inhibitors have already been identified against *M. tuberculosis* PknB[183,209,210,246,257], *S. aureus* Stk1[247,248,254], *L. monocytogenes* PrkA[237], and *E. faecalis* IreK[239].

This dissertation describes the identification and characterization of two chemical scaffolds as novel PASTA kinase inhibitors: the imidazopyridine aminofurazans (**Chapter 2**), and the pyrazolopyridazines (**Chapter 3**). Both scaffolds were identified as PASTA kinase inhibitors by screening live bacteria against libraries of compounds consisting of previously-established eukaryotic kinase inhibitor pharmacophores. This, along with previous studies[247,248], reinforces the concept that the efforts and resources used to develop eukaryotic kinase inhibitors can be repurposed to target bacterial eSTKs. The screening efforts reported here can be further expanded and modified for future screens. For example, the PKIS1, PKIS2, and Selleck libraries could be screened against purified Stk1 and PrkA. The data generated by cross-referencing the biochemical vs microbiologic screens can shed light on just how many compounds are lost simply due to target inaccessibility. If these data are expanded on with larger compound sets, they can begin to shed light on what chemical properties allow entry into these pathogens; such an empirical data set would be invaluable, as successful antibiotics tend to violate the traditional "Lipinski rule of 5" of orally bioactive compounds[6,292–294]. Alternatively, the libraries could be screened against other pathogens of concern such as *E. faecalis* or *S.*

pneumoniae as screens against these pathogens have yet to be done. With more screening data (both biochemical and microbiological) of the PASTA kinases from other pathogens, it may be possible to find patterns among the compiled hits that can aid in determining which types of scaffolds can act as broad or narrow spectrum PASTA kinase inhibitors.

Other compound libraries could also be screened for PASTA kinase inhibitors, thus increasing the overall diversity of tested pharmacophores. Of note, one could screen specifically for allosteric inhibitors, as allosteric regions are less likely to be as conserved as the active site and allow for greater selectivity (as discussed in **Chapter 1**)[295]. This can be achieved by first performing a biochemical screen with purified kinase domains against compound libraries for hits which inhibit kinase activity. Candidates from the screen can then be validated as substrate-noncompetitive inhibitors through enzyme kinetics studies[296]. It is important to keep in mind that the compound libraries to be tested are unbiased, as the libraries in our current screens are biased for ATP-competitive inhibitors.

Since many screens for PASTA kinase inhibitors utilize repurposed human kinase inhibitor libraries, caution must be taken to ensure that PASTA kinase inhibitors are engineered to be selective for prokaryotic kinases to minimize off-target effects on their eukaryotic counterparts. At first glance, this appears to be an impractical barrier given the high structural homology between eukaryotic kinases and the eSTKs (especially within the highly conserved active site, the traditional target for kinase inhibitors). However, previous work with eukaryotic kinases demonstrates that even these highly conserved active sites possess selective characteristics such as gatekeeper-guarded back pockets and the variable ability to contort into "DFG-in" or "DFG-out" conformations (as discussed in **Chapter 1**)[151,153]. We are the first to demonstrate that at least one of these mechanisms, the gatekeeper-guarded back pocket, can also be exploited in the PASTA kinases (**Chapter 2**). To determine if any of the PASTA kinases can adopt the DFG-out conformation, the purified kinase domains can be challenged in an *in vitro* phosphorylation assay with known type-II inhibitors (such as imatinib and sorafenib) that

stabilize the DFG-out conformation. Those kinases that are robustly inhibited can likely adopt the DFG-out conformation. It is important, however, to use an orthogonal approach to validate these findings such as co-crystalizing the kinases with the inhibitors that are effective against them.

As more lead inhibitor scaffolds are discovered, it will be important to chemically optimize them for better PASTA kinase inhibition. One strategy for optimization is to add different sidechains to the scaffolds but leave their core ring systems intact. However, a more bold strategy would be to rationally hybridize the scaffolds of known PASTA kinase inhibitors to discover novel pharmacophores. This strategy has already proven effective in the discovery of novel eukaryotic kinase inhibitors with hybridized properties[165,297,298]. Inhibitors that target a specific kinase domain could be hybridized in an effort to find more potent inhibitors for that particular kinase, or inhibitors that inhibit different kinases could be hybridized in an effort to increase the compound's spectrum of action.

Beyond drug discovery, it is imperative that future work in the PASTA kinase field answer the question of whether PASTA kinase inhibitors in conjunction with β-lactams can improve survival rates in animal infection models. A single study performed by Kant *et al.* shows promise with the MRSA strain MW2 in a murine septicemia model[254]. However, more studies need to be done to determine if these results are broadly applicable to other species, strains, and infection models. Furthermore, the question of how fast resistance arises to kinase inhibition across species needs to be answered. These studies are crucial in determining if PASTA kinase inhibitors warrant further pharmaceutical development and clinical trials.

As with all other antibiotics, eventual resistance to PASTA kinase inhibitors is inevitable. The important questions to answer are how quickly will resistance arise, and by what mechanism. The most straightforward road to resistance would be to mutate the kinase domain in a way that decreases the affinity of the inhibitor; this is a well-established mechanism in eukaryotic protein kinases[299,300]. Alternatively, mutations in proteins downstream of the kinase

can bypass the blockade on kinase signaling. In the latter case, a better understanding of the PASTA kinase signaling cascades would be beneficial to predict where resistance mutations may arise. To begin to address this, we are in the process of screening for substrates of *S. aureus* Stk1 that are important for maintenance of β-lactam resistance (for a discussion of this approach and preliminary results, see **Appendix A**).

In conclusion, we have identified two novel PASTA kinase inhibitor scaffolds which inhibit *L. monocytogenes* PrkA and *S. aureus* Stk1. Perhaps one day PASTA kinase inhibitors will be a new tool to add to the arsenal of antibiotics as we continue to tackle the rise of antibiotic resistance.

Appendix A: Investigation of the downstream signaling cascades of *S. aureus* Stk1

Authors and their contributions

Adam J. Schaenzer: Planned, designed, and conducted all experiments. Organized data and wrote this manuscript.

John-Demian Sauer: Supervised all research and contributed intellectually to the design of experiments.

INTRODUCTION

Over the years, a variety of PASTA kinase substrates have been identified, including substrates with known roles in cell wall metabolism and antibiotic resistance (**Table A.1**). However, to date there is little overlap amongst different organisms in the phosphorylation of specific cell wall metabolism substrates. Furthermore, with the exception of *E. faecalis* IreB[239], none of these substrates have been demonstrated to be directly involved in the PASTA kinase-dependent β-lactam resistance phenotype, suggesting a potential divergence in the mechanisms these kinases utilize to regulate cell wall homeostasis and stress responses. While it is well established that the PASTA kinases regulate cell wall homeostasis, stress responses, and antibiotic resistance, the mechanism(s) by which the PASTA kinases regulate β-lactam resistance are unknown. Furthermore, despite demonstrating a consistent role in β-lactam resistance across species, the extent and patterns of β-lactam susceptibility in the absence of PASTA kinases vary between species and even amongst strains. This is particularly apparent in *S. aureus*, where Δ*stk1* mutants have been studied in 4 different strains. Deletion of Stk1 in the MRSA strain N315 has minor effects on select cephalosporin and carbapenem MICs[213]. On the other hand, both hospital-acquired MRSA strain COL and community-acquired strain LAC Δ*stk1* mutants are significantly sensitized to nafcillin, cloxacillin, and oxacillin (**Chapter 3**)[223]. Finally, deletion of Stk1 in the MSSA strain NCTC 8325 has minimal effects on β-lactam resistance, resulting in a modest 2-fold sensitization to methicillin and oxacillin and no effect on the MICs of the cephalosporins ceftriaxone and cefepime[236]. The interpretation of these data is made even more complicated due to the inconsistency in the choice of β-lactam to use. However, these data suggest overall that there is variation in Stk1 function even within the species.

Several Stk1 substrates have been identified which are known to play roles in cell division and resistance to cell wall-acting antibiotics (**Table A.1**). Three of the five noted substrates (GraR, VraR, and WalR) are involved in signaling that either directly or indirectly involves modifications to the cell wall[141,301,302]. The fourth substrate, BlaR1, is an antirepressor

which regulates the expression of the Class A β-lactamase BlaZ[303]. Finally, FtsZ is essential for septation during cell division. Phosphorylation of VraR by Stk1 was found to decrease its DNA binding ability[225], while phosphorylation of GraR and WalR increases their affinity for their target DNA[196,216]. Phosphorylation of BlaR1 by Stk1 was noted to increase activity of BlaZ[248]. Phosphorylation of FtsZ within its GTP binding domain results in decreased GTP hydrolysis and ultimately decreased FtsZ polymerization[196]. However, although the direct consequences of substrate phosphorylation have been characterized, whether phosphorylation of these substrates is pertinent to Stk1-mediated β-lactam resistance has yet to be determined.

Here, we utilize a two-pronged approach to determine downstream substrates of Stk1 which are likely candidates to be involved in β-lactam resistance. Additionally, we investigate the role of the β-lactamase system in Stk1-dependent β-lactam resistance, as phosphorylation of the β-lactamase antirepressor BlaR1 implies this system as an obvious link between Stk1 and β-lactam resistance.

RESULTS

Stk1 mediates β-lactam resistance independent of the β-lactamase BlaZ

In 2015, Boudreau *et al* discovered that Stk1 was able to phosphorylate the β-lactamase antirepressor protein BlaR1 in the MRSA strain NRS70 which resulted in increased β-lactamase activity[248]; this led to the hypothesis that Stk1 regulates β-lactam resistance through regulation of the β-lactamase BlaZ. They demonstrate that BlaR1 can be phosphorylated on a specific tyrosine residue and that inhibition of Stk1 with their synthesized compounds decreases tyrosine phosphorylation and BlaZ activity[248]. Because their compounds increase the sensitivity of the MRSA strains tested to β-lactams, they conclude that the β-lactam resistance phenotype is due, in part, to BlaR1 phosphorylation by Stk1. However, as epistasis experiments were never

performed, the direct link between the β-lactam resistance phenotype and Stk1-dependent regulation of BlaZ was never validated.

To fully test this hypothesis, we utilized a nitrocefin assay to determine relative β-lactamase activity of the MRSA strain LAC and its Δ*stk1* mutant in the presence of the β-lactamase-inducing β-lactam cefoxitin. In corroboration with Boudreau *et al*, supernatants from the Δ*stk1* mutant displayed a 2-fold decrease in β-lactamase activity relative to the WT (**Figure A.1A**, LAC & Δ*stk1*). Furthermore, treatment with the Stk1 inhibitor GW779439X showed a similar phenotype which was dependent on the presence of Stk1. Importantly, the MRSA strain JE2, which is a derivative of LAC which lacks the β-lactamase operon, failed to show appreciable β-lactamase activity regardless of the status of Stk1 (**Figure A.1A**, JE2 *& stk1::tn*). However, when tested against the β-lactam oxacillin in broth culture, an Stk1-compromised mutant was still sensitized to the antibiotic relative to its WT counterpart regardless of the status of its β-lactamase (**Figure A.1B**). In fact, the JE2 *stk1::tn* mutant is even more sensitive to oxacillin than its BlaZ-competent counterpart, suggesting either an additive or synergistic relationship rather than an epistatic one. Taken together, our data suggest that while BlaZ activity is indeed regulated in part by Stk1, there are almost certainly other factors regulated by Stk1 which are important for β-lactam resistance. These results are in agreement with the finding that various MRSA strains (such as COL)[223] and other bacterial species (such as *L. monocytogenes*)[222] that lack a β-lactamase are considerably sensitized to β-lactams when their respective PASTA kinases are compromised.

A combined genetics/phosphoproteomics approach identifies 6 candidate proteins

To identify candidate Stk1 substrates important for β-lactam resistance, we utilized a combined genetic screen/phosphoproteomics approach (**Figure A.2**). For the genetics arm, we screened the Nebraska Transposon Mutant Library (NTML, an ordered library in the JE2 strain background)[304] for *S. aureus* mutants with increased susceptibility to the β-lactam oxacillin. For

the phosphoproteomics arm, we utilized shotgun phosphoproteomics to identify phosphorylated proteins in *S. aureus* grown in the presence of sublethal concentrations of β-lactams. Cross-referencing overlap between these two data sets will illuminate proteins that are both important for β-lactam resistance and are phosphorylated during β-lactam treatment. We hypothesize that these proteins are likely Stk1 substrates that directly contribute to β-lactam resistance.

In the first arm of the screen, 69 NTML mutants had a 50% or greater growth inhibition relative to their library plate average in the presence of a sublethal dose of oxacillin (listed in **Table A.2**). As expected, we successfully identified various mutants already established to be important for β-lactam resistance such as PBP2A[305], PBP4[306], and VraR/VraS[142]. When compared with other screens for β-lactam resistance determinants[307,308], we were surprised to find considerable variation between the three screens with only one protein identified in all 3 screens (conserved hypothetical protein SAUSA300_1003) (**Figure A.3A**). However, other expected hits such as PBP4 and PBP2A were found to overlap in 2 of the 3 screens.

In our phosphoproteome experiments, we identified 129 phosphorylated proteins with 29 proteins overlapping between both our oxacillin and nafcillin experiments (**Figure A.3B**) (For complete list of phosphorylated proteins, see **Table A.3**). We identified phosphorylated peptides of Stk1 as well as other established Stk1 substrates such as PurA[236], FtsZ[196], and DnaK[220]. Intriguingly, we also identified other proteins that are involved in cell wall metabolism and cell division, including proteins with established functions like MurZ, MurG, GpsB, PBP1, and SepF (SAUSA300_1083) and putative cell division functions like SAUSA300_1086.

When we cross-referenced the hits from both the phosphoproteome data and NTML library screen, we found 6 proteins that overlap (**Figure A.2**): PurA, PurB, SucB, MurZ, glyceraldehyde 3-phosphate dehydrogenase 2 (Gap), and hypothetical protein SAUSA300_0839.

.

DISCUSSION

Although Stk1 is important for the maintenance of β-lactam resistance in *S. aureus*, the exact mechanism(s) by which resistance is maintained remain unknown. Here we utilize a combination of phosphoproteomics and genetics to identify proteins that are both important for β-lactam resistance and are phosphorylated during exposure to β-lactam stress; the overlap between these data sets would, in theory, contain the most likely candidates to be within the Stk1-dependent β-lactam signaling axis. Although this combination strategy limits candidates to nonessential genes (as a gene must be able to be knocked out by a transposon), the phosphoproteomics data alone can be used to identify essential Stk1 substrates as additional candidates.

When comparing our data from the NTML screen with other *S. aureus*-specific β-lactam screens in the literature (see Rajagopal *et al*[307] and Vestergaard *et al*[308]), we were surprised at how little overlap was present between the three data sets (**Figure A.3A**). That being said, the differences between experimental setup and data analysis need to be considered. Both our screen and that performed by Vestergaard *et al* were performed using the NTML in a growth-based approach while the screen performed by Rajagopal *et al* used the strain NCTC 8325 (an MSSA strain) in a Tn-seq-based approach. There were some proteins identified that were unique to either strain, thereby eliminating the possibility of them ever overlapping. For example, PBP2A is absent from the NCTC 8325 strain while the hypothetical protein SAOUHSC_A02189 is unique to NCTC 8325. With respect to the two NTML screens, experimental conditions almost certainly account for the discrepancies between the data sets. Vestergaard *et al* screened lag phase bacteria on tryptic soy agar plates while we screened log phase bacteria in cation-adjusted Mueller-Hinton broth supplemented with 2% w/v NaCl as per CLSI standards laid out for antibiotic susceptibility testing[286]. These differences alone drastically affect the oxacillin MIC of wild-type JE2 (0.5 µg/mL reported by Vestergaard *et al* vs. 16 µg/mL reported throughout this dissertation).

Notably, our screen identified a larger number of mutants compared to Vestergaard *et al*. This may be the result of the differing data analysis strategies. Vestergaard *et al.* defined their hits on a fold-MIC scale with a minimum category being a 2-fold decrease in MIC[308]. We defined our hits based on a percent-inhibition scale with a hit requiring at least a 50% growth inhibition (see **MATERIALS AND METHODS** section). This would allow us to be more inclusive with our hits as we did not require at least a 2-fold decrease in MIC. It is also important to note that our screen did not take into account mutants that might have a natural growth defect in Mueller-Hinton broth. A secondary screen in Mueller-Hinton without antibiotic is needed to remove any false positives from our data.

Stk1 is the only annotated Ser/Thr protein kinase in the LAC genome; as such, it is unlikely that the phosphorylated proteins identified in our phosphoproteomics data are the result of a different ser/thr kinase. Nevertheless, Stk1 needs to be validated as the kinase responsible for the phosphorylation of any substrate chosen as follow up *in vitro*. Beyond *in vitro* kinase assays, the phosphoproteomics experiments are being repeated with a Δ*stk1* mutant, allowing for any remaining phosphorylated proteins to be ruled out as Stk1 substrates. This also would rule out any proteins which utilize ser/thr phosphorylation as part of their catalytic activity.

We identified various proteins involved in cell wall synthesis and cell division that were not previously known to be phosphorylated in *S. aureus*, including MurG, GpsB, and PBP1. MurG performs the final step in muropeptide synthesis before the monomer is flipped across the membrane[309]. Although MurG has not yet been shown to be phosphorylated in other organisms, Lima *et al* have identified MurG as an interaction partner with the *L. monocytogenes* PASTA kinase PrkA[310], suggesting a potential link between these two proteins. On the other hand, GpsB has been shown to be phosphorylated on a single residue (T75) in *Bacillus subtilis* as part of a negative feedback loop on PrkC activity[311]. In *S. pneumoniae*, GpsB is demonstrated to enhance StkP activity rather than suppress it[312]. Furthermore, it has also been linked to cell wall synthesis through PBP2a and MurA/MurZ in *S. pneumoniae* and *L. monocytogenes*,

respectively[312,313]. We identified 5 potential phosphorylation sites on *S. aureus* GpsB within an 11 amino acid stretch (**Table A.3**). However, we did not find an appreciable impact on β-lactam resistance with the *gpsb::tn* mutant in our NTML screen, suggesting a disconnect between GpsB phosphorylation and β-lactam resistance in *S. aureus*.

When the data from the NTML screen and phosphoproteomics are cross-referenced, only 6 hits are present (**Figure A.2**). One limitation to this approach is that cross-referencing the NTML limits our results to nonessential proteins, forcing us to exclude phosphorylated proteins such as MurG, PBP1, and FtsZ described above. This may explain our low number of hits as many proteins that are important for β-lactam resistance are likely essential cell wall synthesis and cell division proteins. Nevertheless, phosphorylated essential proteins of interest can still be further investigated alongside our overlapping hits using conditional expression of phosphoablative versions of essential genes.

Intriguingly, four of our six overlapping hits are directly involved in central metabolic processes: PurA, PurB, SucB, and Gap. The first pair, PurA and PurB, is involved in purine biosynthesis. PurA has already been established as an Stk1 substrate with phosphorylation decreasing its enzymatic activity[236]. Although PurB has not been studied in the context of PASTA kinase signaling, it has been shown to indirectly regulate PBP2A expression via ppGpp and the stringent response[314]. However, in contrast to our findings, inactivation of PurB increases resistance by shunting more inosine monophosphate towards synthesis of GMP and ultimately ppGpp. Further work is needed to elucidate the link between purine metabolism and β-lactam resistance. The other metabolic enzymes, SucB and Gap, are involved in lysine catabolism and glycolysis, respectively. Lysine is the third amino acid incorporated into the pentapeptide stem of the *S. aureus* muropeptide. Therefore, it is conceivable that dysregulation of lysine metabolism might have indirect consequences on cell wall synthesis. On the other hand, speculation about the role of Gap and glycolysis in β-lactam resistance is more difficult

(though global changes in metabolism certainly have an effect on antibiotic resistance, as reviewed in [315]).

The identification of MurZ in our screen is particularly interesting, as it catalyzes the first committed step in peptidoglycan synthesis along with its paralogue MurA[316]. In *E. faecalis*, overexpression of the MurZ homolog MurAA is able to rescue cephalosporin resistance in a Δ*ireK* PASTA kinase mutant[317]. However, whether this phenotype is due to bypass of an IreK-dependent regulation of MurAA or is the result of a general increase in muropeptide production remains to be determined. Nevertheless, MurZ will be the first hit from our screen that we will follow up on.

MATERIALS AND METHODS

Bacterial strains and growth conditions

Bacteria were maintained at 37°C in tryptic soy broth (TSB) or on tryptic soy agar unless otherwise noted. The LAC derivative JE2, *stk1::tn* mutant, and Nebraska Transposon Mutant Library (NTML) were received from BEI Resources through the National Institute for Allergy and Infectious Diseases. The LAC Δ*stk1* mutant was generated as previously described[280].

Nitrocefin assay

Overnight cultures were back-diluted to an OD_{600} of 0.06 in cation-adjusted Mueller-Hinton medium supplemented with 2% w/v NaCl with 20 µM GW779439X added where noted. After 2 hours of outgrowth, β-lactamase expression was induced with 8 µg/mL cefoxitin (Sigma-Aldrich) for an additional 2 hours. The OD_{600} was then measured for each culture after which their supernatants were harvested and filtered through a 0.2 µm filter. Supernatants were then serial-diluted 1:2 in cation-adjusted Mueller-Hinton medium with 2% w/v NaCl. Samples were incubated with 100 µM nitrocefin (Thermo Fisher, catalog # SR0112) for 30 minutes at room

temperature with the OD_{500} monitored throughout. OD_{500} levels were then normalized to the cultures' respective OD_{600} values.

β-lactam dose-response assay

S. aureus overnight cultures were back-diluted to an OD_{600} of 0.06 into cation-adjusted Mueller-Hinton medium supplemented with 2% w/v NaCl in increasing concentrations of nafcillin. Microdilutions were incubated for 12 hours at 37°C with moderate shaking; OD_{600} was measured throughout the experiment.

NTML oxacillin screen

The NTML was stored in 20 96-well plates in TSB + 32% v/v glycerol at -80°C. Plates were inoculated into 100 µL TSB using a 96-prong plate replicator and sealed with Breathe Easier sealing membranes (Sigma-Aldrich). Plates were incubated overnight at 37°C and 250 rpm. Cultures were then back-diluted 1:100 into fresh TSB and sealed as above and incubated for 3 hours at 37°C and 250 rpm. Finally, cultures were back-diluted 1:100 into cation-adjusted Mueller-Hinton broth supplemented with 2% w/v NaCl. Cultures were incubated for 8 hours with 0.5X MIC of oxacillin (8 µg/mL) at 37°C and 250 rpm. OD_{600} values were then measured for each well. Percent growth was then calculated for each well using the formula $(OD_X / OD_{AVG}) * 100$, where OD_X is the OD_{600} of the selected well and OD_{AVG} is the average OD_{600} of that well's respective plate. A hit was defined as a well with a percent growth ≤ 50%.

Phosphoproteomics

Overnight cultures were back-diluted to an OD_{600} of 0.05 into 1L volumes of cation-adjusted Mueller-Hinton media supplemented with 2% NaCl and either oxacillin (8 µg/mL) or nafcillin (8 µg/mL). Cultures were incubated at 37°C and 250 rpm to late exponential phase

(OD_{600} ~ 0.8). Cells were then pelleted, rinsed with 20 mL chilled PBS, and resuspended with 20 mL chilled lysis buffer (50 mM Tris pH 8 + 5 mM dithiotreitol). PhosSTOP tablets (Roche) were then added as per the manufacturer's instruction. Sodium dodecyl sulfate was added to a final concentration of 0.1% w/v as well as ~1/4th volume of 0.1 mm zirconia/silica beads (BioSpec Products). Cells were then lysed by vortexing for 10 minutes. Supernatants were then harvested and filtered through a 0.2 µm filter. Lysates were digested with trypsin and phosphoenriched with titanium dioxide coated beads. Peptides were then analyzed by nanoLC-MS/MS with an Agilent 1100 nanoflow system coupled to a hybrid linear ion trap-orbitrap mass spectrometer equipped with an EASY-Spray™ electrospray source. Raw MS/MS data was analyzed by the *Mascot* search engine 2.2.07.

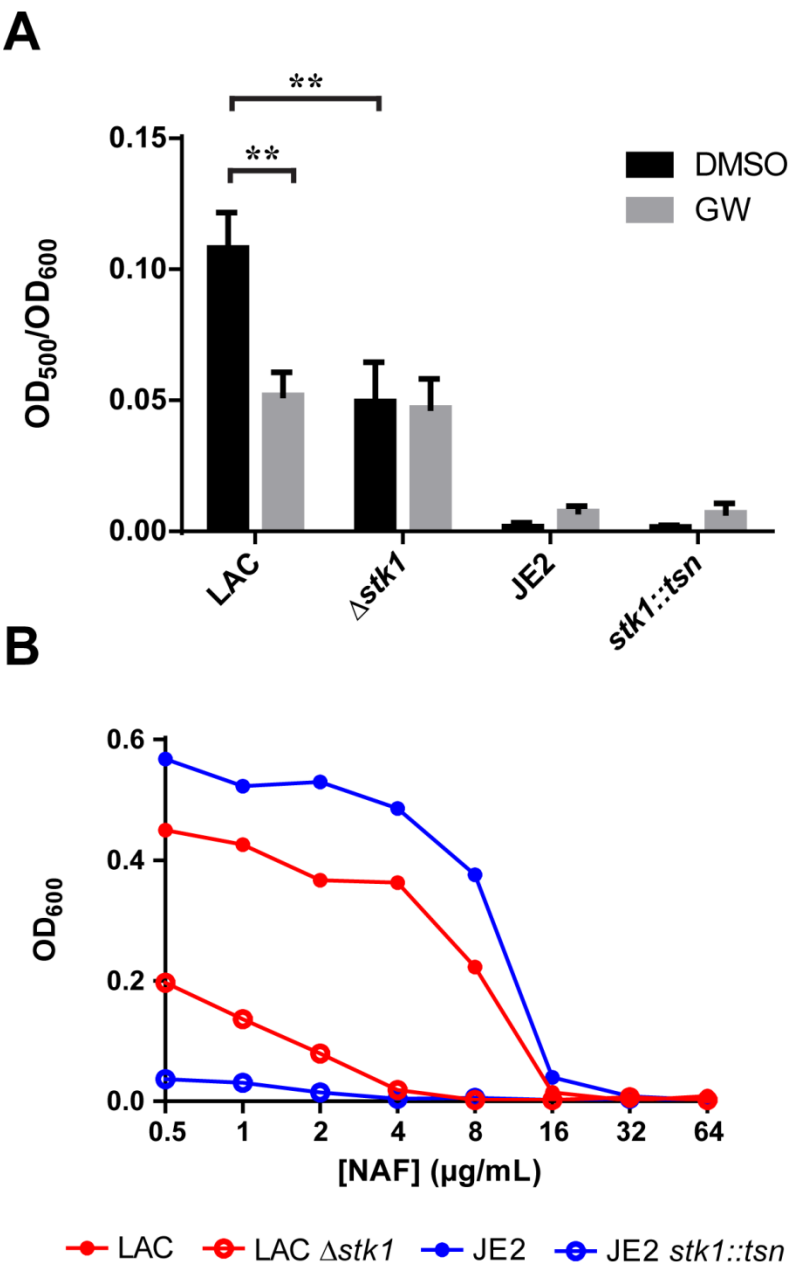

Figure A.1: Stk1 regulates β-lactam resistance in LAC independent of BlaZ. A) Nitrocefin assay. Bacteria were incubated with the BlaZ inducer cefoxitin +/- 20 μM GW779439X, and the supernatants incubated with 100 μM nitrocefin. Error bars represent the SEM of 4 independent trials. ** < 0.005. **B)** Bacteria were back-diluted into increasing concentrations of nafcillin. Curves are representative of 3 independent trials.

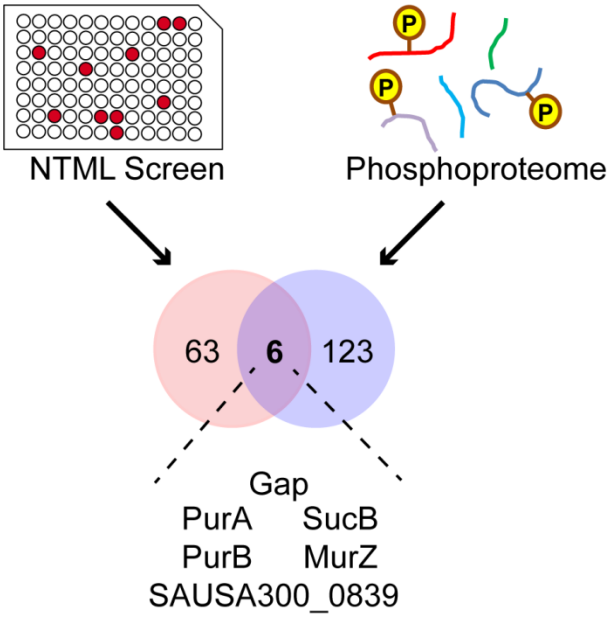

Figure A.2: A two-pronged approach to identify Stk1 substrates important for β-lactam resistance. 6 proteins were identified to be both important for β-lactam resistance in the NTML screen and phosphorylated during β-lactam stress.

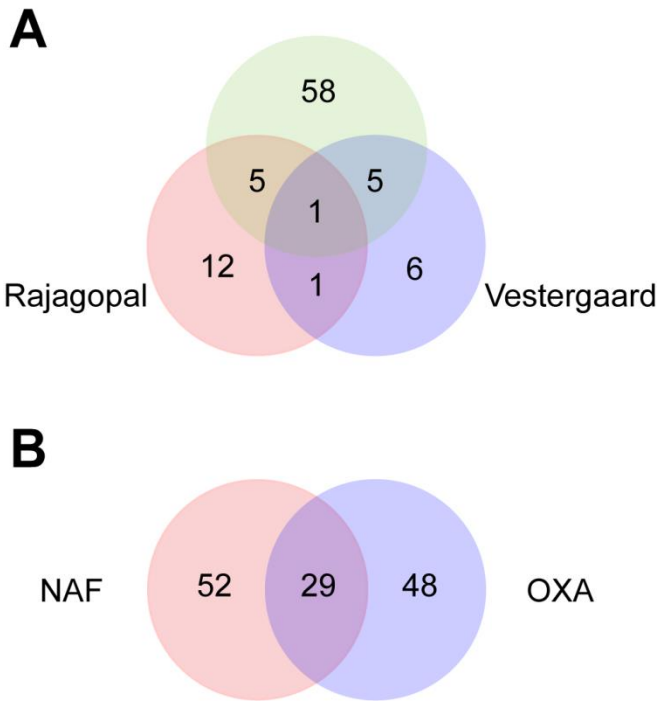

Figure A.3: Data cross-references for NTML screen and phosphoproteome. A) NTML screen data reported here (green circle) cross referenced with NTML screen by Vestergaard *et al*[308] and Tn-seq screen of the *S. aureus* strain NCTC 8325 by Rajagopal *et al*[307]. **B)** Phosphoproteome comparison between trials using nafcillin (NAF) and oxacillin (OXA).

Organism	Substrate	Confirmed kinase-dependent link to β-lactam resistance?
S. aureus	WalR[196]	No
	FtsZ[196]	No
	GraR[216]	No
	VraR[225]	No
	BlaR1[248]	No
L. monocytogenes	YvcK[222]	No
S. pneumoniae	DivIVA[215]	No
	MapZ[318]	No
	GlmM[319]	No
	MacP[320]	No
	MurC[321]	No
E. faecalis	IreB[239]	Yes
M. tuberculosis	CwlM[322]	No
	MviN[323]	No
	FhaA[324]	No
	GlmU[325]	No
	DivIVA[285]	No

Table A.1: PASTA kinase substrates involved in cell wall metabolism, cell division, and cell wall-acting antibiotic resistance

Table A.2: List of NTML mutants with increased OXA sensitivity

Accession number	Gene name	Gene description	% of plate AVG
SAUSA300_0017	purA	adenylosuccinate synthetase	12.5
SAUSA300_0032	mecA	penicillin-binding protein 2'	14.4
SAUSA300_0081	-	conserved hypothetical protein	31.7
SAUSA300_0119	-	ornithine cyclodeaminase	12.3
SAUSA300_0212	-	oxidoreductase, Gfo/Idh/MocA family	23.6
SAUSA300_0449	treC	alpha,alpha-phosphotrehalase	33.0
SAUSA300_0474	-	putative endoribonuclease L-PSP	36.5
SAUSA300_0553	-	hypothetical protein	29.6
SAUSA300_0595	-	conserved hypothetical protein	32.2
SAUSA300_0629	pbp4	penicillin-binding protein 4	12.8
SAUSA300_0711	-	conserved hypothetical protein	47.5
SAUSA300_0726	-	glycerate kinase family protein	40.8
SAUSA300_0794	-	Toprim domain protein	19.8
SAUSA300_0799	int	integrase	39.0
SAUSA300_0839	-	hypothetical protein	46.1
SAUSA300_0867	spsA	signal peptidase IA	46.5
SAUSA300_0901	-	putative competence protein	35.2
SAUSA300_0932	-	hypothetical protein	49.9
SAUSA300_0968	-	phosphoribosylaminoimidazole-succinocarboxamide synthase	34.1
SAUSA300_0974	purN	phosphoribosylglycinamide formyltransferase	20.7
SAUSA300_0980	-	hypothetical protein	22.2
SAUSA300_0994	pdhB	pyruvate dehydrogenase E1 component, beta subunit	20.1
SAUSA300_1003	-	conserved hypothetical protein	17.2
SAUSA300_1019	-	conserved hypothetical protein	26.5
SAUSA300_1047	sdhA	succinate dehydrogenase, flavoprotein subunit	25.5
SAUSA300_1112	-	protein phosphatase 2C domain-containing protein	42.7
SAUSA300_1138	sucC	succinyl-CoA synthetase, beta subunit	33.2
SAUSA300_1139	sucD	succinyl-CoA synthetase subunit alpha	20.1
SAUSA300_1145	xerC	tyrosine recombinase xerC	32.1
SAUSA300_1174	-	conserved hypothetical protein	44.5
SAUSA300_1243	sbcC	exonuclease SbcC	25.7
SAUSA300_1283	-	phosphate ABC transporter, phosphate-binding protein PstS	28.1
SAUSA300_1305	sucB	sucB, E2 component, dihydrolipoamide succinyltransferase	40.8
SAUSA300_1306	sucA	2-oxoglutarate dehydrogenase, E1 component	27.1
SAUSA300_1321	-	hypothetical protein	32.3
SAUSA300_1326	-	putative cell wall enzyme EbsB	46.7
SAUSA300_1356	aroB	3-dehydroquinate synthase	44.0
SAUSA300_1368	ansA	L-asparaginase	34.8

Accession number	Gene name	Gene description	% of plate AVG
SAUSA300_1426	-	conserved hypothetical phage protein	40.6
SAUSA300_1472	xseA	exodeoxyribonuclease VII, large subunit	34.6
SAUSA300_1628	lysP	lysine-specific permease	40.6
SAUSA300_1633	gap	glyceraldehyde 3-phosphate dehydrogenase 2	35.6
SAUSA300_1642	-	D-serine/D-alanine/glycine transporter	20.5
SAUSA300_1674	-	putative serine protease HtrA	35.3
SAUSA300_1712	ribH	6,7-dimethyl-8-ribityllumazine synthase	14.6
SAUSA300_1713	ribBA	riboflavin biosynthesis protein	13.8
SAUSA300_1714	ribE	riboflavin synthase, alpha subunit	14.3
SAUSA300_1731	pckA	phosphoenolpyruvate carboxykinase	33.4
SAUSA300_1801	fumC	fumarate hydratase, class II	35.4
SAUSA300_1865	vraR	DNA-binding response regulator	24.0
SAUSA300_1866	vraS	two-component sensor histidine kinase	21.6
SAUSA300_1889	purB	adenylosuccinate lyase	44.1
SAUSA300_1989	agrB	accessory gene regulator protein B	38.1
SAUSA300_1991	agrC	accessory gene regulator protein C	32.9
SAUSA300_2027	alr	alanine racemase	26.5
SAUSA300_2071	-	HemK family modification methylase	17.3
SAUSA300_2078	murZ	UDP-N-acetylglucosamine 1-carboxyvinyltransferase	50.1
SAUSA300_2108	mtlD	mannitol-1-phosphate 5-dehydrogenase	43.5
SAUSA300_2223	mobB	molybdopterin-guanine dinucleotide biosynthesis protein B	36.3
SAUSA300_2233	-	BioY family protein	32.7
SAUSA300_2249	ssaA	secretory antigen precursor SsaA	40.5
SAUSA300_2278	hutU	urocanate hydratase	36.0
SAUSA300_2297	-	conserved hypothetical protein	25.0
SAUSA300_2302	tcaA	teicoplanin resistance associated membrane protein TcaA protein	32.1
SAUSA300_2312	mqo	malate:quinone oxidoreductase	27.9
SAUSA300_2331	-	transcriptional regulator, MarR family	39.7
SAUSA300_2351	-	Zn-binding lipoprotein adcA-like protein	47.1
SAUSA300_2455	-	putative fructose-1,6-bisphosphatase	21.3
SAUSA300_2462	frp	NAD(P)H-flavin oxidoreductase	37.3

Table A.3: List of phosphorylated proteins under β-lactam stress

(Proteins phosphorylated as part of their own catalytic mechanism are highlighted in red)

Accession Number	Protein Descriptions	Phosphorylation Sites	Condition
SAUSA300_0017	Adenylosuccinate synthetase (purA)	S34	NAF
SAUSA300_0097	Uncharacterized protein	S466	NAF
SAUSA300_0135	Superoxide dismutase (Mn/Fe family) (sodA)	S50	NAF
SAUSA300_0141	Phosphopentomutase (deoB)	S77, S80, T85, T87	Both
SAUSA300_0153	Capsular polysaccharide protein Cap5B	S220	NAF
SAUSA300_0170	Putative aldehyde dehydrogenase AldA	S186, T187	Both
SAUSA300_0177	Uncharacterized protein	S325	NAF
SAUSA300_0181	Non-ribosomal peptide synthetase	Y2297, S2301	Both
SAUSA300_0211	Maltose ABC transporter, permease protein	*Ambiguous*	OXA
SAUSA300_0224	Staphylocoagulase (coa)	T350, T364	NAF
SAUSA300_0278	ESAT-6-like protein	S30, S91	Both
SAUSA300_0279	Putative membrane protein	T166, S167, S702, S703	NAF
SAUSA300_0320	Triacylglycerol lipase	S127, T133, T136	NAF
SAUSA300_0367	Single-stranded DNA-binding protein ssB	S132, S137	NAF
SAUSA300_0379	Alkyl hydroperoxide reductase, subunit F	S454	NAF
SAUSA300_0383	Uncharacterized protein	S295	OXA
SAUSA300_0397	Exotoxin	T18, T22, S109	NAF
SAUSA300_0426	UPF0753 protein	Y835	OXA
SAUSA300_0479	50S ribosomal protein L25 (rplY)	T36, S67	Both
SAUSA300_0481	Transcription-repair coupling factor (mfd)	T431	NAF
SAUSA300_0491	Cysteine synthase (cysK)	T10	OXA
SAUSA300_0507	Transcriptional regulator CtsR	T48	OXA
SAUSA300_0525	50s ribosomal protein L7/L12	S62, S65, S66	Both
SAUSA300_0532	Elongation factor G (fusA)	S238, Y321	OXA
SAUSA300_0533	Elongation Factor Tu (tuF)	S42, S46, S386	Both
SAUSA300_0536	Molecular chaperone Hsp31 and glyoxalase 3 (hchA)	S2, S9	NAF
SAUSA300_0538	Uncharacterized epimerase/dehydratase	T7	NAF
SAUSA300_0540	HAD-superfamily hydrolase, subfamily IA, variant 1	S57, S63, S83	OXA
SAUSA300_0570	Phosphate acetyltransferase (pta)	T129	NAF
SAUSA300_0598	Putative iron compound ABC transporter, iron compound-binding protein	S193	NAF
SAUSA300_0618	ABC transporter, substrate-binding protein	T233	NAF
SAUSA300_0641	Putative lipase/esterase	S338	OXA
SAUSA300_0668	Uncharacterized protein	T55	OXA
SAUSA300_0685	Fructose specific permease (fruA)	S55	OXA

Accession Number	Protein Descriptions	Phosphorylation Sites	Condition
SAUSA300_0717	Ribonucleoside-diphosphate reductase, beta subunit	*Ambiguous*	OXA
SAUSA300_0756	Glyceraldehyde-3 phosphate dehydrogenase	T211	NAF
SAUSA300_0758	Triosephosphate isomerase (tpiA)	*Ambiguous*	OXA
SAUSA300_0764	Ribonuclease R (rnr)	*Ambiguous*	OXA
SAUSA300_0789	Putative thioredoxin	S12, S16, S88	OXA
SAUSA300_0816	UPF0377 protein	T17	NAF
SAUSA300_0839	Uncharacterized protein	*Ambiguous*	OXA
SAUSA300_0861	Glutamate dehydrogenase (gudB)	S264, T267, T269	Both
SAUSA300_0865	Glucose-6 phosphate isomerase (pgi)	T143	Both
SAUSA300_0965	methylenetetrahydrofolate dehydrogenase/methenyltetrahydrofolate cyclohydrolase (folD)	S190	NAF
SAUSA300_0983	Phosphocarrier protein HPr (PtsH)	T12, S46	Both
SAUSA300_0995	Dihydrolipoamide acetyltransferase	T113, T115	Both
SAUSA300_0996	Dihydrolipoyl dehydrogenase (lpdA)	*Ambiguous*	OXA
SAUSA300_1014	Succinate dehydrogenase, flavoprotein subunit (sdhA)	S140, S142, T155	NAF
SAUSA300_1028	Iron-regulated surface determinant protein B (isdB)	*Ambiguous*	OXA
SAUSA300_1044	Thioredoxin (trxA)	S62, T63, S71	Both
SAUSA300_1075	Pencillin-binding-protein 1 (pbpA)	T366, S368, S369	NAF
SAUSA300_1080	Cell division protein FtsZ	S238, S325, T333, S334, T337, S338, T339, T349, S350, S352, S353, S360, S362	Both
SAUSA300_1083	Cell division protein SepF	T43, T44, T84	Both
SAUSA300_1086	Putative cell-division initiation protein	S68	Both
SAUSA300_1087	Isoleucine--tRNA ligase (ileS)	S599	OXA
SAUSA300_1094	Dihydroorotase (pyrC)	T251, T255, T262	OXA
SAUSA300_1113	Ser/Thr Protein kinase Stk1 (pknB)	S159, T161, S162, T164, T166, T168, T230, T288	Both
SAUSA300_1119	Uncharacterized protein	S22	OXA
SAUSA300_1120	ATP-dependent DNA helicase RecG	T601, T604	NAF
SAUSA300_1124	3-oxoacyl-(Acyl-carrier-protein) reductase (fabG)	S76	NAF
SAUSA300_1140	Cell wall hydrolase (lytN)	T137	OXA
SAUSA300_1152	Ribosome-recycling factor (frr)	S27, Y69	OXA
SAUSA300_1217	ABC transporter, ATP-binding protein	S44	OXA
SAUSA300_1249	Glycerol-3-phosphate acyltransferase (plsY)	T42	OXA
SAUSA300_1305	Dihydrolipoyllysine-residue succinyltransferase component (odhB, sucB)	S87, S168, T171, T172	Both
SAUSA300_1311	MurG	S124, T127	NAF

Accession Number	Protein Descriptions	Phosphorylation Sites	Condition
SAUSA300_1337	Cell cycle protein GpsB	S83, S86, T91, T93, S94	Both
SAUSA300_1358	Nucleoside diphosphate kinase (ndk)	T91	NAF
SAUSA300_1365	30S Ribosomal protein S1 (rpsA)	T364, S632	Both
SAUSA300_1370	Elastin-binding protein (ebpS)	S281	Both
SAUSA300_1393	PhiSLT ORF2067-like protein, phage tail tape measure protein	T888, T901	NAF
SAUSA300_1447	Tyrosine recombinase XerD	T143	NAF
SAUSA300_1464	2-oxoisovalerate dehydrogenase, E2 component, dihydrolipoamide acetyltransferase	S177	OXA
SAUSA300_1513	Superoxide dismutase [Mn/Fe] 1 (sodA)	S50, T69	OXA
SAUSA300_1540	Chaperone Protein DnaK	S473, S475, S594, T595	Both
SAUSA300_1541	Protein GrpE	S14, T15	OXA
SAUSA300_1574	UPF0297 protein	T7, Y12	OXA
SAUSA300_1590	GTP pyrophosphokinase	T730	NAF
SAUSA300_1594	Preprotein translocase, YajC subunit (yajC)	S40	OXA
SAUSA300_1603	50S ribosomal protein L21 (rplU)	S45	OXA
SAUSA300_1633	Glyceraldehyde-3-phosphate dehydrogenase (gap)	T211	OXA
SAUSA300_1644	Pyruvate kinase (pyk)	T384, T531, T537, S538	Both
SAUSA300_1646	Acetyl-coenzyme A carboxylase carboxyl transferase subunit alpha (accA)	S292, S294	NAF
SAUSA300_1653	UPF0173 metal-dependent hydrolase	S4	NAF
SAUSA300_1656	Putative universal stress protein	T157	Both
SAUSA300_1662	Aminotransferase, class V	S58	NAF
SAUSA300_1672	Phosphotransferase system, N-acetylglucosamine-specific IIBC component (nagE)	T267,T270	OXA
SAUSA300_1677	Iron-regulated surface determinant protein H (isdH)	T816	NAF
SAUSA300_1685	UPF0478 protein	S109, T151, S156, S159	Both
SAUSA300_1704	Leucine--tRNA ligase (leuS)	Y71	OXA
SAUSA300_1739	Uncharacterized protein	T171, T173	NAF
SAUSA300_1845	Glutamate-1-semialdehyde 2,1-aminomutase 2 (hemL2)	Y296, T300, S307	OXA
SAUSA300_1850	Uncharacterized protein	*Ambiguous*	OXA
SAUSA300_1864	Putative membrane protein	S369, T372	NAF
SAUSA300_1879	Diacylglycerol kinase (dagK)	Y163, T245	Both
SAUSA300_1889	Adenylosuccinate lyase (purB)	T348, S354	NAF
SAUSA300_1983	10 kDa chaperonin OS=Staphylococcus aureus (groS)	S22	OXA
SAUSA300_2012	3-isopropylmalate dehydratase large subunit (leuC)	*Ambiguous*	OXA
SAUSA300_2024	Anti-sigma factor antagonist (rsbV)	*Ambiguous*	OXA

Accession Number	Protein Descriptions	Phosphorylation Sites	Condition
SAUSA300_2030	Putative membrane protein	S100, T104	OXA
SAUSA300_2061	ATP synthase, subunit delta (atpH)	S48, T51, T141	NAF
SAUSA300_2067	Serine hydroxymethyltransferase (glyA)	Y51	OXA
SAUSA300_2076	Putative aldehyde dehydrogenase	S220, S224, S229	NAF
SAUSA300_2078	MurZ	S143	NAF
SAUSA300_2079	Fructose bisphosphate aldolase (fba)	T212, T234	Both
SAUSA300_2097	Uncharacterized protein	T85	NAF
SAUSA300_2132	UPF0457 protein	S53	OXA
SAUSA300_2142	Alkaline shock protein 23 (asp23)	Y12, T16, S80, S110	OXA
SAUSA300_2144	Uncharacterized protein	S143	OXA
SAUSA300_2146	Alcohol dehydrogenase, zinc-containing	S151, S163	NAF
SAUSA300_2186	50S ribosomal protein L30 (rpmD)	S34	NAF
SAUSA300_2192	50S ribosomal protein L5 (rplE)	S47	Both
SAUSA300_2196	50S ribosomal protein L29 (rpmC)	S16	OXA
SAUSA300_2197	50S ribosomal protein L16 (rplP)	S144	NAF
SAUSA300_2204	50S ribosomal protein L3 (rplC)	S153, S161	Both
SAUSA300_2230	Molybdenum ABC transporter, molybdenum-binding protein ModA	T150	NAF
SAUSA300_2235	Iron compound ABC transporter, iron compound-binding protein	S243, S245, S255	NAF
SAUSA300_2240	Urease subunit alpha (ureC)	*Ambiguous*	OXA
SAUSA300_2270	PTS system, arbutin-like IIBC component (glvC)	S444	NAF
SAUSA300_2282	Lysostaphin resistance protein	S249	NAF
SAUSA300_2324	PTS system, sucrose-specific IIBC component	T57	OXA
SAUSA300_2326	Transcription regulatory protein	S503	NAF
SAUSA300_2406	Putative transporter	S384	OXA
SAUSA300_2441	Fibronectin-binding protein A (fnbA)	T246, S248, T253, S257, T258	NAF
SAUSA300_2453	ABC transporter, ATP-binding protein	S178, S183	OXA
SAUSA300_2486	Putative ATP-dependent Clp proteinase	S490, T492, S496	NAF
SAUSA300_2540	Fructose-bisphosphate aldolase class 1 (fda)	S22, S25, S238	Both
SAUSA300_2578	Putative phage infection protein	T697	NAF
SAUSA300_2589	Serine-rich adhesin for platelets	T2199, T2200, T2202	NAF
SAUSA300_0759	2,3-bisphosphoglycerate-independent phosphoglycerate mutase (gpmI)	S62	Both
SAUSA300_2111	Phosphoglucosamine mutase GlmM	S100, S102	Both
SAUSA300_2433	Phosphoglucomutase (pgcA)	T141, S143	Both

REFERENCES

1. Tan, S. Y. & Tatsumura, Y. Alexander Fleming (1881–1955): Discoverer of Penicillin. *Singapore Med. J.* **56,** 366–367 (2015). doi:10.11622/smedj.2015105
2. Houbraken, J., Frisvad, J. C. & Samson', R. A. Fleming's Penicillin Producing Strain Is Not<I> Penicillium Chrysogenum</I> But<I> P. Rubens</I> *IMA Fungus* **2,** 87–95 (2011). doi:10.5598/imafungus.2011.02.01.12
3. Aldridge, S., Parascandola, J. & Sturchio, J. L. The Discovery and Development of Penicillin 1928-1945. *American Chemical Society and Royal Society of Chemistry* 1–10 (1999).
4. Lyddiard, D., Jones, G. L. & Greatrex, B. W. Keeping It Simple: Lessons from the Golden Era of Antibiotic Discovery. *FEMS Microbiol. Lett.* **363,** 2016–2018 (2016). doi:10.1093/femsle/fnw084
5. Waksman, S. A. & Woodruff, H. B. The Soil as a Source of Microorganisms Antagonistic to Disease-Producing Bacteria. *J. Bacteriol.* **40,** 581–600 (1940).
6. Lewis, K. Platforms for Antibiotic Discovery. *Nat. Rev. Drug Discov.* **12,** 371–87 (2013). doi:10.1038/nrd3975
7. Frieden, T. Antibiotic Resistance Threats. *Cdc* 22–50 (2013). doi:CS239559-Bdoi:CS239559-B
8. Projan, S. J. & Shlaes, D. M. Antibacterial Drug Discovery: Is It All Downhill from Here? *Clin. Microbiol. Infect.* **10 Suppl 4,** 18–22 (2004). doi:10.1111/j.1465-0691.2004.1006.x
9. Gaudêncio, S. P. & Pereira, F. Dereplication: Racing to Speed up the Natural Products Discovery Process. *Nat. Prod. Rep.* **32,** 779–810 (2015). doi:10.1039/c4np00134f
10. Watve, M. G., Tickoo, R., Jog, M. M. & Bhole, B. D. How Many Antibiotics Are Produced by the Genus Streptomyces? *Arch. Microbiol.* **176,** 386–390 (2001). doi:10.1007/s002030100345
11. Cox, G., Sieron, A., King, A. M., De Pascale, G., Pawlowski, A. C., Koteva, K. & Wright, G. D. A Common Platform for Antibiotic Dereplication and Adjuvant Discovery. *Cell Chem. Biol.* **24,** 98–109 (2017). doi:10.1016/j.chembiol.2016.11.011
12. Brötz-Oesterhelt, H. & Sass, P. Postgenomic Strategies in Antibacterial Drug Discovery. *Future Microbiol.* **5,** 1553–1579 (2010). doi:10.2217/fmb.10.119
13. Baltz, R. H. Renaissance in Antibacterial Discovery from Actinomycetes. *Curr. Opin. Pharmacol.* **8,** 557–563 (2008). doi:10.1016/j.coph.2008.04.008
14. Maffioli, S. I. A Chemist's Survey of Different Antibiotic Classes. in *Antibiotics* 1–22 (Wiley-VCH Verlag GmbH & Co. KGaA, 2013). doi:10.1002/9783527659685.ch1
15. Spellberg, B., Powers, J. H., Brass, E. P., Miller, L. G. & Edwards, J. E. Trends in Antimicrobial Drug Development: Implications for the Future. *Clin. Infect. Dis.* **38,** 1279–1286 (2004). doi:10.1086/420937
16. Projan, S. J. Why Is Big Pharma Getting out of Antibacterial Drug Discovery? *Curr. Opin. Microbiol.* **6,** 427–430 (2003). doi:10.1016/j.mib.2003.08.003
17. Fair, R. J. & Tor, Y. Antibiotics and Bacterial Resistance in the 21st Century. *Perspect. Medicin. Chem.* **6,** PMC.S14459 (2014). doi:10.4137/PMC.S14459
18. Ventola, C. L. The Antibiotic Resistance Crisis: Part 1: Causes and Threats. *P T* **40,** 277–83 (2015).
19. Alanis, A. J. Resistance to Antibiotics: Are We in the Post-Antibiotic Era? *Arch. Med. Res.* **36,** 697–705 (2005). doi:10.1016/j.arcmed.2005.06.009
20. O'Neill, J. Antimicrobial Resistance : Tackling a Crisis for the Health and Wealth of Nations. (2014).
21. Boucher, H. W., Talbot, G. H., Bradley, J. S., Edwards, J. E., Gilbert, D., Rice, L. B., Scheld, M., Spellberg, B. & Bartlett, J. Bad Bugs, No Drugs: No ESKAPE! An Update from the Infectious Diseases Society of America. *Clin. Infect. Dis.* **48,** 1–12 (2009).

doi:10.1086/595011
22. D'costa, V. M., King, C. E., Kalan, L., Morar, M., Sung, W. W. L., Schwarz, C., Froese, D., Zazula, G., Calmels, F., Debruyne, R., Golding, G. B., Poinar, H. N. & Wright, G. D. Antibiotic Resistance Is Ancient. *Nature* **477,** 457–461 (2011). doi:10.1038/nature10388
23. Wright, G. D. & Poinar, H. Antibiotic Resistance Is Ancient: Implications for Drug Discovery. *Trends Microbiol.* **20,** 157–159 (2012). doi:10.1016/j.tim.2012.01.002
24. Morar, M. & Wright, G. D. The Genomic Enzymology of Antibiotic Resistance. *Annu. Rev. Genet.* **44,** 25–51 (2010). doi:10.1146/annurev-genet-102209-163517
25. Jiang, X., Ellabaan, M. M. H., Charusanti, P., Munck, C., Blin, K., Tong, Y., Weber, T., Sommer, M. O. A. & Lee, S. Y. Dissemination of Antibiotic Resistance Genes from Antibiotic Producers to Pathogens. *Nat. Commun.* **8,** 15784 (2017). doi:10.1038/ncomms15784
26. Barlow, M. What Antimicrobial Resistance Has Taught Us About Horizontal Gene Transfer. in *Horizontal Gene Transfer* **1332,** 397–411 (2009).
27. Munita, J. M. & Arias, C. A. Mechanisms of Antibiotic Resistance. in *Virulence Mechanisms of Bacterial Pathogens, Fifth Edition* **4,** 481–511 (American Society of Microbiology, 2016).
28. Garneau-Tsodikova, S. & Labby, K. J. Mechanisms of Resistance to Aminoglycoside Antibiotics: Overview and Perspectives. *Medchemcomm* **7,** 11–27 (2016). doi:10.1039/C5MD00344J
29. Quirós, L. M., Carbajo, R. J., Braña, A. F. & Salas, J. A. Glycosylation of Macrolide Antibiotics. Purification and Kinetic Studies of a Macrolide Glycosyltransferase from Streptomyces Antibioticus. *J. Biol. Chem.* **275,** 11713–11720 (2000). doi:10.1074/jbc.275.16.11713
30. Yang, W., Moore, I. F., Koteva, K. P., Bareich, D. C., Hughes, D. W. & Wright, G. D. TetX Is a Flavin-Dependent Monooxygenase Conferring Resistance to Tetracycline Antibiotics. *J. Biol. Chem.* **279,** 52346–52352 (2004). doi:10.1074/jbc.M409573200
31. Baysarowich, J., Koteva, K., Hughes, D. W., Ejim, L., Griffiths, E., Zhang, K., Junop, M. & Wright, G. D. Rifamycin Antibiotic Resistance by ADP-Ribosylation: Structure and Diversity of Arr. *Proc. Natl. Acad. Sci.* **105,** 4886–4891 (2008). doi:10.1073/pnas.0711939105
32. Bush, K. Characterization of β-Lactamases. *Antimicrob. Agents Chemother.* 259–263 (1989). doi:10.1006/anae.1996.0030doi:10.1006/anae.1996.0030
33. Bush, K. & Jacoby, G. A. Updated Functional Classification of β-Lactamases. *Antimicrob. Agents Chemother.* **54,** 969–976 (2010). doi:10.1128/AAC.01009-09
34. Korczynska, M., Mukhtar, T. A., Wright, G. D. & Berghuis, A. M. Structural Basis for Streptogramin B Resistance in Staphylococcus Aureus by Virginiamycin B Lyase. *Proc. Natl. Acad. Sci. U. S. A.* **104,** 10388–93 (2007). doi:10.1073/pnas.0701809104
35. Floss, H. G. & Yu, T. W. Rifamycin - Mode of Action, Resistance, and Biosynthesis. *Chem. Rev.* **105,** 621–632 (2005). doi:10.1021/cr030112j
36. Hooper, D. C. Fluoroquinolone Resistance among Gram-Positive Cocci. *Lancet Infect. Dis.* **2,** 530–538 (2002). doi:10.1016/S1473-3099(02)00369-9
37. Mendes, R. E., Deshpande, L. M. & Jones, R. N. Linezolid Update: Stable in Vitro Activity Following More than a Decade of Clinical Use and Summary of Associated Resistance Mechanisms. *Drug Resist. Updat.* **17,** 1–12 (2014). doi:10.1016/j.drup.2014.04.002
38. Weisblum, B. Erythromycin Resistance by Ribosome Modification. *Antimicrob. Agents Chemother.* **39,** 577–585 (1995). doi:10.1128/AAC.39.3.577
39. Leclercq, R. Mechanisms of Resistance to Macrolides and Lincosamides: Nature of the Resistance Elements and Their Clinical Implications. *Clin. Infect. Dis.* **34,** 482–492 (2002). doi:10.1086/324626
40. Katz, L. & Ashley, G. W. Translation and Protein Synthesis: Macrolides. *Chem. Rev.* **105,**

499–527 (2005). doi:10.1021/cr030107f
41. Locke, J. B., Zurenko, G. E., Shaw, K. J. & Bartizal, K. Tedizolid for the Management of Human Infections: In Vitro Characteristics. *Clin. Infect. Dis.* **58,** 35–42 (2014). doi:10.1093/cid/cit616
42. Long, K. S. & Vester, B. Resistance to Linezolid Caused by Modifications at Its Binding Site on the Ribosome. *Antimicrob. Agents Chemother.* **56,** 603–612 (2012). doi:10.1128/AAC.05702-11
43. Giessing, A. M. B., Jensen, S. S., Rasmussen, A., Hansen, L. H., Gondela, A., Long, K., Vester, B. & Kirpekar, F. Identification of 8-Methyladenosine as the Modification Catalyzed by the Radical SAM Methyltransferase Cfr That Confers Antibiotic Resistance in Bacteria. *Rna* **15,** 327–336 (2009). doi:10.1261/rna.1371409
44. Fuda, C., Suvorov, M., Vakulenko, S. B. & Mobashery, S. The Basis for Resistance to β-Lactam Antibiotics by Penicillin-Binding Protein 2a of Methicillin-Resistant Staphylococcus Aureus. *J. Biol. Chem.* **279,** 40802–40806 (2004). doi:10.1074/jbc.M403589200
45. Lim, D. & Strynadka, N. C. J. Structural Basis for the β Lactam Resistance of PBP2a from Methicillin-Resistant Staphylococcus Aureus. *Nat. Struct. Biol.* **9,** (2002). doi:10.1038/nsb858
46. Leski, T. a & Tomasz, A. Role of Penicillin-Binding Protein 2 (PBP2) in the Antibiotic Susceptibility and Cell Wall Cross-Linking of Staphylococcus Aureus. *J. Bacteriol.* **2,** 1815–1824 (2005). doi:10.1128/JB.187.5.1815
47. Reynolds, P. E. Structure, Biochemistry and Mechanism of Action of Glycopeptide Antibiotics. *Eur. J. Clin. Microbiol. Infect. Dis.* **8,** 943–950 (1989). doi:10.1007/BF01967563
48. Miller, W. R., Munita, J. M. & Arias, C. A. Mechanisms of Antibiotic Resistance in Enterococci. *Expert Rev. Anti. Infect. Ther.* **12,** 1221–1236 (2014). doi:10.1586/14787210.2014.956092
49. Webber, M. A. The Importance of Efflux Pumps in Bacterial Antibiotic Resistance. *J. Antimicrob. Chemother.* **51,** 9–11 (2003). doi:10.1093/jac/dkg050
50. Chopra, I. & Roberts, M. Tetracycline Antibiotics: Mode of Action, Applications, Molecular Biology, and Epidemiology of Bacterial Resistance. *Microbiol. Mol. Biol. Rev.* **65,** 232–260 (2001). doi:10.1128/MMBR.65.2.232-260.2001
51. Wang, W., Guo, Q., Xu, X., Sheng, Z. -k., Ye, X. & Wang, M. High-Level Tetracycline Resistance Mediated by Efflux Pumps Tet(A) and Tet(A)-1 with Two Start Codons. *J. Med. Microbiol.* **63,** 1454–1459 (2014). doi:10.1099/jmm.0.078063-0
52. Fernandez, L. & Hancock, R. E. W. Adaptive and Mutational Resistance: Role of Porins and Efflux Pumps in Drug Resistance. *Clin. Microbiol. Rev.* **25,** 661–681 (2012). doi:10.1128/CMR.00043-12
53. Delcour, A. H. Outer Membrane Permeability and Antibiotic Resistance. *Biochim. Biophys. Acta - Proteins Proteomics* **1794,** 808–816 (2009). doi:10.1016/j.bbapap.2008.11.005
54. Ballestero, S., Fernández-Rodríguez, A., Villaverde, R., Escobar, H., Pérez-Díaz, J. C. & Baquero, F. Carbapenem Resistance in Pseudomonas Aeruginosa from Cystic Fibrosis Patients. *J. Antimicrob. Chemother.* **38,** 39–45 (1996).
55. Arbing, M. A., Dahan, D., Boismenu, D., Mamer, O. A., Hanrahan, J. W. & Coulton, J. W. Charged Residues in Surface-Located Loops Influence Voltage Gating of Porin from Haemophilus Influenzae Type B. *J. Membr. Biol.* **178,** 185–193 (2000). doi:10.1007/s002320010026
56. Bishop, N. D., Lea, E. J. A., Mobasheri, H. & Spiro, S. Altered Voltage Sensitivity of Mutant OmpC Porin Channels. *FEBS Lett.* **379,** 295–298 (1996). doi:10.1016/0014-5793(95)01535-3

57. Tamaki, S., Sato, T. & Matsuhashi, M. Role of Lipopolysaccharides in Antibiotic Resistance and Bacteriophage Adsorption of Escherichia Coli K-12. *J. Bacteriol.* **105,** 968–975 (1971).
58. Snyder, D. S. & McIntosh, T. J. The Lipopolysaccharide Barrier: Correlation of Antibiotic Susceptibility with Antibiotic Permeability and Fluorescent Probe Binding Kinetics †. *Biochemistry* **39,** 11777–11787 (2000). doi:10.1021/bi000810n
59. Llobet, E., Tomas, J. M. & Bengoechea, J. A. Capsule Polysaccharide Is a Bacterial Decoy for Antimicrobial Peptides. *Microbiology* **154,** 3877–3886 (2008). doi:10.1099/mic.0.2008/022301-0
60. Nishi, H., Komatsuzawa, H., Fujiwara, T., McCallum, N. & Sugai, M. Reduced Content of Lysyl-Phosphatidylglycerol in the Cytoplasmic Membrane Affects Susceptibility to Moenomycin, as Well as Vancomycin, Gentamicin, and Antimicrobial Peptides, in Staphylococcus Aureus. *Antimicrob. Agents Chemother.* **48,** 4800–4807 (2004). doi:10.1128/AAC.48.12.4800-4807.2004
61. Peschel, A., Otto, M., Jack, R. W., Kalbacher, H., Jung, G. & Götz, F. Inactivation of the Dlt Operon in Staphylococcus Aureus Confers Sensitivity to Defensins, Protegrins, and Other Antimicrobial Peptides. *J. Biol. Chem.* **274,** 8405–8410 (1999). doi:10.1074/jbc.274.13.8405
62. Jones, T., Yeaman, M. R., Sakoulas, G., Yang, S.-J., Proctor, R. A., Sahl, H.-G., Schrenzel, J., Xiong, Y. Q. & Bayer, A. S. Failures in Clinical Treatment of Staphylococcus Aureus Infection with Daptomycin Are Associated with Alterations in Surface Charge, Membrane Phospholipid Asymmetry, and Drug Binding. *Antimicrob. Agents Chemother.* **52,** 269–278 (2008). doi:10.1128/AAC.00719-07
63. Yang, S.-J., Mishra, N. N., Rubio, A. & Bayer, A. S. Causal Role of Single Nucleotide Polymorphisms within the MprF Gene of Staphylococcus Aureus in Daptomycin Resistance. *Antimicrob. Agents Chemother.* **57,** 5658–5664 (2013). doi:10.1128/AAC.01184-13
64. Elander, R. P. Industrial Production of β-Lactam Antibiotics. *Appl. Microbiol. Biotechnol.* **61,** 385–392 (2003). doi:10.1007/s00253-003-1274-y
65. Tipper, D. J. & Strominger, J. L. Mechanism of Action of Penicillins: A Proposal Based on Their Structural Similarity to Acyl-D-Alanyl-D-Alanine. *Proc. Natl. Acad. Sci.* **54,** 1133–1141 (1965). doi:10.1073/pnas.54.4.1133
66. Cho, H., Uehara, T. & Bernhardt, T. G. Beta-Lactam Antibiotics Induce a Lethal Malfunctioning of the Bacterial Cell Wall Synthesis Machinery. *Cell* **159,** 1300–1311 (2014). doi:10.1016/j.cell.2014.11.017
67. Poole, K. Resistance to β-Lactam Antibiotics. *Cell. Mol. Life Sci.* **61,** 2200–2223 (2004). doi:10.1007/s00018-004-4060-9
68. Fisher, J. F. & Mobashery, S. β-Lactam Resistance Mechanisms: Gram-Positive Bacteria and Mycobacterium Tuberculosis. *Cold Spring Harb. Perspect. Med.* **6,** a025221 (2016). doi:10.1101/cshperspect.a025221
69. Toussaint, K. A. & Gallagher, J. C. β-Lactam/β-Lactamase Inhibitor Combinations-From Then to Now. *Ann. Pharmacother.* **49,** 86–98 (2015). doi:10.1177/1060028014556652
70. Queenan, A. M. & Bush, K. Carbapenemases: The Versatile β-Lactamases. *Clin. Microbiol. Rev.* **20,** 440–458 (2007). doi:10.1128/CMR.00001-07
71. Zhanel, G. G., Lawrence, C. K., Adam, H., Schweizer, F., Zelenitsky, S., Zhanel, M., Lagacé-Wiens, P. R. S., Walkty, A., Denisuik, A., Golden, A., Gin, A. S., Hoban, D. J., Lynch, J. P. & Karlowsky, J. A. Imipenem–Relebactam and Meropenem–Vaborbactam: Two Novel Carbapenem-β-Lactamase Inhibitor Combinations. *Drugs* **78,** 787–787 (2018). doi:10.1007/s40265-018-0910-x
72. Zhanel, G. G., Lawson, C. D., Adam, H., Schweizer, F., Zelenitsky, S., Lagacé-Wiens, P. R. S., Denisuik, A., Rubinstein, E., Gin, A. S., Hoban, D. J., Lynch, J. P. & Karlowsky, J.

A. Ceftazidime-Avibactam: A Novel Cephalosporin/β-Lactamase Inhibitor Combination. *Drugs* **73,** 159–177 (2013). doi:10.1007/s40265-013-0013-7
73. Meini, M.-R., Llarrull, L. & Vila, A. Evolution of Metallo-β-Lactamases: Trends Revealed by Natural Diversity and in Vitro Evolution. *Antibiotics* **3,** 285–316 (2014). doi:10.3390/antibiotics3030285
74. Page, M. I. & Badarau, A. The Mechanisms of Catalysis by Metallo β-Lactamases. *Bioinorg. Chem. Appl.* **2008,** 1–14 (2008). doi:10.1155/2008/576297
75. Rotondo, C. M. & Wright, G. D. Inhibitors of Metallo-β-Lactamases. *Curr. Opin. Microbiol.* **39,** 96–105 (2017). doi:10.1016/j.mib.2017.10.026
76. Bush, K., Heep, M., Macielag, M. J. & Noel, G. J. Anti-MRSA β-Lactams in Development, with a Focus on Ceftobiprole: The First Anti-MRSA β-Lactam to Demonstrate Clinical Efficacy. *Expert Opin. Investig. Drugs* **16,** 419–429 (2007). doi:10.1517/13543784.16.4.419
77. Duplessis, C. & Crum-Cianflone, N. F. Ceftaroline: A New Cephalosporin with Activity Against Methicillin-Resistant Staphylococcus Aureus (MRSA). *Clin. Med. Rev. Ther.* **3,** 1–17 (2011). doi:10.4137/CMRT.S1637
78. Davies, T. A., Page, M. G. P., Shang, W., Andrew, T., Kania, M. & Bush, K. Binding of Ceftobiprole and Comparators to the Penicillin-Binding Proteins of Escherichia Coli, Pseudomonas Aeruginosa, Staphylococcus Aureus, and Streptococcus Pneumoniae. *Antimicrob. Agents Chemother.* **51,** 2621–2624 (2007). doi:10.1128/AAC.00029-07
79. Mushtaq, S., Warner, M., Ge, Y., Kaniga, K. & Livermore, D. M. In Vitro Activity of Ceftaroline (PPI-0903M, T-91825) against Bacteria with Defined Resistance Mechanisms and Phenotypes. *J. Antimicrob. Chemother.* **60,** 300–311 (2007). doi:10.1093/jac/dkm150
80. Long, S. W., Olsen, R. J., Mehta, S. C., Palzkill, T., Cernoch, P. L., Perez, K. K., Musick, W. L., Rosato, A. E. & Musser, J. M. PBP2a Mutations Causing High-Level Ceftaroline Resistance in Clinical Methicillin-Resistant Staphylococcus Aureus Isolates. *Antimicrob. Agents Chemother.* **58,** 6668–6674 (2014). doi:10.1128/AAC.03622-14
81. Alm, R. A., McLaughlin, R. E., Kos, V. N., Sader, H. S., Iaconis, J. P. & Lahiri, S. D. Analysis of Staphylococcus Aureus Clinical Isolates with Reduced Susceptibility to Ceftaroline: An Epidemiological and Structural Perspective. *J. Antimicrob. Chemother.* **69,** 2065–2075 (2014). doi:10.1093/jac/dku114
82. Chan, L. C., Basuino, L., Diep, B., Hamilton, S., Chatterjee, S. S. & Chambers, H. F. Ceftobiprole- and Ceftaroline-Resistant Methicillin-Resistant Staphylococcus Aureus. *Antimicrob. Agents Chemother.* **59,** 2960–2963 (2015). doi:10.1128/AAC.05004-14
83. Mendes, R. E., Tsakris, A., Sader, H. S., Jones, R. N., Biek, D., McGhee, P., Appelbaum, P. C. & Kosowska-Shick, K. Characterization of Methicillin-Resistant Staphylococcus Aureus Displaying Increased MICs of Ceftaroline. *J. Antimicrob. Chemother.* **67,** 1321–1324 (2012). doi:10.1093/jac/dks069
84. Lahiri, S. D. & Alm, R. A. Identification of Non-PBP2a Resistance Mechanisms in Staphylococcus Aureus after Serial Passage with Ceftaroline: Involvement of Other PBPs. *J. Antimicrob. Chemother.* **71,** 3050–3057 (2016). doi:10.1093/jac/dkw282
85. Coates, A. R., Halls, G. & Hu, Y. Novel Classes of Antibiotics or More of the Same? *Br. J. Pharmacol.* **163,** 184–194 (2011). doi:10.1111/j.1476-5381.2011.01250.x
86. Stewart, E. J. Growing Unculturable Bacteria. *J. Bacteriol.* **194,** 4151–4160 (2012). doi:10.1128/JB.00345-12
87. Thaker, M. N., Wang, W., Spanogiannopoulos, P., Waglechner, N., King, A. M., Medina, R. & Wright, G. D. Identifying Producers of Antibacterial Compounds by Screening for Antibiotic Resistance. *Nat. Biotechnol.* **31,** 922–927 (2013). doi:10.1038/nbt.2685
88. Kaeberlein, T. Isolating 'Uncultivable' Microorganisms in Pure Culture in a Simulated Natural Environment. *Science (80-.).* **296,** 1127–1129 (2002). doi:10.1126/science.1070633

89. Zengler, K., Toledo, G., Rappe, M., Elkins, J., Mathur, E. J., Short, J. M. & Keller, M. Cultivating the Uncultured. *Proc. Natl. Acad. Sci.* **99,** 15681–15686 (2002). doi:10.1073/pnas.252630999
90. Rutledge, P. J. & Challis, G. L. Discovery of Microbial Natural Products by Activation of Silent Biosynthetic Gene Clusters. *Nat. Rev. Microbiol.* **13,** 509–523 (2015). doi:10.1038/nrmicro3496
91. Becerril, A., Álvarez, S., Braña, A. F., Rico, S., Díaz, M., Santamaría, R. I., Salas, J. A. & Méndez, C. Uncovering Production of Specialized Metabolites by Streptomyces Argillaceus: Activation of Cryptic Biosynthesis Gene Clusters Using Nutritional and Genetic Approaches. *PLoS One* **13,** e0198145 (2018). doi:10.1371/journal.pone.0198145
92. Saha, S., Zhang, W., Zhang, G., Zhu, Y., Chen, Y., Liu, W., Yuan, C., Zhang, Q., Zhang, H., Zhang, L., Zhang, W. & Zhang, C. Activation and Characterization of a Cryptic Gene Cluster Reveals a Cyclization Cascade for Polycyclic Tetramate Macrolactams. *Chem. Sci.* **8,** 1607–1612 (2017). doi:10.1039/C6SC03875A
93. Li, S., Wu, X., Zhang, L., Shen, Y. & Du, L. Activation of a Cryptic Gene Cluster in Lysobacter Enzymogenes Reveals a Module/Domain Portable Mechanism of Nonribosomal Peptide Synthetases in the Biosynthesis of Pyrrolopyrazines. *Org. Lett.* **19,** 5010–5013 (2017). doi:10.1021/acs.orglett.7b01611
94. Gupta, A., Bedre, R., Thapa, S. S., Sabrin, A., Wang, G., Dassanayake, M. & Grove, A. Global Awakening of Cryptic Biosynthetic Gene Clusters in Burkholderia Thailandensis. *ACS Chem. Biol.* **12,** 3012–3021 (2017). doi:10.1021/acschembio.7b00681
95. Tanaka, Y., Kasahara, K., Hirose, Y., Murakami, K., Kugimiya, R. & Ochi, K. Activation and Products of the Cryptic Secondary Metabolite Biosynthetic Gene Clusters by Rifampin Resistance (RpoB) Mutations in Actinomycetes. *J. Bacteriol.* **195,** 2959–2970 (2013). doi:10.1128/JB.00147-13
96. Riddell, J. 2018 IAS-USA Recommendations for the Use of Antiretroviral Therapy for HIV. *JAMA* **320,** 347 (2018). doi:10.1001/jama.2018.9184
97. Ocampo, P. S., Lázár, V., Papp, B., Arnoldini, M., Abel zur Wiesch, P., Busa-Fekete, R., Fekete, G., Pál, C., Ackermann, M. & Bonhoeffer, S. Antagonism between Bacteriostatic and Bactericidal Antibiotics Is Prevalent. *Antimicrob. Agents Chemother.* **58,** 4573–4582 (2014). doi:10.1128/AAC.02463-14
98. Corsonello, A., Abbatecola, A. M., Fusco, S., Luciani, F., Marino, A., Catalano, S., Maggio, M. G. & Lattanzio, F. The Impact of Drug Interactions and Polypharmacy on Antimicrobial Therapy in the Elderly. *Clin. Microbiol. Infect.* **21,** 20–26 (2015). doi:10.1016/j.cmi.2014.09.011
99. Macy, E., Romano, A. & Khan, D. Practical Management of Antibiotic Hypersensitivity in 2017. *J. Allergy Clin. Immunol. Pract.* **5,** 577–586 (2017). doi:10.1016/j.jaip.2017.02.014
100. Abedon, S. T., Kuhl, S. J., Blasdel, B. G. & Kutter, E. M. Phage Treatment of Human Infections. *Bacteriophage* **1,** 66–85 (2011). doi:10.4161/bact.1.2.15845
101. Lin, D. M., Koskella, B. & Lin, H. C. Phage Therapy: An Alternative to Antibiotics in the Age of Multi-Drug Resistance. *World J. Gastrointest. Pharmacol. Ther.* **8,** 162 (2017). doi:10.4292/wjgpt.v8.i3.162
102. Chang, R. Y. K., Wallin, M., Lin, Y., Leung, S. S. Y., Wang, H., Morales, S. & Chan, H.-K. Phage Therapy for Respiratory Infections. *Adv. Drug Deliv. Rev.* 1–11 (2018). doi:10.1016/j.addr.2018.08.001doi:10.1016/j.addr.2018.08.001
103. Fish, R., Kutter, E., Wheat, G., Blasdel, B., Kutateladze, M. & Kuhl, S. Bacteriophage Treatment of Intransigent Diabetic Toe Ulcers: A Case Series. *J. Wound Care* **25,** S27–S33 (2016). doi:10.12968/jowc.2016.25.Sup7.S27
104. Schooley, R. T. et al. Development and Use of Personalized Bacteriophage-Based Therapeutic Cocktails To Treat a Patient with a Disseminated Resistant Acinetobacter Baumannii Infection. *Antimicrob. Agents Chemother.* **61,** 1–14 (2017).

doi:10.1128/AAC.00954-17
105. Wright, A., Hawkins, C. H., Änggård, E. E. & Harper, D. R. A Controlled Clinical Trial of a Therapeutic Bacteriophage Preparation in Chronic Otitis Due to Antibiotic-Resistant Pseudomonas Aeruginosa ; a Preliminary Report of Efficacy. *Clin. Otolaryngol.* **34,** 349–357 (2009). doi:10.1111/j.1749-4486.2009.01973.x
106. Labrie, S. J., Samson, J. E. & Moineau, S. Bacteriophage Resistance Mechanisms. *Nat. Rev. Microbiol.* **8,** 317–327 (2010). doi:10.1038/nrmicro2315
107. Chan, B. K., Abedon, S. T. & Loc-Carrillo, C. Phage Cocktails and the Future of Phage Therapy. *Future Microbiol.* **8,** 769–783 (2013). doi:10.2217/fmb.13.47
108. Núñez, M. E., Martin, M. O., Duong, L. K., Ly, E. & Spain, E. M. Investigations into the Life Cycle of the Bacterial Predator Bdellovibrio Bacteriovorus 109J at an Interface by Atomic Force Microscopy. *Biophys. J.* **84,** 3379–3388 (2003). doi:10.1016/S0006-3495(03)70061-7
109. Willis, A. R., Moore, C., Mazon-Moya, M., Krokowski, S., Lambert, C., Till, R., Mostowy, S. & Sockett, R. E. Injections of Predatory Bacteria Work Alongside Host Immune Cells to Treat Shigella Infection in Zebrafish Larvae. *Curr. Biol.* **26,** 3343–3351 (2016). doi:10.1016/j.cub.2016.09.067
110. Shatzkes, K., Tang, C., Singleton, E., Shukla, S., Zuena, M., Gupta, S., Dharani, S., Rinaggio, J., Connell, N. D. & Kadouri, D. E. Effect of Predatory Bacteria on the Gut Bacterial Microbiota in Rats. *Sci. Rep.* **7,** 43483 (2017). doi:10.1038/srep43483
111. Wright, G. D. Antibiotic Adjuvants: Rescuing Antibiotics from Resistance. *Trends Microbiol.* **24,** 862–871 (2016). doi:10.1016/j.tim.2016.06.009
112. Neu, H. C. & Fu, K. P. Clavulanic Acid, a Novel Inhibitor of -Lactamases. *Antimicrob. Agents Chemother.* **14,** 650–655 (1978). doi:10.1128/AAC.14.5.650
113. Tehrani, K. H. M. E. & Martin, N. I. β-Lactam/β-Lactamase Inhibitor Combinations: An Update. *Medchemcomm* (2018). doi:10.1039/C8MD00342Ddoi:10.1039/C8MD00342D
114. Shakya, T., Stogios, P. J., Waglechner, N., Evdokimova, E., Ejim, L., Blanchard, J. E., McArthur, A. G., Savchenko, A. & Wright, G. D. A Small Molecule Discrimination Map of the Antibiotic Resistance Kinome. *Chem. Biol.* **18,** 1591–1601 (2011). doi:10.1016/j.chembiol.2011.10.018
115. Stogios, P. J., Spanogiannopoulos, P., Evdokimova, E., Egorova, O., Shakya, T., Todorovic, N., Capretta, A., Wright, G. D. & Savchenko, A. Structure-Guided Optimization of Protein Kinase Inhibitors Reverses Aminoglycoside Antibiotic Resistance. *Biochem. J.* **454,** 191–200 (2013). doi:10.1042/BJ20130317
116. Ejim, L., Farha, M. A., Falconer, S. B., Wildenhain, J., Coombes, B. K., Tyers, M., Brown, E. D. & Wright, G. D. Combinations of Antibiotics and Nonantibiotic Drugs Enhance Antimicrobial Efficacy. *Nat. Chem. Biol.* **7,** 348–350 (2011). doi:10.1038/nchembio.559
117. Perry, J. A., Koteva, K., Verschoor, C. P., Wang, W., Bowdish, D. M. & Wright, G. D. A Macrophage-Stimulating Compound from a Screen of Microbial Natural Products. *J. Antibiot. (Tokyo).* **68,** 40–46 (2015). doi:10.1038/ja.2014.83
118. Kobir, A., Shi, L., Boskovic, A., Grangeasse, C., Franjevic, D. & Mijakovic, I. Protein Phosphorylation in Bacterial Signal Transduction. *Biochim. Biophys. Acta - Gen. Subj.* **1810,** 989–994 (2011). doi:10.1016/j.bbagen.2011.01.006
119. Manning, G., Whyte, D. B., Martinez, R., Hunter, T. & Sudarsanam, S. The Protein Kinase Complement of the Human Genome. *Science* **298,** 1912–1934 (2002). doi:10.1126/science.1075762
120. Kannan, N., Taylor, S. S., Zhai, Y., Venter, J. C. & Manning, G. Structural and Functional Diversity of the Microbial Kinome. *PLoS Biol.* **5,** e17 (2007). doi:10.1371/journal.pbio.0050017
121. Hunter, T. Protein Kinases and Phosphatases: The Yin and Yang of Protein Phosphorylation and Signaling. *Cell* **80,** 225–236 (1995). doi:10.1016/0092-

8674(95)90405-0
122. Adams, J. a. Kinetic and Catalytic Mechanisms of Protein Kinases. *Chem. Rev.* **101,** 2271–2290 (2001). doi:10.1021/cr000230w
123. Hanks, S. K., Quinn, A. M. & Hunter, T. The Protein Kinase Family: Conserved Features and Deduced Phylogeny of the Catalytic Domains. *Science (80-.).* **241,** 42–52 (1988).
124. La Sala, G., Riccardi, L., Gaspari, R., Cavalli, A., Hantschel, O. & De Vivo, M. HRD Motif as the Central Hub of the Signaling Network for Activation Loop Autophosphorylation in Abl Kinase. *J. Chem. Theory Comput.* **12,** 5563–5574 (2016). doi:10.1021/acs.jctc.6b00600
125. Shaw, A. S., Kornev, A. P., Hu, J., Ahuja, L. G. & Taylor, S. S. Kinases and Pseudokinases: Lessons from RAF. *Mol. Cell. Biol.* **34,** 1538–1546 (2014). doi:10.1128/MCB.00057-14
126. Adams, J. A. Activation Loop Phosphorylation and Catalysis in Protein Kinases: Is There Functional Evidence for the Autoinhibitor Model? †. *Biochemistry* **42,** 601–607 (2003). doi:10.1021/bi020617o
127. Pucheta-Martínez, E., Saladino, G., Morando, M. A., Martinez-Torrecuadrada, J., Lelli, M., Sutto, L., D'Amelio, N. & Gervasio, F. L. An Allosteric Cross-Talk Between the Activation Loop and the ATP Binding Site Regulates the Activation of Src Kinase. *Sci. Rep.* **6,** 24235 (2016). doi:10.1038/srep24235
128. Stock, J. B., Stock, a M. & Mottonen, J. M. Signal Transduction in Bacteria. *Nature* **344,** 395–400 (1990).
129. Hoch, J. a. Two-Component and Phosphorelay Signal Transduction. *Curr Opin Microbiol* **3,** 165–170 (2000). doi:10.1016/S1369-5274(00)00070-9
130. Laub, M. T. & Goulian, M. Specificity in Two-Component Signal Transduction Pathways. *Annu. Rev. Genet.* **41,** 121–145 (2007). doi:10.1146/annurev.genet.41.042007.170548
131. Skerker, J. M., Perchuk, B. S., Siryaporn, A., Lubin, E. A., Ashenberg, O., Goulian, M. & Laub, M. T. Rewiring the Specificity of Two-Component Signal Transduction Systems. *Cell* **133,** 1043–54 (2008). doi:10.1016/j.cell.2008.04.040
132. Munoz-dorado, J., Inouye, S. & Inouye, M. A Gene Encoding a Protein Serine/Threonine Kinase Is Required for Normal Development of M. Xanthus, a Gram-Negative Bacterium. *Cell* **67,** 995–1006 (1991). doi:10.1016/0092-8674(91)90372-6
133. Zhang, W., Munoz-Dorado, J., Inouye, M. & Inouye, S. Identification of a Putative Eukaryotic-like Protein Kinase Family in the Developmental Bacterium Myxococcus Xanthus. *J. Bacteriol.* **174,** 5450–5453 (1992). doi:10.1128/jb.174.16.5450-5453.1992
134. Burnside, K. & Rajagopal, L. Regulation of Prokaryotic Gene Expression by Eukaryotic-like Enzymes. *Curr. Opin. Microbiol.* **15,** 125–131 (2012). doi:10.1016/j.mib.2011.12.006
135. Shi, L., Potts, M. & Kennelly, P. J. The Serine , Threonine , and / or Tyrosine-Specific Protein Kinases and Protein Phosphatases of Prokaryotic Organisms : A Family Portrait. *FEMS Microbiol. Rev.* **22,** 229–253 (1998).
136. Perez, J., Castaneda-Garcia, A., Jenke-Kodama, H., Muller, R. & Munoz-Dorado, J. Eukaryotic-like Protein Kinases in the Prokaryotes and the Myxobacterial Kinome. *Proc. Natl. Acad. Sci.* **105,** 15950–15955 (2008). doi:10.1073/pnas.0806851105
137. Wright, D. P. & Ulijasz, A. T. Regulation of Transcription by Eukaryotic-like Serine-Threonine Kinases and Phosphatases in Gram-Positive Bacterial Pathogens. *Virulence* **5,** 863–885 (2014). doi:10.4161/21505594.2014.983404
138. Pereira, S. F. F., Goss, L. & Dworkin, J. Eukaryote-like Serine/Threonine Kinases and Phosphatases in Bacteria. *Microbiol. Mol. Biol. Rev.* **75,** 192–212 (2011). doi:10.1128/MMBR.00042-10
139. Prisic, S. & Husson, R. N. Mycobacterium Tuberculosis Serine/Threonine Protein Kinases. *Microbiol. Spectr.* **2,** (2014). doi:10.1128/microbiolspec.MGM2-0006-2013
140. Tiwari, S., Jamal, S. B., Hassan, S. S., Carvalho, P. V. S. D., Almeida, S., Barh, D.,

Ghosh, P., Silva, A., Castro, T. L. P. & Azevedo, V. Two-Component Signal Transduction Systems of Pathogenic Bacteria As Targets for Antimicrobial Therapy: An Overview. *Front. Microbiol.* **8,** 1–7 (2017). doi:10.3389/fmicb.2017.01878

141. Dubrac, S., Boneca, I. G., Poupel, O. & Msadek, T. New Insights into the WalK/WalR (YycG/YycF) Essential Signal Transduction Pathway Reveal a Major Role in Controlling Cell Wall Metabolism and Biofilm Formation in Staphylococcus Aureus. *J. Bacteriol.* **189,** 8257–8269 (2007). doi:10.1128/JB.00645-07
142. Kuroda, M., Kuroda, H., Oshima, T., Takeuchi, F., Mori, H. & Hiramatsu, K. Two-Component System VraSR Positively Modulates the Regulation of Cell-Wall Biosynthesis Pathway in Staphylococcus Aureus. *Mol. Microbiol.* **49,** 807–821 (2003). doi:10.1046/j.1365-2958.2003.03599.x
143. Hong, H.-J., Hutchings, M. I. & Buttner, M. J. Vancomycin Resistance VanS/VanR Two-Component Systems. in *Bacterial Signal Transduction: Networks and Drug Targets* **631,** 200–213 (Springer New York, 2008).
144. Barrett, J. F. et al. Antibacterial Agents That Inhibit Two-Component Signal Transduction Systems. *Proc. Natl. Acad. Sci.* **95,** 5317–5322 (1998). doi:10.1073/pnas.95.9.5317
145. Stephenson, K., Yamaguchi, Y. & Hoch, J. A. The Mechanism of Action of Inhibitors of Bacterial Two-Component Signal Transduction Systems. *J. Biol. Chem.* **275,** 38900–38904 (2000). doi:10.1074/jbc.M006633200
146. Roychoudhury, S., Zielinski, N. A., Ninfa, A. J., Allen, N. E., Jungheim, L. N., Nicas, T. I. & Chakrabarty, A. M. Inhibitors of Two-Component Signal Transduction Systems: Inhibition of Alginate Gene Activation in Pseudomonas Aeruginosa. *Proc. Natl. Acad. Sci.* **90,** 965–969 (1993). doi:10.1073/pnas.90.3.965
147. Ulijasz, A. T. & Weisblum, B. Dissecting the VanRS Signal Transduction Pathway with Specific Inhibitors. *J. Bacteriol.* **181,** 627–31 (1999).
148. Okada, A., Igarashi, M., Okajima, T., Kinoshita, N., Umekita, M., Sawa, R., Inoue, K., Watanabe, T., Doi, A., Martin, A., Quinn, J., Nishimura, Y. & Utsumi, R. Walkmycin B Targets WalK (YycG), a Histidine Kinase Essential for Bacterial Cell Growth. *J. Antibiot. (Tokyo).* **63,** 89–94 (2010). doi:10.1038/ja.2009.128
149. Hilliard, J. J., Goldschmidt, R. M., Licata, L., Baum, E. Z. & Bush, K. Multiple Mechanisms of Action for Inhibitors of Histidine Protein Kinases from Bacterial Two-Component Systems. *Antimicrob. Agents Chemother.* **43,** 1693–9 (1999).
150. Macielag, M. J. & Goldschmidt, R. Inhibitors of Bacterial Two-Component Signalling Systems. *Expert Opin. Investig. Drugs* **9,** 2351–69 (2000). doi:10.1517/13543784.9.10.2351
151. Norman, R. A., Toader, D. & Ferguson, A. D. Structural Approaches to Obtain Kinase Selectivity. *Trends Pharmacol. Sci.* **33,** 273–278 (2012). doi:10.1016/j.tips.2012.03.005
152. Roskoski, R. A Historical Overview of Protein Kinases and Their Targeted Small Molecule Inhibitors. *Pharmacol. Res.* **100,** 1–23 (2015). doi:10.1016/j.phrs.2015.07.010
153. Roskoski, R. Classification of Small Molecule Protein Kinase Inhibitors Based upon the Structures of Their Drug-Enzyme Complexes. *Pharmacol. Res.* **103,** 26–48 (2016). doi:10.1016/j.phrs.2015.10.021
154. Davis, M. I., Hunt, J. P., Herrgard, S., Ciceri, P., Wodicka, L. M., Pallares, G., Hocker, M., Treiber, D. K. & Zarrinkar, P. P. Comprehensive Analysis of Kinase Inhibitor Selectivity. *Nat. Biotechnol.* **29,** 1046–1051 (2011). doi:10.1038/nbt.1990
155. Knight, Z. A. & Shokat, K. M. Features of Selective Kinase Inhibitors. *Chem. Biol.* **12,** 621–637 (2005). doi:10.1016/j.chembiol.2005.04.011
156. Noble, M. E. M. Protein Kinase Inhibitors: Insights into Drug Design from Structure. *Science (80-.).* **303,** 1800–1805 (2004). doi:10.1126/science.1095920
157. Liao, J. J.-L. Molecular Recognition of Protein Kinase Binding Pockets for Design of Potent and Selective Kinase Inhibitors. *J. Med. Chem.* **50,** 409–424 (2007).

doi:10.1021/jm0608107
158. Wang, Q., Zorn, J. A. & Kuriyan, J. A Structural Atlas of Kinases Inhibited by Clinically Approved Drugs. in *Methods in Enzymology* **548,** 23–67 (Elsevier Inc., 2014).
159. Levinson, N. M., Kuchment, O., Shen, K., Young, M. A., Koldobskiy, M., Karplus, M., Cole, P. A. & Kuriyan, J. A Src-Like Inactive Conformation in the Abl Tyrosine Kinase Domain. *PLoS Biol.* **4,** e144 (2006). doi:10.1371/journal.pbio.0040144
160. Vogtherr, M., Saxena, K., Hoelder, S., Grimme, S., Betz, M., Schieborr, U., Pescatore, B., Robin, M., Delarbre, L., Langer, T., Wendt, K. U. & Schwalbe, H. NMR Characterization of Kinase P38 Dynamics in Free and Ligand-Bound Forms. *Angew. Chemie Int. Ed.* **45,** 993–997 (2006). doi:10.1002/anie.200502770
161. Pargellis, C., Tong, L., Churchill, L., Cirillo, P. F., Gilmore, T., Graham, A. G., Grob, P. M., Hickey, E. R., Moss, N., Pav, S. & Regan, J. Inhibition of P38 MAP Kinase by Utilizing a Novel Allosteric Binding Site. *Nat. Struct. Biol.* **9,** 268–272 (2002). doi:10.1038/nsb770
162. Wan, P. T. C., Garnett, M. J., Roe, S. M., Lee, S., Niculescu-Duvaz, D., Good, V. M., Project, C. G., Jones, C. M., Marshall, C. J., Springer, C. J., Barford, D. & Marais, R. Mechanism of Activation of the RAF-ERK Signaling Pathway by Oncogenic Mutations of B-RAF. *Cell* **116,** 855–867 (2004). doi:10.1016/S0092-8674(04)00215-6
163. Schindler, T. Structural Mechanism for STI-571 Inhibition of Abelson Tyrosine Kinase. *Science (80-.).* **289,** 1938–1942 (2000). doi:10.1126/science.289.5486.1938
164. Hari, S. B., Merritt, E. a. & Maly, D. J. Sequence Determinants of a Specific Inactive Protein Kinase Conformation. *Chem. Biol.* **20,** 806–815 (2013). doi:10.1016/j.chembiol.2013.05.005
165. Dietrich, J., Hulme, C. & Hurley, L. H. The Design, Synthesis, and Evaluation of 8 Hybrid DFG-out Allosteric Kinase Inhibitors: A Structural Analysis of the Binding Interactions of Gleevec ??, Nexavar??, And BIRB-796. *Bioorganic Med. Chem.* **18,** 5738–5748 (2010). doi:10.1016/j.bmc.2010.05.063
166. Zuccotto, F., Ardini, E., Casale, E. & Angiolini, M. Through the “Gatekeeper Door”: Exploiting the Active Kinase Conformation. *J. Med. Chem.* **53,** 2681–2694 (2010). doi:10.1021/jm901443h
167. Liu, Y., Shah, K., Yang, F., Witucki, L. & Shokat, K. M. A Molecular Gate Which Controls Unnatural ATP Analogue Recognition by the Tyrosine Kinase V-Src. *Bioorganic Med. Chem.* **6,** 1219–1226 (1998). doi:10.1016/S0968-0896(98)00099-6
168. Wood, E. R., Truesdale, A. T., McDonald, O. B., Yuan, D., Hassell, A., Dickerson, S. H., Ellis, B., Pennisi, C., Horne, E., Lackey, K., Alligood, K. J., Rusnak, D. W., Gilmer, T. M. & Shewchuk, L. A Unique Structure for Epidermal Growth Factor Receptor Bound to GW572016 (Lapatinib). *Cancer Res.* **64,** 6652–6659 (2004). doi:10.1158/0008-5472.CAN-04-1168
169. Tomita, N., Hayashi, Y., Suzuki, S., Oomori, Y., Aramaki, Y., Matsushita, Y., Iwatani, M., Iwata, H., Okabe, A., Awazu, Y., Isono, O., Skene, R. J., Hosfield, D. J., Miki, H., Kawamoto, T., Hori, A. & Baba, A. Structure-Based Discovery of Cellular-Active Allosteric Inhibitors of FAK. *Bioorg. Med. Chem. Lett.* **23,** 1779–1785 (2013). doi:10.1016/j.bmcl.2013.01.047
170. Ohren, J. F. et al. Structures of Human MAP Kinase Kinase 1 (MEK1) and MEK2 Describe Novel Noncompetitive Kinase Inhibition. *Nat. Struct. Mol. Biol.* **11,** 1192–1197 (2004). doi:10.1038/nsmb859
171. Mahadevan, D., Powis, G., Mash, E. a, George, B., Gokhale, V. M., Zhang, S., Shakalya, K., Du-Cuny, L., Berggren, M., Ali, M. A., Jana, U., Ihle, N., Moses, S., Franklin, C., Narayan, S., Shirahatti, N. & Meuillet, E. J. Discovery of a Novel Class of AKT Pleckstrin Homology Domain Inhibitors. *Mol. Cancer Ther.* **7,** 2621–2632 (2008). doi:10.1158/1535-7163.MCT-07-2276
172. Cohen, P. Protein Kinases--the Major Drug Targets of the Twenty-First Century? *Nat.*

Rev. Drug Discov. **1,** 309–315 (2002). doi:10.1038/nrd773
173. Cohen, P. & Alessi, D. R. Kinase Drug Discovery--What's next in the Field? *ACS Chem. Biol.* **8,** 96–104 (2013). doi:10.1021/cb300610s
174. Wu, P., Nielsen, T. E. & Clausen, M. H. FDA-Approved Small-Molecule Kinase Inhibitors. *Trends Pharmacol. Sci.* **36,** 422–439 (2015). doi:10.1016/j.tips.2015.04.005
175. Drewry, D. H., Willson, T. M. & Zuercher, W. J. Seeding Collaborations to Advance Kinase Science with the GSK Published Kinase Inhibitor Set (PKIS). *Curr Top Med Chem* **14,** 340–342 (2014). doi:10.2174/1568026613666131127160819
176. Miller, J. R. et al. A Class of Selective Antibacterials Derived from a Protein Kinase Inhibitor Pharmacophore. *Proc. Natl. Acad. Sci.* **106,** 1737–1742 (2009). doi:10.1073/pnas.0811275106
177. Rudolf, A. F., Skovgaard, T., Knapp, S., Jensen, L. J. & Berthelsen, J. A Comparison of Protein Kinases Inhibitor Screening Methods Using Both Enzymatic Activity and Binding Affinity Determination. *PLoS One* **9,** e98800 (2014). doi:10.1371/journal.pone.0098800
178. Bi, K., Lebakken, C. S. & Vogel, K. W. Transformation of in Vitro Tools for Kinase Profiling: Keeping an Eye over the off-Target Liabilities. *Expert Opin. Drug Discov.* **6,** 701–712 (2011). doi:10.1517/17460441.2011.575776
179. Martić, S. & Kraatz, H.-B. Chemical Biology Toolkit for Exploring Protein Kinase Catalyzed Phosphorylation Reactions. *Chem. Sci.* **4,** 42–59 (2013). doi:10.1039/C2SC20846F
180. Ferrè, F., Palmeri, A. & Helmer-Citterich, M. Computational Methods for Analysis and Inference of Kinase/Inhibitor Relationships. *Front. Genet.* **5,** 1–5 (2014). doi:10.3389/fgene.2014.00196
181. Jones, G. & Dyson, P. Evolution of Transmembrane Protein Kinases Implicated in Coordinating Remodeling of Gram-Positive Peptidoglycan: Inside versus Outside. *J. Bacteriol.* **188,** 7470–7476 (2006). doi:10.1128/JB.00800-06
182. Fiuza, M., Canova, M. J., Zanella-Cléon, I., Becchi, M., Cozzone, A. J., Mateos, L. M., Kremer, L., Gil, J. A. & Molle, V. From the Characterization of the Four Serine/Threonine Protein Kinases (PknA/B/G/L) of Corynebacterium Glutamicum toward the Role of PknA and PknB in Cell Division. *J. Biol. Chem.* **283,** 18099–18112 (2008). doi:10.1074/jbc.M802615200
183. Fernandez, P., Saint-Joanis, B., Barilone, N., Jackson, M., Gicquel, B., Cole, S. T. & Alzari, P. M. The Ser/Thr Protein Kinase PknB Is Essential for Sustaining Mycobacterial Growth. *J. Bacteriol.* **188,** 7778–7784 (2006). doi:10.1128/JB.00963-06
184. Chawla, Y., Upadhyay, S., Khan, S., Nagarajan, S. N., Forti, F. & Nandicoori, V. K. Protein Kinase B (PknB) of Mycobacterium Tuberculosis Is Essential for Growth of the Pathogen in Vitro as Well as for Survival within the Host. *J. Biol. Chem.* **289,** 13858–13875 (2014). doi:10.1074/jbc.M114.563536
185. Yeats, C., Finn, R. D. & Bateman, A. The PASTA Domain: A Beta-Lactam-Binding Domain. *Trends Biochem. Sci.* **27,** 438 (2002).
186. Calvanese, L., Falcigno, L., Squeglia, F., D'Auria, G. & Berisio, R. PASTA in Penicillin Binding Proteins and Serine/Threonine Kinases: A Recipe of Structural, Dynamic and Binding Properties. *Curr. Med. Chem.* **24,** 4038–4056 (2017). doi:10.2174/0929867324666170216112746
187. Gordon, E., Mouz, N., Duée, E. & Dideberg, O. The Crystal Structure of the Penicillin-Binding Protein 2x from Streptococcus Pneumoniae and Its Acyl-Enzyme Form: Implication in Drug Resistance. *J. Mol. Biol.* **299,** 477–485 (2000). doi:10.1006/jmbi.2000.3740
188. Paracuellos, P., Ballandras, A., Robert, X., Kahn, R., Hervé, M., Mengin-Lecreulx, D., Cozzone, A. J., Duclos, B. & Gouet, P. The Extended Conformation of the 2.9-Å Crystal Structure of the Three-PASTA Domain of a Ser/Thr Kinase from the Human Pathogen

Staphylococcus Aureus. *J. Mol. Biol.* **404,** 847–858 (2010). doi:10.1016/j.jmb.2010.10.012
189. Ruggiero, A., Squeglia, F., Marasco, D., Marchetti, R., Molinaro, A. & Berisio, R. X-Ray Structural Studies of the Entire Extracellular Region of the Serine/Threonine Kinase PrkC from Staphylococcus Aureus. *Biochem. J.* **435,** 33–41 (2011). doi:10.1042/BJ20101643
190. Barthe, P., Mukamolova, G. V., Roumestand, C. & Cohen-Gonsaud, M. The Structure of PknB Extracellular PASTA Domain from Mycobacterium Tuberculosis Suggests a Ligand-Dependent Kinase Activation. *Structure* **18,** 606–615 (2010). doi:10.1016/j.str.2010.02.013
191. Lemmon, M. A. & Schlessinger, J. Cell Signaling by Receptor Tyrosine Kinases. *Cell* **141,** 1117–1134 (2010). doi:10.1016/j.cell.2010.06.011
192. Shah, I. M., Laaberki, M.-H., Popham, D. L. & Dworkin, J. A Eukaryotic-like Ser/Thr Kinase Signals Bacteria to Exit Dormancy in Response to Peptidoglycan Fragments. *Cell* **29,** 997–1003 (2008). doi:10.1016/j.cell.2008.08.039
193. Squeglia, F., Marchetti, R., Ruggiero, A., Lanzetta, R., Marasco, D., Dworkin, J., Petoukhov, M., Molinaro, A., Berisio, R. & Silipo, A. Chemical Basis of Peptidoglycan Discrimination by PrkC, a Key Kinase Involved in Bacterial Resuscitation from Dormancy. *J. Am. Chem. Soc.* **133,** 20676–20679 (2011). doi:10.1021/ja208080r
194. Lee, M., Hesek, D., Shah, I. M., Oliver, A. G., Dworkin, J. & Mobashery, S. Synthetic Peptidoglycan Motifs for Germination of Bacterial Spores. *Chembiochem* **11,** 2525–9 (2010). doi:10.1002/cbic.201000626
195. Mir, M., Asong, J., Li, X., Cardot, J., Boons, G. J. & Husson, R. N. The Extracytoplasmic Domain of the Mycobacterium Tuberculosis Ser/Thr Kinase PknB Binds Specific Muropeptides and Is Required for PknB Localization. *PLoS Pathog.* **7,** (2011). doi:10.1371/journal.ppat.1002182
196. Hardt, P., Engels, I., Rausch, M., Gajdiss, M., Ulm, H., Sass, P., Ohlsen, K., Sahl, H. G., Bierbaum, G., Schneider, T. & Grein, F. The Cell Wall Precursor Lipid II Acts as a Molecular Signal for the Ser/Thr Kinase PknB of Staphylococcus Aureus. *Int. J. Med. Microbiol.* **307,** 1–10 (2017). doi:10.1016/j.ijmm.2016.12.001
197. Maestro, B., Novaková, L., Hesek, D., Lee, M., Leyva, E., Mobashery, S., Sanz, J. M. & Branny, P. Recognition of Peptidoglycan and β-Lactam Antibiotics by the Extracellular Domain of the Ser/Thr Protein Kinase StkP from Streptococcus Pneumoniae. *FEBS Lett.* **585,** 357–363 (2011). doi:10.1016/j.febslet.2010.12.016
198. Leeds, J. A. & Beckwith, J. Lambda Repressor N-Terminal DNA-Binding Domain as an Assay for Protein Transmembrane Segment Interactions in Vivo. *J. Mol. Biol.* **280,** 799–810 (1998). doi:10.1006/jmbi.1998.1893
199. Madec, E., Laszkiewicz, A., Iwanicki, A., Obuchowski, M. & Séror, S. Characterization of a Membrane-Linked Ser/Thr Protein Kinase in Bacillus Subtilis, Implicated in Developmental Processes. *Mol. Microbiol.* **46,** 571–86 (2002).
200. Pallová, P., Hercík, K., Sasková, L., Nováková, L. & Branny, P. A Eukaryotic-Type Serine/Threonine Protein Kinase StkP of Streptococcus Pneumoniae Acts as a Dimer in Vivo. *Biochem. Biophys. Res. Commun.* **355,** 526–530 (2007). doi:10.1016/j.bbrc.2007.01.184
201. Beilharz, K., Novakova, L., Fadda, D., Branny, P., Massidda, O. & Veening, J.-W. Control of Cell Division in Streptococcus Pneumoniae by the Conserved Ser/Thr Protein Kinase StkP. *Proc. Natl. Acad. Sci.* **109,** E905–E913 (2012). doi:10.1073/pnas.1119172109
202. Zucchini, L., Mercy, C., Garcia, P. S., Cluzel, C., Gueguen-Chaignon, V., Galisson, F., Freton, C., Guiral, S., Brochier-Armanet, C., Gouet, P. & Grangeasse, C. PASTA Repeats of the Protein Kinase StkP Interconnect Cell Constriction and Separation of Streptococcus Pneumoniae. *Nat. Microbiol.* **3,** 197–209 (2018). doi:10.1038/s41564-017-0069-3

203. Morlot, C., Bayle, L., Jacq, M., Fleurie, A., Tourcier, G., Galisson, F., Vernet, T., Grangeasse, C. & Di Guilmi, A. M. Interaction of Penicillin-Binding Protein 2x and Ser/Thr Protein Kinase StkP, Two Key Players in Streptococcus Pneumoniae R6 Morphogenesis. *Mol. Microbiol.* **90,** n/a-n/a (2013). doi:10.1111/mmi.12348
204. Mieczkowski, C., Iavarone, A. T. & Alber, T. Auto-Activation Mechanism of the Mycobacterium Tuberculosis PknB Receptor Ser/Thr Kinase. *EMBO J.* **27,** 3186–3197 (2008). doi:10.1038/emboj.2008.236
205. Boitel, B., Ortiz-Lombardía, M., Durán, R., Pompeo, F., Cole, S. T., Cerveñansky, C. & Alzari, P. M. PknB Kinase Activity Is Regulated by Phosphorylation in Two Thr Residues and Dephosphorylation by PstP, the Cognate Phospho-Ser/Thr Phosphatase, in Mycobacterium Tuberculosis. *Mol. Microbiol.* **49,** 1493–1508 (2003). doi:10.1046/j.1365-2958.2003.03657.x
206. Young, T. a, Delagoutte, B., Endrizzi, J. a, Falick, A. M. & Alber, T. Structure of Mycobacterium Tuberculosis PknB Supports a Universal Activation Mechanism for Ser/Thr Protein Kinases. *Nat. Struct. Biol.* **10,** 168–174 (2003). doi:10.1038/nsb897
207. Zheng, W., Cai, X., Li, S. & Li, Z. Autophosphorylation Mechanism of the Ser/Thr Kinase Stk1 From Staphylococcus Aureus. *Front. Microbiol.* **9,** (2018). doi:10.3389/fmicb.2018.00758
208. Bryant-Hudson, K. M., Shakir, S. M. & Ballard, J. D. Autoregulatory Characteristics of a Bacillus Anthracis Serine/Threonine Kinase. *J. Bacteriol.* **193,** 1833–1842 (2011). doi:10.1128/JB.01401-10
209. Ortiz-Lombardia, M., Pompeo, F., Boitel, B. & Alzari, P. M. Crystal Structure of the Catalytic Domain of the PknB Serine/Threonine Kinase from Mycobacterium Tuberculosis. *J. Biol. Chem.* **278,** 13094–13100 (2003). doi:10.1074/jbc.M300660200
210. Wehenkel, A., Fernandez, P., Bellinzoni, M., Catherinot, V., Barilone, N., Labesse, G., Jackson, M. & Alzari, P. M. The Structure of PknB in Complex with Mitoxantrone, an ATP-Competitive Inhibitor, Suggests a Mode of Protein Kinase Regulation in Mycobacteria. *FEBS Lett.* **580,** 3018–3022 (2006). doi:10.1016/j.febslet.2006.04.046
211. Lombana, T. N., Echols, N., Good, M. C., Thomsen, N. D., Ng, H.-L., Greenstein, A. E., Falick, A. M., King, D. S. & Alber, T. Allosteric Activation Mechanism of the Mycobacterium Tuberculosis Receptor Ser/Thr Protein Kinase, PknB. *Structure* **18,** 1667–1677 (2010). doi:10.1016/j.str.2010.09.019
212. Damle, N. P. & Mohanty, D. Mechanism of Autophosphorylation of Mycobacterial PknB Explored by Molecular Dynamics Simulations. *Biochemistry* **53,** 4715–4726 (2014). doi:10.1021/bi500245v
213. Beltramini, A. M., Mukhopadhyay, C. D. & Pancholi, V. Modulation of Cell Wall Structure and Antimicrobial Susceptibility by a Staphylococcus Aureus Eukaryote-like Serine/Threonine Kinase and Phosphatase. *Infect. Immun.* **77,** 1406–1416 (2009). doi:10.1128/IAI.01499-08
214. Foulquier, E., Pompeo, F., Freton, C., Cordier, B., Grangeasse, C. & Galinier, A. PrkC-Mediated Phosphorylation of Overexpressed YvcK Regulates PBP1 Localization in Bacillus Subtilis MreB Mutant Cells. *J. Biol. Chem.* 0–17 (2014). doi:10.1074/jbc.M114.562496doi:10.1074/jbc.M114.562496
215. Fleurie, A., Manuse, S., Zhao, C., Campo, N., Cluzel, C., Lavergne, J. P., Freton, C., Combet, C., Guiral, S., Soufi, B., Macek, B., Kuru, E., VanNieuwenhze, M. S., Brun, Y. V., Di Guilmi, A. M., Claverys, J. P., Galinier, A. & Grangeasse, C. Interplay of the Serine/Threonine-Kinase StkP and the Paralogs DivIVA and GpsB in Pneumococcal Cell Elongation and Division. *PLoS Genet.* **10,** (2014). doi:10.1371/journal.pgen.1004275
216. Fridman, M., Williams, G. D., Muzamal, U., Hunter, H., Siu, K. W. M. & Golemi-Kotra, D. Two Unique Phosphorylation-Driven Signaling Pathways Crosstalk in Staphylococcus Aureus to Modulate the Cell-Wall Charge: Stk1/Stp1 Meets GraSR. *Biochemistry* **52,**

7975–7986 (2013). doi:10.1021/bi401177n
217. Liebeke, M., Meyer, H., Donat, S., Ohlsen, K. & Lalk, M. A Metabolomic View of Staphylococcus Aureus and Its Ser/Thr Kinase and Phosphatase Deletion Mutants: Involvement in Cell Wall Biosynthesis. *Chem. Biol.* **17,** 820–830 (2010). doi:10.1016/j.chembiol.2010.06.012
218. Ortega, C., Liao, R., Anderson, L. N., Rustad, T., Ollodart, A. R., Wright, A. T., Sherman, D. R. & Grundner, C. Mycobacterium Tuberculosis Ser/Thr Protein Kinase B Mediates an Oxygen-Dependent Replication Switch. *PLoS Biol.* **12,** (2014). doi:10.1371/journal.pbio.1001746
219. Leiba, J., Hartmann, T., Cluzel, M. E., Cohen-Gonsaud, M., Delolme, F., Bischoff, M. & Molle, V. A Novel Mode of Regulation of the Staphylococcus Aureus Catabolite Control Protein A (CcpA) Mediated by Stk1 Protein Phosphorylation. *J. Biol. Chem.* **287,** 43607–43619 (2012). doi:10.1074/jbc.M112.418913
220. Lomas-Lopez, R., Paracuellos, P., Riberty, M., Cozzone, A. J. & Duclos, B. Several Enzymes of the Central Metabolism Are Phosphorylated in Staphylococcus Aureus. *FEMS Microbiol. Lett.* **272,** 35–42 (2007). doi:10.1111/j.1574-6968.2007.00742.x
221. Liu, Q., Fan, J., Niu, C., Wang, D., Wang, J., Wang, X., Villaruz, A. E., Li, M., Otto, M. & Gao, Q. The Eukaryotic-Type Serine/Threonine Protein Kinase Stk Is Required for Biofilm Formation and Virulence in Staphylococcus Epidermidis. *PLoS One* **6,** 1–13 (2011). doi:10.1371/journal.pone.0025380
222. Pensinger, D. A., Boldon, K. M., Chen, G. Y., Vincent, W. J. B., Sherman, K., Xiong, M., Schaenzer, A. J., Forster, E. R., Coers, J., Striker, R. & Sauer, J. D. The Listeria Monocytogenes PASTA Kinase PrkA and Its Substrate YvcK Are Required for Cell Wall Homeostasis , Metabolism , and Virulence. *PLoS Pathog.* 1–28 (2016). doi:10.1371/journal.ppat.1006001doi:10.1371/journal.ppat.1006001
223. Tamber, S., Schwartzman, J. & Cheung, A. L. Role of PknB Kinase in Antibiotic Resistance and Virulence in Community-Acquired Methicillin-Resistant Staphylococcus Aureus Strain USA300. *Infect. Immun.* **78,** 3637–3646 (2010). doi:10.1128/IAI.00296-10
224. Kristich, C. J., Wells, C. L. & Dunny, G. M. A Eukaryotic-Type Ser/Thr Kinase in Enterococcus Faecalis Mediates Antimicrobial Resistance and Intestinal Persistence. *Proc. Natl. Acad. Sci. U. S. A.* **104,** 3508–3513 (2007). doi:10.1073/pnas.0608742104
225. Canova, M. J., Baronian, G., Brelle, S., Cohen-Gonsaud, M., Bischoff, M. & Molle, V. A Novel Mode of Regulation of the Staphylococcus Aureus Vancomycin-Resistance-Associated Response Regulator VraR Mediated by Stk1 Protein Phosphorylation. *Biochem. Biophys. Res. Commun.* **447,** 165–171 (2014). doi:10.1016/j.bbrc.2014.03.128
226. Débarbouillé, M., Dramsi, S., Dussurget, O., Nahori, M. A., Vaganay, E., Jouvion, G., Cozzone, A., Msadek, T. & Duclos, B. Characterization of a Serine/Threonine Kinase Involved in Virulence of Staphylococcus Aureus. *J. Bacteriol.* **191,** 4070–4081 (2009). doi:10.1128/JB.01813-08
227. Didier, J. P., Cozzone, A. J. & Duclos, B. Phosphorylation of the Virulence Regulator SarA Modulates Its Ability to Bind DNA in Staphylococcus Aureus. *FEMS Microbiol. Lett.* **306,** 30–36 (2010). doi:10.1111/j.1574-6968.2010.01930.x
228. Sun, F., Ding, Y., Ji, Q., Liang, Z., Deng, X., Wong, C. C. L., Yi, C., Zhang, L., Xie, S., Alvarez, S., Hicks, L. M., Luo, C., Jiang, H., Lan, L. & He, C. Protein Cysteine Phosphorylation of SarA/MgrA Family Transcriptional Regulators Mediates Bacterial Virulence and Antibiotic Resistance. *Proc. Natl. Acad. Sci.* **109,** 15461–15466 (2012). doi:10.1073/pnas.1205952109
229. Burnside, K., Lembo, A., de los Reyes, M., Iliuk, A., BinhTran, N. T., Connelly, J. E., Lin, W. J., Schmidt, B. Z., Richardson, A. R., Fang, F. C., Tao, W. A. & Rajagopal, L. Regulation of Hemolysin Expression and Virulence of Staphylococcus Aureus by a Serine/Threonine Kinase and Phosphatase. *PLoS One* **5,** (2010).

doi:10.1371/journal.pone.0011071
230. Cheung, A. & Duclos, B. Stp1 and Stk1: The Yin and Yang of Vancomycin Sensitivity and Virulence in Vancomycin-Intermediate Staphylococcus Aureus Strains. *J. Infect. Dis.* **205,** 1625–1627 (2012). doi:10.1093/infdis/jis255
231. Arora, G., Sajid, A., Virmani, R., Singhal, A., Kumar, C. M. S., Dhasmana, N., Khanna, T., Maji, A., Misra, R., Molle, V., Becher, D., Gerth, U., Mande, S. C. & Singh, Y. Ser/Thr Protein Kinase PrkC-Mediated Regulation of GroEL Is Critical for Biofilm Formation in Bacillus Anthracis. *npj Biofilms Microbiomes* **3,** 7 (2017). doi:10.1038/s41522-017-0015-4
232. Bugrysheva, J., Froehlich, B. J., Freiberg, J. a. & Scott, J. R. Serine/Threonine Protein Kinase Stk Is Required for Virulence, Stress Response, and Penicillin Tolerance in Streptococcus Pyogenes. *Infect. Immun.* **79,** 4201–4209 (2011). doi:10.1128/IAI.05360-11
233. Arvidson, S. & Tegmark, K. Regulation of Virulence Determinants in Staphylococcus Aureus. *Int. J. Med. Microbiol.* **291,** 159–170 (2001). doi:10.1078/1438-4221-00112
234. Wang, B. & Muir, T. W. Regulation of Virulence in Staphylococcus Aureus : Molecular Mechanisms and Remaining Puzzles. *Cell Chem. Biol.* **23,** 214–224 (2016). doi:10.1016/j.chembiol.2016.01.004
235. Cheung, A. L., Chien, Y. T. & Bayer, A. S. Hyperproduction of Alpha-Hemolysin in a SigB Mutant Is Associated with Elevated SarA Expression in Staphylococcus Aureus. *Infect. Immun.* **67,** 1331–7 (1999).
236. Donat, S., Streker, K., Schirmeister, T., Rakette, S., Stehle, T., Liebeke, M., Lalk, M. & Ohlsen, K. Transcriptome and Functional Analysis of the Eukaryotic-Type Serine/Threonine Kinase PknB in Staphylococcus Aureus. *J. Bacteriol.* **191,** 4056–4069 (2009). doi:10.1128/JB.00117-09
237. Pensinger, D. a., Aliota, M. T., Schaenzer, A. J., Boldon, K. M., Ansari, I. U. H., Vincent, W. J. B., Knight, B., Reniere, M. L., Striker, R. & Sauer, J. D. Selective Pharmacologic Inhibition of a PASTA Kinase Increases Listeria Monocytogenes Susceptibility to β-Lactam Antibiotics. *Antimicrob. Agents Chemother.* **58,** 4486–4494 (2014). doi:10.1128/AAC.02396-14
238. Dias, R., Félix, D., Caniça, M. & Trombe, M.-C. The Highly Conserved Serine Threonine Kinase StkP of Streptococcus Pneumoniae Contributes to Penicillin Susceptibility Independently from Genes Encoding Penicillin-Binding Proteins. *BMC Microbiol.* **9,** 121 (2009). doi:10.1186/1471-2180-9-121
239. Hall, C. L., Tschannen, M., Worthey, E. A. & Kristich, C. J. IreB, a Ser/Thr Kinase Substrate, Influences Antimicrobial Resistance in Enterococcus Faecalis. *Antimicrob. Agents Chemother.* **57,** 6179–6186 (2013). doi:10.1128/AAC.01472-13
240. Kristich, C. J., Little, J. L., Hall, C. L. & Hoff, J. S. Reciprocal Regulation of Cephalosporin Resistance in Enterococcus Faecalis. *MBio* **2,** e00199-11 (2011). doi:10.1128/mBio.00199-11
241. Desbonnet, C., Tait-Kamradt, A., Garcia-Solache, M., Dunman, P., Coleman, J., Arthur, M. & Rice, L. B. Involvement of the Eukaryote-like Kinase-Phosphatase System and a Protein That Interacts with Penicillin-Binding Protein 5 in Emergence of Cephalosporin Resistance in Cephalosporin-Sensitive Class A Penicillin-Binding Protein Mutants in Enterococcus Faeci. *MBio* **7,** 1–10 (2016). doi:10.1128/mBio.02188-15
242. Murray, B. E. The Life and Times of the Enterococcus. *Clin. Microbiol. Rev.* **3,** 46–65 (1990). doi:10.1128/CMR.3.1.46
243. Hof, H., Nichterlein, T. & Kretschmar, M. Management of Listeriosis. *Clin. Microbiol. Rev.* **10,** 345–57 (1997).
244. Hof, H. Listeriosis: Therapeutic Options. *FEMS Immunol. Med. Microbiol.* **35,** 203–5 (2003).
245. Lougheed, K. E. a, Osborne, S. a., Saxty, B., Whalley, D., Chapman, T., Bouloc, N.,

Chugh, J., Nott, T. J., Patel, D., Spivey, V. L., Kettleborough, C. a., Bryans, J. S., Taylor, D. L., Smerdon, S. J. & Buxton, R. S. Effective Inhibitors of the Essential Kinase PknB and Their Potential as Anti-Mycobacterial Agents. *Tuberculosis* **91,** 277–286 (2011). doi:10.1016/j.tube.2011.03.005

246. Chapman, T. M., Bouloc, N., Buxton, R. S., Chugh, J., Lougheed, K. E. A., Osborne, S. A., Saxty, B., Smerdon, S. J., Taylor, D. L. & Whalley, D. Substituted Aminopyrimidine Protein Kinase B (PknB) Inhibitors Show Activity against Mycobacterium Tuberculosis. *Bioorganic Med. Chem. Lett.* **22,** 3349–3353 (2012). doi:10.1016/j.bmcl.2012.02.107
247. Vornhagen, J., Burnside, K., Whidbey, C., Berry, J., Qin, X. & Rajagopal, L. Kinase Inhibitors That Increase the Sensitivity of Methicillin Resistant Staphylococcus Aureus to β-Lactam Antibiotics. *Pathog. (Basel, Switzerland)* **4,** 708–21 (2015). doi:10.3390/pathogens4040708
248. Boudreau, M. A., Fishovitz, J., Llarrull, L. I., Xiao, Q. & Mobashery, S. Phosphorylation of BlaR1 in Manifestation of Antibiotic Resistance in Methicillin-Resistant Staphylococcus Aureus and Its Abrogation by Small Molecules. *ACS Infect. Dis.* **1,** 454–459 (2015). doi:10.1021/acsinfecdis.5b00086
249. Kurosu, M. & Begari, E. Bacterial Protein Kinase Inhibitors. *Drug Dev. Res.* **71,** 168–187 (2010). doi:10.1002/ddr.20362
250. Pensinger, D. A.; Schaenzer, A. J.; Sauer, J. Do Shoot the Messenger: PASTA Kinases as Virulence Determinants and Antibiotic Targets. *Trends Microbiol* **26,** 56–69 (2017). doi:10.1016/j.tim.2017.06.010
251. Ruegg, U. T. & Burgess, G. M. Staurosporine, K-252 and UCN-01: Potent but Nonspecific Inhibitors of Protein Kinases. *Trends Pharmacol. Sci.* **10,** 218–220 (1989). doi:10.1016/0165-6147(89)90263-0
252. Elkins, J. M. et al. Comprehensive Characterization of the Published Kinase Inhibitor Set. *Nat. Biotechnol.* **34,** 95–103 (2016). doi:10.1038/nbt.3374
253. Heerding, D. a et al. Identification of 4-(2-(4-Amino-1,2,5-Oxadiazol-3-Yl)-1-Ethyl-7{[(3S)-3-Piperidinylmethyl]Oxy}-1H-Imidazo [4 , 5-c] Pyridin-4-Yl) -2-Methyl-3-Butyn-2-Ol (GSK690693), a Novel Inhibitor of AKT Kinase. *J. Med. Chem.* 5663–5679 (2008). doi:10.1021/jm8004527doi:10.1021/jm8004527
254. Kant, S., Asthana, S., Missiakas, D. & Pancholi, V. A Novel STK1-Targeted Small-Molecule as an " Antibiotic Resistance Breaker " against Aureus. *Sci. Rep.* **7,** 1–19 (2017). doi:10.1038/s41598-017-05314-z
255. Tsatsanis, C. & Spandidos, D. a. The Role of Oncogenic Kinases in Human Cancer (Review). *International journal of molecular medicine* **5,** 583–590 (2000).
256. Bellacosa, a & Kumar, C. Activation of AKT Kinases in Cancer: Implications for Therapeutic Targeting. *Adv. cancer …* (2005). doi:10.1016/S0065-230X(04)94002-Xdoi:10.1016/S0065-230X(04)94002-X
257. Lougheed, K. E. A., Osborne, S. A., Saxty, B., Whalley, D., Chapman, T., Bouloc, N., Chugh, J., Nott, T. J., Patel, D., Spivey, V. L., Kettleborough, C. A., Bryans, J. S., Taylor, D. L., Smerdon, S. J. & Buxton, R. S. Effective Inhibitors of the Essential Kinase PknB and Their Potential as Anti-Mycobacterial Agents. *Tuberculosis* **91,** 277–286 (2011). doi:10.1016/j.tube.2011.03.005
258. Francino, M. P. Antibiotics and the Human Gut Microbiome: Dysbioses and Accumulation of Resistances. *Front. Microbiol.* **6,** 1–11 (2016). doi:10.3389/fmicb.2015.01543
259. Langdon, A., Crook, N. & Dantas, G. The Effects of Antibiotics on the Microbiome throughout Development and Alternative Approaches for Therapeutic Modulation. *Genome Med.* **8,** 39 (2016). doi:10.1186/s13073-016-0294-z
260. Xu, J., Wang, J., Zhou, J., Xu, C., Huang, B., Xing, Y., Wang, B., Luo, R., Wang, Y., You, X., Lu, Y. & Yu, L. A Novel Protein Kinase Inhibitor IMB-YH-8 with Anti-Tuberculosis Activity. *Sci. Rep.* **7,** 5093 (2017). doi:10.1038/s41598-017-04108-7

261. Åberg, E., Lund, B., Pflug, A., Gani, O. A. B. S. M., Rothweiler, U., De Oliveira, T. M. & Engh, R. A. Structural Origins of AGC Protein Kinase Inhibitor Selectivities: PKA as a Drug Discovery Tool. *Biol. Chem.* **393,** 1121–1129 (2012). doi:10.1515/hsz-2012-0248
262. Hancock, I. C., Wiseman, G. & Baddiley, J. Biosynthesis of the Unit That Links Teichoic Acid to the Bacterial Wall: Inhibition by Tunicamycin. *FEBS Lett.* **69,** 75–80 (1976). doi:10.1016/0014-5793(76)80657-6
263. Brandish, P. E., Kimura, K. I., Inukai, M., Southgate, R., Lonsdale, J. T., Brandish, P. E., Kimura, K., Inukai, M., Southgate, R., Lonsdale, J. T. & Bugg, T. D. H. Modes of Action of Tunicamycin , Liposidomycin B , and Mureidomycin A : Inhibition of Phospho-N-Acetylmuramyl- Pentapeptide Translocase from Escherichia Coli. *Antimicrob. Agents Chemother.* **40,** 1640–1644 (1996).
264. Fiuza, M., Canova, M. J., Patin, D., Letek, M., Zanella-Cléon, I., Becchi, M., Mateos, L. M., Mengin-Lecreulx, D., Molle, V. & Gil, J. A. The MurC Ligase Essential for Peptidoglycan Biosynthesis Is Regulated by the Serine/Threonine Protein Kinase PknA in Corynebacterium Glutamicum. *J. Biol. Chem.* **283,** 36553–36563 (2008). doi:10.1074/jbc.M807175200
265. Dasgupta, A., Datta, P., Kundu, M. & Basu, J. The Serine/Threonine Kinase PknB of Mycobacterium Tuberculosis Phosphorylates PBPA, a Penicillin-Binding Protein Required for Cell Division. *Microbiology* **152,** 493–504 (2006). doi:10.1099/mic.0.28630-0
266. Jani, C., Eoh, H., Lee, J. J., Hamasha, K., Sahana, M. B., Han, J. S., Nyayapathy, S., Lee, J. Y., Suh, J. W., Lee, S. H., Rehse, S. J., Crick, D. C. & Kang, C. M. Regulation of Polar Peptidoglycan Biosynthesis by Wag31 Phosphorylation in Mycobacteria. *BMC Microbiol* **10,** 327 (2010). doi:10.1186/1471-2180-10-327
267. Bose, J. L., Fey, P. D. & Bayles, K. W. Genetic Tools to Enhance the Study of Gene Function and Regulation in Staphylococcus Aureus. *Appl. Environ. Microbiol.* **79,** 2218–2224 (2013). doi:10.1128/AEM.00136-13
268. Kelly, L. A., Mezulis, S., Yates, C., Wass, M. & Sternberg, M. The Phyre2 Web Portal for Protein Modelling, Prediction, and Analysis. *Nat. Protoc.* **10,** 845–858 (2015). doi:10.1038/nprot.2015-053
269. Tripos International. SYBYL-X.
270. Irwin, J. J., Sterling, T., Mysinger, M. M., Bolstad, E. S. & Coleman, R. G. ZINC: A Free Tool to Discover Chemistry for Biology. *J. Chem. Inf. Model.* **52,** 1757–1768 (2012). doi:10.1021/ci3001277
271. Morris, G. M., Goodsell, D. S., Halliday, R. S., Huey, R., Hart, W. E., Belew, R. K. & Olson, A. J. Automated Docking Using a Lamarckian Genetic Algorithm and an Empirical Binding Free Energy Function. *J. Comput. Chem.* **19,** 1639–1662 (1998). doi:10.1002/(SICI)1096-987X(19981115)19:14<1639::AID-JCC10>3.0.CO;2-B
272. Schrödinger, L. The PyMOL Molecular Graphics System.
273. Bishop, D. K. & Hinrichs, D. J. Adoptive Transfer of Immunity to Listeria Monocytogenes. The Influence of in Vitro Stimulation on Lymphocyte Subset Requirements. *J Immunol* **139,** 2005–2009 (1987).
274. Kreiswirth, B. N., Löfdahl, S., Betley, M. J., O'Reilly, M., Schlievert, P. M., Bergdoll, M. S. & Novick, R. P. The Toxic Shock Syndrome Exotoxin Structural Gene Is Not Detectably Transmitted by a Prophage. *Nature* **305,** 709–12 (1983). doi:10.1088/1751-8113/44/8/085201
275. Diep, B. A., Gill, S. R., Chang, R. F., Phan, T. H. Van, Chen, J. H., Davidson, M. G., Lin, F., Lin, J., Carleton, H. A., Mongodin, E. F., Sensabaugh, G. F. & Perdreau-Remington, F. Complete Genome Sequence of USA300, an Epidemic Clone of Community-Acquired Meticillin-Resistant Staphylococcus Aureus. *Lancet* **367,** 731–739 (2006). doi:10.1016/S0140-6736(06)68231-7
276. Appelbaum, P. C. The Emergence of Vancomycin-Intermediate and Vancomycin-

Resistant Staphylococcus Aureus. *Clin. Microbiol. Infect.* **12,** 16–23 (2006). doi:10.1111/j.1469-0691.2006.01344.x

277. Marty, F. M., Yeh, W., Wennersten, C. B., Venkataraman, L., Albano, E., Alyea, E. P., Gold, H. S., Baden, L. R. & Pillai, S. K. Emergence of a Clinical Daptomycin Resistant Staphylococcus Aureus Isolate during Treatment of Methicillin Resistant Staphylococcus Aureus Bacteremia and Osteomyelitis. *J. Clin. Microbiol.* **44,** 595–597 (2006). doi:10.1128/JCM.44.2.595
278. Gu, B., Kelesidis, T., Tsiodras, S., Hindler, J. & Humphries, R. M. The Emerging Problem of Linezolid-Resistant Staphylococcus. *J. Antimicrob. Chemother.* **68,** 4–11 (2013). doi:10.1093/jac/dks354
279. Lee, N., Yuen, K.-Y. & Kumana, C. R. Clinical Role of Beta-Lactam/Beta-Lactamase Inhibitor Combinations. *Drugs* **63,** 1511–24 (2003). doi:63146 [pii]
280. Schaenzer, A. J., Wlodarchak, N., Drewry, D. H., Zuercher, W. J., Rose, W. E., Striker, R. & Sauer, J. D. A Screen for Kinase Inhibitors Identifies Antimicrobial Imidazopyridine Aminofurazans as Specific Inhibitors of the Listeria Monocytogenes PASTA Kinase PrkA. *J. Biol. Chem.* **292,** 17037–17045 (2017). doi:10.1074/jbc.M117.808600
281. Stevens, K. L., Reno, M. J., Alberti, J. B., Price, D. J., Kane-Carson, L. S., Knick, V. B., Shewchuk, L. M., Hassell, A. M., Veal, J. M., Davis, S. T., Griffin, R. J. & Peel, M. R. Synthesis and Evaluation of Pyrazolo[1,5-b]Pyridazines as Selective Cyclin Dependent Kinase Inhibitors. *Bioorg. Med. Chem. Lett.* **18,** 5758–5762 (2008). doi:10.1016/j.bmcl.2008.09.069
282. Diekema, D. J., Richter, S. S., Heilmann, K. P., Dohrn, C. L., Riahi, F., Tendolkar, S., McDanel, J. S. & Doern, G. V. Continued Emergence of USA300 Methicillin-Resistant Staphylococcus Aureus in the United States: Results from a Nationwide Surveillance Study. *Infect. Control Hosp. Epidemiol.* **35,** 285–292 (2014). doi:10.1086/675283
283. Otero, L. H., Rojas-Altuve, a, Llarrull, L. I., Carrasco-Lopez, C., Kumarasiri, M., Lastochkin, E., Fishovitz, J., Dawley, M., Hesek, D., Lee, M., Johnson, J. W., Fisher, J. F., Chang, M., Mobashery, S. & Hermoso, J. a. How Allosteric Control of Staphylococcus Aureus Penicillin Binding Protein 2a Enables Methicillin Resistance and Physiological Function. *Proc Natl Acad Sci U S A* **110,** 16808–16813 (2013). doi:10.1073/pnas.1300118110
284. Mir, M., Prisic, S., Kang, C. M., Lun, S., Guo, H., Murry, J. P., Rubin, E. J. & Husson, R. N. Mycobacterial Gene CuvA Is Required for Optimal Nutrient Utilization and Virulence. *Infect. Immun.* **82,** 4104–4117 (2014). doi:10.1128/IAI.02207-14
285. Kang, C., Abbott, D. W., Park, S. T., Dascher, C. C., Cantley, L. C. & Husson, R. N. The Mycobacterium Tuberculosis Serine/Threonine Kinases PknA and PknB: Substrate Identification and Regulation of Cell Shape. *Genes Dev.* **19,** 1692–1704 (2005). doi:10.1101/gad.1311105.nism
286. M. P. Weinstein, B. L. Z. F. R. C. M. A. W. J. A. M. N. D. G. M. E. M. J. F. D. J. H. D. W. H. J. A. H. J. B. P. M. P. J. M. S. R. B. T. M. M. T. J. D. T. *Methods for Dilution Antimicrobial Susceptibility Tests for Bacteria That Grow Aerobically ; Approved Standard — Ninth Edition*. *Methods for Dilution Antimicrobial Susceptibility Tests for Bacteria That Grow Aerobically; Approved Standard- Ninth Edition* **32,** (2012).
287. Baba, T., Takeuchi, F., Kuroda, M., Yuzawa, H., Aoki, K. I., Oguchi, A., Nagai, Y., Iwama, N., Asano, K., Naimi, T., Kuroda, H., Cui, L., Yamamoto, K. & Hiramatsu, K. Genome and Virulence Determinants of High Virulence Community-Acquired MRSA. *Lancet* **359,** 1819–1827 (2002). doi:10.1016/S0140-6736(02)08713-5
288. Gill, S. R. et al. Insights on Evolution of Virulence and Resistance from the Complete Genome Analysis of an Early Methicillin-Resistant Staphylococcus Aureus Strain and a Biofilm-Producing Methicillin-Resistant Staphylococcus Epidermidis Strain. *J. Bacteriol.* **187,** 2426–2438 (2005). doi:10.1128/JB.187.7.2426

289. Mcdougal, L. K., Steward, C. D., George, E., Chaitram, J. M., Mcallister, S. K., Tenover, C., Killgore, G. E. & Tenover, F. C. Pulsed-Field Gel Electrophoresis Typing of Oxacillin-Resistant Staphylococcus Aureus Isolates from the United States : Establishing a National Database Pulsed-Field Gel Electrophoresis Typing of Oxacillin-Resistant Staphylococcus Aureus Isolates from The. *J. Clin. Microbiol.* **41,** 5113–5120 (2003). doi:10.1128/JCM.41.11.5113
290. Baba, T., Bae, T., Schneewind, O., Takeuchi, F. & Hiramatsu, K. Genome Sequence of Staphylococcus Aureus Strain Newman and Comparative Analysis of Staphylococcal Genomes: Polymorphism and Evolution of Two Major Pathogenicity Islands. *J. Bacteriol.* **190,** 300–310 (2008). doi:10.1128/JB.01000-07
291. Peng, H. L., Novick, R. P., Kreiswirth, B., Kornblum, J. & Schlievert, P. Cloning, Characterization and Sequencing of an Accessory Gene Regulator (Agr) in Staphylococcus Aureus. *J. Bacteriol.* **170,** 4365–4372 (1988). doi:10.1128/jb.170.9.4365-4372.1988
292. Blaskovich, M. A. T., Zuegg, J., Elliott, A. G. & Cooper, M. A. Helping Chemists Discover New Antibiotics. *ACS Infect. Dis.* **1,** 285–287 (2015). doi:10.1021/acsinfecdis.5b00044
293. Lipinski, C. A., Lombardo, F., Dominy, B. W. & Feeney, P. J. Experimental and Computational Approaches to Estimate Solubility and Permeability in Drug Discovery and Development Settings. *Adv. Drug Deliv. Rev.* **46,** 3–26 (2001).
294. Lipinski, C. A. Drug-like Properties and the Causes of Poor Solubility and Poor Permeability. *J. Pharmacol. Toxicol. Methods* **44,** 235–49 (2000).
295. Wu, P., Clausen, M. H. & Nielsen, T. E. Allosteric Small-Molecule Kinase Inhibitors. *Pharmacol. Ther.* **156,** 59–68 (2015). doi:10.1016/j.pharmthera.2015.10.002
296. Roussel, M. R. & Fraser, S. J. Global Analysis of Enzyme Inhibition Kinetics. *J. Phys. Chem.* **97,** 8316–8327 (1993). doi:10.1021/j100133a031
297. Innocenti, P., Cheung, K. J., Solanki, S., Mas-droux, C., Rowan, F., Yeoh, S., Boxall, K., Westlake, M., Pickard, L., Hardy, T., Baxter, J. E., Aherne, G. W., Bayliss, R., Fry, A. M. & Hoelder, S. Design of Potent and Selective Hybrid Inhibitors of the Mitotic Kinase Nek2: Structure − Activity Relationship, Structural Biology, and Cellular Activity †. (2012).
298. Beckers, T., Mahboobi, S., Sellmer, A., Winkler, M., Eichhorn, E., Pongratz, H., Maier, T., Ciossek, T., Baer, T., Kelter, G., Fiebig, H.-H. & Schmidt, M. Chimerically Designed HDAC- and Tyrosine Kinase Inhibitors. A Series of Erlotinib Hybrids as Dual-Selective Inhibitors of EGFR, HER2 and Histone Deacetylases. *Medchemcomm* **3,** 829 (2012). doi:10.1039/c2md00317a
299. Barouch-bentov, R. Mechanisms of Drug-Resistance in Kinases. *Expert Opin. Investig. Drugs* **20,** 153–208 (2012). doi:10.1517/13543784.2011.546344.Mechanisms
300. Blencke, S., Zech, B., Engkvist, O., Greff, Z., Őrfi, L., Horváth, Z., Kéri, G., Ullrich, A. & Daub, H. Characterization of a Conserved Structural Determinant Controlling Protein Kinase Sensitivity to Selective Inhibitors. *Chem. Biol.* **11,** 691–701 (2004). doi:10.1016/j.chembiol.2004.02.029
301. Yang, S. J., Bayer, A. S., Mishra, N. N., Meehl, M., Ledala, N., Yeaman, M. R., Xiong, Y. Q. & Cheung, A. L. The Staphylococcus Aureus Two-Component Regulatory System, Grars, Senses and Confers Resistance to Selected Cationic Antimicrobial Peptides. *Infect. Immun.* **80,** 74–81 (2012). doi:10.1128/IAI.05669-11
302. Daum, R. S., Yin, S., Yin, S., Boyle-Vavra, S., Daum, R. S. & Boyle-vavra, S. VraSR Two-Component Regulatory System and Its Role in Induction Of. *Microbiology* **50,** 336–343 (2006). doi:10.1128/AAC.50.1.336
303. Hackbarth, C. J. & Chambers, H. F. BlaI and BlaR1 Regulate Beta-Lactamase and PBP 2a Production in Methicillin-Resistant Staphylococcus Aureus. *Antimicrob. Agents Chemother.* **37,** 1144–1149 (1993). doi:10.1128/AAC.37.5.1144
304. Fey, P. D., Endres, J. L., Yajjala, V. K., Widhelm, T. J., Boissy, R. J., Bose, J. L. &

Bayles, K. W. A Genetic Resource for Rapid and Comprehensive Phenotype Screening of Nonessential Staphylococcus Aureus Genes. *MBio* **4,** 1–8 (2013). doi:10.1128/mBio.00537-12

305. Beck, W. D., Berger-Bachi, B. & Kayser, F. H. Additional DNA in Methicillin-Resistant Staphylococcus Aureus and Molecular Cloning of Mec-Specific DNA. *J. Bacteriol.* **165,** 373–378 (1986).
306. Memmi, G., Filipe, S. R., Pinho, M. G., Fu, Z. & Cheung, A. Staphylococcus Aureus PBP4 Is Essential for β-Lactam Resistance in Community-Acquired Methicillin-Resistant Strains. *Antimicrob. Agents Chemother.* **52,** 3955–3966 (2008). doi:10.1128/AAC.00049-08
307. Rajagopal, M., Martin, M. J., Santiago, M., Lee, W., Kos, V. N., Meredith, T., Gilmore, M. S. & Walker, S. Multidrug Intrinsic Resistance Factors in Staphylococcus Aureus Identified by Profiling Fitness within High-Diversity Transposon Libraries. *MBio* **7,** 1–11 (2016). doi:10.1128/mBio.00950-16
308. Vestergaard, M., Leng, B., Haaber, J., Bojer, M. S., Vegge, C. S. & Ingmer, H. Genome-Wide Identification of Antimicrobial Intrinsic Resistance Determinants in Staphylococcus Aureus. *Front. Microbiol.* **7,** 1–10 (2016). doi:10.3389/fmicb.2016.02018
309. Mengin-Lecreulx, D., Texier, L., Rousseau, M. & van Heijenoort, J. The MurG Gene of Escherichia Coli Codes for the UDP-N-Acetylglucosamine: N-Acetylmuramyl-(Pentapeptide) Pyrophosphoryl-Undecaprenol N-Acetylglucosamine Transferase Involved in the Membrane Steps of Peptidoglycan Synthesis. *J. Bacteriol.* **173,** 4625–4636 (1991). doi:10.1128/jb.173.15.4625-4636.1991
310. Lima, A., Duran, R., Schujman, G. E., Marchissio, M. J., Portela, M. M., Obal, G., Pritsch, O., de Mendoza, D. & Cervenansky, C. Serine/Threonine Protein Kinase PrkA of the Human Pathogen Listeria Monocytogenes: Biochemical Characterization and Identification of Interacting Partners through Proteomic Approaches. *J. Proteomics* **74,** 1720–1734 (2011). doi:10.1016/j.jprot.2011.03.005
311. Pompeo, F., Foulquier, E., Serrano, B., Grangeasse, C. & Galinier, A. Phosphorylation of the Cell Division Protein GpsB Regulates PrkC Kinase Activity through a Negative Feedback Loop in Bacillus Subtilis. *Mol. Microbiol.* **97,** 139–150 (2015). doi:10.1111/mmi.13015
312. Rued, B. E., Zheng, J. J., Mura, A., Tsui, H. C. T., Boersma, M. J., Mazny, J. L., Corona, F., Perez, A. J., Fadda, D., Doubravová, L., Buriánková, K., Branny, P., Massidda, O. & Winkler, M. E. Suppression and Synthetic-Lethal Genetic Relationships of ΔgpsB Mutations Indicate That GpsB Mediates Protein Phosphorylation and Penicillin-Binding Protein Interactions in Streptococcus Pneumoniae D39. *Mol. Microbiol.* **103,** 931–957 (2017). doi:10.1111/mmi.13613
313. Rismondo, J., Bender, J. K. & Halbedel, S. Suppressor Mutations Linking GpsB with the First Committed Step of Peptidoglycan Biosynthesis in Listeria Monocytogenes. *J. Bacteriol.* **199,** (2017). doi:10.1128/JB.00393-16
314. Pardos de la Gandara, M., Borges, V., Chung, M., Milheiriço, C., Gomes, J. P., de Lencastre, H. & Tomasz, A. Genetic Determinants of High-Level Oxacillin Resistance in Methicillin-Resistant Staphylococcus Aureus. *Antimicrob. Agents Chemother.* **62,** (2018). doi:10.1128/AAC.00206-18
315. Martínez, J. L. & Rojo, F. Metabolic Regulation of Antibiotic Resistance. *FEMS Microbiol. Rev.* **35,** 768–789 (2011). doi:10.1111/j.1574-6976.2011.00282.x
316. Blake, K. L., O'Neill, A. J., Mengin-Lecreulx, D., Henderson, P. J. F., Bostock, J. M., Dunsmore, C. J., Simmons, K. J., Fishwick, C. W. G., Leeds, J. A. & Chopra, I. The Nature of Staphylococcus Aureus MurA and MurZ and Approaches for Detection of Peptidoglycan Biosynthesis Inhibitors. *Mol. Microbiol.* **72,** 335–343 (2009). doi:10.1111/j.1365-2958.2009.06648.x

317. Vesić, D. & Kristich, C. J. MurAA Is Required for Intrinsic Cephalosporin Resistance of Enterococcus Faecalis. *Antimicrob. Agents Chemother.* **56,** 2443–2451 (2012). doi:10.1128/AAC.05984-11
318. Fleurie, A., Lesterlin, C., Manuse, S., Zhao, C., Cluzel, C., Lavergne, J. P., Franz-Wachtel, M., MacEk, B., Combet, C., Kuru, E., VanNieuwenhze, M. S., Brun, Y. V., Sherratt, D. & Grangeasse, C. MapZ Marks the Division Sites and Positions FtsZ Rings in Streptococcus Pneumoniae. *Nature* **516,** 260–262 (2014). doi:10.1038/nature13966
319. Nováková, L., Sasková, L., Pallová, P., Janeček, J., Novotná, J., Ulrych, A., Echenique, J., Trombe, M. C. & Branny, P. Characterization of a Eukaryotic Type Serine/Threonine Protein Kinase and Protein Phosphatase of Streptococcus Pneumoniae and Identification of Kinase Substrates. *FEBS J.* **272,** 1243–1254 (2005). doi:10.1111/j.1742-4658.2005.04560.x
320. Fenton, A. K., Manuse, S., Flores-Kim, J., Garcia, P. S., Mercy, C., Grangeasse, C., Bernhardt, T. G. & Rudner, D. Z. Phosphorylation-Dependent Activation of the Cell Wall Synthase PBP2a in *Streptococcus Pneumoniae* by MacP. *Proc. Natl. Acad. Sci.* **115,** 2812–2817 (2018). doi:10.1073/pnas.1715218115
321. Falk, S. P. & Weisblum, B. Phosphorylation of the Streptococcus Pneumoniae Cell Wall Biosynthesis Enzyme MurC by a Eukaryotic-like Ser/Thr Kinase. *FEMS Microbiol. Lett.* **340,** 19–23 (2013). doi:10.1111/1574-6968.12067
322. Boutte, C. C., Baer, C. E., Papavinasasundaram, K., Liu, W., Chase, M. R., Meniche, X., Fortune, S. M., Sassetti, C. M., Ioerger, T. R. & Rubin, E. J. A Cytoplasmic Peptidoglycan Amidase Homologue Controls Mycobacterial Cell Wall Synthesis. *Elife* **5,** 1–22 (2016). doi:10.7554/eLife.14590
323. Gee, C. L., Papavinasasundaram, K. G., Blair, S. R., Baer, C. E., Falick, A. M., King, D. S., Griffin, J. E., Venghatakrishnan, H., Zukauskas, A., Wei, J.-R., Dhiman, R. K., Crick, D. C., Rubin, E. J., Sassetti, C. M. & Alber, T. A Phosphorylated Pseudokinase Complex Controls Cell Wall Synthesis in Mycobacteria. *Sci. Signal.* **5,** ra7-ra7 (2012). doi:10.1126/scisignal.2002525
324. Roumestand, C., Leiba, J., Galophe, N., Margeat, E., Padilla, A., Bessin, Y., Barthe, P., Molle, V. & Cohen-Gonsaud, M. Structural Insight into the Mycobacterium Tuberculosis Rv0020c Protein and Its Interaction with the PknB Kinase. *Structure* **19,** 1525–1534 (2011). doi:10.1016/j.str.2011.07.011
325. Parikh, A., Verma, S. K., Khan, S., Prakash, B. & Nandicoori, V. K. PknB-Mediated Phosphorylation of a Novel Substrate, N-Acetylglucosamine-1-Phosphate Uridyltransferase, Modulates Its Acetyltransferase Activity. *J. Mol. Biol.* **386,** 451–464 (2009). doi:10.1016/j.jmb.2008.12.031